Synthesis, Structural Elucidation, and Application of Tetrelylenes

A thesis submitted in the partial fulfillment of the requirement for the degree of

Doctor of Philosophy

By

Shiv Pal

ID: 20133268

Indian Institute of Science Education and Research (IISER), Pune

2018

मम्मी - पापा को समर्पित

Certificate

It is hereby certified that the work described in this thesis entitled "Synthesis, Structural Elucidation and Application of Tetrelylenes" submitted by Mr. Shiv Pal was carried out by the candidate, under my supervision. The work presented here or any part of it has not been included in any other thesis submitted previously for the award of any degree or diploma from any other university or institution.

Date: 26th Oct 2018

Dr. Shabana Khan

Research Supervisor

Email: shabana@iiserpune.ac.in

Contact No.: +91-20-2590-8137

Declaration

I declare that the written submission represents my ideas in my own words and wherever other's ideas have been included, I have adequately cited and referenced the original sources. I also declare that I have adhered to all principle of academic honesty and integrity and have not misrepresented or fabricated or falsified any idea/data/fact/source in my submission. I understand that the violation of the above will cause for disciplinary action by the institute and an also evoke penal action from the sources which have thus not been properly cited or from whom proper permission has not been taken when needed.

Date: 26th Oct, 2018

Shiv Pal

ID: 20133268

Acknowledgment

First of all, I would like to express my immense gratitude to my supervisor Dr. Shabana Khan to give me the opportunity to work under her guidance. When joined the IISER Pune, I had no idea which field I should choose and fortunately I met to my supervisor and joined the Ph.D. under her supervision. At the time of joining, we had no proper research lab but subsequently, we set up the lab from scratch, and it is always a unique pleasure and satisfaction to work with your supervisor to set-up the lab and work under her/his as if she/he is your senior, not a supervisor. I have learned a lot from my ma'am in the last five years and again I thanks her for support and guidance.

I, also express my sincere gratitude to our former Director Prof. K. N. Ganesh for providing an excellent research facility, interdisciplinary research atmosphere, and funding. Also, I would like to acknowledge our present Director Prof. Jayant B. Udgaonkar for taking over the responsibility and continuing with same directorship spirit.

I am delighted to express my gratitude to my Research Advisory Committee (RAC) member, Dr. Sakya S. Sen (NCL) and Dr. R. Boomi Shankar (IISER Pune). They have given me invaluable suggestions during research advisory committee meeting which helped me a lot to improve my research. I am thankful to my collaborator, Dr. Parameswaran Pattiyil (NIT Calicut), Dr. Nirmalya Ballav (IISER Pune), Dr. Arun Venkatanathan (IISER Pune), Mr.Rakesh Pant and Ms. Meghna Manae for their appreciable input in my thesis. Among them, Dr. Nirmalya Ballav which whom I interacted most gave me the immensely helpful suggestion which improved my way of learning the various technique. I am also extremely thankful to Prof. M. Jayakannan (Chair, Department of Chemistry) and all the faculty members of our Chemistry department for their valuable suggestion bestowed on myself during my research period.

Now it's time to thanks my labmates who supported me directly, throughout my research tenure. I specially thanks to my batchmate-cum-labmate, Ms. Neha Kathewad. We were only two students in the newly founded inorganic lab, so I spend research period with her more than other lab members, and so as a consequence we learn together and also fought together, but I thank her again because without her the journey would not have

been as exciting and memorable as it has been. I will miss the deep scientific and non-scientific discussions with Mr. Rajarshi Dasgupta and Ms. Nasrina Parvin. I also thank newly joined lab member, Nilanjana Sen, Moushakhi Ghosh, and Md. Jabed Hossain.

I am grateful to technical services staff, Mr. Parveen Nasa (Sr. Technical officer, Instrumentation) Neeta Deo (System Administrator), Nisha Kurkure (Sr. Technical Officer, High Performance Computing), Mr. Mahesh Jadhav (Technical Officer), Mr. Nitin Dalvi, Mr. S. Suresh Kumar, Mr. Sachin Behra, Mr. T. S. Yatish, Mrs. Megha Paygude, Mr. Ganesh Dimbar, Mr. Sandeep Kanade. I, thanks to Mrs. Deepali Jadhav, Mr. Chinmay Lowalekar, Ms. Swati and Mrs. Nayana for spectroscopic measurements. I, also, would like to appreciate to administrative staff, especially, Mr. Mayuresh Kulkarni (Office Assistant) and Tushar Kurulkar (Office Assistant).

I am very grateful to my IISER senior, Dr. Anant Kumar Srivastava, Dr. Ashok Kumar Yadav, Dr. Mahesh S. Deshmukh, and Dr. Gopalakrishna, for helping me in the field of X-ray Crystallography. Like every other, my friends also contributed in this journey and so thanks to all my friends especially to Reman Kumar Singh, Plawan K. Jha, Mahesh Gudem, Sathish Dasari, Korra Pravin, Veer Kumar, Varchswal Kashyap, and Santosh Kumar Singh. I acknowledge to my batchmate Yashwant Kumar, R. Manoharan, Nilesh Deshpandey, Shiv Shanker, Desbasis Shaha, Partha Samantha, and Himani Rawat.

Any achievement is not meaningful unless it deliver happiness to our parent and they appreciate it. They, always, keep faith in me and support to do whatever right thing I want to do. I, also acknowledge my brothers here, Satya Pal, Satyabrat, Priyabrat and Yash Pal for their affection and love.

I gratefully acknowledge the University Grant Commissions (UGC), India for providing the fellowship throughout the tenure. I acknowledge the DST-SERB for financial support to attend the IRIS-15 held in Kyoto, Japan. I would like to acknowledge American Chemical Society (ACS), Royal Society of Chemistry (RSC), John Wiley & Sons, Springer, etc. for publishing my research articles as well as for providing the permission and reprinting the materials under copyright.

Shiv Pal

Contents

Synopsis

*The thesis entitled "**Synthesis, Structural Elucidation, and Application of Tetrelylenes**" is about the synthesis of the group 14th (Si, Ge, and Sn) divalent compounds based on α-phosphinoamido-, α-borylamido- and benzamidinato- ligands. The present thesis is divided into five chapters starting with the brief introduction of the chemistry of low valent compounds of group 14 element. Each chapter contains the details of experimental as well as theoretical investigations of tetrelylenes reported in this thesis.*

Chapter 1: Introduction

This chapter starts with the introduction of tetrelylenes and furthers their thermal and kinetic stabilities are discussed. The brief history of tetrelylenes *i. e.* silylenes, germylenes, stannylenes and plumbylenes have been discussed in the middle part of the chapter. Moreover, the general route of synthesis which is being widely used for the isolation of tetrelylenes has also been discussed in brief. At the end of the chapter, selected reactivity of tetrelylenes towards various small molecules and catalytic applications are mentioned.

Chapter 2: Amidinato-Phosphinoamido-Silylene, Its Gold (I) Complex and Comparison with Heavier Congeners

In the chapter 2, The silylene (PhC(N*t*Bu)$_2$SiN(PPh$_2$)(2,6-*i*Pr$_2$-C$_6$H$_3$)) (**2.2**) was prepared from the previously reported (PhC(N*t*Bu)$_2$SiCl) by salt elimination method. The reaction of **2.2** with AuCl·SMe$_2$ afforded [(PhC(N*t*Bu)$_2$SiN(PPh$_2$)(2,6-*i*Pr$_2$-C$_6$H$_3$))AuCl] (**2.3**) (*Scheme 1*). It is noteworthy to mentions that in complex **2.3** that only Si(II) is coordinated to Au(I), while P(III) remains uncoordinated. The higher negative value of electrostatic potential (ESP) at the Si-center (-28.8 kcal/mol) as compared to that at the P-center (-15.3 kcal/mol) justifies this observation. Furthermore, the chloride abstraction from **2.3** with AgSbF$_6$ led to the formation of a dinuclear Au(I) cationic complex, [PhC(N*t*Bu)$_2$Si(2,6-*i*Pr$_2$-C$_6$H$_3$NPPh$_2$)(Au)]$_2$[SbF$_6$]$_2$ (**2.4**) which displays intra-molecular Au···Au interaction of 2.865 Å. The analogues germylene, PhC(N*t*Bu)$_2$SnN(PPh$_2$)(2,6-*i*Pr$_2$-C$_6$H$_3$)) (**2.7**) and stannylene, PhC(N*t*Bu)$_2$SnN(PPh$_2$)(2,6-*i*Pr$_2$-C$_6$H$_3$)) (**2.8**) have also been prepared. The comparison of the molecular orbitals and

the molecular electrostatic potential (ESP) maps on the van der Waal's surface of the atoms in silylene (**2.2**), germylene (**2.7**), and stannylene (**2.8**) indicate that the nucleophilicity of the group-14 atom reduces from silylene to stannylene. The Si-center is more nucleophilic than P-center in **2.2**, whereas Ge and P- centers have similar nucleophilicity in **2.7** and Sn-center is much less nucleophilic than P-center in **2.8**.

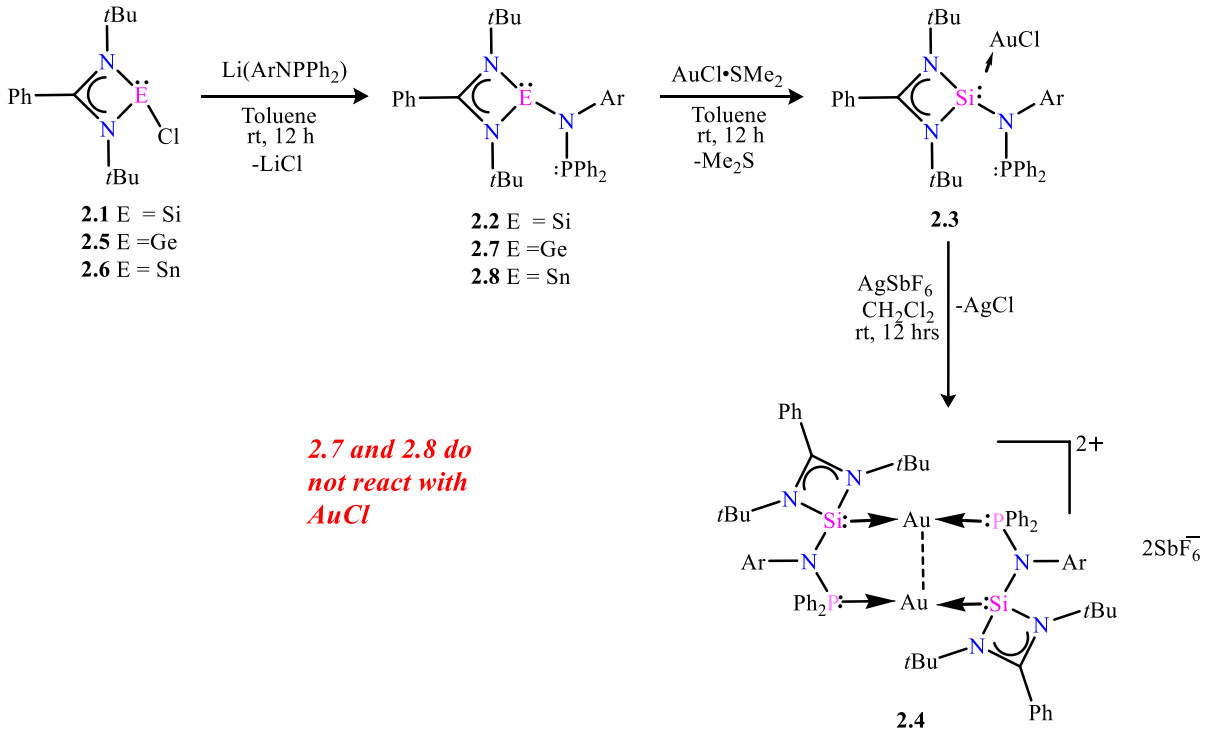

Scheme 1. *Synthesis of amidinato-phosphinoamido-silylene (**2.2**), germylene (**2.7**) and stannylene (**2.8**) and gold complexes of amidinato-phosphinoamido-silylene (**2.3**-**2.4**)*

The global minimum of the ESP of **2.2** is in the direction of the lone pair on Si, whereas the global minimum of the ESP of **2.7** and **2.8** is located above 2, 6-*i*Pr$_2$-C$_6$H$_3$ ring on the N-atom and in the opposite direction of the P-center. This is supported by the observation that silylene **2.2** forms complex with AuCl by coordinating with Si-center, whereas germylene **2.7** and stannylene **2.8** do not form the analogous adducts.

Chapter 3: Acyclic α-Phosphinoamido-Germylenes Experimental and Theoretical Study of Their Nucleophilic Behaviour

The reaction of lithium salt of ligand [**3.1**; (2,6-*i*Pr$_2$C$_6$H$_3$NH)(PPh$_2$)] with GeCl$_2$·dioxane in 1:1 stoichiometry gives a dimeric chlorogermylene, (2,6-*i*Pr$_2$C$_6$H$_3$NGeClPPh$_2$)$_2$ (**3.2**). Following the same synthetic route, with 2:1 stoichiometric ratio, germylene, (2,6-

*i*Pr$_2$C$_6$H$_3$NPPh$_2$)$_2$Ge (**3.3**) was synthesized. Compounds **3.2** and **3.3** were characterized by means of X-ray diffraction studies, NMR and mass spectrometry. Compound **3.2** is a dimer and forms a non-planner

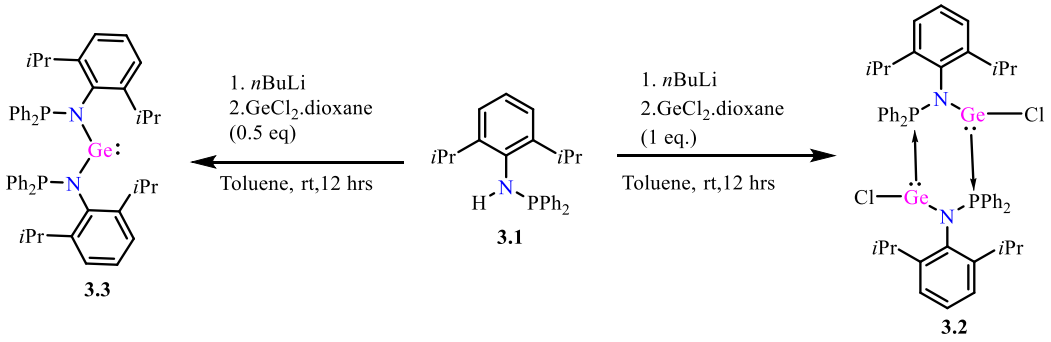

Scheme 2. *Synthesis of α-Phosphinoamido-Germylenes **3.2** and **3.3**.*

six-membered ring with Ge, P, and N atoms. For a deeper understanding of the structure and bonding, DFT calculations were performed at the M06/Def2-TZVPP//BP86/Def2-TZVPP level of theory which shows that the HOMO and LUMO are located on P- and Ge-centers respectively. At the same level of theory, population analysis was also performed to investigate the nature and composition of molecular orbitals (MOs). The analysis of electrostatic potential (ESP) mapped onto constant electron density surface show that the nucleophilic center in **3.3** is P-center rather than the Ge-center.

Chapter 4: Acyclic α -Borylamido-Germylene and Stannylene: Synthesis and Application in Hydroboration Reaction

The acyclic α-borylamido-germylene and stannylene of composition (2, 6-*i*Pr$_2$C$_6$H$_3$NBCy$_2$)$_2$E (E= Ge (**4.2**), Sn (**4.3**)) are synthesized via the reaction of lithium salt of ligand **4.1** (2, 6-*i*Pr$_2$C$_6$H$_3$NBCy$_2$) with 0.5 equivalent of GeCl$_2$·dioxane and SnCl$_2$, respectively. Compounds **4.2** and **4.3** are characterized by using routine multinuclear NMR techniques, mass spectroscopy, and single crystal X-ray diffraction studies. To get more insight about the structures, DFT calculations were performed at the BP86/Def2-TZVPP level of theory. The theoretical calculation shows both HOMO-LUMO both are reside of tetrel (Ge/Sn) center unlike that of α -phosphinoamido-germylenes where both are on two different centers. Moreover, α-borylamido-germylene (**4.2**) and stannylene (**4.3**) are used as catalysts in hydroboration reaction of aromatic aldehydes. The yield of hydroborated products (**4.4**) are quite good at the catalyst loading of 2.5 mol% for germylenes and 0.5 mol% for stannylene with reaction time of 6 hrs and 15 min respectively.

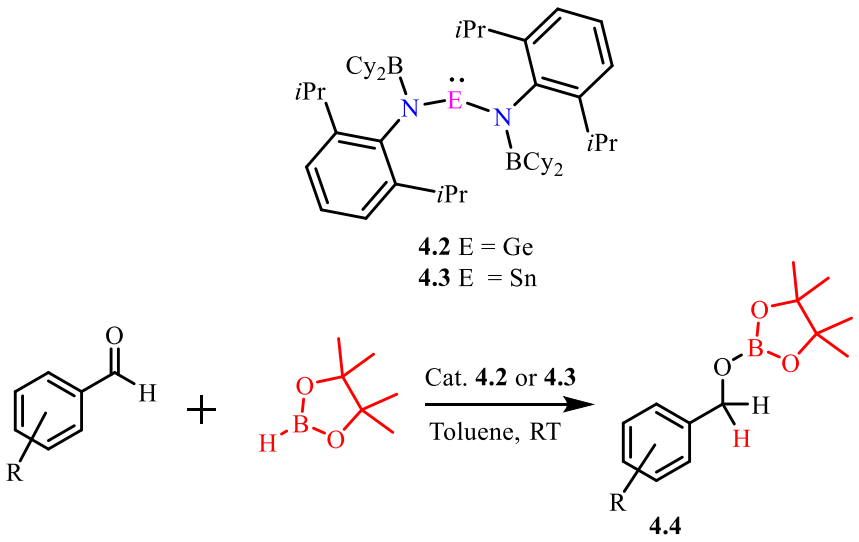

Scheme 3. *Hydroboration of aldehydes using α-borylamido-germylene (**4.2**) and stannylene (**4.3**)*

For comparison purpose, we also performed the same catalytic reaction using α -phosphinoamido-germylenes (**3.3**) as catalyst and the catalytic activity is comparable to that of α-borylamido-germylene (**4.2)** and stannylene (**4.3**).

Chapter 5: $Sn_{19}I_6 \cdot 6PPh_3$: A High-nuclearity Metalloid Tin Cluster

In the last three chapters, we discussed the mono-nuclear tetrelylenes having the oxidation state of +2. In this chapter, we have synthesized a metalloid tin cluster which could be considered as the multi-nuclear low valent species of tin whose average oxidation state is 0.3. Since the oxidation state of such types of metalloid cluster falls between the oxidation state of molecular species (+2) and elemental species (0) *i. e.* 0.1 0.2 0.6 etc., their electronic and physical properties are different than what are observed for molecular species and elemental species.

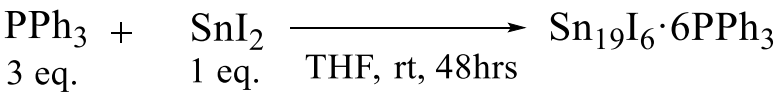

Scheme 4. *Synthesis of the metalloid tin cluster, $Sn_{19}I_6 \cdot 6PPh_3$*

The tin cluster, $Sn_{19}I_6 \cdot 6PPh_3$ was synthesized by treating the 3.0 equivalent of triphenylphosphine (PPh_3) with 1.0 equivalent of tindiiodie (SnI_2) together in dried THF for 48 hrs. The orange crystals of $Sn_{19}I_6 \cdot 6PPh_3$ were characterized by X-ray crystallography, NMR and Raman spectroscopy. Its thermal behavior was also checked by performing the thermogravimetric analysis.

Abbreviations

Anal.	Analysis
Calcd.	Calculated
CCDC	Cambridge Crystallographic Data Centre
CIF	Crystallographic Information file
CAACs	Cyclic (Alkyl)(Amino)Carbenes
Cy	Cyclohexyl
DCM	Dichloromethane
DFT	Density Functional Theory
Dipp	Diisopropylaniline
DMF	N, N-Dimethyl Formamide
DMSO	Dimethyl Sulphoxide
HBPin	Pinacolborane
HRMS	High-Resolution Mass Spectroscopy
hrs	Hours
HBPin	Pinacolborane
*i*Pr	Isopropyl
M.P.	Melting Point
MALDI-TOF	Matrix-Assisted Laser Desorption/Ionization – Time of Flight
Mes	Mesitylene
MeCN	Acetonitrile
mg	Milligram
min	Minutes
µL	Microliter
mL	Milliliter
mm	Millimeter
mmol	Millimoles
ppm	Parts per million
RT	Room Temperature
NMR	Nuclear Magnetic Resonance
NHC	N-Heterocyclic Carbene
NHSi	N-Heterocyclic Silylene
NHGe	N-Heterocyclic Germylene
NHSn	N-Heterocyclic Stannylene
*t*Bu	Tertiary Butyl
TGA	Thermogravimetric analysis
THF	Tetrahydrofuran
XRD	X-ray Diffraction

List of Publications

Publications included in the thesis

1. Cover Page Communication: Stepwise isolation of an unprecedented silylene supported dinuclear gold(I) cation with aurophilic interaction
   Shabana Khan, **Shiv Pal**, Neha Kathewad, Pattiyil Parameswaran, Susmita De and Indu Purushothaman, *Chem. Commun.* **2016**, *52*, 3880–3882.
2. Comparing Nucleophilicity of Heavier Heteroleptic Amidinato-Amido Tetrelylenes: An Experimental and Theoretical Study
   Nasrina Parvin, **Shiv Pal**, Vallyanga Chalil Rojisha, Susmita De, Pattiyil Parameswaran, and Shabana Khan, *ChemistrySelect* **2016** ,*1*,1991–1995.
3. Acyclic α-Phosphinoamido-Germylene: Synthesis and Characterization
   Shiv Pal, Rajarshi Dasgupta, and Shabana Khan, *Organometallics* **2016**, *35*, 3635-3640.
4. Acyclic α-Borylamido- Germylene and Stannylene: Synthesis, Structural Elucidation and Catalytic Application in Hydroboration Reactions
   Shiv Pal, Neha Kathewad, Nilanjana Sen, Rajarshi Dasgupta and Shabana Khan, *Manuscript under preparation*
5. $Sn_{19}I_6 \cdot 6PPh_3$: A High-nuclearity Metalloid Tin Cluster
   Shiv Pal, Moushakhi Ghosh, Neha Kathewad, Shabana Khan, *Manuscript under preparation*

*Publications **not** included in the thesis*

6. Cations and dications of heavier group 14 elements in low oxidation state
   V.S.V.S.N. Swamy, **Shiv Pal**, Shabana Khan and Sakya Singha Sen, *Dalton Trans.* **2015** , *44*, 12903-12923.
7. Synthesis, Characterization, and Luminescence Studies of Gold(I) Complexes with PNP- and PNB-Based Ligand Systems
   Shiv Pal, Neha Kathewad, Rakesh Pant, and Shabana Khan, *Inorg. Chem.*, **2015**, *54*, 10172-10183.

8. Reactivity of N-heterocyclic carbene, 1,3-bis(2,6-diisopropylphenyl)imidazol-2-ylidene, towards heavier halogens (Br_2 and I_2)
   Shiv Pal, Meghna A. Manae, Vikas V. Khade and Shabana Khan, *J. Ind. Chem. Soc.* **2018**, *95*, 765-770
9. Silicon(II) Bis(trimethylsilyl)amide ($LSiN(SiMe_3)_2$, L = $PhC(NtBu)_2$) Supported Copper, Silver, and Gold Complexes
   Shabana Khan, Saurabh K. Ahirwar, **Shiv Pal**, Nasrina Parvin, and Neha Kathewad, *Organometallics* **2015**, *34*, 5401–5406.
10. Facile access to a Ge(II) dication stabilized by isocyanides
    V. S. V. S. N. Swamy, Sandeep Yadav, **Shiv Pal**, Tamal Das, Kumar Vanka And Sakya S. Sen, *Chem. Commun.* **2016**, *52*, 7890 – 7892.
11. Unique Approach to Copper(I) Silylene Chalcogenone Complexes
    Nasrina Parvin, **Shiv Pal**, Shabana Khan, Shubhajit Das, Swapan K. Pati, and Herbert W. Roesky, *Inorg. Chem.* **2017**, *56*, 1706–1712.
12. Strikingly diverse reactivity of structurally identical silylene and stannylene
    Nasrina Parvin, Rajarshi Dasgupta, **Shiv Pal**, Sakya S. Sen and Shabana Khan, *Dalton Trans.* **2017**, *46*, 6528-6532.
13. Catalyst free boron carbon bond cleavage and facile formation of five-membered PNBCC heterocycles
    Rajarshi Dasgupta, Atanu Panda, **Shiv Pal**, Puthan V. Muhasina, Susmita De, attiyil Parameswaran, and Shabana Khan, *Dalton Trans.* **2017**, *46*, 15190-15194.
14. Synthetic Diversity and Luminescence Property of $ArN(PPh_2)_2$ Based Copper(I) Complexes
    Neha Kathewad, **Shiv Pal**, Rameshwar L. Kumawat, Ehesan Ali, and Shabana Khan, *Eur. J. Inorg. Chem.*, **2018**, DOI: 10.1002/ejic.201800096.
15. Taming Monomeric $[Cu(\eta^6\text{-}C_6H_6)]^+$ Complex with Silylene
    Nasrina Parvin, **Shiv Pal**, Jorge Echeverría, Santiago Alvarez, and Shabana Khan, *Chem. Sci.* **2018**, *9*, 4333-4337.
16. Conformational Studies of Triazole Based Flexible Molecules: A Comparative Analysis of Crystal Structure and Optimized Structure for DNA Binding Ability
    Ranjeet Kumar, Pratima Yadav, **Shiv Pal**, KR Kumar, B Sridhar, AK Tewari, *ChemistrySelect* **2017**, *2*, 3444-3451.

17. Reverse Intramolecular Stacking in o-Xylene Bridge Symmetrical Dimers of 2-Thiopyridine Derivative: Assessment of the Conformational Stability
    Ranjeet Kumar, Archana Gaurav, **Shiv Pal**, KR Kumar, B Sridhar, Ashis K Tewari, *ChemistrySelect* **2017**, *2*, 3249-3255.
18. A Case of Folding Pattern in Flexible Tripodal of N-Substituted Bisethylenamine Bridged Pyridazinone Dimers
    R Kumar, Archana Gaurav, **Shiv Pal**, AK Tewari, *ChemistrySelect* **2017**, *2,* 1479-1483.

CHAPTER 1

Introduction

The word "Tetrelylenes" refers to the heavier congeners of carbene which are low valent species of carbon in +2 oxidation state. Initially, the carbenes were observed as reactive intermediates in various chemical reactions and were characterized only spectroscopically.[1] However, the carbene-metal complexes were characterized long before its isolation in free form[2] but since the isolation of free and stable N- heterocyclic carbene (NHC) by Arduengo *et al.* in 1991,[3] its chemistry have thoroughly been studied and now is well-understood.[4] The tetrelylenes, being a heavier congeners of carbene, followed the same path of development.[5] The chemistry of group 14 elements in their low oxidation state is entirely different from their analogues in normal oxidation state because of their unique electronic property *i. e.* the possession of a lone pair and vacant *p*-orbital on the same center. In the past few decades the carbene and its heavier congeners, *i.e.,* silylenes, germylenes, stannylenes, and plumbylenes have been studied extensively used as synthetic reagents, a precursor for reactive intermediates, functional materials and catalysts.[6]

1.1 Thermodynamic and kinetic stability of tetrelylenes

If we talk about the stability of tetrelylenes, it increases as we proceed down the group because of inert pair effect and consequently the divalent species of tin and lead, i.e. $SnCl_2$, SnI_2, $PbCl_2$, *etc.* are stable at ambient condition but they exist as ion pair or polymeric form in solution as well as in the solid state.[7] In contrast to divalent species of tin and lead, the divalent species of silicon are barely stable without proper electronic and steric protection whereas compound of germanium have moderate stability.[8] Since the outermost *s* orbital (ns) electrons of tetrel atoms are tightly bound to the nucleus as compared to carbon atom, they are reluctant to participate in bonding and therefore prefer to $(ns)^2$ $(np)^2$ valence electronic configuration in their divalent species. The presence of two valence *s* electron as paired, the singlet state of tetrelylenes are more stable as compare to the triplet state.[9] The empty *p*-orbital on tetrel center are highly reactive and vulnerable, and it is responsible for the high reactivity of tetrelylenes toward other molecules as well as themselves. Hence, to make them thermally and kinetically stable for isolation, the highly reactive *p*-orbital need to be protected by means of electronic donation and the use of bulky ligands, respectively.[10] The hetero donor atom near the tetrel center donates the electron density to the vacant *p*-orbital of the tetrel atom and consequently make it less reactive and provide thermodynamic stabilization.

The inclusion of bulky ligands in tetrelylenes synthesis provides the steric protection of reactive *p*- orbitals and, therefore, the tetrelylenes become kinetically stable *i. e.* the reactivity towards other molecule and themselves is suppressed (*Figure. 1.1*).

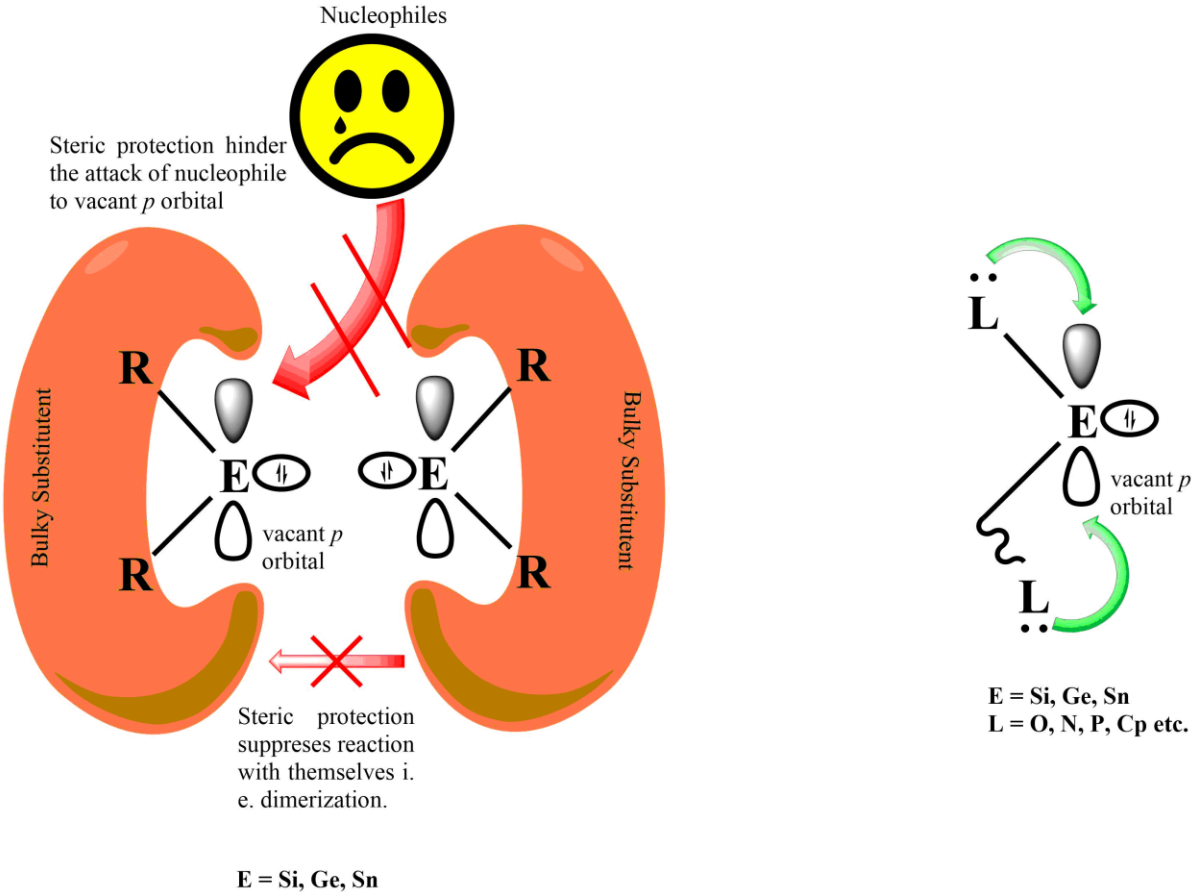

Figure 1.1 *Graphical representation for the role of the bulky substituent (left) and substitution of heteroatom (right) for stabilization of tetrelylenes*

1.2 A brief history of tetrelylenes

1.2.1 Silylenes

Silylenes are, comparatively, as reactive as carbenes and it was first observed as transient species by Skell and Goldstein,[11] and subsequently, it was spectroscopically characterized by Michl and West.[12] However, their structures were not much explored until the isolation of first stable N-heterocyclic silylene (NHSi), **1a**, by West *et al.* in 1994 (*Chart 1.1*).[13] R. West utilized the advantage of the *p*π-*p*π interaction between the vacant *p* orbital of silicon center and filled *p* orbital of the nitrogen atom of amino-ligand. This pπ-pπ interaction facilitates the cyclic (4n + 2) π electron delocalization which provides

exceptional thermal stability (**1a**).[14] After isolation of first stable silylene, its saturated analogues (**2a-2e**)[15] and benzo-fused silylene, **4a-4c**,[16] have been reported in the next ten years. Although the first divalent silylene was isolated in 1994, decamethylsilicocene, **3**, which is stabilized by η^5-coordination of pentamethylcyclopentadienyl ligand and formally could also be considered as silylene, was isolated by Jutzi et al. in 1986.[17] In 1999, Kira et al. reported the cyclic dialkylsilylene, **5**, which was kinetically stabilized by putting the bulky helmet-like bidentate substituent (-C(SiMe$_3$)$_2$CH$_2$CH$_2$(SiMe$_3$)$_2$C-) on silicon. This dialkylsilylene (**5**) undergo 1, 2 migration of trimethylsilyl group giving the corresponding silaethene derivative.[18] The nitrogen-based ligands have been used extensively in comparison to other types of ligands *i. e.* carbon, or phosphorus-based ligands, for the isolation of silylenes. In the class of N-supported ligands, benzamidianto- is the leading player to being used for isolation the four-membered tricoordinate N-heterocyclic silylenes (**7a-7f**).[19]

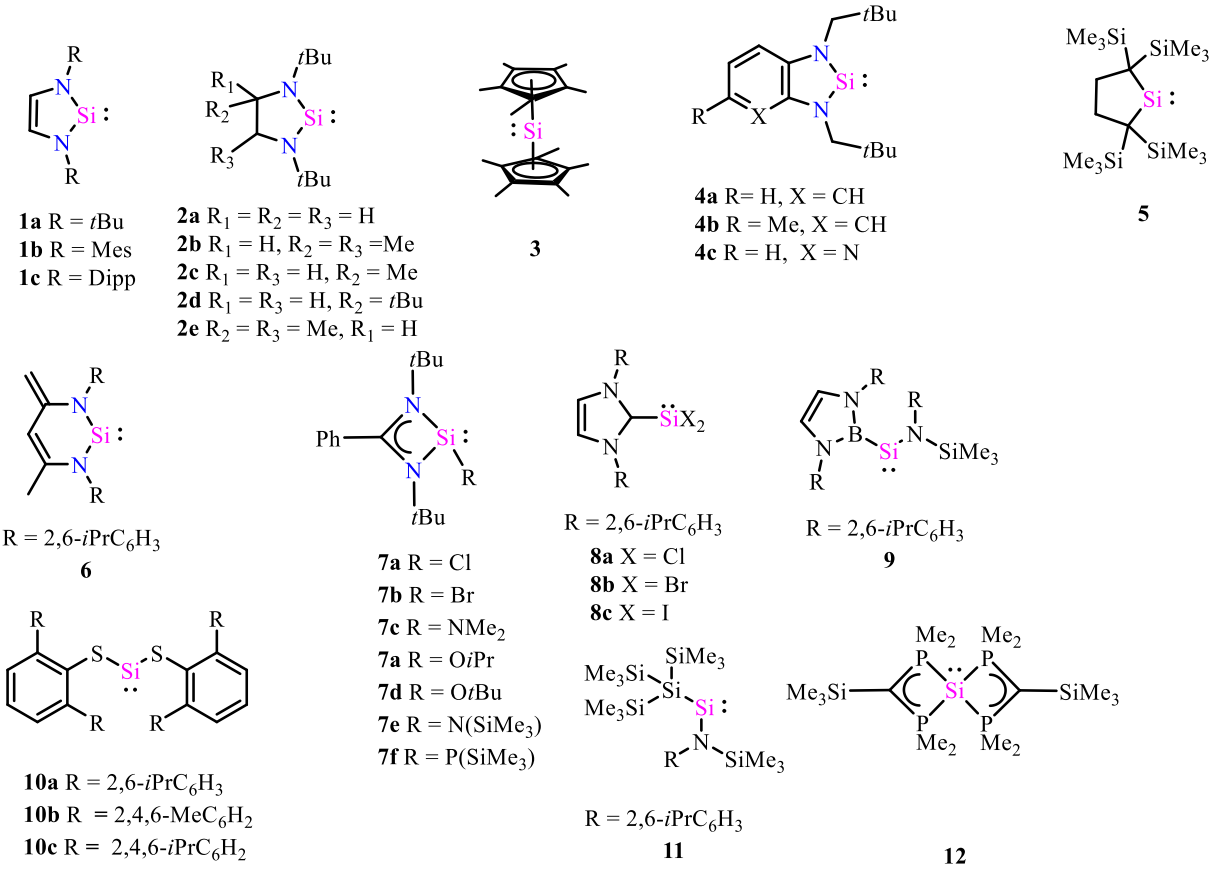

Chart 1.1 *Representative examples of silylenes*

In 2006, a six-membered N-heterocyclic silylene **6**, supported through β-diketiminate-(nacnac) derived ligand was reported[20], and interestingly the backbone could not be easily altered since it was observed that changing the substituent on N from 2,6-diisopropyl- to *t*-Butyl- or 2,6-dimethylphenyl- didn't give the corresponding silylenes.[21] The silicon dichloride (:$SiCl_2$), **8a** which exist in the gaseous phase have also been reported from the group of Roesky in 2009[22a] which was followed by the isolation of silicon dibromide, (:$SiBr_2$), **8b**, and diiodide (:SiI_2), **8c**, by Filippou *et al.*[22b-c] In the last few years, silylenes supported through P, B, Si, S and O based ligands have been isolated (**9-12**).[23]

1.2.2 Germylenes

After silylenes, the next heavier congeners of carbenes are germylenes which are not as much reactive as silylene. Actually, the chemistry of germylenes predates that of silylenes with the isolation of the alkyl-germylenes, $[(Me_3Si)_2CH]_2Ge$: (**13**), by Lappert *et al.* in 1976.[24] However, the compound **13** was monomeric in solution phase but exist as dimer in solid state. Later, Jutzi et al. reported the monomeric alkyl-germylenes, $[(Me_3Si)_3C][(Me_3Si)_2CH]Ge$: (**14**), in solid state.[25] The diarylgermylenes (**15a-15c**) reported between 1996-1997 are stabilized by intramolecular interaction of $-CF_3$ group with Ge center (**15a**) or kinetically stabilized by bulky substituent (**15b -15d**).[26] The **15d** is extremely stable since here the Ge center is protected through extremely bulky substituents, 2,4,6-tris[bis(trimethylsilyl)methyl]phenyl (Tbt) and 2,4,6-triisopropylphenyl (Tip) groups.[27a] The **15d** have been shown to display the reactivity towards alcohols, butadienes, acetylenes, hydrosilanes, and elemental chalcogens.[27] In 1999, Kira et al. isolated the cyclic alkyl-germylenes (**19**), a Ge analogue of silylene **5**.[28] Usually, ligands used for isolation of silylene *i. e.* saturated/unsaturated, benzo-fused or annelated diamino- derivative, amidinate, β-diketiminate, *etc.* were also used to synthesize germylenes (**16-21**).[16b, 29] In the last decades, the use of variously substituted β-diketiminate ligands afforded the cyclic six-membered N-heterocyclic halo-germylenes (NHGe) (**20a-20g**)[30] and dicoordinated germylene (**22**)[31]. The germylenes, **20a-20g,** were easily accessible by deprotonation of the β-diketiminate ligand followed by addition of $GeCl_2$·dioxane. The amidinate or guanidinate ligands, as they are used for isolation of silylenes, have also been employed to afford the germanium (**21a-21e**)[32] and tin analogue of silylene.

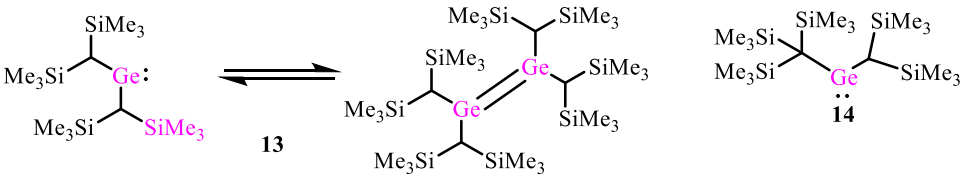

13 **14**

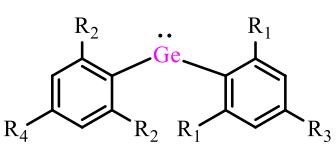

15a $R_1 = R_2 = R_3 = R_4 = CF_3$
15b $R_1 = R_2 = R_3 = R_4$ = t-Bu
15c $R_1 = R_2$ = Mes, $R_3 = R_4 = H$
15d $R_1 = R_3 = i$Pr $R_2 = R_4 = -C(SiMe_3)_2$

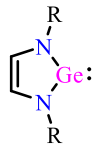

16a R = *t*-Bu
16b R = Np
16c R = 2,6-iPrC_6H_3
16d R =Mess

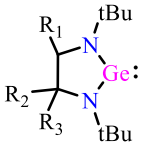

17a $R_1 = R_2 = R_3$ = H
17b $R_1 = R_2$ =Me R_3 = H
17c $R_1 = R_2$ = H, R_3 = Me
17d $R_1 = R_2$ = H, $R_3 = t$-Bu

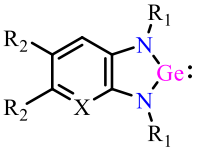

18a R_1 = Me, R_2 = H, X = CH
18b R_1 = TMS, R_2 = H, X = CH
18c R_1 = Np, R_2 = -$(CH)_4$-, X = CH
18d R_1 = Np, R_2 = H, X = CH
18e R_1 = Np, R_2 = H, X = N

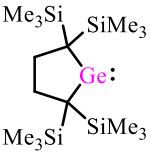

19

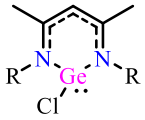

20a R =Dipp, X = Cl
20b R = C_6F_5, X = Cl
20c R = Mes, X = Cl
20d R = 2,6-MePh, X = Cl
20e R = Ph, X = Cl
20f R = Ph, X = I
20g R = Dipp, X = F

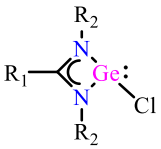

21a R = *t*Bu, R_2 = Dipp
21b R_1 = Ph, R_2 = *t*Bu
21c $R_1 = N(i\text{Pr})_2$, R_2 = Dipp
21d $R_1 = N(\text{Cy})_2$, R_2 = Dipp
21e R_1 = 2,6-$Me_2C_5H_8N$, R_2 = Dipp

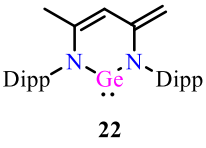

22

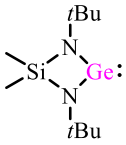

23

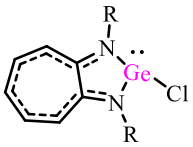

24a R = Me
24b R = *i*Pr

Dipp = 2,6-*i*PrC_6H_3 , Mes = 2,4,6-MeC_6H_2

Chart 1.2 *Representative examples of germylenes*

In 1987, Veith *et al.* reported a four-membered germylene, **23**, followed by its tin and lead analogues, however, the silicon analogue could not be isolated.[33] The aminotroponiminate based chloro-germylenes, **24a-24b**, which are similar to amidinate or guanidinate species regarding stabilization by donation, have also been reported in 1997.[34] Jones and coworkers have published a number of research articles on chloro-germylenes and stannylene which are stabilized by extremely bulky amido- ligands.[35a-b]

1.2.3 Stannylenes and plumbylenes

Unlike silylenes and germylenes, the +2 oxidation state of the last two members of tetrelylenes family *i. e.* stannylenes and plumbylenes are relatively thermodynamically stable.

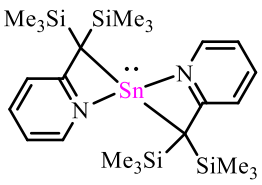

25

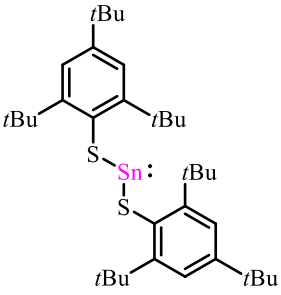

26

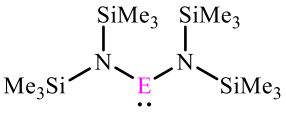

27a E = Sn
27b E = Pb

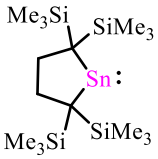

28

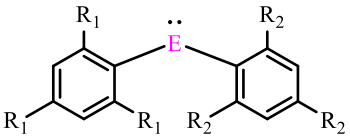

29a E = Sn, R_1= R_2 = t-Bu
29b E = Sn, R_1= R_2= CF_3
29c E =Sn, R_1= iPr, R_2 =-$CH(SiMe_3)_2$
29d E = Pb, R_1= R_2= CF_3

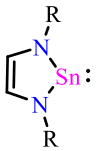

30a R = tBu
30c R = Dipp
30c R = Mes

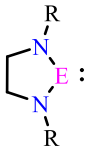

31a E = Sn, R =Dipp
31b E = Sn, R = Mes
31c E = Pb, R =Dipp
31d E = Pb, R = Mes

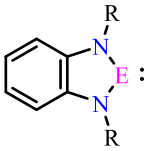

32a E = Sn, R = (CH_2)*t*Bu
32b E =Sn, R = Et
32c E = Sn, R = Me
32d E =Sn, R = $(CH_2)_2$OMe
32e E = Sn, R = $(CH_2)_3$Ome
32f E = Sn, R = $(CH_2)_2NMe_2$
32g E = Sn, R = $(CH_2)_3NMe_2$
32h E = Pb, R = (CH_2)*t*Bu
32i E = Pb, R = (CH_2)*i*Pr
32j E =Pb, R = *t*Bu
32k E = Pb, R = Me

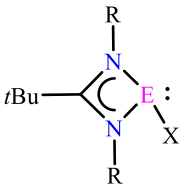

33a E = Sn, R = TMS, X = $N(TMS)_2$
33b E = Sn, R = Dipp, X = Cl
33c E =Sn, R = Dipp, X = OiPr
33d E = Sn, R = Dipp, X = NMe_2
33e E =Sn, R = Cy, X = $N(TMS)_2$
33f E = Pb, R =Dipp, X = Cl

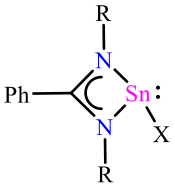

34a R = TMS, X = $N(TMS)_2$
34b R = $SiMe_2Ph$, X = $N(TMS)_2$
34c R = TMS. X = $OCPh_3$
34d R = $SiMe_2Ph$, X = $OCPh1_3$

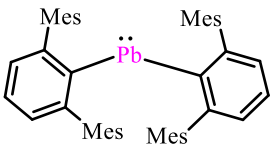

37

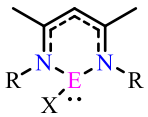

35a E = Sn, R = Ph, X = Cl
35b E = Sn, R = Ph, X = I
35c E = Sn, R = Dipp X =Cl
35d E = Sn, R = Mes, X =Cl
35e E = Pb, R = Dipp, X =Br
35f E = Pb, R = Dipp, X =$N(TMS)_2$
35g E = Pb, R = Dipp, X =$P(TMS)_2$

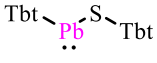

36
Tbt = 2,4,6-$[(Me_3Si)_2CH]C_6H_2$

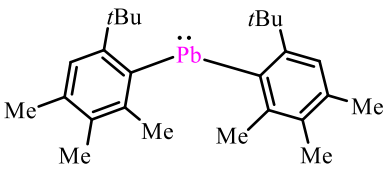

38

Chart 1.3 *Representative examples of stannylenes and plumbylenes*

The dilkylstannylene, a tin analogue of dialkylgermylene (**13**) reported by Lappert et al. was found to exist as monomer in gaseous phase but do exist as dimer in solid state and in equilibrium between the monomeric and dimeric form in solution phase.[24, 36] In 1983, dialkylbenzenethiolate- (**26**) and trimethylsilyamide- (**27**) supported stannylene and plumbylenes, stabilized by donation from heteroatom (S and N) to empty p-orbitals, were reported.[37] In 1991, Kira *et al.* reported the tin analogue (**28**) of alkyl-germylene (**19**) which was the first examples of dicoordinated dialkylstannylene.[38] However, first monomeric dialkyl stannylene in the solid state, bis[2-pyridyl-2,2-bis(trimethylsilyl) methyl]stannylene (**25**) was synthesized and structurally characterized by Lappert *et al.* in 1988, and it was found to be four coordinated, and the stabilization was considerably due to intramolecular contacts between the tin and pyridyl-nitrogen atom.[39] The diarylstannylene **29a** is the first example of kinetically stabilized aryl substituted stannylene reported by Weidenbruch *et al*.[40] The substitution of *t*Bu group with -CF_3 and -$CH(SiMe_3)_2$/*i*Pr and leads to the diarylstannylenes **29b-29c**.[41] The Saturated, unsaturated and annelated diamine have been employed to synthesize the tin analogue of Arduengo carbenes, **30a-30c**,[42] five-membered saturated analogue, **31a-31b**, [43] and five-membered benzo-fused stannylenes **32a-32g,**[16b, 44] respectively. In the last decade, amidiniate/guanidinate and β-diketiminate derived ligands has been proven to be a good candidate for isolation of four-membered (**33a-33e,**[45, 32c] **34a-34d**[46]) and six-membered (**35a-35d**) stannylenes,[47] respectively.

The chemistry of plumbylenes is limited, and it is not as much explored as for the rest of the tetrelylenes. The plumbylenes, usually, occurs as intermediate in the process of synthesis of tetravalent organo-lead compounds, R_4Pb (R = Ligands) and undergo disproportionation or polymerization reactions in the absences of suitable ligands.[48] The first plumbylenes supported through amido- ligand $[(Me_3Si)_2N]_2Pb$ (**27b**) in 1974 by Lappert *et al.*[49] In 1997, Okazaki *et al.* reported the heteroleptic aryl(arylthio)plumbylenes, TbtPbSTbt (**36**) (Tbt = 2,4,6-tris[bis(trimethylsilyl)methyl]phenyl).[50] Only few examples of monomeric plumbylenes have been reported till to date, and some of them are listed in Chart 1.3.[51]

1.3 General Method of preparations

The preparation methods of tetrelylenes could be broadly divided into three groups - (i) De-hydro halogenation of tetravalent precursors, (ii) Reduction of tetravalent precursor (iii) Substitution on divalent precursor (**Scheme 1.1**). Most of the silylenes are synthesized by de-hydrohalogenation and reduction of tetravalent precursor because their tetravalent precursors *i. e.* $SiCl_4$, $HSiCl_3$, $PhHSiCl_2$, *etc.* are thermodynamically stable and commercially available.

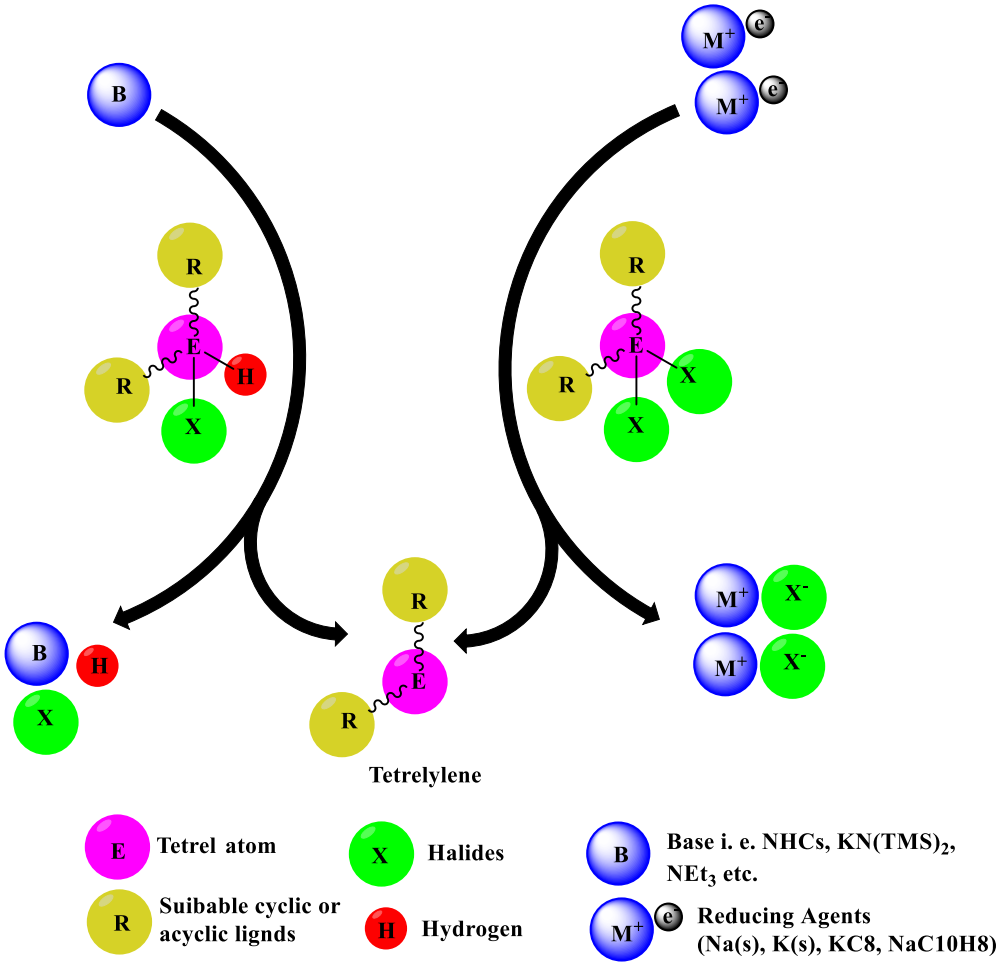

Scheme 1.1 *Schematic representation of the synthesis of tetrelylenes by (i) De-hydrohalogenation and (ii) reduction of the tetravalent precursor.*

Moreover, the synthesis of germylenes, stannylenes, and plumbylenes are readily being accomplished by the substitution of halide on divalent halo-precursor with suitable ligands.

1.3.1 De-hydro halogenation of tetravalent (E^{IV}) precursors

In this preparative method, the tetravalent precursors are being treated with the strong bases like potassium or lithium bis(trimethylsilyl)amide ($KN(TMS)_2$, $LiN(TMS)_2$) or with carbenes (NHCs or cCACs) which abstract the proton from the precursor to form the tetrelylenes. In 2010, Roesky *et al.* first reported the chloro- amidinate silylenes (**7a**) by abstraction of the proton using $Li(TMS)_2$ or NHCs (*Scheme 1.2a*).[19b] The synthesis of choro- amidinate silylenes (**7a**) was also reported by the reduction method, but unfortunately the yield was only 10%. [19a]

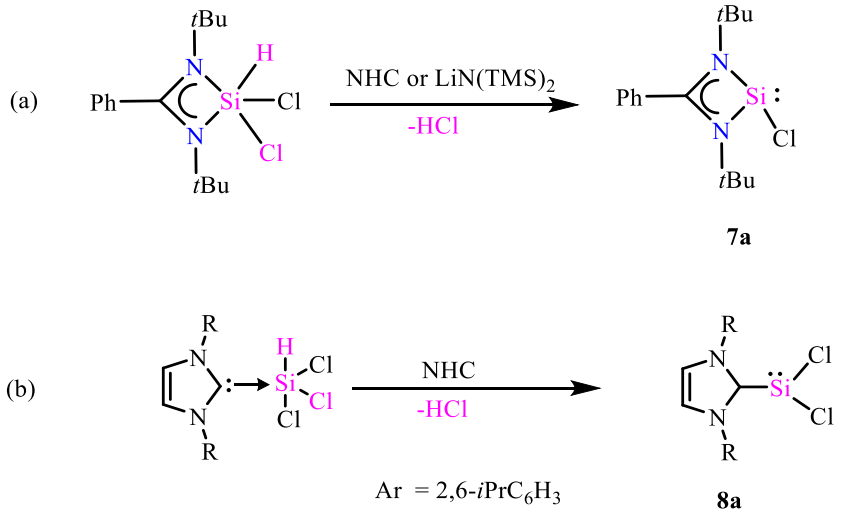

Scheme 1.2 *Selected examples of dehydrohalogenation method*

In the scheme 1.2(a), the use of two equivalent of $LiN(TMS)_2$ leads to the heteroleptic silylene (**7e**) where elimination of 2 equivalent of LiCl, as well as 1 equivalent of HN(TMS)2 groups, took place. Similarly, the NHC stabilized dichlorsilylenes (**8a**) are synthesized by treating the NHC-$SiHCl_3$ proton scavenger NHC (*Scheme 1.2b)*.[22a]

1.3.2 Reduction of the tetravalent (E^{IV}) precursor

This method is being used since the initial days of tetrelylene's chemistry. Almost all the five-membered tetrelylenes are synthesized via this method. In this method, a suitable dihalo- tetravalent precursor are treated with strong to mild reducing agents *i. e*. $Na_{(s)}$, $K_{(s)}$, KC_8, lithium naphthalenide *etc*. The first reported monomeric silylene by West, was synthesized by the reduction of tetravalent dichlorosilane with potassium metal (*Scheme 1.3(a)*)[13,] and its germanium analogue was synthesized by both the reduction (with lithium metals) and substitution (substitutions of chloride of $GeCl_2$ with ligands) methods.[29d] The five-membered saturated or unsaturated alkyl-tetrelylenes (**5**,[18] **19**,[28] **and 28**[38]) are synthesized by reduction of the corresponding dihalo- precursors with potassium graphite (KC_8) at low temperature (*Scheme 1.3 (b)*)

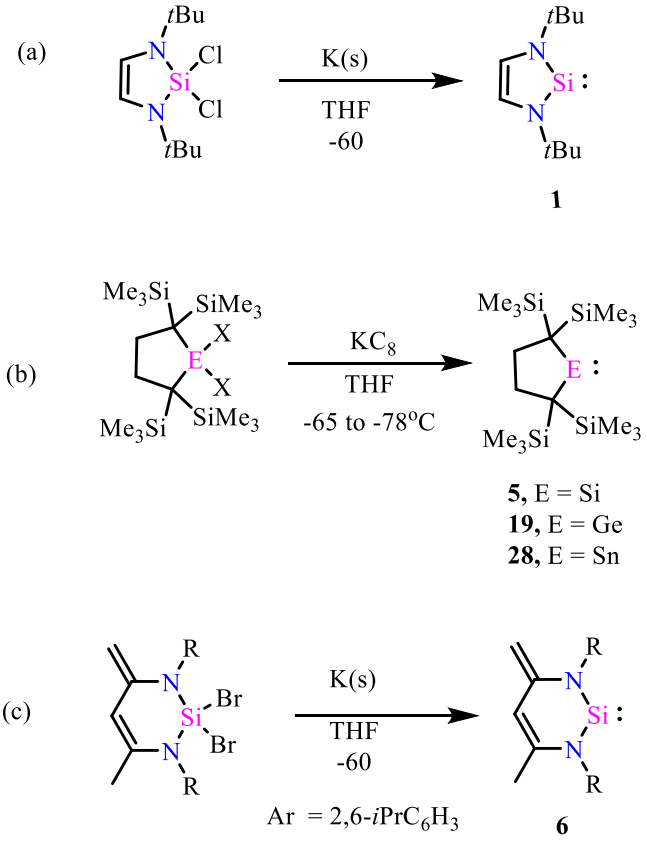

Scheme 1.3 *Selected examples of synthesis of silylenes via reduction method*

1.3.3 Substitution on divalent precursor

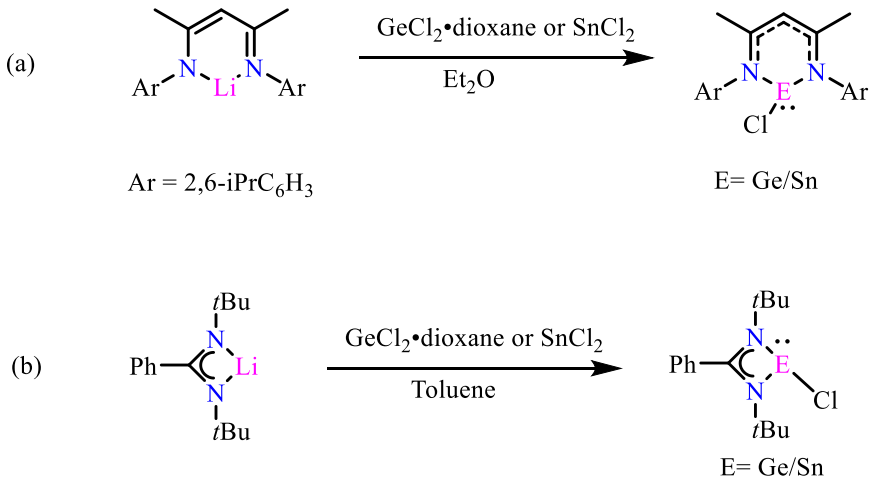

Scheme 1.4 *Selected examples of substitution method*

The substitution methods are only suitable for synthesis of tetrelylenes whose divalent precursor is easily accessible and stable at ambient conditions. Except for carbon and silicon, all the other group 14 element are commercially available in +2 state as divalent halide *i. e.* $GeCl_2$·dixoane, GeI_2, $SnCl_2$, SnI_2, $PbCl_2$, *etc.* and the halide atom could be replaced with suitable ligands by treating them with LiR (R = ligands). The scheme 1.4 (a) shows an example of substitution of chloride on Ge/Sn center with variously substituted (2,6-$CH_3C_6H_3$, Mes, Ph *i*Pr, *etc.)* nacnac ligand. [30a, b, d] The amidinate and guanidinate germylenes (**21**) (*Scheme 1.4*) could easily be accessed by treating amidinate or guanidinate lithium salts with $GeCl_2$.dioxane.[32] The acyclic germylene, stannylene, and plumbylene supported through bulky amido- [35a-b] and terphenyl ligands[35c], all are prepared by the substituting the chloride by lithium salt of ligands.

1.4 Selected reactivities of tetrelylenes, R_2E: (E =Si, Ge, Sn, and Pb)

Since the group 14 low valent compounds of general formula R_2E: (E = Si, Ge, Sn, or Pb) possess a lone pair as well as an empty *p*-orbitals on the same tetrel center, and therefore their frontier orbitals are almost similar to that of transition metals. [52] In regards of interaction with small molecules, they behave like transition metals complexes, and therefore they have been employed for the activation of small molecule and in catalytic applications.[53]

1.4.1 Activation of small molecules

1.4.1.1 Reaction with hydrocarbons

The silylenes are known to react with multiply bonded hydrocarbons *i. e.* alkene, alkyne to form cyclo-derivatives.[54] The benzamidinato-chlorosilylene, **7a**, reacts with the biphenyl acetylene in 1:1 ratio to afford the disilacyclobutene system (**39**).[19b] The reduction of **7a** gives the bis-silylene (**40**) which upon reaction with 2.0 equivalent of diphenyl acetylenes rupture the Si-Si bond of bis-silylene and form a six-membered 1, 4-disilabenzene derivative (**41**).[55] Similarly, six-membered β-diketiminato- silylene **6**, upon reaction with acetylene, phenylacetylene, and diphenylacetylene at low temperature, unveils the 2+1 cycloaddition process and gives the corresponding silacyclopropene derivatives (**42a-42c**), but when they are treated together at room temperature, the C-H insertion product (**43a-43b**) was observed.[56] Unlike silylene **6**, its germanium analogue, **22**, didn't undergo 2+ 1 cycloaddition with acetylene and phenyl acetylene, instead lead to the formation of [2.2.2]bicyclooctane-like structures (**44a-44b**) via 2 + 4 cycloaddition.[57] Recently, Aldridge and co-workers shown various mode of insertion reaction of boryl- and silyl- substitute acyclic tetrelylenes towards phenyl-substituted alkynes.[58]

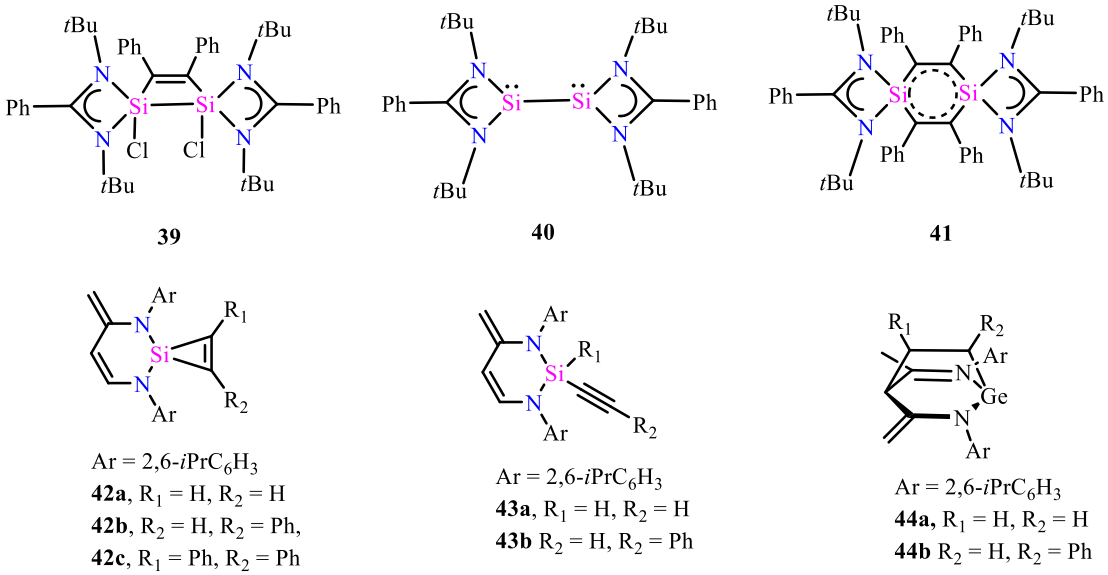

Chart 1.4 *Selected examples of reactivity of tetrelylenes towards hydrocarbon*

1.4.1.2 Reactions with H_2O, H_2, N_2O, NH_3, P_4, etc.

The tetrelylenes, mostly silylenes and germylenes show the insertion reaction in the various type of bonds *i. e.* O-H (H_2O, alcohol), N-H (NH_3, amine), B-H (boranes) C-X (alkyl aryl halides), *etc.*[16a, 59] Both the saturated and unsaturated silylenes, **1-2**, are reported to show the insertion of Si atom across the O-H bond of alcohol (**47**) and water (**46**) (*Scheme 1.5a*).[60] Similarly, the β-diketiminato silylene **6,** reacts H_2O to give the oxo-bridged silane derivative[61] and when its NHC adduct is treated N_2O or chalcogen (S, Se, Te) gives the Si=O and S=Ch (Ch = S, Se, Te) (**51**), respectively.[62]

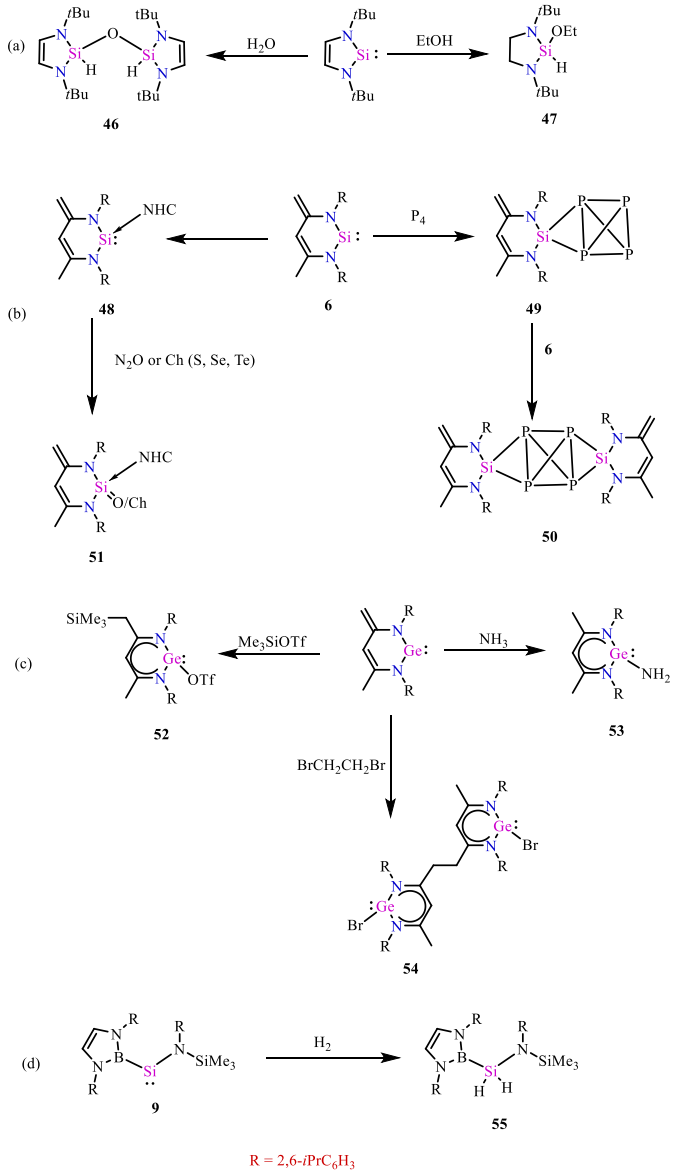

Scheme 1.5 *Selected examples of small molecules activation*

The β-diketiminato- and amindinato- silylenes have been shown to activate the phosphorus (P_4).[63] The β-diketiminato silylene reacts with 1.0 equivalent of P_4 to afford **49** and further addition of 1.0 equivalent **6** results in the formation of **50**.[64] Like β-diketiminato silylenes, the β-diketiminato germylene has also been shown to cleave various σ-bonds *i. e.* N-H (**53**), C-X (**54**) Si-O (**52**), *etc.* (*Scheme 1.5*).[31, 65] In recent years, the tetrelylenes have been studied extensively to activate the H_2, but most of them are irreversible activation of hydrogen in nature.[66] In 2012, Aldridge and co-workers, first experimentally observed the activation of H_2 by a silylene utilizing the acyclic silylene, Si{B(NArCH)$_2$}{N-(SiMe$_3$)Ar} (Ar = 2,6-*i*Pr$_2$C$_6$H$_3$) (**9**). The silylene **9,** having the low singlet-triplet gap (103.9 kJ mol^{-1}), undergo facile oxidation addition with H_2 and gives the compound **55**, following the mode of reactivity similar to that of transition metal systems.[23a]

1.4.2 Coordination with transitions metal

The transition metal catalysts have a wide application in the synthesis of various drugs and natural product.[67] The most common ligands used in transition metal catalyst are based on phosphine derived ligands[68] which could be replaced with group 14 low valent compounds.[69] The tetrelylenes having the active lone pair could act as donor ligands for transition metals, and the modification of ligands could alter the reactivity of the tetrelylenes-transition metal catalysts and consequently may also enhance the catalytic activity.[70] The seminal work on of isolation of silylene-transition metal complex was accomplished by Welz and Schmid via the synthesis of a thermolabile NHSi-iron complex, **56**.[71]

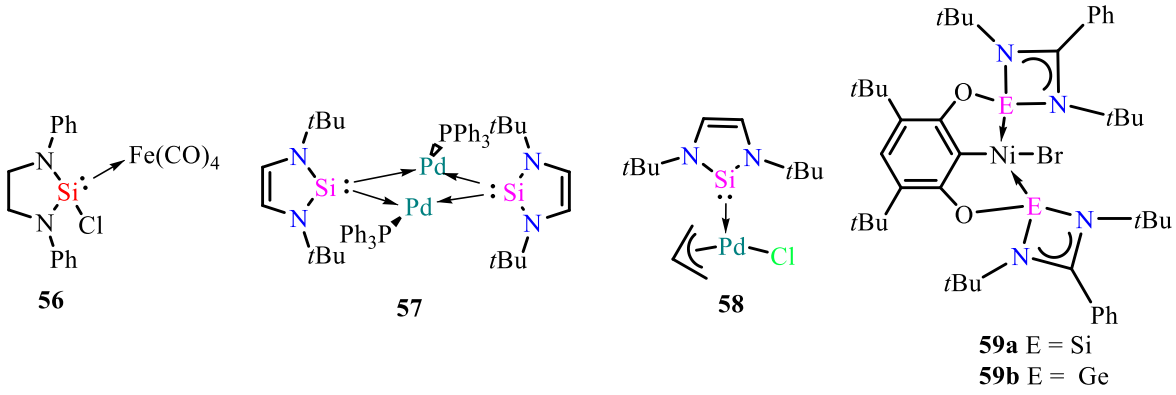

Chart 1.5 *Selected examples of Silylenes-transition metal complexes*

In last two decade the tetrelylenes, especially silylenes have been used to isolate the transition metal complexes of Fe, Mn, Rh, Ir, Os, Pd, *etc*. and also they have been demonstrated for catalytic applications.[72, 6a] The selected examples of tetrelylenes-transition metal complexes (**57-59**) are given in *chart 1.5.*[73]

1.4.3 Catalysis

The NHC–transition metal complexes have been found to be useful in various organic transformation[74] and tetrelylenes being the heavier congeners of carbenes caught the attention of the scientific community in recent years.[72] The silylene transition metal complexes have been demonstrated in several showcases of organic transformations including the Heck coupling,[73b] Suzuki coupling,[73a] hydrosilylation of carbonyls,[75] amination of arenes,[76] cyclotrimerization of alkynes[77] and Sonogashira cross-coupling reactions.[73c] The tetrelylenes have also been employed as single site catalyst in cyanosilylation, hydroboration, and hydrosilylation of the carbonyl compound.[78]

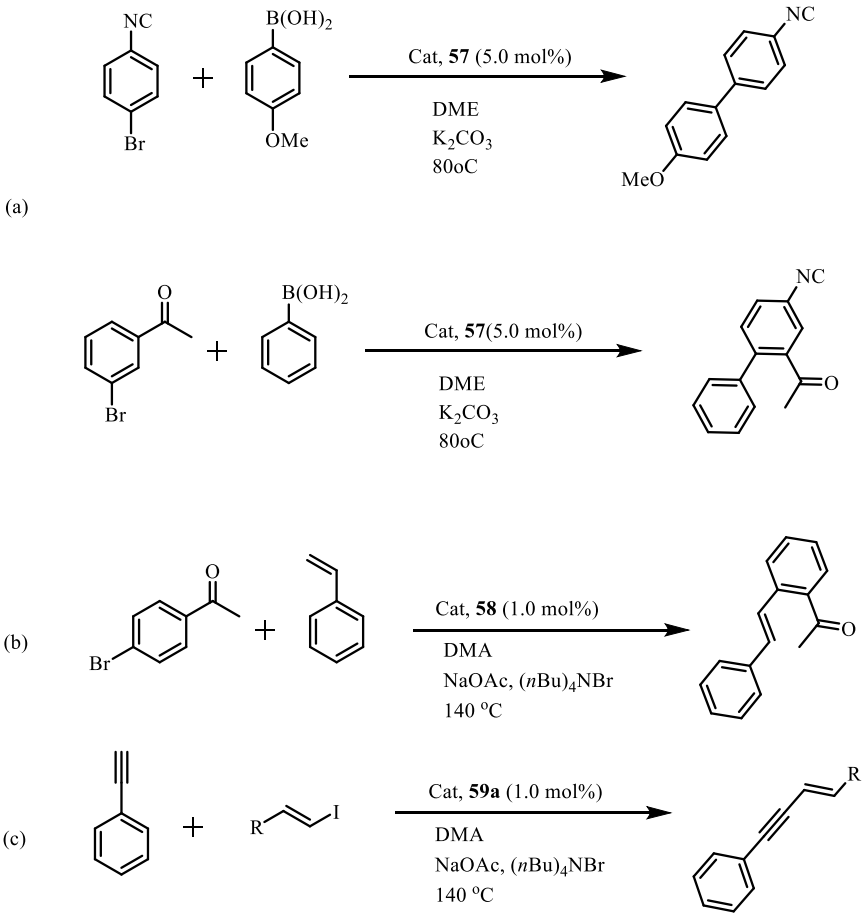

Scheme 1.6 *Selected examples of silylene-transition metal complexes used in catalysis (a) Suzuki Coupling, (b) Heck coupling and (c) Sonogashira cross-coupling*

In 2001, Fürstner and co-workers reported the dinuclear silylene-palladium complex **57** for the Suzuki coupling reaction of aryl boronic acids with bromoarenes (*Scheme 1.6 (a)*).[73a] Later, In 2008, Roesky and co-workers isolated the second example of silylene-palladium complex **58** by treating the NHSi with $[Pd(\eta^3\text{-}C_3H_5)Cl]_2$ precursor and the complex was used for the heck coupling of styrene and bromoacetophenone (*Scheme 1.6 (b)*).[73b] Recently, Dries and co-workers synthesized the Ni complex of silylene **59a** through the reaction of pincer-type silylene (bis-silylene) with $NiBr_2(dme)$ in the presence of NEt_3 in excess. The silylene-nickel complex **59a** was proved to be a good candidate for C-H activations and used for the Sonogashira cross-coupling reaction of phenylacetylene with 1-octenyl iodide (*Scheme 1.6(c)*)[73c]

So for, we have discussed the various aspects of group 14 low valent (R_2E: E, = Si, Ge, Sn, Pb) species we have realized the importance of these species for the development of new functional materials and catalyst which could mimic the transition metal chemistry. Moreover, the study of the group 14 low valent species is also important to understand their structure and bonding. The main objective of the present thesis is the synthesis of new group 14 low valent species, their coordination complexes, and catalytic application.

1.5 Reference

1. (a) Herzberg, G.; Shoosmith, J. *Nature* **1959**, *183*, 1801; (b) Cvetanovic, R. J.; Avery, H. E.; Irwin, R. S. *J. Chem. Phys.* **1967**, *46*, 1993; (c) Anet, F. A. L.; Bader, R. F. W.; Auwera, A.-M. V. d. *J. Am. Chem. Soc.* **1960**, *82*, 3217; (d) Wanzlick, H.-W. *Angew. Chem., Int. Ed. Engl.* **1962**, *1*, 75.
2. (a) Fischer, E. O.; Maasbol, A. *Angew. Chem. Int. Ed.* **1964**, 580; (c) Öfele, K. *J. Organomet. Chem.* **1968**, *12*, 42.
3. Arduengo, III, A. J.; Harlow R. L.; Kline, M. *J. Am. Chem. Soc.* **1991**, *113*, 361.
4. (a) Liddle, S. T.; Edworthy, I. S.; Arnold, P. L. *Chem. Soc. ReV.* **2007**, *36*, 1732. (b) Bourissou, D.; Guerret, O.; Gabbai, F. P.; Bertrand, G. *Chem. ReV.* **2000**, *100*, 39. (c) Hahn, F. E. *Angew. Chem., Int. Ed.* **2006**, *45*, 1348. (d) Cantat, T.; Mezailles, N.; Auffrant, A.; Le Floch, P. *Dalton Trans.* **2008**, 1957. (e) Hahn, F. E.; Jahnke, M. C. *Angew. Chem., Int. Ed.* **2008**, *47*, 3122 (f) Matthew N. Hopkinson, M. N.; Richter, C.; Schedler, M.;

Glorius, F. *Nature* **2004**, *510*, 485; (g) Hermann, W. A. *Angew. Chem., Int. Ed.* **2002**, *41*, 1290; (h) Flanigan, D. M.; Romanov-Michailidis, F.; White, N. A.; Rovis, T. *Chem. Rev.* **2015**, *115*, 9307.

5. (a) Neumann, W. P. *Chem. Rev.* **1991**, *91*, 311; (a) Tokitoh, N.; Okazaki, R. *Coord. Chem. Rev.* **2000**, *210*, 251; (b) Kira, M.; Ishida, S.; Iwamoto, T. *Chem. Rec*. **2004**, *4*, 243; (c) Asay, M.; Jones, C.; Driess, M. *Chem. Rev.* **2011**, *111*, 354; (d) Sen, S. S.; Khan, S.; Samuel, P. P.; Roesky, H. W. *Chem. Sci.* **2012**, *3*, 659; (e) Mizuhata, Y.; Sasamori, T.; Tokitoh, N. *Chem. Rev.*, **2009**, *109*, 3479; (f) Kira, M. *J. Org. Chem.* **2004**, *689*, 4475; (g) Nagendran, S.; Roesky, H. W. *Organometallics* **2008**, *27*, 457.
6. (a) Blom, B.; Gallego, D.; Driess, M. *Inorg. Chem. Front.* **2014**, *1*, 134; (b) Sen, S. S.; Khan, S.; Nagendran, S.; Roesky, H. W. *Acc. Chem. Res.* **2012**, *45*, 578; (c) Weidenbruch, M. *Chem. Rev.* **1995**, *95*, 1479; (d) Barrau, J.; Escudie, J.; Satge J. *Chem. Rev.*, **1990**, *90*, 283.
7. Drago, R. S. *J. Phys. Chem.* **1958**, *62*, 353.
8. (a) du Mont, W. W.; Gust, T.; Seppälä, E.; Wismach, C. *J. Organomet. Chem.* **2004**, *689*, 1331; (b) Gynane, M. J. S.; Harris, D. H.; Lappert, M. F.; Power, P. P.; Rivière, P.; Rivière-Baudet, M. *J. Chem. Soc., Dalton Trans.*, **1977**, 2004.
9. (a) Sasamori, T.; Tokitoh, N. *Encyclopedia of Inorganic Chemistry II, John Wiley & Sons: Chichester, U.K.*, **2005**; 1698; (b) Trinquier, G. *J. Am. Chem. Soc.* **1990**, *112*, 2130.
10. (a) Weidenbruch, M. *Organometallics* **2003**, *22*, 4348; (b) Weidenbruch, M. *J. Organomet. Chem*. **2002**, *646*, 39.
11. Skell, P. S.; Goldstein, E. J. *J. Am. Chem. Soc*. **1964**, *86*, 1442.
12. Drahnak, T. J.; Michl, J.; West, R. *J. Am. Chem. Soc.* **1979**, *101*, 5427.
13. Denk, M.; Lennon, R.; Hayashi, R.; West, R.; Belyakov, A. V.; Verne, H. P.; Haaland, A.; Wagner, M.; Metzler, N. *J. Am. Chem. Soc.* **1994**, *116*, 2691.
14. (a) Denk, M.; Green, J. C.; Metzler, N.; Wagner, M. *J. Chem. Soc., Dalton Trans.* **1994**, 2405; (b) Kong, L.; Zhang, J.; Song, H.; Cui, C. *Dalton Trans.* **2009**, 5444.
15. (a) Denk, M.; Lennon, R.; Hayashi, R.; West, R.; Belyakov, A. V.; Verne, H. P.; Haaland, A.; Wagner, M.; Metzler, N. *J. Am. Chem. Soc.* **1994**, *116*, 2691; (b) Li, W.; Hill, N. J.; Tomasik, A. C.; Bikzhanova, G.; West, R. *Organometallics* **2006**, *25*, 3802; (c) Tomasik, A. C.; Mitra, A.; West, R. *Organometallics* **2009**, *28*, 378.
16. (a) Gehrhus, B.; Lappert, M. F.; Heinicke, J.; Boese, R.; Blaeser, D. *J. Chem. Soc., Chem. Commun.* **1995**, 1931; (b) Heinicke, J.; Oprea, A.; Kindermann, M. K.; Karpati, T.;

Nyulaszi, L.; Veszpremi, T. *Chem. Eur. J.* **1998**, *4*, 541; (c) Gehrhus, B.; Hitchcock, P. B.; Lappert, M. F. *Z. Anorg. Allg. Chem.* **2005**, *631*, 1383.

17. Jutzi, P.; Kanne, K.; Krueger, C. *Angew. Chem. Int. Ed. Engl.* **1986**, *25*, 164.
18. Kira, M.; Ishida, S.; Iwamoto, T.; Kabuto, C. *J. Am. Chem. Soc.* **1999**, *121*, 9722.
19. (a) So, C.-W.; Roesky, H. W.; Magull, J.; Oswald, R. B. *Angew. Chem., Int. Ed.* **2006**, *45*, 3948; (b) Sen, S. S.; Roesky, H. W.; Stern, D.; Henn, J.; Stalke, D. *J. Am. Chem. Soc.* **2010**, *132*, 1123; (c) So, C.-W.; Roesky, H. W.; Gurubasavaraj, P. M.; Oswald, R. O.; Gamer, M. T.; Jones, P. G.; Blaurock, S. *J. Am. Chem. Soc.* **2007**, *129*, 12049; (d) Yeong, H.-X.; Lau, K.-C.; Xi, H.-W.; Lim, K. H.; So, C.-W. *Inorg. Chem.* **2010**, *49*, 371.
20. Driess, M.; Yao, S.; Brym, M.; van Wuellen, C.; Lentz, D. *J. Am. Chem. Soc.* **2006**, *128*, 9628.
21. (a) Xiong, Y.; Yao, S.; Driess, M. *Chem. Asian J.* **2009**, *4*, 1323; (b) Xiong, Y.; Yao, S.; Driess, M. *Dalton Trans.* **2009**, 421; (c) Kassaee, M. Z.; Zandi, H.; Momeni, M. R.; Shakib, R. A.; Ghambarian, M. *J. Mol. Struct. Theochem.* **2009**, *912*, 16.
22. (a) Ghadwal, R. S.; Roesky, H. W.; Merkel, S.; Henn J.; Stalke, D. *Angew. Chem., Int. Ed.* **2009**, *48*, 5683; (b) Filippou, A. C.; Chernov, O.; Schnakenburg, G. *Angew. Chem., Int. Ed.* **2009**, *48*, 5687; (c) Filippou, A. C.; Lebedev, Y. N.; Chernov, O.; Straßmann, M.; Schnakenburg, G. *Angew. Chem., Int. Ed.* **2013**, *52*, 6974.
23. (a) Protchenko, A. V.; Birjkumar, K. H.; Dange, D.; Schwarz, A. D.; Vidovic, D.; Jones, C.; Kaltsoyannis, N.; Mountford, P.; Aldridge, S. *J. Am. Chem. Soc.*, **2012**, *134*, 6500; (b) Rekken, B. D.; Brown, T. M.; Fettinger, J. C.; Tuononen H. M.; Power, P. P. *J. Am. Chem. Soc.* **2012**, *134*, 6504; (c) Protchenko, A. V.; Schwarz, A. D.; Blake, M. P.; Jones, C.; Kaltsoyannis, N.; Mountford, P.; Aldridge, S. *Angew. Chem., Int. Ed.* **2013**, *52*, 568; (d) Rekken, B. D.; Brown, T. M.; Lips, J. C. F. F.; Tuononen, H. M.; Herber, R. H.; Power, P. P. *J. Am. Chem. Soc.* **2013**, *135*, 10134.
24. Davidson, P. J.; Harris, D. H.; Lappert, M. F. *J. Chem. Soc., Dalton Trans.* **1977**, 2268.
25. Jutzi, P.; Becker, A.; Stammler, H. G.; Neumann, B. *Organometallics* **1991**, *10*, 1647.
26. (a) Bender IV, J.; Holl, M. M. B.; Kamp, J. W. *Organometallics* **1997**, *16*, 2743; (b) Jutzi, P.; Schmidt, H.; Neumann, B.; Stammler, H. G.; *Organometallics*, **1996**, *15*, 741; (c) Simons, R. S.; Pu, L.; Olmstead, M. M.; Power, P. P. *Organometallics* **1997**, *16*, 1920.
27. (a) Tokitoh, N.; Manmaru, K.; Okazaki R. *Organometallics* **1994**, *13*, 167 (b) Tokitoh, N.; Matsumoto, T.; Manmaru, Okazaki, R.; *J. Am. Chem. Soc.* **1993**, *115* 8855; (c) Tokitoh, N.; Kishikawa, K.; Matsumoto, T.; Okazaki, R. *Chem. Lett.*, **1995**, 827.

28. Kira, M.; Ishida, S.; Iwamoto, T.; Ichinohe, M.; Kabuto, C.; Ignatovich, L.; Sakurai, H. *Chem. Lett.* **1999**, 263.
29. (a) Pfeiffer, J.; Noltemeyer, M.; Meller, A. *Z. Anorg. Allg. Chem.* **1989**, 145; (b) Heinicke, J.; Operea, A. *Heteroat. Chem.* **1998**, *9*, 439; (c) Baker, R. J.; Jones, C.; Mills, D. P.; Pierce, G. A.; Waugh, M. *Inorg. Chim. Acta* **2008**, *361*, 427; (d) Herrmann, W. A.; Denk, M.; Behm, J.; Scherer, W.; Klingan, F.-R.; Bock, H.; Solouki, B.; Wagner, M. *Angew. Chem., Int. Ed. Engl.* **1992**, *31*, 1485; (e) Kuehl, O.; Loennecke, P.; Heinicke, J. *Polyhedron* **2001**, *20*, 2215; (f) Tomasik, A. C.; Hill, N. J.; West, R. *J. Organomet. Chem*. **2009**, 694, 2122.
30. Ding, Y.; Roesky, H. W.; Noltemeyer, M.; Schmidt, H.-G. *Organometallics* **2001**, *20*, 1190; (b) Ding, Y.; Hao, H.; Roesky, H. W.; Noltemeyer, M.; Schmidt, H.-G. *Organometallics* **2001**, *20*, 4806; (c) Akkari, A.; Byrne, J. J.; Saur, I.; Rima, G.; Gornitzka, H.; Barrau, J. *J. Organomet. Chem.* **2001**, *622*, 190; (d) Ayers, A. E.; Klapoetke, T. M.; Dias, H. V. R. *Inorg. Chem.* **2001**, *40*, 1000; (e) Arii, H.; Nakadate, F.; Mochida, K. *Organometallics,* **2009**, *28*, 4909; (f) Yang, Z.; Ma, X.; Roesky, H. W.; Yang, Y.; Zhu, H.; Magull, J.; Ringe, A. *Z. Anorg. Allg. Chem.* **2008**, *634*, 1490; (g) Mcheik, A.; Katir, N.; Castel, A.; Gornitzka, H.; Massou, S.; Riviere, P.; Hamieh, T. *Eur. J. Inorg. Chem.* **2008**, 5397;
31. (a) Driess, M.; Yao, S.; Brym, M.; van Wuellen, C. *Angew. Chem., Int. Ed.* **2006**, *45*, 4349.
32. (a) Jones, C.; Rose, R. P.; Stasch, A. *Dalton Trans.* **2008**, 2871; (b) Foley, S. R.; Bensimon, C.; Richeson, D. S. *J. Am. Chem. Soc.* **1997**, *119*, 10359; (c) Foley, S. R.; Zhou, Y.; Yap, G. P. A.; Richeson, D. S. *Inorg. Chem.* **2000**, *39*, 924; (d) Nagendran, S.; Sen, S. S.; Roesky, H. W.; Koley, D.; Grubmüller, H.; Pal, A.; Herbst-Irmer, R. *Organometallics* **2008**, *27*, 5459.
33. (a) Veith, M. *Angew. Chem., Int. Ed. Engl.* **1987**, *26*, 1; (b) Veith, M.; Werle, E.; Lisowsky, R.; Koppe, R.; Schnockel, H. *Chem. Ber.* **1992**, *125*, 1375.
34. Dias, H. V. R.; Wang, Z. *J. Am. Chem. Soc.* **1997**, *119*, 4650.
35. (a) Hadlington, T. J.; Li, J.; Jones, C. *Can. J. Chem.* **2014**, 92, 427; (b) Li, J.; Stasch, A.; Schenk, C.; Jones, C. *Dalton Trans.* **2011**, *40,* 10448; (c) Pu, L.; Olmstead, M. M.; Power, P. P.; Schiemenz, B.; *Organometallics* **1998**, *17*, 5602;
36. (a)Goldberg, D. E.; Harris, D. H.; Lappert, M. F.; Thomas, K. M.; *J. Chem. Soc. Chem. Commun.* **1976**, 261. (b) Cotton, J.D.; Davidson, P. J.; Lappert, M. F. *J. Chem. Soc. Dalton Trans.* **1976**, 2275.

37. (a) Hitchcock, P. B.; Lappert, M. F.; Samways, B. J.; Weinberg, E. L. *J. Chem. Soc. Chem. Commun.* **1983**,1492; (b) Fjeldberg, T.; Hope, H.; Lappert, M. F.; Power, P. P.; Thorne, A. J.; *J. Chem. Soc. Chem. Commun.* **1983**, 639.
38. Kira, M.; Yauchibara, R.; Hirano, R.; Kabuto, C.; Sakurai, H.; *J. Am. Chem. Soc.* **1991**, *113*, 7785.
39. Engelhardt, L. M.; Jolly, B. S.; Lappert, M. F.; Raston, C. L.; White, A. H.; *J. Chem. Soc. Chem. Commun.* **1988**, 336.
40. Weidenbruch, M.; Schlaefke, J.; Schäfer, A.; Peters, K.; Schnering, H. G. V.; Marsmann, H.; *Angew. Chem. Int. Ed. Engl.* **1994**, *33,* 1846.
41. (a) Lay, U.; Pritzkow, H.; Grützmacher, H. *J. Chem. Soc., Chem. Commun.* **1992**, 260; (b) Tokitoh, N.; Saito, M.; Okazaki, R. *J. Am. Chem. Soc.* **1993**, *115*, 2065.
42. Gans-Eichler, T.; Gudat, D.; Nieger, M. *Angew. Chem. Int. Ed.*, **2002**, *41*, 1888.
43. Mansell, S. M.; Russell, C. A.; Wass, D. F. *Inorg. Chem.* **2008**, *47*, 11367.
44. Hahn, F. E.; Wittenbecher, L.; Van, D. L.; Zabula, A. V. *Inorg. Chem.* **2007**, *46*, 7662.
45. (a) Nimitsiriwat, N.; Gibson, V. C.; Marshall, E. L.; White, A. J. P.; Dale, S. H.; Elsegood, M. R. J. *Dalton Trans.* **2007**, 4464; (b) Foley, S. R.; Yap, G. P. A.; Richeson, D. S. *Organometallics* **1999**, *18*, 4700.
46. (a) Aubrecht, K. B.; Hillmyer, M. A.; Tolman, W. B. *Macromolecules,* **2002**, *35*, 644; (b) Sen, S. S.; Kritzler-Kosch, M. P.; Nagendran, S.; Roesky, H. W.; Beck, T.; Pal, A.; Herbst-Irmer, R. *Eur. J. Inorg. Chem*. **2010**, 5304.
47. (a) Dove, A. P.; Gibson, V. C.; Marshall, E. L.; Rzepa, H. S.; White, A. J. P.; Williams, D. J. *J. Am. Chem. Soc.* **2006**, *128*, 9834; (b) Jana, A.; Roesky, H. W.; Schulzke, C.; Doering, A.; Beck, T.; Pal, A.; Herbst-Irmer, R. *Inorg. Chem.* **2009**, *48*, 193.
48. Leeper, R. W.; Summers, L.; Gilman, H. *Chem. Rev.* **1954**, *54*, 101.
49. Harris, D. H.; Lappert, M. F. *J. Chem. Soc. Chem. Commun.* **1974**, 895.
50. Kano, N.; Tokitoh, N.; Okazaki, R. *Organometallics* **1997**, *16*, 4237.
51. (a) Brooker, S.; Buijink, J.-K.; Edelmann, F. T. *Organometallics*, **1991**, *10*, 25; (b) Stü rmann, M.; Weidenbruch, M.; Klinkhammer, K. W.; Lissner, F.; Marsmann, H. *Organometallics* **1998**, *17*, 4425; (c) Hino, S.; Olmstead, M.; Phillips, A. D.; Wright, R. J.; Power, P. P. *Inorg. Chem.* **2004**, *43*, 7346; (d) Stasch, A.; Forsyth, C. M.; Jones, C.; Junk, P. C. *New. J. Chem.* **2008**, *32*, 829; (e) Fulton, J. R.; Hitchcock, P. B.; Johnstone, N. C.; Tam, E. C. Y. *Dalton Trans.* **2007**, 3360; (f) Chen, M.; Fulton, J. R.; Hitchcock, P. B.; Johnstone, N. C.; Lappert, M. F.; Protchenko, A. V. *Dalton Trans.* **2007**, 2770; (g) Jana,

A.; Sarish, S. P.; Roesky, H. W.; Schulzke, C.; Doering, A.; John, M. *Organometallics* **2009**, *28*, 2563; (h) Yao, S.; Block, S.; Brym, M.; Driess, M. *Chem. Commun.* **2007**, 3844.

52. Power, P. P. *Nature*, **2010**, 463, 171.
53. (a) Xiong, Y.; Yao, S.; Mueller, R.; Kaupp, M.; Driess, M. *Nat. Chem.* **2010**, *2*, 577; (b)
54. (a) Takeda, N.; Tokitoh, N.; Okazaki, R. *Chem. Lett.* **2000**, *29*, 622; (b) Bobbitt, K. L.; Gaspar, P. P. *J. Organomet. Chem.* **1995**, *499*, 17.
55. (a) Sen, S. S.; Jana, A.; Roesky, H. W.; Schulzke, C. *Angew. Chem., Int. Ed.* **2009**, *48*, 8536; (b) Sen, S. S.; Roesky, H. W.; Meindl, K.; Stern, D.; Henn, J.; Stückl, A. C.; Stalke, D. *Chem. Commun.* **2010**, *46*, 5873.
56. Yao, S. L.; van Wullen, C.; Sun, X. Y.; Driess, M. *Angew. Chem., Int. Ed.* **2008**, *47*, 3250.
57. Yao, S.; Wüllen, C. v.; Driess, M. Chem. Commun. **2008**, 5393.
58. Protchenko, A. V.; Blake, M. P.; Schwarz, A. D.; Jones, C.; Mountford, P.; Aldridge S. *Organometallics* **2015**, *34*, 2126.
59. (a) Kajiwara, T.; Takeda, N.; Sasamori, T.; Tokitoh, N. *Organometallics* **2004**, *23*, 4723; (b) Moser, D. F.; Bosse, T.; Olson, J.; Moser, J. L.; Guzei, I. A.; West, R. *J. Am. Chem. Soc.* **2002**, *124*, 4186.; (c) Gehrhus, B.; Hitchcock, P. B.; Lappert, M. F.; Heinicke, J.; Boese, R.; Blaeser, D. *J. Organomet. Chem.* **1996**, *521*, 211; (d) Yao, S. L.; Xiong, Y.; Brym, M.; Driess, M. *Chem. Asian J.* **2008**, *3*, 113; (e) Kajiwara, T.; Takeda, N.; Sasamori, T.; Tokitoh, N. *Chem. Commun.* **2004**, 2218.
60. Haaf, M.; Schmiedl, A.; Schmedake, T. A.; Powell, D. R.; Millevolte, A. J.; Denk, M.; West, R. *J. Am. Chem. Soc.,* **1998**, *120*, 12714.
61. Yao, S. L.; Brym, M.; Van Wullen, C.; Driess, M. *Angew. Chem., Int. Ed.* **2007**, *46*, 4159.
62. (a) Xiong, Y.; Yao, S.; Driess, M. *J. Am. Chem. Soc.,* **2009**, *131*, 7562; (b) Yao, S.; Xiong, Y.; Driess, M. *Chem. Eur. J.* **2010**, *16*, 1281.
63. (a) Scheer, M.; Balázs, G.; Seitz, A. *Chem. Rev.* **2010**, *110*, 4236; (b) Sen, S. S.; Khan, S.; Roesky, H. W.; Kratzert, D.; Meindl, K.; Henn, J.; Stalke, D.; Demers, J.-P.; Lange, A. *Angew. Chem., Int. Ed.* **2011**, *50*, 2322.
64. Xiong, Y.; Yao, S.; Brym, M.; Driess, M. *Angew. Chem. Int. Ed.,* **2007**, *46*, 4511.
65. Jana, A.; Objartel, I.; Roesky, H. W.; Stalke, D. *Inorg. Chem.* **2009**, *48*, 798.
66. (a) Peng, Y.; Ellis, B. D.; Wang, X.; Power, P. P. *J. Am. Chem. Soc.*, **2008**, *130*, 12268; (b) Peng, Y.; Guo, J.-D.; Ellis, B. D.; Zhu, Z.; Fettinger, J. C.; Nagase, S.; Power, P. P. J. Am. Chem. Soc. **2009**, *131*, 16272; (c) Inomata, K.; Watanabe, T.; Miyazaki, Y.; Tobita, H. *J. Am. Chem. Soc.* **2015**, *137*, 11935.

67. (a) Crabtree, R. H. *The Organometallic Chemistry of the Transition Metals; John Wiley & Sons: New York*, **2009**; (b) Beller, M.; Bolm, C. *Transition Metals for Organic Syntheses, Wiley*, **2004**; (c) Crawley M. L.;Trost, B. M. *Applications of Transition Metal Catalysis in Drug Discovery and Development, Wiley*, **2012**.
68. (a) Kamer, P. C. J.; Leeuwen, P. W. N. M. V. *Phosphorus(III) ligands in homogeneous catalysis: Design and synthesis, Wiley*, **2012**; (b) Pignolet, L. M. *Homogeneous Catalysis with Metal Phosphine Complexes, Springer*, **2013**.
69. (a) Benedek, Z.; Szilvási, T. *RSC Adv.,* **2015**, *5*, 5077; (b) Brück, A.; Gallego, D.; Wang, W.; Irran, E.; Driess, M.; Hartwig, J. F. *Angew. Chem., Int. Ed.* **2012**, *51*, 11478.
70. B. Blom, M. Stoelzel, M. Driess, *Chem. Eur. J.* **2013**, *19*, 40.
71. Schmid G.; Welz, E. *Angew. Chem., Int. Ed. Engl.* **1977**, *16*, 785.
72. Raoufmoghaddam, S.; Zhou, Y.-P.; Wang, Y.; Driess, M. *J. Organomet. Chem.* **2017**, *829*, 2.
73. (a) Fürstner, A.; Krause, H.; Lehmann, C. W. *Chem. Commun.* **2001**, 2372; (b) Zhang, M.; Liu, X.; Shi, C.; Ren, C.; Ding, Y.; Roesky, H. W. *Z. Anorg. Allg. Chem.* **2008**, *634*, 1755; (c) Gallego, D.; Brück, A.; Irran, E.; Meier, F.; Kaupp, M.; Driess, M.; Hartwig, J. F. *J. Am. Chem. Soc.* **2013**, *135*, 15617.
74. (a) Zhang , L.; Hou, Z. *Pure Appl. Chem.*, **2012**, *84*, 1705; (b) Valente, C.; Calimsiz, S.; Hoi, K. H.; Mallik, D.; Sayah M.; Organ, M. G. *Angew. Chem., Int. Ed.* **2012**, *51*, 3314; (c) Marion N.; Nolan, S. P. *Chem. Soc. Rev.* **2008**, *37*, 1776; (d) Velazquez, H. D.; Verpoort, F. *Chem. Soc. Rev.*, **2012**, *41*, 7032.
75. (a) Blom, B.; Enthaler, S.; Inoue, S.; Irran, E.; Driess, M. *J. Am. Chem. Soc.* **2013**, *135*, 6703; (b) Metsänen, T. T.; Gallego, D.; Szilvási, T.; Driess, M.; Oestreich, M. *Chem. Sci.* **2015**, *6*, 7143; (c) Gallego, D.; Inoue, S.; Blom, B.; Driess, M. *Organometallics* **2014**, *33*, 6885.
76. Zhou, Y.-P.; Raoufmoghaddam S.; Szilvási, T.; Driess, M. *Angew. Chem. Int. Ed.* **2016**, *55*, 12868.
77. Wang, W.; Inoue, S.; Enthaler, S.; Driess, M. *Angew. Chem. Int. Ed.* **2012**, *51*, 6167.
78. (a) Hadlington, T. J.; Hermann, M.; Frenking, G.; Jones, *J. Am. Chem. Soc.* **2014**, *136*, 3028; (b) Wu, Y.; Shan, C.; Sun, Y.; Chen, P.; Ying, J.; Zhu, J.; Liu, L.; Zhao, Y. *Chem. Commun.*, **2016**, *52*, 13799; (c) Schneider, J.; Sindlinger, C. P.; Freitag, S. M.; Schubert, H.; Wesemann, L. *Angew. Chem. Int. Ed.* **2017**, *56*, 333.

CHAPTER 2

Amidinato-Phosphinoamido-Silylene, its Gold(I) Complexes and Comparison with Higher Congeners

2.1 Introduction

The propensity of silylene to donate the lone pair of electron to a transition metal fragment led to the isolation of a range of silylene-transition metal complexes *i. e.* complexes with Fe, Ni, Co, Rh Ir *etc.*.[1] In contrast, the silylene-gold complex is highly unprecedented.

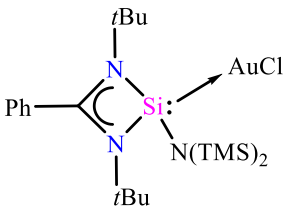

60

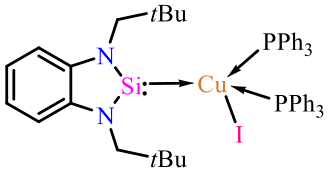

61

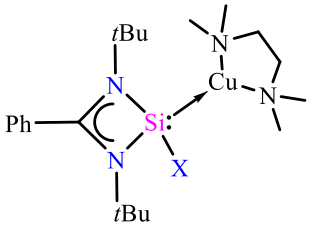

62a X = Cl
62b X = O*t*Bu
62c X = NMe_2

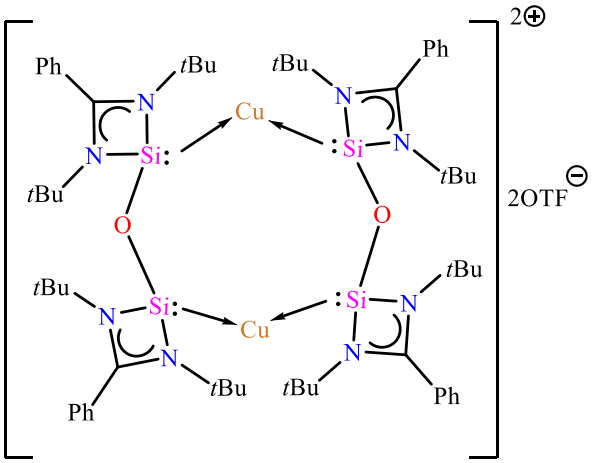

63

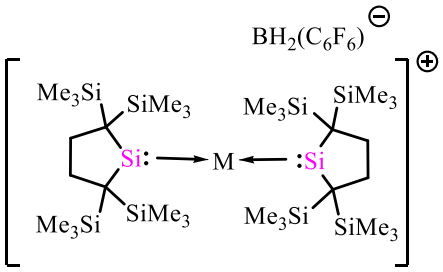

64a M = Cu
64b M = Ag

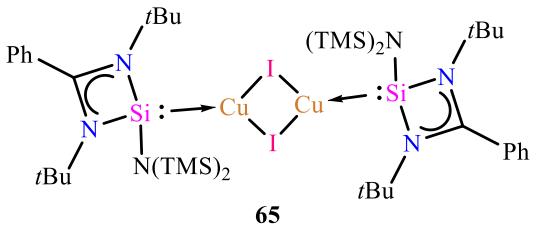

65

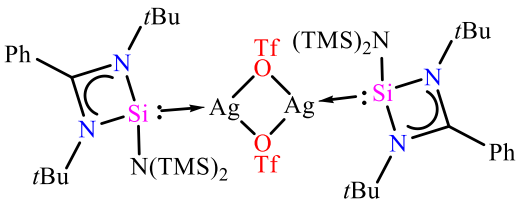

66

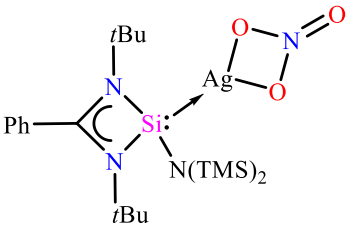

67

Chart 2.1 *Selected examples of Silylene-Coinage metal Complexes*

Although Frenking had predicted that the gold would form stronger bond with silylene as compared to copper and silver,[2] there was no report on silylene –gold complex until we isolated benz-amidinato stabilized silylene gold complex [{PhC(N*t*Bu)$_2$}Si{N(SiMe$_3$)$_2$}]AuCl (**60**) in 2016 (*Chart 2.1)*.[3] However, the quest for the silylene-complex having aurophilic interaction was remained un-answered. Moreover, there are few reports available on silylene complexes of copper and silver. In 2003, Lappert et al. reported copper complex of diaminosilyene (**61**).[4] Recently, Dries et al. isolated the cationic Silylene-Copper complex, **62-63**, which are supported through functionalized silylenes *i. e.* oxo-bridged amidinato-bisslilylene, chloro-amidinatosilylene, *etc.*[5] The alkylsilylenes of Kira is also used to isolate Cu and Ag complexes of silylenes (**64a-64b**).[6] Recently, We have also isolated the copper and silver complexes of amidinato-silylene (**65**– **67**). In this chapter, we isolated the silylene-Au(I) complex (**2.4**) having aurophilic interaction and detailed study of their structure, bonding and nucleophilicity were performed experimentally and theoretically. Further, we synthesized the heavier congeners of silylene (**2.2**) and tried to isolate their gold complexes but unlike, silylene (**2.2**), germylene (**2.7**) and stannylene (**2.8**) do not show any propensity towards coordinating to gold chloride.

2.2 Experimental section

2.2.1 General remarks

All manipulations were carried out in an inert gas atmosphere of dinitrogen using standard Schlenk techniques and in a dinitrogen filled glove box. The solvents used were purified by MBRAUN solvent purification system MB SPS-800. Compound **2.1**, [7a] **2.5**,[7b] **2.6**,[7c] and LiN(PPh$_2$)(2,6-*i*Pr$_2$C$_6$H$_3$)$_2$[7d] were prepared by literature methods. All chemicals purchased from Aldrich were used without further purification. ^{1}H, ^{13}C, ^{31}P, and ^{29}Si NMR spectra were recorded in C$_6$D$_6$, and CD$_2$Cl$_2$ using Bruker 400 MHz spectrometer. NMR spectra were referenced to external SiMe$_4$ (^{1}H, ^{13}C, and ^{29}Si) and 85% H$_3$PO$_4$ (^{31}P). Mass spectra were recorded using AB Sciex, 4800 plus MALDI TOF/TOF.

2.2.2 Synthesis

2.2.2.1 Synthesis of **2.2**

Toluene (30 mL) was added to the mixture of chlorosilylene **2.1** (0.295 g, 1mmol) and LiN(PPh$_2$)(2,6-*i*Pr$_2$C$_6$H$_3$) (0.367 g, 1mmol) at room temperature and stirred for overnight.

The resulting solution was filtered off and solvent was removed to yield pale yellow solid. Single crystals suitable for X-ray analysis were grown in toluene at -30 ˚C. M. P.: 121-123˚C. Yield: 80% (0.486 g). ^{1}H NMR (C_6D_6, 400 MHz, TMS): δ 0.43 (d, 6H, $(CH_3)_2CH$, J = 6.7 Hz), 1.32 (d, 6H, $(CH_3)_2CH$, J = 6.7 Hz), 1.44 (s, 18H, $(CH_3)_3N$), 3.57-3.63 (sept, 2H, $(CH3)_2CH$), 6.88-7.57 (m, 18H, Ph) ppm; ^{13}C NMR (C_6D_6, 100.61 MHz): δ 22.58, 27.44, 28.6, 32.31, 53.81, 124.53, 126.92, 132.04, 135.08, 135.32, 141.38, 144.06, 144.17, 148.72, 166.54 ppm ; ^{31}P NMR (C_6D_6, 161.97 MHz) : δ 54.09 (s) ppm ; ^{29}Si NMR (C_6D_6, 79.49 MHz): δ 10.72 ppm (d, $^{2}J_{Si-P}$ = 10.6 Hz). Elemental analysis ($C_{39}H_{50}N_3PSi$): calculated C, 75.44; H, 8.28; N, 6.77; obtained C, 74.89; H, 7.97; N, 6.54.

2.2.2.2 Synthesis of **2.3**

20 mL of toluene was added to the flask containing mixture of **2.2** (0.620 g, 1mmol) and $AuCl{\cdot}SMe_2$ (0.3 g, 1 mmol). It was left for stirring overnight at ambient temperature. The solvent was removed under vacuum to afford **2.3** as colorless solid. Single crystals suitable for X-ray analysis were grown from the CH_2Cl_2/n-pentane mixture (1:1). Yield 78% (0.664 g); M. P.: 128-130 ˚C (decomposition). ^{1}H NMR (CD_2Cl_2, 400 MHz, TMS): δ 0.91- 1.36 (m, 12H, $(CH_3)_2CH$), 1.53 (s, 18H, $(CH_3)_2C$), 3.07-3.10 (m, 2H, $(CH_3)_2CH$), 7.07 (d, 2H, Ph, J = 7.6 Hz), 7.22-7.32 (m, 9H, Ph), 7.38 (t, 2H, Ph, J = 7.1 Hz), 7.55-7.66 (m, 5H, Ph) ppm; ^{13}C NMR (CD_2Cl_2, 100.61 MHz): δ 21.48, 28.29, 28.77, 34.44, 56.13, 126.98, 127.65, 128.41, 128.48, 130.33, 131.63, 135.72, 137.21, 148.32, 178.28 ppm; ^{31}P{H}NMR (CD_2Cl_2, 161.97 MHz) : δ 55.69 (s) ppm; ^{29}Si NMR (CD_2Cl_2, 79.49 MHz): δ 24.87 (d, $^{2}J_{Si-P}$ = 20.90 Hz) ppm: Elemental analysis ($C_{39}H_{50}AuClN_3PSi$) (dried overnight to remove the solvent): calculated C, 54.96; H, 5.91; N, 4.93; obtained C, 54.64; H, 5.23; N, 4.35. MS (Positive ESI) m/z for $C_{39}H_{50}N_3PSi$ (851.2866): 815.32 $[M\text{-}Cl]^+$ (10%), 632.43 $[M\text{-}(Cl+PPh_2)]^+$ (30%).

2.2.2.3 Synthesis of **2.4**

25 mL of DCM was added to the flask containing **2.3** (0.430 g, 0.5 mmol) and $AgSbF_6$ (0.172 g, 0.5 mmol), and stirred overnight under the dark. The solution was filtered through a pad of celite and concentrated to dryness to afford **2.4** as a beige solid. Single crystals suitable for X-ray analysis were grown in CH_2Cl_2/*n*-pentane (1:1) mixture. Yield: 62% (0.331 g). M. P.: ~140 ˚C. ^{1}H NMR (CD_2Cl_2, 400 MHz, TMS): δ 0.98 (s, 36H, $(CH_3)_3C$), 1.62-1.66 (m, 24H, $(CH_3)_2CH$), 3.48-3.55 (m, 4H, $(CH_3)_2CH$), 7.28-7.85 (m, 36H, Ph) ; ^{13}C

NMR (CD_2Cl_2, 100.61 MHz): δ 24.66, 27.68, 32.08, 48.40, 57.19, 126.91, 128.03, 128.73, 129.74, 129.86, 132.56, 133.20, 133.60, 134.68, 139.44, 146.59 ppm; $^{31}P\{H\}$NMR (CD_2Cl_2, 161.97 MHz) : δ 97.10 (s) ppm ; ^{29}Si NMR (CD_2Cl_2, 79.49 MHz): δ 78.04-78.36 (m) ppm; ^{19}F NMR (CD_2Cl_2, 376.49 MHz) δ **:** -192.66 to -161.96 (br) ppm ; MS (Positive ESI) for $[C_{78}H100Au_2N_6P_2Si_2]^{2+}$ (1632.6354): m/z = 815.41.

2.2.2.4 Synthesis of **2.7**

40 mL toluene was added to the mixture of 1.023 g (3 mmol) of **2.5** and 1.1001 g (3 mmol) of lithium salt of ligand ($LiN(PPh_2)(2,6\text{-}iPr_2C_6H_3)_2$) and stirred overnight at room temperature. A precipitate was formed and filtered off. The solvent was partially removed in vaccuo. Storage of the remaining solution at room temperature afforded colorless crystals of **2.7** (73.8%) (1.5 g); M.p. 78-81°C. ^1H NMR (400 MHz, $CDCl_3$, 298K): δ 1.07 (d, J = 6.8 Hz, 12H, CH*Me*$_2$), 1.18 (s, 18H, C*Me*$_3$), 2.97-3.04 (m, 2H, C*H*Me$_2$), 7.02-7.14 (m, 3H, Ph), 7.19-7.33 (m, 4H, Ph), 7.35-7.46 (m, 6H, Ph), 7.49-7.76 (m, 5H, Ph) ppm; ^{13}C $\{^1H\}$ NMR (100.613 MHz, $CDCl_3$, 298K): δ 23.76, 28.42, 28.83, 32.34, 53.59, 123.67, 124.10, 126.74, 128.68, 131.29, 131.49, 134.97, 135.22, 142.53, 148.75, 171.60 ppm. $^{31}P\{^1H\}$ NMR (161.976 MHz, $CDCl_3$, 298K): δ 54.91 ppm. MALDI-MS: m/z ($C_{40}H_{53}N_3PGe$): 685.44 $[M+Na]^+$.

2.2.2.5 Synthesis of **2.8**

40 mL toluene was added to a mixture of 0.772 g (2 mmol) of **2.6** and 0.734 g (2 mmol) of lithium salt of ligand ($LiN(PPh_2)(2,6\text{-}iPr_2C_6H_3)_2$) and stirred overnight at room temperature. The light yellow colored solution was filtered using frit and volume was reduced to 10 mL. Pale yellow colored crystals of **2.8** were obtained immediately. Yield: 72.41% (1.05 g); M.p. 82-86°C. ^1H NMR (400 MHz, $CDCl_3$, 298K): δ 1.07 (d, J = 6.8 Hz, 12H, CH*Me*$_2$), 1.20 (s, 18H, C*Me*$_3$), 2.98-3.04 (m, 2H, C*H*Me$_2$), 7.01-7.11 (m, 3H, *Ph*), 7.23-7.33 (m, 5H, *Ph*), 7.38-7.44 (m, 6H, *Ph*), 7.52-7.57 (m, 4H, *Ph*) ppm. ^{13}C $\{^1H\}$ NMR (100.613 MHz, $CDCl_3$, 298K): δ 23.78, 28.04, 30.60, 31.776, 50.67, 123.48, 127.63, 127.74, 128.16, 28.35, 128.41, 128.86, 129.01, 131.26, 131.46, 142.63 ppm. $^{31}P\{^1H\}$ NMR (161.976 MHz, $CDCl_3$, 298K): 56.15 ppm. $^{119}Sn\{^1H\}$ NMR (111.92 Hz, $CDCl_3$, 298K): δ -122.70 ppm. MALDI-MS: *m/z* ($C_{40}H_{53}N_3PSn$): 523.25 $[M\text{-}PPh_2]^+$.

2.3 X-ray crystallography

Crystallography Reflections were collected on a Bruker Smart Apex Duo diffractometer at 100 K using Mo Kα radiation (λ = 0.710 73 Å) for **2.2**, **2.3**, **2.4**, **2.7** and **2.8**. All the structures were solved by direct methods and refined by full-matrix least-squares methods against F^2 (SHELXL-2014/6).[8] Crystallographic data for **2.2**, **2.3**, **2.4**, **2.7** and **2.8** are given in Appendix 2, Table 2A.1 and Table 2A.2, respectively. CCDC CIF Nos **2.2**-**2.7**. 1437075 (**2.2**), 1437076 (**2.3**), 1437077 (**2.4**), 1447731 (**2.7**) and 1447732 (**2.8**).

2.4 Computational methodology

All the geometry optimizations were performed with Gaussian 09 program[9] using BP86[10]/def2-SVP basis set.[11] Meta-GGA exchange correlation functional M06[12] with def2-TZVPP basis set[11] was used for the single point calculations on the optimized geometries and the energies were corrected by adding the zero point energies from the BP86/def2-SVP level of theory. Natural Bond Order (NBO)[13] analysis and the quantitative analysis of electrostatic potential (ESP) on the van der Waals surface of molecules using Multiwfn program[14] were done at the same level of theory. Quantum theory of atoms in molecules (QTAIM)[15] method implemented in AIMALL program package[16] was used for the topological analysis of electron density. Wave function for this analysis was generated at M06/def2-TZVPP//BP86/def2-SVP level of theory using Gaussian 09 program.

The nature of Si–Au bond was studied using EDA-NOCV method at the BP86/TZ2P level of theory using ADF 2013.01 program.[17] Scalar relativistic effects were incorporated using Zeroth Order Regular Approximation (ZORA).[18] The core electrons were treated by the frozen-core approximations. Energy Decomposition Analysis (EDA)[19] gives the instantaneous interaction energy (ΔE_{int}) between two fragents in the frozen geometry of the compound. The interaction energy can be divided into three parts:

$$\Delta E_{int} = \Delta E_{elstat} + \Delta E_{Pauli} + \Delta E_{orb}$$

ΔE_{elstat} gives the electrostatic interaction energy between the frozen charge densities of the two fragents. ΔE_{Pauli} is the result of repulsive interaction between two fragents, which are caused by the electrons of same spin. ΔE_{orb} is the lowering in energy due to the overlap of orbitals of the two fragents. Sum of ΔE_{int} and ΔE_{prep} (energy necessary to promote the

fragents from their ground state geometry to the geometry in the compound) gives –De (dissociation energy).

$-De = \Delta E_{int} + \Delta E_{prep}$

In the EDA-NOCV analysis method, ΔE_{orb} term is decomposed into the contributions from different natural orbitals of chemical valence (NOCV).[20] It provides the energy contributions for each specific orbital interaction between fragments to the total bond energy.

2.5 Results and discussion

2.5.1 Synthesis and characterization of compounds **2.2**, **2.3** and **2.4**

We first prepared a tailored Si(II) compound $(PhC(NtBu)_2SiN(PPh_2)(2,6\text{-}iPr_2\text{-}C_6H_3))$ (**2.2**) and then reacted the latter with $AuCl{\cdot}SMe_2$ to form a Si(II)-Au(I) complex, $[(PhC(NtBu)_2SiN(PPh_2)(2,6\text{-}iPr_2\text{-}C_6H_3))AuCl]$ (**2.3**). Subsequent dehalogenation from **2.3** led to the first Si(II) supported Au(I) cation $[PhC(NtBu)_2Si(2,6\text{-}iPr_2C_6H_3NPPh_2)(Au)]_2[SbF_6]_2$ (**2.4**), which exhibits aurophilic interaction. The functionalized silylene **2.2** was synthesized in 80% yield by reacting the chlorosilylene $[\{PhC(NtBu)_2\}SiCl]$ (**2.1**)[7a] with $[(2,6\text{-}iPr_2C_6H_3NPPh_2)Li]$ (*Scheme 2.1*). The main feature of **2.2** is the presence of two donor sites,

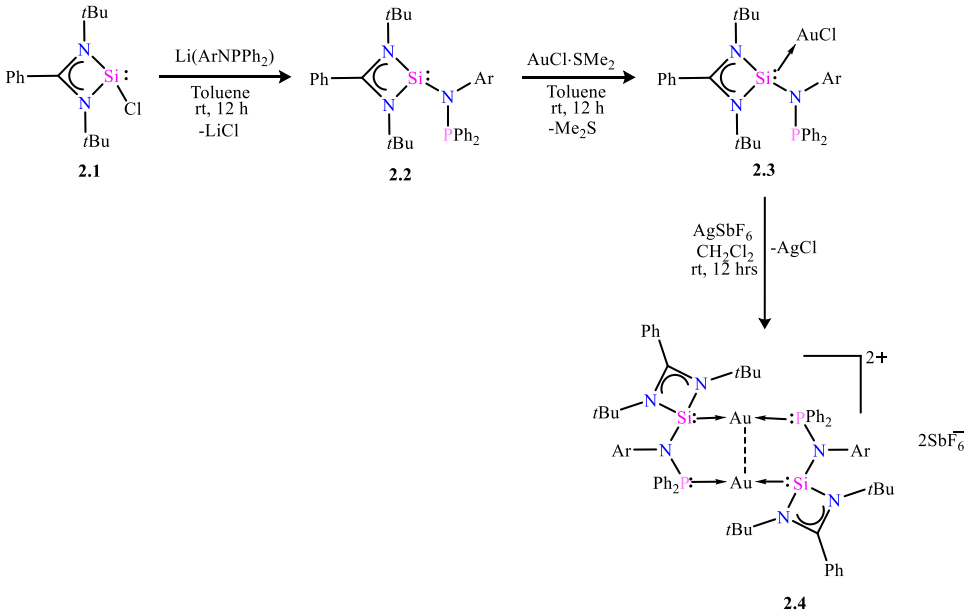

Scheme 2.1 *Syntheses of compounds* ***2.2-2.4****.*

Si and P respectively. The ^{29}Si NMR spectrum of exhibits one doublet at δ 10.72 ppm ($^{2}J_{Si-P}$ = 10.6 Hz) (*Appendix 2, Figure 2A.1*) which is slightly upfield shifted as compared to the parent compound **2.1** (δ 14.6 ppm) but downfield with respect to the previously reported Si(II) amides, [{PhC(N*t*Bu)$_2$}SiNMe$_2$] (δ –2.62 ppm)[21] and [{PhC(N*t*Bu)$_2$}SiN(SiMe$_3$)$_2$] (δ –8.07 ppm).[22] The X-ray structure analysis of **2.2** shows that the Si(II) center in **2.2** is tricoordinated (*Figure. 2.1*) and exhibits a pyramidal geometry with the sum of the bond angles around Si1 atom of 277.9°. The geometry is consistent with the presence of a lone pair of electrons at the Si(II) atom. The Si1-N3 bond distance (1.796(2) Å) is in good agreement with the Si-N bond lengths in the previously reported Si(II) amide, [{PhC(N*t*Bu)$_2$}SiNMe$_2$] (1.724(2) Å) and [{PhC(N*t*Bu)$_2$}SiN(SiMe$_3$)$_2$] (1.769 (7) Å).

The reaction of **2.2** with AuCl·SMe$_2$ exclusively afforded 1:1 complex, **2.3**, where the Si(II) atom is coordinated to the Au(I) center but P(III) atom remains uncoordinated. This is indicated by the downfield shift in the ^{29}Si NMR spectrum of **2.3** (δ 24.87) in comparison to that of **2.2**. The formulation of **2.3** was further confirmed by single crystal diffraction study (*Figure 2.1*). The Si1-Au1 bond distance in **2.3** is 2.246(2) Å, which is very close to the Si–Au distances in **60** (2.265(1) Å) and the theoretically calculated Si(II)–Au(I) bond length of (2.227Å).[2] The linearity of the Au(I) atom is proved by the Si1-Au1-Cl1 angle of 177.39°, marginally shorter than that in **60** (179.47(3)°).

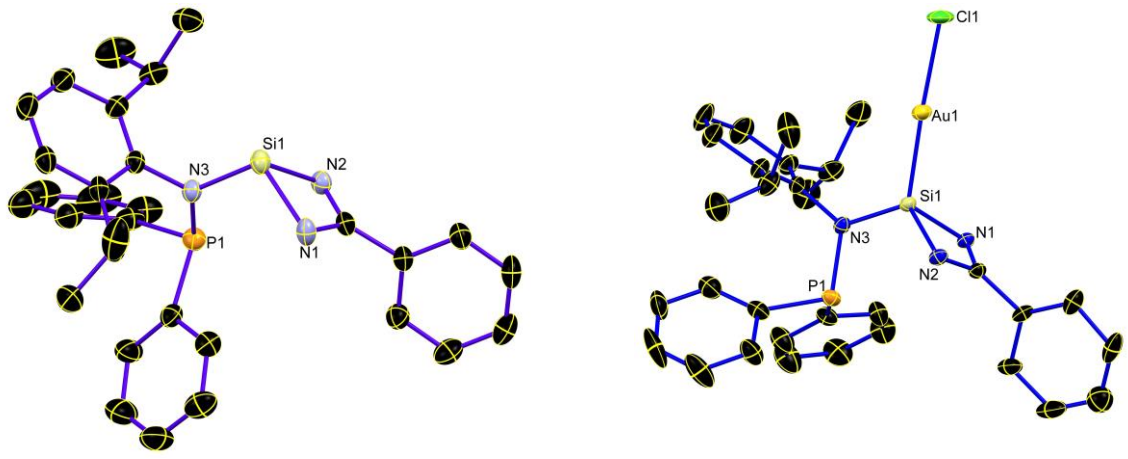

Figure 2.1 *Molecular structure of **2.2** (left) and **2.3** (right) with anisotropic displacement parameters depicted at the 50 % probability level. Hydrogen atoms, iPr, and tBu groups are not shown for clarity. The calculated geometrical parameters at the BP86/def2-SVP level of theory are given in square brackets. Selected bond lengths (Å) and bond angles (°) for **2.2**: N3–P1 1.726(2) [1.777], Si1–N3 1.796(2)*

*[1.845], Si1–N1 1.899(2) [1.962], Si1-N2 1.911(2) [1.982]. Selected bond lengths (Å) and bond angles (°) for **2.3**: Si1–Au1 2.246(2) [2.280], Si1-Au1-Cl1 177.39(9) [177.6]*

The reaction of **2.3** with $AgSbF_6$ resulted in the formation of cation **2.4** (*Scheme 2.1*). A singlet resonance at δ 97.10 (s) ppm in the ^{31}P NMR spectrum, shifted downfield in comparison to that of **2.3** (δ 55.69 ppm), indicated the coordination of P to the Au(I) centre in **2.4**. Similarly, the ^{29}Si NMR also showed a more downfield shifted multiplet at δ 78.04-78.36. The compound **2.4** is very stable and there is no change in the structure even after keeping it in open air for a month. The X-ray diffraction studies of **2.4** confirmed the formation of a dimeric Au cation where both P and Si atoms are coordinating to the Au(I) atom (*Figure 2.2*). The molecular structure of **2.4** reveals a fully supported dimeric dinuclear Au(I) cationic complex with SbF_6^- anion. The most remarkable feature of **2.4** is the presence of intramolecular aurophilic interaction (Au···Au) of 2.875(1) Å.[7a, 23] The calculated Au···Au distance at the BP86/def2-SVP level of theory is 2.962 Å, which is slightly longer than the Au···Au distance observed in the crystal structure. **2.4** contains an eight-membered ring N-Si-Au-P-N-Si-Au-P**,** where all the atoms lie in a plane except the nitrogen atoms, which are slightly above and below the plane. The *trans*-annular bending between the two arms is almost negligible which can be attributed to the highly crowded amidinato moieties at the Si(II) centres. The geometry of the Au(I) atom is nearly linear with the bond angle of 175.0(1)°.

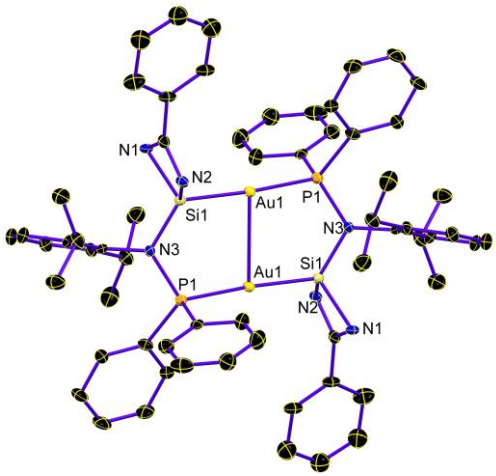

***Figure 2.2** The molecular structure of **2.4** with anisotropic displacement parameters depicted at the 50 % probability level. Hydrogen atoms and tBu groups are not shown for clarity. Selected bond lengths and bond angles are given in Å and °. The calculated geometrical parameters at the BP86/def2-SVP level of*

theory are given in square brackets. Au1···Au1 2.875(1) [2.962], P1–Au1 2.360(2) [2.456], Si1–Au1 2.318(2) [2.388], P1-Au1-Si1 175.0(1) [177.3]

The P-Au and the Si-Au bond distances are 2.360(2) and 2.318(2) Å, respectively. The Si-Au bond lengths are slightly increased if compared to that of **2.3** while the P-Au bond distance matches well with the literature values reported for the analogous systems.[24] Note that, **2.4** represents the first example of a silylene ligand supported Au(I) cation with aurophilic interaction.

2.5.2 Synthesis and characterizations of compounds **2.7** and **2.8**

After isolating the silylene-Au complexes, we moved to synthesize the gold complexes of heavier congeners of silylene *i. e.* germylenes and stannylene. The reaction of LGeCl[7b] and LSnCl[7c] [L= PhC(NtBu)$_2$] with one equivalent of 2,6-*i*Pr$_2$C$_6$H$_3$N(Li)PPh$_2$ in toluene afforded the targeted complexes (2,6 *i*Pr$_2$C$_6$H$_3$NPPh$_2$)GePhC(NtBu)$_2$ (**2.7**) and (2,6-iPr$_2$C$_6$H$_3$NPPh$_2$)SnPhC(NtBu)$_2$ (**2.8)**; (*Scheme 2.2*). Both compounds contain three lone pairs on M (M= Ge, Sn), N, and P in the same framework. Compound **2.7** was obtained as a colorless crystalline solid in 73.8% yield whereas a pale yellow crystalline solid of compound **2.8** was yielded in 72.4% yield. Both compounds were characterized by multinuclear NMR spectroscopy, HRMS spectrometry, and single crystal X-ray structural analysis.

In the ^{1}H NMR spectra of **2.7** and **2.8**, there are sharp singlets at δ 1.18 and 1.20 ppm, respectively indicating the *t*Bu substituents in the amidinate moieties, which are downfield shifted compared to those of **2.5** and **2.6** (**2.5**: δ 1.08 and **2.6**: δ 1.02 ppm).[7b,c] The proton of the methyl group of C*H*Me$_2$ for both **2.7** and **2.8** appear at δ 1.07 ppm as doublets with the same coupling constant of 6.8 Hz. In the ^{31}P NMR of **2.7** and **2.8,** a singlet resonance appeared at δ 54.91, and 56.15 ppm, respectively, which are also downfield shifted compared to that of [(2,6-*i*Pr$_2$C$_6$H$_3$NPPh$_2$)Li] (δ 51.0).[25, 7d] Compound **2.8** resonates at δ -122.70 ppm in the ^{119}Sn NMR spectrum, which is remarkably upfield when compared to that of **2.6** (δ 29.6 ppm) and related LSnN(SiMe$_3$)$_2$ (δ -33.16 ppm).[7c] This can be attributed to the electron withdrawing nature of the PPh$_2$ unit bound to the *N* atom in **2.8**.

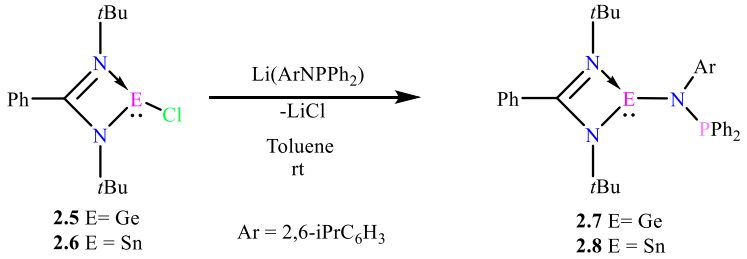

Scheme 2.2 *Syntheses of compounds* ***2.7*** *and* ***2.8.***

Colorless single crystals of **2.7** suitable for X-ray structural analysis were grown by slow evaporation of the toluene solution. Figure 2.3 depicts the molecular structure and the bond parameters for **2.7** which crystallizes in the triclinic space group *P*-1.[8] The geometry at the germanium atom may be qualitatively described (see theoretical calculations below) on the basis of an sp^2 hybridization with one hybrid orbital representing the lone pair and the others engaged in bonding to the substituents, which is similar to the previously reported Ge(II) amides e.g.[(CyNC(R)NCy)M(NSiMe$_3$)$_2$], [M=Ge, Sn and R=Me, *t*Bu] and [Me$_3$SiNC(*t*Bu)NSiMe$_3$]M[N(SiMe$_3$)$_2$], (M=Ge, Sn).[26]

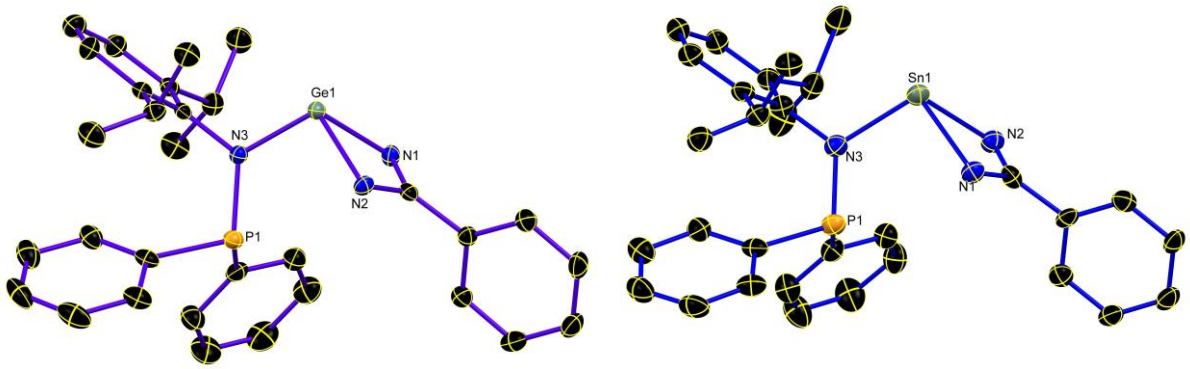

Figure 2.3 *The molecular structure of* ***2.7*** *(left) and* ***2.8*** *(right) with anisotropic displacement parameters depicted at the 50% probability level. Hydrogen atoms and tBu groups are not shown for clarity. Selected bond lengths (Å) and bond angles (deg). Calculated values at the BP86/def2-TZVPP level of theory are given in square brackets: Compound* ***2.7****: Ge1-N1 2.047(2) [2.103], Ge1-N2 2.033(2) [2.079], Ge1-N3 1.920(2) [1.966], N3-P1 1.717(2) [1.737]; P1-N3-Ge1 120.73(9) [120.2], N1-Ge1-N3 102.86(6) [104.9], N2-Ge1-N3 101.13(6) [103.8]. Compound* ***2.8****: Sn1-N1 2.189(9)*

[2.260], Sn1-N2 2.247(6) [2.300], Sn1-N3 2.106(7) [2.168], N3-P1 1.689(8) [1.729]; P1-N3-Sn1 123.2(4) [120.2], N3-Sn1-N1 97.7(3) [102.0], N3-Sn1-N2 104.4(3) [104.6].

This interpretation is supported by the observed N(1)-Ge(1)-N(3) and N(2)-Ge(1)-N(3) angles of 102.86(6) and 101.13(6)°, respectively. The average Ge1-$N_{amidinato}$ [Ge1-N1= 2.047 (2) and Ge1-N2= 2.033 (2) Å] bond length is similar to those of **2.5**.[7b] The Ge1-N3 bond distance is 1.920(2) Å. The coordination of the nitrogen atoms is almost planar with angular sums $\Sigma_{\text{bond angle}}$N of 359.15(1).

Single crystals suitable for X-ray structural analysis of compound **2.8** was also obtained by slow evaporation of toluene solution. Molecular structure and bond parameters of **2.8** are given in the legend of Figure 2.3. The compound **2.8** crystallizes in monoclinic space group $P2_1/c$.[8] The molecular structure of compound **2.8** is similar to that of **2.7** where the Sn(II) atom is three coordinated and exhibits a distorted trigonal-pyramidal geometry with a lone pair of electrons at the apex. The two sites of the Sn(II) center are occupied by the N atoms from the amidinato ligand, and the other site is occupied by the N atom from the amide ligand. The Sn1-N1 and Sn1-N2 bond distances are 2.189(9) Å and 2.247(6) Å respectively, which are markedly longer than those of **2.7** but similar to those in **2.6**.[7c] The amido nitrogen atom in **2.8** contains a lone pair of electrons and three valance bonds with Sn(II), P1 center, and the aryl ring and adopts a nearly planar geometry with Sn-N_{amide} distance of 2.106(7) Å, which is comparable to the Sn-N_{amide} bond lengths in the previously reported [PhC(N*t*Bu)$_2$SnN(SiMe$_3$)$_2$] (2.125(mean) Å)[7c] and [Me$_3$SiNC(*t*Bu)NSiMe$_3$]Sn[N(SiMe$_3$)$_2$] (2.121(5) Å).[26c] The P1-N3 Bond length [1.689(8) Å] is quite similar to that in **2.7**. The N1-Sn1-N3 bond angle [97.7(3)°] is larger than that in **2.7** [92.28(7)°].

2.5.3 Theoretical investigation of compounds **2.2**, **2.3** and **2.4**

We have carried out quantum mechanical calculations at the M06/def2-TZVPP//BP86/def2-SVP level of theory[9-16] to explore the greater nucleophilicity of Si(II) center with respect to P(III) center in **2.2** as well as to understand the bonding interaction of the Si center with the Au atom in **2.3**. The HOMO (-5.46 eV) and HOMO-1 (-5.87 eV) of silylene **2.2** (*Figure 2.4*) are mainly lone pair orbital on Si and P centers respectively, which indicates that lone pair on Si-center is highly nucleophilic center as compared to that on the P-center. It is well supported by the ESP on the molecular van der Waals

surface of **2.2**. The global minimum (-28.8 kcal/mol) of ESP is observed close to Si-center, whereas the ESP value at the P-center is only -15.3 kcal/mol (*Figure 2.8*).

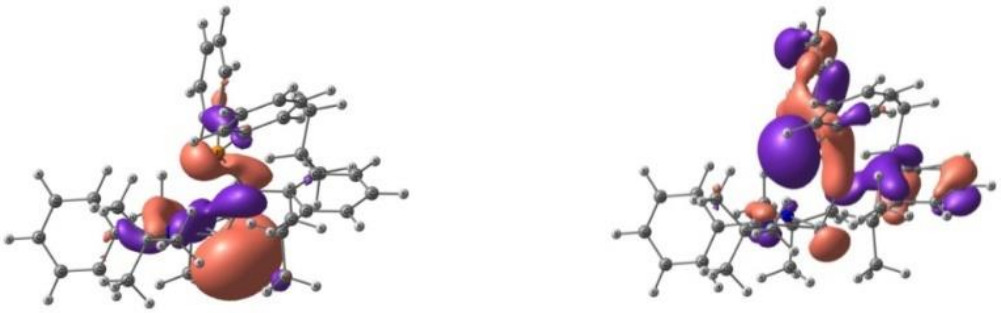

HOMO (-5.46) LUMO (-5.87)

Figure 2.4 *Plots of molecular orbitals of silylene,* ***2.2****, at the M06/def2-TZVPP//BP86/def2-SVP level of theory. Eigen values in eV are given in the parenthesis.*

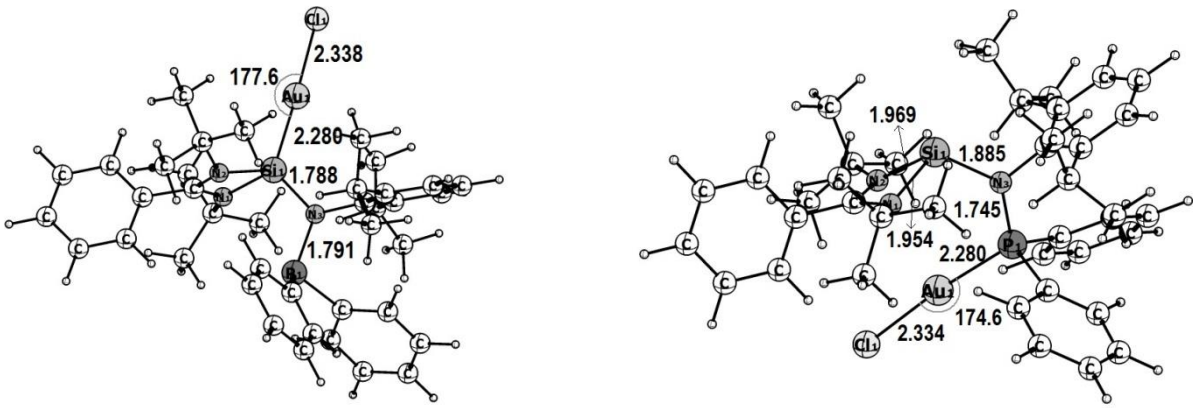

(0.0) (14.5)

Figure 2.5 *Optimized geometries and important geometrical parameters of* ***2.3*** *(Si→Au) and* ***2.3'*** *(P→Au, hypothetical) at the M06/def2-TZVPP//BP86/def2-SVP level of theory. Relative energies of* ***2.3*** *and* ***2.3'*** *are in kcal/mol (given in the parenthesis).*

Accordingly, the hypothetical P-coordinated Au complex is found to be 14.5 kcal/mol higher in energy than the Si-coordinated Au complex (*Figure 2.5*). The electrostatic interaction contributes 75.8% to the total attractive interaction of the Si-Au bond. The high negative NBO charge (*Appendix 2, Table 2A.5*) on the Au-Cl group (-0.47 e) also supports a predominant electrostatic nature of the Si-Au bond. The σ- donation from the Si-lone pair orbital to the vacant *sd*-hybrid orbital on Au (Δρ1, ΔE = -28.6 kcal/mol, *see*

the Appendix 2, Figure 2A.11) is the major contributor to the Si-Au interaction and contributes 41.7% towards the total covalent interaction. The back donation from the filled d-orbitals of Au to the antibonding orbital of Si-N bonds (Δρ2 + Δρ3 + Δρ4, ΔE = -20.9 kcal/mol) also contributes significantly to the Si-Au bond. The bond dissociation energy of 62.2 kcal/mol indicates rather strong Si-Au interaction.[2]

In order to understand the nature of the bonding interaction between two Au centers in compound **2.4**, we have further carried out topological analysis of electron density on **2.4** according to the quantum theory of atoms in molecules (QTAIM) using AIMALL program package. A bond critical point (BCP) is observed between the two Au-atoms (*Figure 2.6*). The positive Laplacian of electron density ($\nabla^2\rho(r)$ = 2.0098 e Å^{-5}) at the bcp typically indicates closed shell interactions. Note that, the experimentally reported $\nabla^2\rho(r)$ values at the bcp of Mn-Mn bond in $Mn_2(CO)_{10}$ and Co-Co bond in $Co_2(CO)_6(AsH_3)_2$, where there are metal-metal direct bonds, are 0.720 e Å^{-5} and -0.043 e Å^{-5} respectively. However, the values of electron density ρ (r) at the bcp of Mn-Mn (0.144 e Å^{-3}) and Co-Co (0.271 e Å^{-3}) bonds are much close to the ρ(r) value at the bcp of Au---Au interaction in **2.4**.[27] However, the high electron density (ρ(r) = 0.2207 e Å^{-3}) and negative total energy density (H(r) = -0.0216 hartree Å^{-3}) at bcp indicates a relatively strong interaction in **2.4**.[15] Thus, the Au···Au interaction in **2.4** can be described as a strong aurophilic closed shell interaction between the two d^{10} Au atoms.

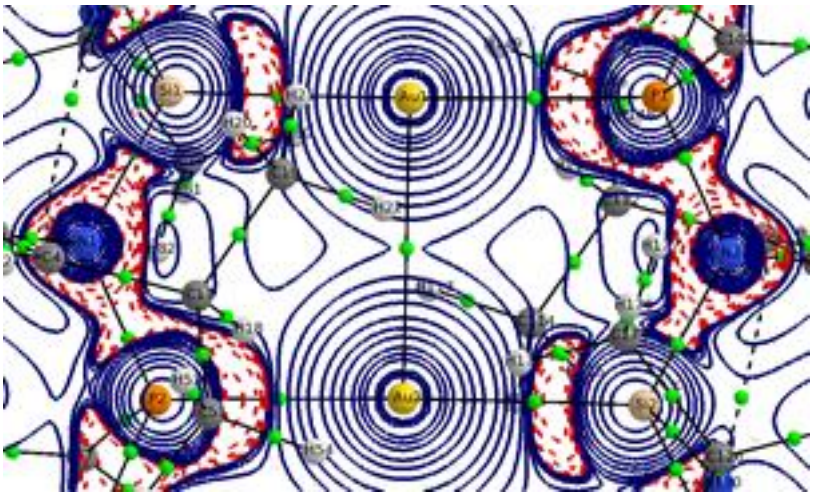

Figure 2.6 *Contour line diagram of the Laplacian of electron density ($\nabla^2\rho(r)$) in the plane of Au1-Au2-N2 of Silylene-$(Au)_2$,* ***2.4****, at the M06/def2-TZVPP//BP86/def2-SVP level of theory. The small green circles represent bond critical points (BCPs). The blue solid and red dotted lines indicate regions with $\nabla^2\rho(r) < 0$ and $\nabla^2\rho(r) > 0$ respectively.*

Table 2.1 *Topological analysis of electron density (ρ), Laplacian of electron density ($\nabla^2\rho$), total energy density (H), potential energy density (V) and kinetic energy density (G) of* ***2.4*** *at the selected bond critical points (BCPs) at the M06/def2-TZVPP//BP86/ def2-SVP level of theory*

Atoms	ρ (e Å^{-3})	$\nabla^2\rho$ (e Å^{-5})	H (hartree Å^{-3})	V (hartree Å^{-3})	G (hartree Å^{-3})
Au1-Au2	0.2207	2.0098	-0.0216	-0.1842	0.1626
Au1-Si1	0.6344	-1.1471	-0.3057	-0.5311	0.2254
Au1-P1	0.5811	2.4774	-0.1950	-0.5635	0.3685
Au2-Si2	0.6344	-1.1471	-0.3057	-0.5311	0.2254
Au2-P2	0.5811	2.4774	-0.1950	-0.5635	0.3685

The Si–Au and P–Au interactions on the contrary show high ρ(r) value at the bcp of Si–Au and P–Au bonds, respectively indicating stronger metal ligand interaction (*Table 2.1*). A positive $\nabla^2\rho(r)$ at the bcp of the P–Au bond indicates a closed-shell donor-acceptor interaction. The negative $\nabla^2\rho(r)$ at the bcp of Si–Au bond is in the range of dative bond with the significant covalent character as evident from the Laplacian plot.[2]

The nature of the Au-P and Au-Si bonding interactions is further elucidated by EDA-NOCV analysis by taking $[Au{---}Au]^{2+}$ as one fragment and rest of the molecule as another. The results indicate that the energy corresponding to the electrostatic interaction (52.2%) is slightly higher than that of the covalent interaction (47.8%). In addition to the donation of Si and P lone pair to the *sp*-type orbitals on Au (Δρ1 - Δρ4; ΔEL→Au = -248.2 kcal/mol), the back donation (Δρ9 - Δρ14; ΔEAu→L = -51.6 kcal/mol) from the Au d-orbitals to the Si–N and P–N σ*-orbitals also contribute to the covalent nature of the Au-Si and Au-P bonds (*see the Appendix 2.8*).

2.5.4 Theoretical investigation of **2.7** and **2.8** and comparison of their nucleophilicity with that of silylene (**2.2**)

The computed geometrical parameters of **2.7** and **2.8** are in good agreement with the experimental values. As we have discussed above, that the HOMO and HOMO-1 of silylene, **2.2** are mainly the lone pairs on Si- and P-centers, respectively but the order of the molecular orbital energy levels is reversed in germylene, **2.7** and stannylene, **2.8**, where the lone-pair orbital on the heavier Ge and Sn centers (HOMO-1) is more stabilized as compared to the Si analogue. This is, in accordance with the increasing percentage of *s*-

character of the lone pair on group-14 elements (73.4% in **2.2**, 79.5 % in **2.7** and 86.0% in **2.8**, *Table 2.2*). The stabilization of the lone pair on heavier group-14 elements is commonly observed for the five- and six-membered tetrylenes.[17] Thus, the nucleophilicity of the lone pair on Si in silylene (**2.2**) is higher than that of the lone pairs on Ge and Sn in germylene (**2.7**) and stannylene (**2.8**).

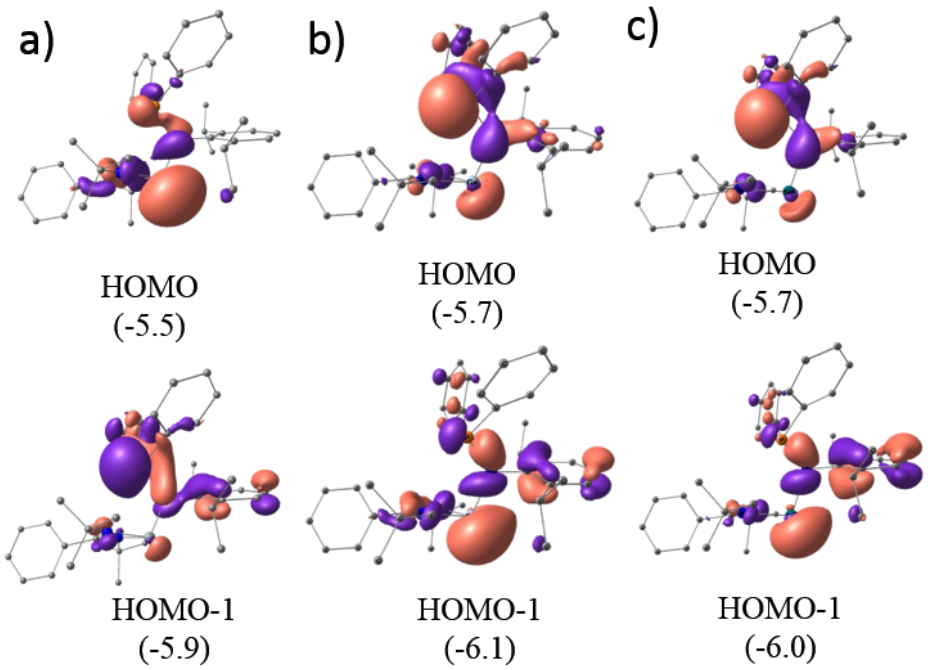

Figure 2.7 *Comparison of HOMO and HOMO-1 of (a) silylene (**2.2**) (b) germylene (**2.7**) and (c) stannylene (**2.8**) at the M06/def2-TZVPP//BP86/ def2-SVP (for **2.2**) and M06/def2-TZVPP//BP86def2-TZVPP[a] (for **2.7**, **2.8**) level of theory The eigen values in eV are given in parentheses.*

For all these molecules, the lone pair orbital on N-center is highly stabilize and is engaged in bonding interaction with the Si-N, Ge-N and Sn-N σ*-MOs. The MO analysis suggests that the nucleophilicity of the lone pair on Si-atom is higher than that of the lone pair on P-center in **2.2**, whereas the nucleophilicity of the lone pair on Ge and Sn-centers in **2.7** and **2.8** are lower than that of the lone pair on P-center. We have further analyzed the molecular electrostatic potential (ESP) map on the van der Waal's surface of atoms in silylene (**2.2**), germylene (**2.7**), and stannylene (**2.8**) (*Figure 2.8*). The global minimum of ESP for **2.2**, **2.7,** and **2.8** are -28.8, -23.4, and -22.4 kcal/mol, respectively.

Table 2.2 *Lone pair occupancy and their percentage s and p character on X, P and N atoms in silylene* ***2.2****, germylene* ***2.7*** *and stannylene* ***2.8*** *by natural bond orbital analysis at the M06/def2-TZVPP//BP86/ def2-SVP (for* ***2.2****) and M06/def2-TZVPP//BP86def2-TZVPP[a] (for* ***2.7****,* ***2.8****) level of theory*

Atom	Lone pair occupancy			% *s* character			% *p* character		
	X = Si	X = Ge	X = Sn	X = Si	X = Ge	X = Sn	X = Si	X = Ge	X = Sn
X	1.92	1.94	1.93	73.4	79.5	86.0	26.5	20.5	13.9
P	1.89	1.89	1.89	50.0	48.2	48.1	50.0	51.8	51.9
N	1.83	1.82	1.83	0.4	0.54	0.01	99.6	99.4	99.9

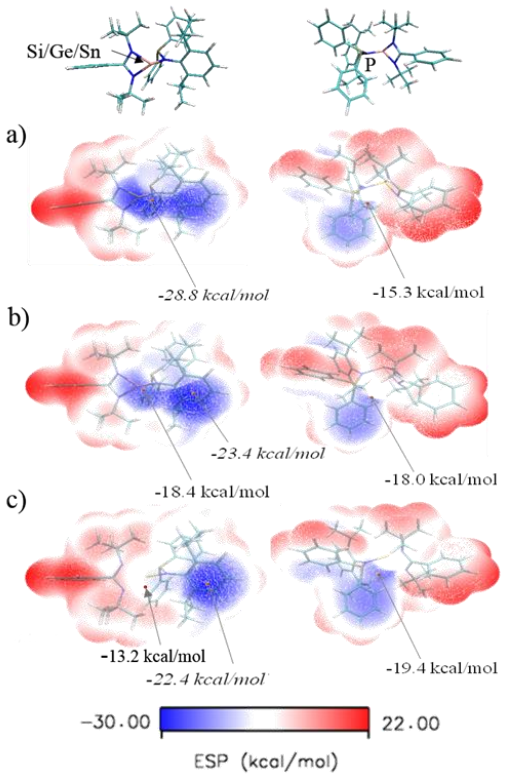

Figure 2.8 *Plot of electrostatic potential on the molecular van der Waals surface of (a) silylene (****2.2****), (b) germylene (****2.7****) and (c) stannylene (****2.8****) at the M06/Def2-TZVPP//BP86/Def2-TZVPP level of* theory. *The global minimum of ESP are shown in italics. The minima at the direction of lone pair on Si, Ge, Sn (left column) and P-centers (right column) are also indicated.*

Note that, the global minimum ESP value of **2.2** is observed in the direction of the lone pair on Si-center, whereas it is observed slightly above the 2,6-*i*PrPh ring connected to

N3-atom and in the opposite direction of P-centers in **2.7** and **2.8**. The ESP values in the direction of the lone pair of Ge and Sn-centers in **2.7** and **2.8** are only -18.4 and -13.2 kcal/mol. Moreover, the minima in the direction of the lone pair on P- centers in **2.2** (-15.3 kcal/mol), **2.7** (-18.0 kcal/mol) and **2.8** (-19.4 kcal/mol) are also less as compared to their global minimum ESP values. Thus, Si-center is more nucleophilic than the P-center in **2.2**, whereas the Ge and P-centers have similar nucleophilicity in **2.7** and the Sn-center is much less nucleophilic than the P-center in **2.8**. Hence, the low nucleophilicity of Ge/Sn and P-centers explains why the complexation reaction of **2.7** and **2.8** with AuCl·SMe_2 is not successful.

2.6 Conclusions

In summary, we have demonstrated the isolation of a functionalized silylene **2.2** with two donor atoms, Si(II) and P(III), and its reaction with AuCl·SMe_2 leading to a 1:1 complex **2.3**, where the Si(II) center is coordinating to the Au atom while the P atom remains intact. Subsequent halide abstraction from **2.3** led to the formation of the cationic complex **2.4**, which is the first example of a Si(II) supported dimeric Au(I) cation with an aurophilic interaction of 2.875(1) Å. The theoretical investigation shows that the nucleophilicity of Si-center is higher than P-center in **2.2**. Further, we have also synthesized the heavier congeners of **2.2**, germylene **2.7** and **2.8**. Notably, **2.7** and **2.8** do not react with AuCl unlike their lighter congener **2.2**. Quantum mechanical calculations revealed that nucleophilicity of the group-14 atom reduces from silylene to stannylene. The global minimum of the ESP of **2.2** is in the direction of the lone pair on Si-center whereas the global minima of the ESP of **2.7** and **2.8** is located above the 2,6-*i*PrPh ring connected to N-atom and in the opposite direction of P-center. Thus, unlike in **2.2** where the Si-center is highly nucleophilic, the nucleophilicity of the Ge/Sn-centers are much less in **2.7** and **2.8**. This corroborates well with the complexation reaction of **2.2** with AuCl.

2.7 References

1. (a) Blom, B.; Enthaler, S.; Inoue, S.; Irran, E.; Driess, M. *J. Am. Chem. Soc.* **2013**, *135*, 6703; (b) Wang, W.; Inoue, S.; Enthaler, S.; Driess, M. *Angew. Chem., Int. Ed.* **2012**, *51*, 6167; (c) Wang, W.; Inoue, S.; Irran, E.; Driess, M. *Angew. Chem., Int. Ed.* **2012**,

51, 3691; (d) Wang, W.; Inoue, S.; Yao S.; Driess, M. *J. Am. Chem. Soc.* **2010**, *132*, 15890; (e) Blom, B.; Gallego, D.; Driess, M. *Inorg. Chem. Front.* **2014**, *1*, 134; (f) Gallego, D.; Inoue, S.; Blom, B.; Driess, M. *Organometallics* **2014**, *33*, 6885; (g) Tan, G.; Enthaler, S.; Inoue, S.; Blom, B.; Driess, M. *Angew. Chem., Int. Ed.* **2015**, *54*, 2214; (h) Breit, N.C.; Szilvási, T.; Inoue, S. *Chem. Commun.* **2015**, *51*, 11272; (i) Tavčar, G.; Sen, S. S.; Azhakar, R.; Thorn, A.; Roesky, H. W. *Inorg. Chem.* **2010**, *49*, 10199; (j) Azhakar, R.; Sarish, S. P.; Roesky, H. W.; Hey, J.; D. Stalke, D. *Inorg. Chem.* **2011**, *50*, 5039; (k) Waterman, R.; Hayes, P. G.; Tilley, T. D. *Acc. Chem. Res.*, **2007**, *40,* 712.

2. Boehme, C.; Frenking, G. *Organometallics* **1998**, *17*, 580.
3. Khan, S.; Ahirwar, S. K.; Pal, S.; Parvin, N.; Kathewad, N. *Organometallics* **2015**, *34*, 5401.
4. Avent, A. G.; Gehrhus, B.; Hitchcock, P. B.; Lappert, M. F.; Maciejewski, H. *J. Organomet. Chem.* **2003**, *686*, 321.
5. Tan, G.; Blom, B.; Gallego, D.; Driess, M. *Organometallics* **2014**, *33*, 363.
6. Inagawa, Y.; Ishida, S.; Iwamoto, T. *Chem. Lett.* **2014**, *43*, 1665.
7. (a) Sen, S. S.; Roesky, H. W.; Stern, D.; Henn, J.; Stalke, D. *J. Am. Chem. Soc.* **2010**, *132*, 1123; (b) Nagendran, S.; Sen, S. S.; Roesky, H. W.; Koley, D.; Grubmüller, H.; Pal, A.; Herbst-Irmer, R. *Organometallics* **2008**, *27*, 5459; (c) Sen, S. S.; Kritzler-Kosch, M. P.; Nagendran, S.; Roesky, H. W.; Beck, T.; Pal, A.; Herbst-Irmer, R. *Eur. J. Inorg. Chem.* **2010**, *2010*, 5304; (d) Pal, S.; Kathewad, N.; Pant, R.; Khan, S. *Inorg. Chem.* **2015**, *54*, 10172.
8. (a) Kottke, T.; Stalke, D. *J. Appl. Crystallogr*. **1993**, *26*, 615; (b) Stalke, D. *Chem. Soc. Rev.* **1998**, *27*, 171; (c) Sheldrick, G. M. *Acta Crystallogr.* **2015**, *A71*, 3; (d) Sheldrick, G. M. *Acta Crystallogr.* **2015**, *C71*, 3; (e) Schulz, T.; Meindl, K.; Leusser, D.; Stern, D.; Ruf, M.; Sheldrick, G. M.; Stalke, D. *J. Appl. Crystallogr*. **2009**, *42*, 885; (f) Krause, L.; Herbst-Irmer, R.; Sheldrick, G. M.; Stalke, D. *J. Appl. Crystallogr.* **2015**, *48*, 3.
9. Gaussian 09, Revision D.01, M. J. Frisch, G. W. Trucks, H. B. Schlegel, G. E. Scuseria, M. A. Robb, J. R. Cheeseman, G. Scalmani, V. Barone, B. Mennucci, G. A. Petersson, H. Nakatsuji, M. Caricato, X. Li, H. P. Hratchian, A. F. Izmaylov, J. Bloino, G. Zheng, J. L. Sonnenberg, M. Hada, M. Ehara, K. Toyota, R. Fukuda, J. Hasegawa, M. Ishida, T. Nakajima, Y. Honda, O. Kitao, H. Nakai, T. Vreven, J. A. Montgomery, Jr., J. E. Peralta, F. Ogliaro, M. Bearpark, J. J. Heyd, E. Brothers, K. N. Kudin, V. N. Staroverov, T. Keith, R. Kobayashi, J. Normand, K. Raghavachari, A. Rendell, J. C. Burant, S. S. Iyengar, J.

Tomasi, M. Cossi, N. Rega, J. M. Millam, M. Klene, J. E. Knox, J. B. Cross, V. Bakken, C. Adamo, J. Jaramillo, R. Gomperts, R. E. Stratmann, O. Yazyev, A. J. Austin, R. Cammi, C. Pomelli, J. W. Ochterski, R. L. Martin, K. Morokuma, V. G. Zakrzewski, G. A. Voth, P. Salvador, J. J. Dannenberg, S. Dapprich, A. D. Daniels, O. Farkas, J. B. Foresman, J. V. Ortiz, J. Cioslowski, and D. J. Fox, Gaussian, Inc., Wallingford CT, 2013.

10. (a) Becke, A. D. *Phys. Rev. A* **1988**, *38*, 3098; (b) Perdew, J. P. *Phys. Rev. B* **1986**, *33*, 8822; (c) Perdew, J. P. *Phys. Rev. B* **1986**, *34*, 7406.
11. Weigend, F.; Ahlrichs, R. *Phys. Chem. Chem. Phys.* **2005**, *7*, 3297.
12. Zhao, Y.; Truhlar, D. G. *Theor. Chem. Acc.* **2008**, *120*, 215.
13. (a) Reed, A. E.; Curtiss, L. A.; Weinhold, F. *Chem. Rev.* **1988**, *88*, 899; (b) Glendening, E. D.; Reed, A. E.; Carpenter, J. E.; Weinhold, F. *NBO Version 5.9*.
14. (a) Lu, T.; Chen, F. *J. Comput. Chem.* **2012**, *33*, 580; (b) Lu T.; Chen, F. *J. Mol. Graphics Modell.* **2012**, *38*, 314.
15. (a) Bader, R. F. W. *Atoms in Molecules. A Quantum Theory, Oxford University Press, Oxford*, **1990**; (b) Matta, C. F.; Boyd, R. J. *The Quantum Theory of Atoms in Molecules*, Wiley-VCH, Weinheim, **2007**.
16. Keith, T. A.; AIMAll (Version 15.05.18), TK Gristmill Software, Overland Park KS, USA, **2015** (aim.tkgristmill.com).
17. ADF 2013.01, SCM, *Theoretical Chemistry*, Vrije Universiteit, Amsterdam, http://www.scm.com; Tevelde, G.; Bickelhaupt, F. M.; Baerends, E. J.; Guerra, C. F.; Gisbergen, S. J. A. V.; Snijders, J. G.; Ziegler, T. *J. Comput. Chem.* **2001**, *22*, 931.
18. (a) Chang, C.; Pelissier, M.; Durand, Ph. *Phys. Scr.* **1986**, *34*, 394; (b) Heully, J. –L.; Lindgren, I.; Lindroth, E.; Lundquist, S.; Pendrill, A.-M. M. *J. Phys. B* **1986**, *19*, 2799; (c) Lenthe, E. V.; Baerends, E. J.; Snijders, J. G. *J. Chem. Phys.* **1993**, *99*, 4597; (d) Lenthe, E. V.; Snijders, J. G.; Baerends, E. J. *J. Chem. Phys.* **1996**, *105*, 6505; (e) Lenthe, E. V.; Leeuwen, R. V.; Baerends, E. J.; Snijders, J. G. *Int. J. Quantum Chem*. **1996**, *57*, 281; (f) VanLenthe E.; Baerends, E. J. *J. Comput. Chem.* **2003**, *24*, 1142.
19. (a) Morokuma, K. *J. Chem. Phys.* **1971**, *55,* 1236; (b) Zeigler, T.; A. Rauk, A. *Inorg. Chem.* **1979**, *18*, 1755; (b) Zeigler, T.; Rauk, A. *Inorg. Chem.* **1979**, *18*, 1558; (c) Hopffgarten, M. V.; Frenking, G. *WIREs Comput. Mol. Sci.* **2012**, *2*, 43.
20. (a) Mitoraj, M.; Michalak, A. *Organometallics* **2007**, *26*, 6576; (b) Mitoraj M.; Michalak, A. *J, Mol. Model*. **2007**, *13*, 347; (c) Michalak, A.; Mitoraj, M.; Zeigler, T. *J. Phys. Chem. A* **2008,** *112*, 1933; (d) Mitoraj. M.; Michalak, A. *J. Mol. Model*. **2008**, *14*, 681; (d) Mitoraj,

M. P.; Michalak, A.; Ziegler, T. *J. Chem. Theory Comput*. **2009**, *5*, 962; (e) Nguyen, T. A. N.; Frenking, G. *Chem. Eur. J*. **2012**, *18*, 12733; (f) Mousavi, M.; Frenking, G. *Organometallics* **2013**, *32*, 1743.

21. So, C.-W.; Roesky, H. W.; Gurubasavaraj, P. M.; Oswald, R. B.; Gamer, M. T.; Jones, P. J.; Blaurock, S. *J. Am. Chem. Soc.* **2007**, *129*, 12049.
22. Sen, S. S.; Hey, J.; Herbst-Irmer, R.; Roesky, H. W.; Stalke, D. *J. Am. Chem. Soc.* **2011**, *133*, 12311.
23. (a) Schmidbaur, H.; A. Schier, A. *Chem. Soc. Rev*. **2008**, *37*, 1931; (b) H. Schmidbaur, H.; Schier, A. *Chem. Soc. Rev.* **2012**, *41*, 370; (c) Deák. A.; Megyes, T.; Tárkányi, G.; Király, P.; Biczók, L.; Pálinkás, G.; Stang, P. J. *J. Am. Chem. Soc.* **2006**, *128*, 12668; (d) Wiedemann, D.; Gamer, M. T.; Roesky, P. W. *Z. Anorg. Allg. Chem*. **2009**, *635*, 125.
24. (a) Balch, A. L. *Struct. Bonding* (Berlin), **2007**, *123*, 1; (b) Yam, V. W.-W.; Cheng, E. C.-C. *Chem. Soc. Rev*. **2008**, *37*, 1806; (c) He, X.; Yam, V. W.-W. *Coord. Chem. Rev*. **2011**, *255,* 2111; (d) Yam, V. W.-W.; Cheng, E. C.-C. *Top. Curr. Chem*. **2007**, *281*, 269.
25. Stasch, A. *Angew. Chem. Int. Ed.*, **2012**, *51*, 1930;
26. (a) Foley, S. R.; Bensimon, C.; Richeson, D. S. *J. Am. Chem. Soc.* **1997**, *119*, 10359; (b) Foley, S. R.; Yap, G. P . A.; Richeson, D. S. *Organometallics* **1999**, *18*, 4700; (c) Foley, S. R.; Zhou, Y.; Yap, G. P. A.; Richeson, D. S. *Inorg. Chem.* **2000**, *39*, 924.
27. *Electron Density and Chemical Bonding I: Experimental Charge Density Studies (Structure and Bonding)*, Stalke, D. Vol. 146, **2012**, Springer, New York

CHAPTER 3

Acyclic α-Phosphinoamido-Germylenes

Experimental and Theoretical Study of their Nucleophilic Behaviour

3.1 Introduction

Carbenes and its heavier analogues are the most targeted species in 14th group chemistry.[1] Several research groups across the world are working to exploit their ability to do the numerous chemical transformations, *e.g.*, activation of small molecules (CO, NH_3, CO_2, H_2, H_2O, etc.) and homogeneous catalysis, *etc.*[2] Several reports on monomeric chlorogermylenes (LGeCl) and N-heterocyclic germylenes (L_2G or LGeL') (L, L'= bulky ligand) supported by C-, N- and P- based ligands are present in literature.[3, 1e] Moreover, the germylenes, supported by metals or metal complexes are also known and have been used in catalysis.[4] During the initial phase of development of Ge(II) chemistry, dialkyl- and diaryl- germylenes were synthesized by reduction of Ge(IV) precursor, substitution reactions on Ge(II) precursors or by photochemical reactions.[5] These germylenes were monomeric in solution as well as in gas phase but dimeric in the solid state. In 1991, Jutzi *et al*. isolated the stable dialkylgermylene, $(Me_3Si)_2CHGeC(SiMe_3)_3$.[6] Both steric as well as electronic factors are important for the stabilization of Ge(II) species and can be efficiently provided by using amido- and/or phosphido- ligands. Following this, a series of amido- ligands (*Chart 3.1*) have been used to stabilize many germylenes.[7] The first amide based germylene $[Ge\{N(SiMe_3)_2\}_2]$ (**68**) (*Chart 3.1*)

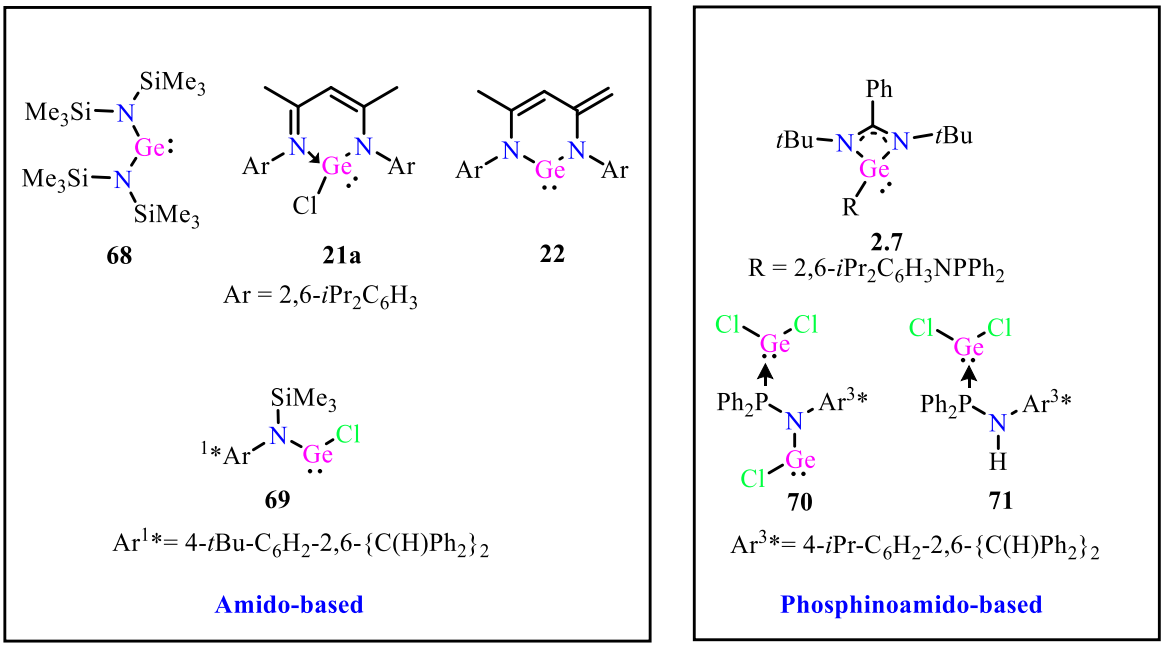

Chart 3.1 *Selected examples of structurally characterized germylenes*

was isolated in 1992 by Chorley *et al.* Later in 2001, Roesky *et al.* utilized bulky *β*-diketiminato ligand [HC(CHMeNAr)$_2$] (Ar = 2,6-*i*Pr$_2$C$_6$H$_3$) and prepared a monomeric chlorogermylene [HC-(CMeNAr)$_2$]GeCl (**21a**).[8] Later, in 2006, Driess *et al.* synthesized the N-heterocyclic germylene [CH{(C=CH$_2$) (CMe)(NAr)$_2$}Ge], (Ar = 2,6-*i*Pr$_2$C$_6$H$_3$) (**22**)[9] by employing the same framework. Recently, Jones *et al.* synthesized a series of chlorogermylenes by utilizing a very bulky aryl amido group L^{1}GeCl [L^1= -N(Ar*)(R) (Ar* = 4-*i*Pr-C$_6$H$_2$-2,6-{C(H)Ph$_2$}$_2$, 4-*t*Bu-C$_6$H$_2$-2,6-{C(H)Ph$_2$}$_2$, R= SiMe$_3$); Ar* = 4-Me-C$_6$H$_2$-2,6-{C(H)Ph$_2$}$_2$, R=2,4,6-*i*Pr$_3$-C$_6$H$_2$; Ar* = 4-Me-C$_6$H$_2$-2,6-{C(H)Ph$_2$}$_2$, R=3,5,-(CF$_3$)$_2$-C$_6$H$_3$.[10] Among these chlorogermylenes, Me$_3$SiNGeClAr^{1*} (Ar^{1*}= *t*Bu-C$_6$H$_2$-2,6-{C(H)Ph$_2$}$_2$) (**69**) was structurally characterized by X-ray diffraction analysis. These bulky ligands provide steric as well as electronic stabilization which is reflected in the short C···Ge distances between *ipso*- and *ortho*- aromatic carbons of flanking phenyl groups and Ge. Attempt to isolate L^{2}GeCl (L^2= -NAr^2*SiMe$_3$, Ar^2*= 2,6-*i*-Pr$_2$-4-(CPh$_3$)-C$_6$H$_2$) with bulky aryl group led to a mixture of products. The endeavor to synthesize monomeric phosphido-M complexes [M = Sn and Pb] with -P(SiMe$_3$)$_2$ substituent by Buhro *et al.* was not successful as the reaction led to the phosphorus-bridged dimeric products.[11] In 1995, Driess *et al.* reported phosphido-germylene by introducing a very bulky phosphido groups, -PR^{1}R^2 (R^1 = Si(2,4,6-*i*Pr$_3$C$_6$H$_2$)$_2$F, Si(*t*-Bu)(2,4,6-*i*Pr$_3$C$_6$H$_2$)F; R^2 = Si*i*Pr$_3$).[12] However, the compound could not be authenticated structurally, but characterized by NMR spectroscopy and elemental analysis. Although there are plenty of reports on germylene bearing amido or phosphido- ligands, there are hardly few reports on α-phosphinoamido-germylene. In the previous chapter, we reported one example of amidinate based phosphinoamido-germylene (**2.7**) showing a highly nucleophilic phosphorus center as compared to Ge.[13] However; there was no report of acyclic phosphinoamido-germylenes. Recently Jones *et al*. tried to synthesize L^{3}GeCl, [L^3= (Ar^3*(PPh$_2$)N)-, Ar^3* =4-*i*Pr-2,6-{C(H)Ph$_2$}$_2$C$_6$H$_2$], but they obtained amido-germanium chloride [GeCl$_2$(κ^1-*P*-L^{3}GeCl)] and amino-germanium chloride, [GeCl$_2$(κ^1-*P*-L^{3}H)] (**70** and **71** respectively) complexes (*Chart 3.1*).[14] In this chapter, we are reporting the first example of acyclic α-phosphinoamido-germylene and dimeric chlorogermylene.

3.2 Experimental section

3.2.1 General remarks

All manipulations were carried out under an inert gas atmosphere of argon using standard Schlenk techniques and in a dinitrogen-filled glove box. The solvents used, were

purified by MBraun MB SPS-800 solvent purification system. All chemicals purchased from Sigma-Aldrich were used without further purification. All the NMR spectra (^{1}H, ^{13}C, and ^{31}P) were recorded in C_6D_6 (purchased from Sigma-Aldrich) using a Bruker 400 MHz spectrometer. Mass spectra were recorded using an AB Sciex 4800 plus MALDI TOF/TOF instrument.

3.2.2 Synthesis

3.2.2.1 Synthesis of (2, 6-*i*Pr$_2$C$_6$H$_3$NGeClPPh$_2$)$_2$ (**3.2**)

To the solution of **3.1** (2.166 g, 6.0 mmol in 60 mL toluene), *n*-BuLi (3 mL of 2M solution in hexane, 6.0 mmol) was added at room temperature. The reaction mixture was stirred for overnight. After a 12 hours of stirring, $GeCl_2$·dioxane (1.392 g, 6.0 mmol) was added at the room temperature. Again, the reaction mixture was stirred for 12 hours. The reaction mixture was filtered to separate out the precipitated LiCl, concentrated, and kept at 0 °C for crystallization. Yield = 45% (1.26 g). M.P. Decomposes around 145 °C. ^{1}H NMR (400 MHz, C_6D_6, 298 K): δ 1.15 (*d*, 12H, -C*H*$_3$, *J* = 6.8 Hz), 1.56 (*d*, 12H, -CH$_3$, *J* = 6.7 Hz), 4.03 (*m*, 4H, -C*H*), 6.76–7.19 (m, 14H, Ph), 7.56–7.7 (m, 12H, Ph); ^{31}P NMR (C_6D_6, 161.976 MHz, ppm): δ 48.26; ^{13}C NMR (C_6D_6, 100.613 MHz, ppm): 23.96 (-*C*H3), 28.67 (-*C*HCH$_3$), 120.14, 126.44, 129.11, 132.70, 133.15, 141.05 142.58, 141.56, 142.71 (Ph). MALDI MS: *m/z* 901.89 [M$^+$–(Cl)].

3.2.2.2 Synthesis of (2,6-*i*Pr$_2$C$_6$H$_3$N PPh$_2$)$_2$Ge (**3.3**)

To the solution of **3.1** (2.166 g, 6.0 mmol in 60 mL toluene), *n*-BuLi (3 mL of 2M solution in hexane, 6.0 mmol) was added at room temperature. The reaction mixture was stirred for overnight. After 12 hours of stirring, $GeCl_2$·dioxane (0.693 g, 3.0 mmol) was added at the room temperature and additionally, reaction mixture was stirred for 12 hrs. It was filtered, concentrated and kept at 0 °C for crystallization. After five days of keeping, pale yellow colored crystals were obtained. Yield = 40% (0.95 g). Melting Point: 80-84 °C. ^{1}H NMR (400 MHz, C_6D_6, 298 K): δ 1.18 (*d*, 24H, -C*H*$_3$, *J* = 6.9 Hz), 3.46 (*m*, 4H, -C*H*CH$_3$), 7.01-7.12 (*m*, 14H, Ph), 7.45-7.51 (*m*, 12H, Ph); ^{31}P NMR (C_6D_6, 161.976 MHz, ppm): δ 59.79; ^{13}C NMR (C_6D_6, 100.613 MHz, ppm): δ 23.8 (-*C*H3), 28.15 (-*C*HCH$_3$), 123.68, 124.19, 128.40, 128.72, 131.42, 139.75, 142.58, 142.71 (Ph). MALDI MS: *m/z* 795.21 [M+H]$^+$.

3.2.3 X-ray crystallography details

The X-ray data for **3.2**, **3.3** and **3.4** were collected on a Bruker Smart Apex Duo diffractometer at 100 K using Mo Kα radiation (λ = 0.710 73 Å) and solved by direct methods and refined by full-matrix least-squares methods against F^2 (SHELXL-2014/6).[15] The crystallographic data file (including structure factors) for the **3.2, 3.3** and **3.4** have been deposited with the Cambridge Crystallographic Data Centre. The CCDC numbers are 1500994, 1500995, and 1500996 for **3.2, 3.3** and **3.4,** respectively. Copies of the data can be obtained free of charge upon application to the CCDC, 12 Union Road, Cambridge CB2 1EZ, U.K. (fax (international) + 44(1223)336-033; e-mail deposit@ccdc.cam.ac.uk).

3.2.4 Computational methodology

All the structures are optimized by DFT at the M06/def2-TZVPP//BP86/Def2-TZVPP level of theory[16] *Gaussian 09* program packages[17]. All the geometrical parameter are in good agreement with experimentally observed values. To calculate the orbital composition, NBO calculations were performed at the M06/Def2-TZVPP level of theory in *NBO 3.0* suite integrated into *Gaussian09*. The orbital composition was analyzed using *Multiwfn* program.[18] Molecular orbitals (MOs) and Electrostatic Potential (ESP) surface diagram are obtained by using *GaussView 5.0.9*.

3.3 Results and discussion

3.3.1 Synthesis and characterization

Chlorogermylene (2,6-*i*$Pr_2C_6H_3$NGeClPPh_2)$_2$ (**3.2**) was synthesized by the reaction of 2,6-*i*$Pr_2C_6H_3$N(Li)PPh_2 with one equivalent $GeCl_2$·dioxane in toluene at room temperature. The reaction of 2,6-*i*$Pr_2C_6H_3$N(Li)PPh_2 with $GeCl_2$·dioxane in 2:1 stoichiometry affords germylene (2,6-*i*$Pr_2C_6H_3$NPPh_2)$_2$Ge (**3.3**) (*Scheme 3.1*). Dimerization of chlorogermylene can be attributed to the insufficient bulk provided by amido ligand to protect the monomeric germanium center. Compounds **3.2** and **3.3** are characterized by NMR spectroscopy, mass spectrometry, and X-ray crystallography.

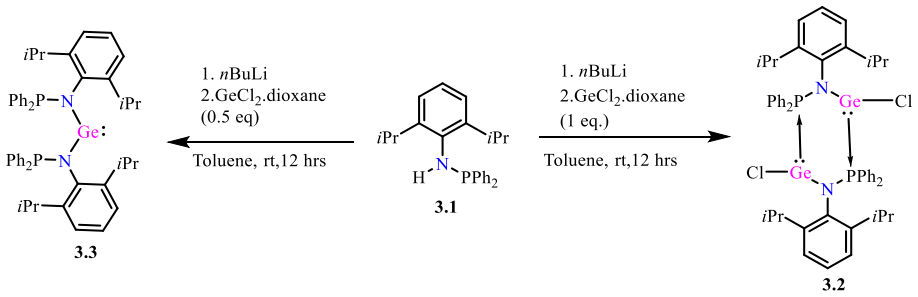

Scheme 3. 1**. Synthesis of **3.2** and **3.3

In the ^{1}H NMR spectrum of **3.2**, two doublets (δ 1.10, and 1.56 ppm) for -C*H*$_3$ for isopropyl groups and a multiplet at 4.03 ppm for -C*H*- are observed. The ^{31}P NMR spectrum shows a singlet at δ 48.26 ppm. The ^{1}H NMR spectrum for **3.3** shows one doublet at δ 1.18 ppm, which is slightly downfield shifted compared to that of ligand **3.1**. A multiplet at δ 3.45 ppm for the -C*H* proton of isopropyl group was observed. The ^{31}P NMR for **3.3** have one singlet peak at δ 59.69 ppm, which is downfield shifted compared to that of **3.2**.

Crystals for both the complexes suitable for X-ray crystallography were grown in toluene at 0 °C. The germylenes **3.2** crystallizes in the monoclinic space group *Pn* (Summary of crystal data is given in Table 1). The molecular structure of **3.2** is given in Figure 3.1. Although **3.2** is a dimer, the central $Ge_2P_2N_2$ six-membered ring is not formed by a center of symmetry. Geometrical parameters at both the germanium center are different. The Ge1-N1 and Ge2-N2 bond lengths were found to be 1.955(9) Å and 1.910(8) Å, respectively and they agree with those of Ge-N bond lengths reported in the literature.[8,19] The average Ge-P bond distance in **3.2** is 2.568 Å which matches with the compounds **70** and **71** (2.5725 and 2.5435 Å respectively)[14]. The bond angles connecting the two dimers [P2-Ge1-N1 102.3(3)°, N2-Ge2-P1 101.0(3)°] are almost equal. The two chlorine atoms are directed opposite to each other and form different angles at the germanium center with respective nitrogen atom [Cl1-Ge1-N1 97.9(3)°, N2-Ge2-Cl2 100.4(3)°. The latter is notably wider than that reported for a cyclic chlorogermylene [HC-(CMeNAr)2]GeCl [N1-Ge1-Cl1 95.00(8)°] [N1-Ge1-Cl1 95.00(8)°].[8]

Crystals of **3.3** were pale yellow and crystallized in triclinic space group *P-1*. In the molecular structure of **3.3** (*Figure 3.1*). The average Ge-N bond distance is of 1.865 Å, and it is slightly shorter than the Ge-N bond length observed in dimeric chlorogermylene. The N1-Ge1-N2 bond angle is 107.1(2)° and matches well to the N1-Ge1-N2 bond angles reported for $Ge\{N(SiMe_3)_2\}_2$ [107.1(2)°].[7b] Also, this bond angle is quite large compared

to that of PhC(N*t*Bu)$_2$Ge(2,6-*i*Pr$_2$C$_6$H$_3$NPPh$_2$) [101.13(6)°].[13] The sum of angles around both the N1 and N2 atoms are 360.1° and 360.0°, respectively, and it is concluded as there is planer geometry at nitrogen atoms.

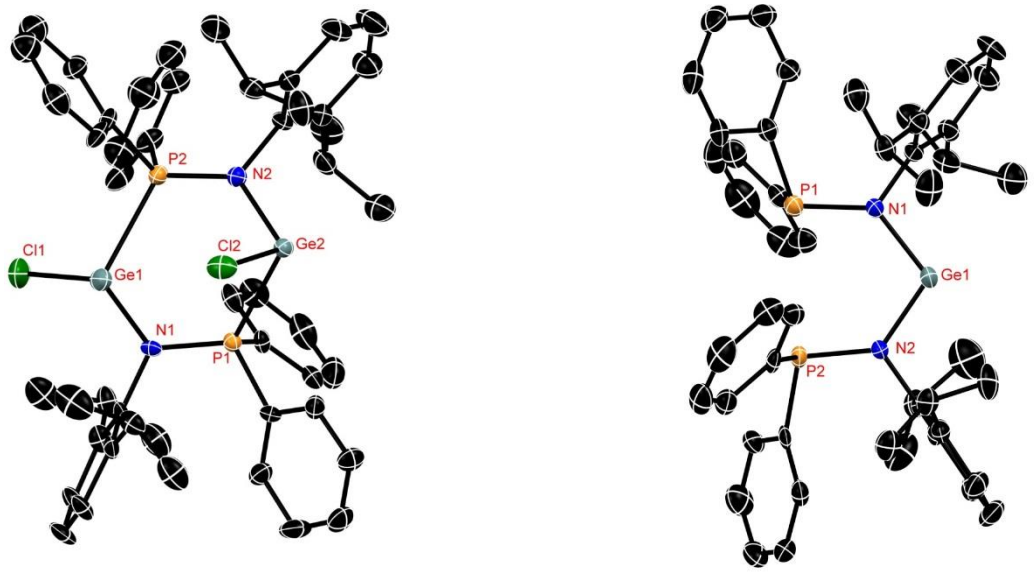

Figure 3.1 *Molecular structure of* ***3.2*** *(left) and* ***3.3*** *(right)at probability level of 30 %. Hydrogen atoms are omitted for clarity. Selected bond lengths (Å) and bond angles (deg). Calculated values at the BP86/def2-TZVPP level of theory are given in square brackets: for compoud* ***3.2****: Ge1-P2 2.612(3)[2.655], Ge2-P1 2.525(3)[2.572], Ge1-Cl1 2.293(4)[2.346], Ge2-Cl2 2.311(4)[2.365], Ge1-N1 1.955(9)[1.975], N1-P1 1.682(9)[1.681], Ge2-N2 1.910(8)[1.928], N2-P2 1.684(8)[1.704], N2-Ge2 1.910(8)[1.982]; P2-Ge1-Cl1 93.5(1)[95.0], Cl1-Ge1-N1 97.9(3)[98.6], P2-Ge1-N1 102.3(3)[107.6], N2-Ge2-Cl2 100.4(3)[100.4], Cl2-Ge2-P1 91.5[91.5](1), N2-Ge2-P1 101.0(3)[103.7]. for compond* ***3.3*** *: P1- N1 1.734(4)[1.756], N1-Ge1 1.870(3)[1.920], Ge1-N2 1.859(4)[1.920], N2 -P2 1.734(4)[1.756]; N1-Ge1-N2 107.1(2)[109.3].*

3.3.2 Serendipitous observation of compound 3.4

In the course of preparation of compound **3.2**, serendipitously, we also obtained few crystals of μ-oxo-bridged germylene **3.4** in the same flask. The formation of compound **3.4** is perhaps due to the hydrolysis of **3.2** in the presence of a little amount of moisture coming from the solvent. However, attempts to do the separate hydrolysis of **3.2** to establish the route for the synthesis of **3.4** were not successful. Therefore we could not perform the routine NMR characterization for **3.4** due to the lack of sufficient material. The compound **3.4** crystallizes in the triclinic space group *P*-1 (*Summary of crystal data*

is given in Appendix 1). The molecular structure of **3.4** is given in Figure 3.3. The Ge1-N1 and Ge2-N2 bond lengths are 1.978(3) Å and 1.983(3) Å, respectively and match well with the previous compounds. The Ge1-O1 and Ge2-O2 bond lengths are observed to be 1.821(3) Å and 1.806(3) Å, respectively and are in good accordance to the values reported for $\{(Bu^{i}_2ATI)Ge(O)OSiPh_3\}_2$ [Ge-O 1.787(3), 1.844(3) Å].[19b]

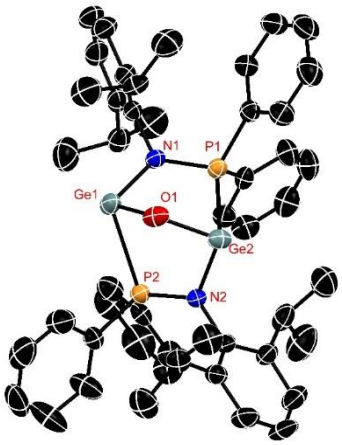

Figure 3.3 *Molecular structure of* ***3.4*** *at probability level of 50 %. Hydrogen atoms are omitted for clarity. Selected bond lengths (Å) and bond angles (deg). N1-Ge1 1.978(3), Ge1-P2 2.633(2), P2-N2 1.656(3), N2-Ge2 1.983(3), Ge2-P1 2.689(1), P1-N1 1.664(3), Ge1-O1 1.821(3), O1-Ge2 1.806(3); N1-Ge1-P2 101.92(8), P1-Ge2-N2 98.96(8), Ge1-O1-Ge2 122.9(1), Ge1-N1-P1 118.2(1), Ge2-N2-P2 116.9(1).*

3.3.3 Theoretical investigation compounds of 3.2 and 3.3

All the geometrical parameter of the computationally optimized structures are in good agreement with experimentally observed values. The NBO analysis of compound **3.2**, shows that the HOMO of **3.2** is non-bonding in nature and primarily based on lone pair of Ge (44.4 %) and also delocalized on P (17.1%), N (15.2%) and Cl (14.0%). The HOMO-1 is also dominated by germanium character and contributions from other non-C, H atom is relatively low. Dominance of lone pair of Ge atom, in MOs decrease from HOMO to HOMO-2 unlike that of 2,5-Bis-{(pyrrolidino)-methyl}-pyrrole based germylene where HOMO is based on π-electron of pyrrole ring and the lone pair of germanium is predominantly present in HOMO-1 and HOMO-2.[20] The LUMO is delocalized over the

phenyl ring of the phosphido moiety, Ge and P atoms. The energy gap between HOMO-LUMO is 249.90 kJ/mol.

In contrast to HOMO of **3.2**, HOMO of **3.3** is based on lone pair of phosphorus (63.2%). The lone pair of Ge are much stabilized, and it is present in HOMO-2 and HOMO-3 (*Figure 3.4*). The LUMO of **3** is the empty *4p* orbital of Ge (75% contribution). The lone pair of nitrogen for both the complexes is highly stabilized (HOMO-6, and HOMO-7 for **3.2** and HOMO-6 for **3.3**). Since the lone pair of the Ge is more stabilized than that of P, its nucleophilicity is less compare to the phosphorus center.

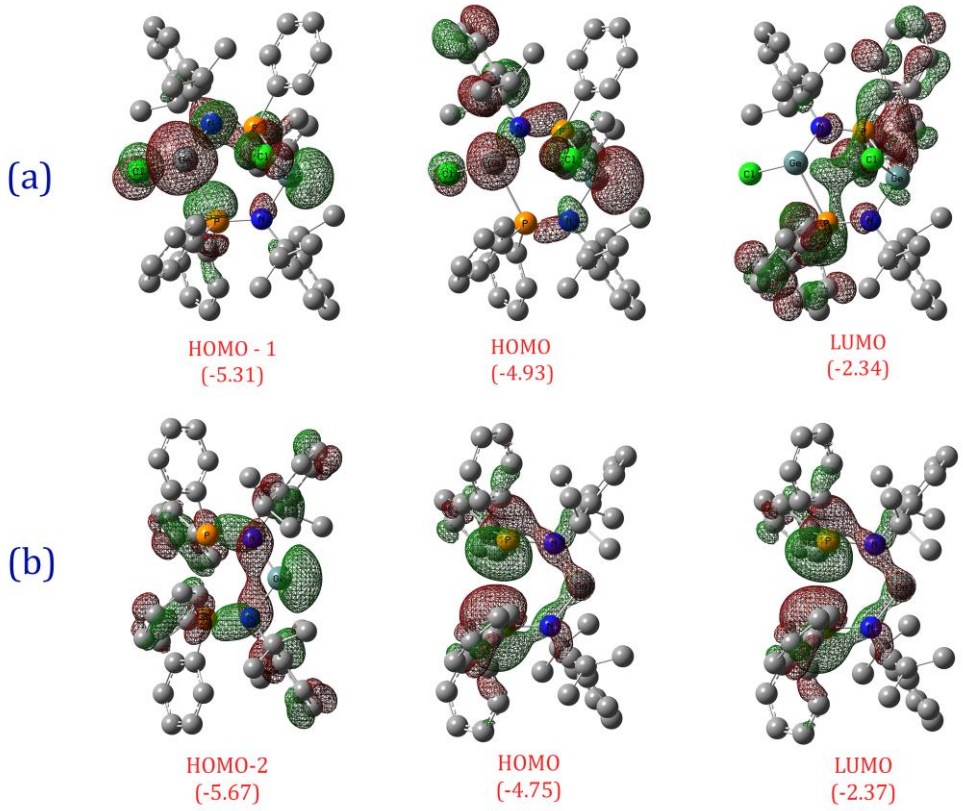

Figure 3.4 *DFT derived surface diagrams of relevant MOs of (a)* ***3.2*** *and (b)* ***3.3*** *at the BP86/Def2-TZVPP level of theory (isosurface value = 0.03). The energy of MOs in eV are given in parentheses.*

We have also analyzed the molecular electrostatic potential (ESP) surface mapped onto a constant electron density surface to investigate the nucleophilic center further. For complex **3.2**, the global minimum value (-28.0 kcal/mol) of ESP is observed on the one Cl center (as shown in red in ESP surface diagram). The global minimum of ESP in **3.3** [-22.4 kcal/mol] is found in the direction of the lone pair of phosphorus atom while the ESP

value observed in the direction of germanium's lone pair is -13.61 kcal/mol. The comparison of ESP for **3.3** shows that the P-center is more nucleophilic than the Ge-center and this result is reminiscent to our previous report on amidinato-amido-germylene PhC(NtBu)$_2$Ge(2,6-iPr$_2$C$_6$H$_3$NPPh$_2$).[43]

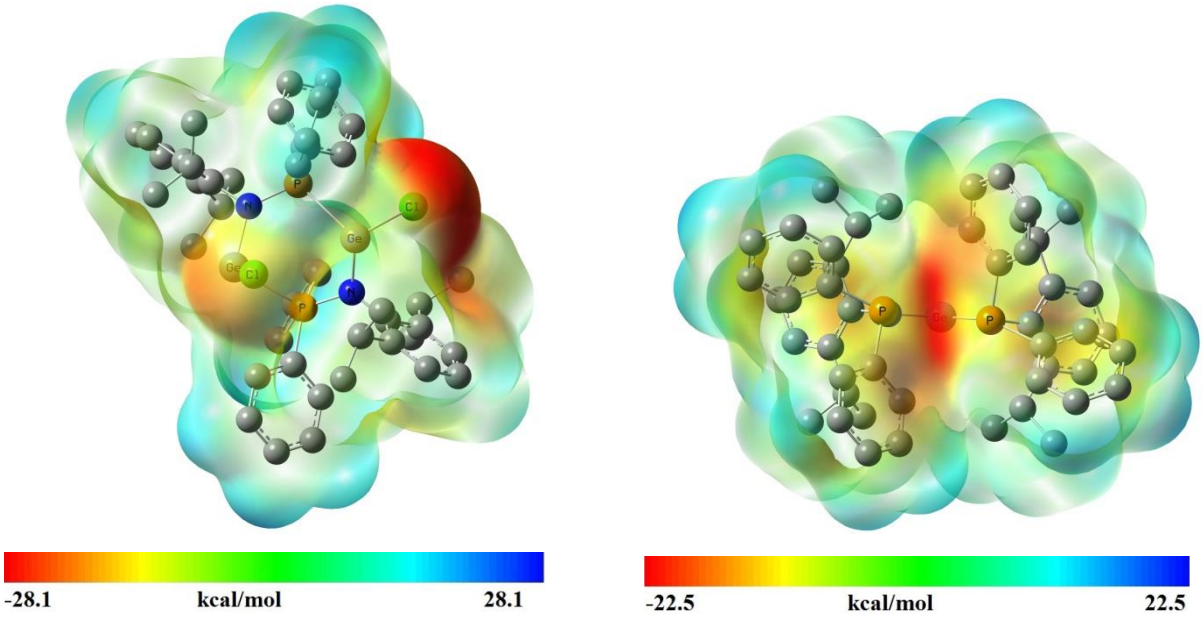

Figure 3.5 *Electrostatic potential of (a)* ***3.2****, and (b)* ***3.3*** *mapped onto electron density surface (Isosurface value=0.001) at BP86/Def2-TZVPP level of theory.*

3.3.4 Reactivity of compound 3.3

As it has been shown that the nucleophilicity of P center is more in comparison to Ge center in compound **3.3**, we wanted to investigate it experimentally. For that, we treated compound **3.3** with AuCl·SMe$_2$ and Me$_3$NO.

3.3.4.1 Reaction with AuCl and subsequent addition of AgSbF$_6$

The compound **3.3** was treated with 1 equivalent of AuCl·SMe$_2$ in toluene. After stirring of 8hrs, the chloride scavenger AgSbF$_6$ (1 eq.) was added in reaction mixture to abstract the chloride from AuCl for generation of Au$^+$ coordinated through germylenes **3.3** (*Scheme 3.2*). It was expected that the active lone pair of Ge would donate to electrophilic, Au$^+$ species. However, the observed compound was **3.5**, where P, instead of Ge, donates and the molecule was cleaved from Ge-N bond. Since it was a mixture of the **3.5** and some unidentified product, the NMR spectra were not interpretable. The compound **3.5** was

only characterized by X-ray crystallography, and the molecular structure is given in *Appendix 3, Figure 3A.1*.

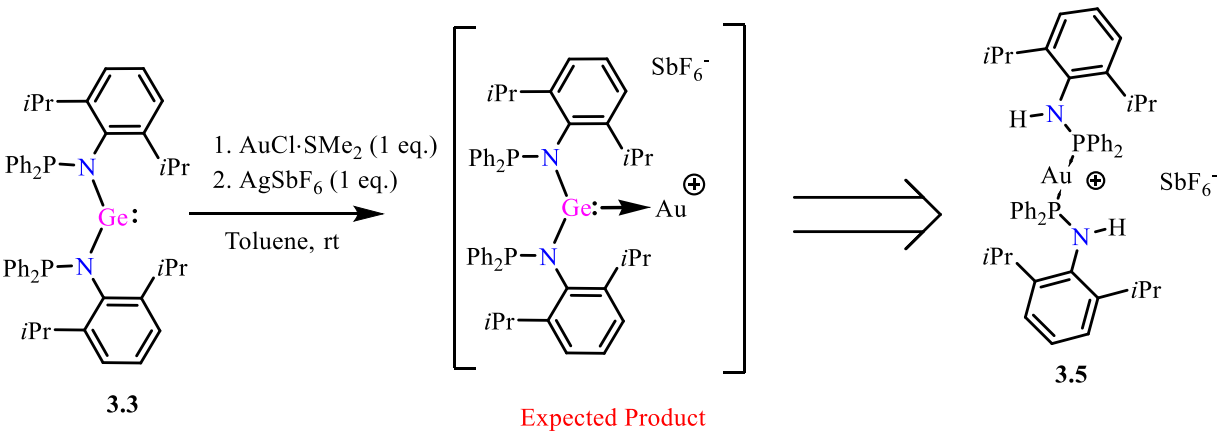

Scheme 3.2 *Reaction of* ***3.3*** *with* $AuCl{\cdot}SMe_2$

3.3.4.2 Reaction with Me_3NO

We treated compound **3.3** with Me_3NO the hope that the nascent oxygen generated form Me_3NO would react with **3.3** to afford the product where Ge would be singly or doubly bonded to oxygen (*Scheme 3.3*). However, we observed product **3.6** where phosphorus is bonded to oxygen. The addition of oxygen to phosphorus confirms that the P center is more nucleophilic as compare to Ge center. The molecular structure is given in *Appendix 3, Figure 3A.1.*

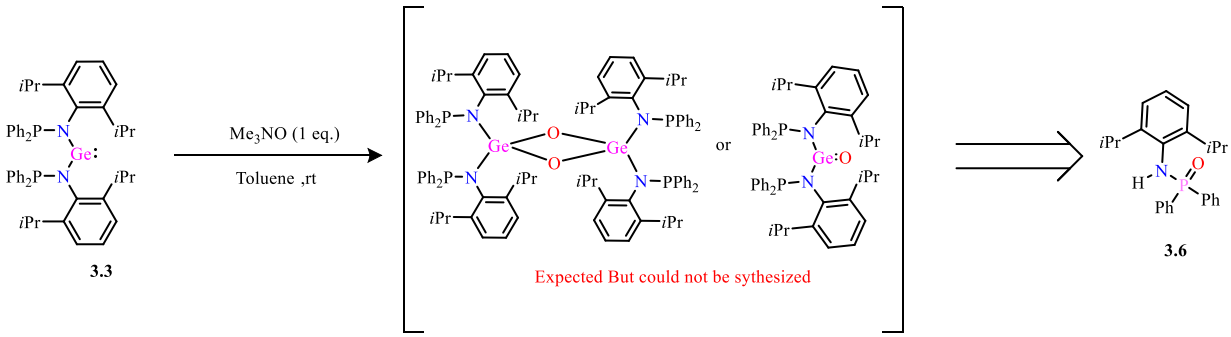

Scheme 3.3 *Reaction of* ***3.3*** *with* Me_3NO

3.4 Conclusions

In summary, we have synthesized α-phsphinoamido- supported chlorogermylene (**3.2**) and germylene (**3.3**). Both the complexes are well characterized and a new addition to the 14th group low valent complexes supported by α-phsphinoamido- ligand (**3.1**). Also, we serendipitously obtained oxygen bridged (μ_2-O) bis-germylene (**3.4**). The theoretical calculation indicates that nucleophilic center in **3.2** is on the one Cl while in the case of **3.3**, it is present on both the P-center. In complex **3.3**, comparison of electrostatic potential in the direction of the lone pair of Ge and P shows that P-center is more nucleophilic. The experimental confirmation of high nucleophilicity of phosphorus is the reactivity of P-center is greater towards electrophilic species (Au^+ and nascent oxygen) as compared to that of Ge center.

3.5 References

1. (a) Mizuhata, Y.; Sasamori, T.; Tokitoh, N. *Chem. Rev.* **2009**, *109,* 3479; (b) Barrau, J.; Escudie, J.; Satge, J. *Chem. Rev.* **1990**, *90*, 283; (b) Kuhl, O. Coord. *Chem. Rev.* **2004**, *248*, 411; (c) Nagendran, S.; Roesky, H. W. *Organometallics* **2008**, *27*, 457; (d) Fischer, R. C.; Power, P. P. *Chem. Rev.* **2010**, *110*, 3877; (e) Tokitoh, N.; Okazaki, R. *Coord. Chem. Rev*. **2000**, *210*, 251; (f) Escudie´, J.; Ranaivonjatovo, H.; Rigon, L. *Chem. Rev.* **2000**, *100*, 3639; (g) Escudie´, J.; Ranaivonjatovo, H. *Organometallics* **2007**, *26*, 1542.
2. (a) Frey, G. D.; Lavallo, V.; Donnadieu, B.; Schoeller, W. W.; Bertrand, G. *Science* **2007**, *316*, 439; (b) Peng, Y.; Ellis, B. D.; Wang, X.; Power, P. P. *J. Am. Chem. Soc.* **2008**, *130*, 12268; (c) Jana, A.; Objartel, I.; Roesky, H. W.; Stalke, D. *Inorg. Chem.* **2009***, 48,* 798; (d) Wang, W.; Inoue, S.; Yao, S.; Driess, M. *Organometallics* **2011**, *30*, 6490. (e) Rodriguez, R.; Gau, D.; Contie, Y.; kato, T.; Saffon-Merceron, N.; Baceire-do, A. *Angew. Chem. Int. Ed.* **2011**, *50*, 11492; (f) Tan, G.; Wang, W.; Blom, B.; Driess, M. *Dalton Trans.* **2014**, *43*, 6006; (g) Lawrence, N. J.; Bushell, S. M. *Tetrahedron Letters* **2000**, *41*, 4507; (h) Hadlington, T. J.; Hermann, M.; Frenking, G.; Jones, C. *J. Am. Chem. Soc.* **2014**, *136*, 3028; (i) Siwatch, R. K.; Nagendran, S. *Chem. Eur. J.* **2014**, *20*, 13551; (j) Blom, B.; Enthaler, S.; Inoue, S.; Irran, E.; Driess, M. *J. Am. Chem. Soc.* **2013**, *135*, 6703; (k) A´lvarez-Rodríguez, L.; Cabeza, J. A.; Ferná ndez-Colinas, J. M.; García-A´ lvarez, P.; Polo, D. *Organometallics* **2016**, *35*, 2526.

3. (a) Jutzi, P.; Burford, N. *Chem. Rev*. **1999**, *99*, 969; (b) Kira, M.; Ishida, S.; Iwamoto, T. *Chem. Rec*. **2004**, *4*, 243; (c) Kira, M. *J. Organomet. Chem*. **2004**, *689*, 4475; (d) Wang, W.; Inoue, S.; Yao, S.; Driess, M. *Chem. Commun.*, **2009**, 2661.
4. (a) Wang, W.;Inoue, S.; Enthaler, S.; Driess, M. *Angew. Chem. Int. Ed.* **2012**, *51*, 6167; (b) Ochiai,T.; Franz, D.; Wu, Xiao-Nan;Inoue, S. *Dalton Trans*. **2015**, *44*, 10952; (c) Inoue, S.; Driess, M. *Organometallics* **2009**, *28*, 5032.
5. (a) Hurni, K. L.; Rupar, P. A.; Payne, N. C.; Baines, K. M. *Organometallics* **2007**, *26*, 5569; (b) Tsumuraya, T.; Sato, S.; Ando, W. *Organometallics* **1988**, *7*, 2015; (c) Masamune, S.; Hanzawa, Y.; Williams, D. J. *J. Am. Chem. Soc.* **1982**, *104*, 6136; (d) Snow, J. T.; Murakami, S.; Masamune, S.; Williams, D. J. *Tetrahedron Lett*. **1984**, *25*, 4191.
6. Jutzi, P.; Becker, A.; Stammler, H. G.; Neumann, B. *Organometallics* **1991**, *10*, 1647.
7. (a) Gynane, M. J. S.; Harris, D. H.; Lappert, M. F.; Power, P. P.; Riviere, P.; Rivierebaudet, M. *J. Chem. Soc., Dalton Trans.* **1977**, 2004; (b) Chorley, R. W.; Hitchcock, P. B.; Lappert, M. F.; Leung, W. P.; Power, P. P.; Olmstead, M. M. *Inorg. Chim. Acta.* **1992**, *200*, 203; (c) Lappert, M. F.; Slade, M. J.; Atwood, J. L.; Zaworotko, M. J. *J. Chem. Soc., Chem. Commun*. **1980**, 621; (d) Riviere-Baudet, M.; Dahrouch, M.; Gornitzka, H. *J. Organomet. Chem.* **2000**, *595*, 153; (e) Hitchcock, P. B.; Lappert, M. F.; Thorne, A. J. *J. Chem. Soc., Chem. Commun.* **1990**, 1587-1589; (f) Veith, M. *Angew. Chem., Int. Ed. Engl.* **1987**, *26*, 1.
8. Ding, Y.; Roesky, H. W.; Noltemeyer, M.; Schmidt, H. G.; Power, P. P.; *Organometallics* **2001**, *20*, 1190.
9. Driess, M.; Yao, S.; Brym, M.; Wüllen; C. *Angew. Chem. Int. Ed*. **2006**, *45*, 4349.
10. Hadlington, T. J.; Li, J.; Jones, C. *Can. J. Chem.* **2014**, *92*, 427.
11. Goel, S. C.; Chiang, M. Y.; Rauscher, D. J.; Buhro, W. E. *J. Am. Chem. Soc.* **1993**, *115*, 160.
12. Driess, M.; Janoschek, R.; Pritzkow, H.; Rell, S.; Winkler, U. *Angew. Chem., Int. Ed. Engl.* **1995**, *34*, 1614.
13. Parvin, N.; Pal, S.; Rojisha, V. C.; De, S.; Parameswaran, P.; Khan, S. *ChemistrySelect*, **2016**, *1*, 1991 .
14. Böttcher, T.; Jones, C. *Main Group Met. Chem.* **2015**, *38*, 165.
15. (a) T. Kottke, D. Stalke, *J. Appl. Crystallogr*. **1993**, *26*, 615; (b) D. Stalke, *Chem. Soc. Rev.* **1998**, *27*, 171; (c) Sheldrick, G. M. *Acta Crystallogr.* **2015**, *A71*, 3; (d) Sheldrick, G. M. *Acta Crystallogr.* **2015**, *C71*, 3; (e) T. Schulz, K. Meindl, D. Leusser, D. Stern, M. Ruf, G. M. Sheldrick, D. Stalke, *J. Appl. Crystallogr*. **2009**, *42*, 885; (f) Krause, L.; Herbst-Irmer, R.; Sheldrick, G. M.; Stalke, D. *J. Appl. Crystallogr.* **2015**, *48*, 3.

16. (a) Becke, A. D. *Phys. Rev. A* **1988**, *38*, 3098; (b) Perdew, J. P. *Phys. Rev. B* **1986**, *33*, 8822; (c) Zhao, Y.; Truhlar, D. G. *Theor. Chem. Acc.* **2008**, 120, 215; (d) Weigend, F.; Ahlrichs, R. *Phys. Chem. Chem. Phys.* **2005**, *7*, 3297.
17. Gaussian 09, Revision D.01, M. J. Frisch, G. W. Trucks, H. B. Schlegel, G. E. Scuseria, M. A. Robb, J. R. Cheeseman, G. Scalmani, V. Barone, B. Mennucci, G. A. Petersson, H. Nakatsuji, M. Caricato, X. Li, H. P. Hratchian, A. F. Izmaylov, J. Bloino, G. Zheng, J. L. Sonnenberg, M. Hada, M. Ehara, K. Toyota, R. Fukuda, J. Hasegawa, M. Ishida, T. Nakajima, Y. Honda, O. Kitao, H. Nakai, T. Vreven, J. A. Montgomery, Jr., J. E. Peralta, F. Ogliaro, M. Bearpark, J. J. Heyd, E. Brothers, K. N. Kudin, V. N. Staroverov, T. Keith, R. Kobayashi, J. Normand, K. Raghavachari, A. Rendell, J. C. Burant, S. S. Iyengar, J. Tomasi, M. Cossi, N. Rega, J. M. Millam, M. Klene, J. E. Knox, J. B. Cross, V. Bakken, C. Adamo, J. Jaramillo, R. Gomperts, R. E. Stratmann, O. Yazyev, A. J. Austin, R. Cammi, C. Pomelli, J. W. Ochterski, R. L. Martin, K. Morokuma, V. G. Zakrzewski, G. A. Voth, P. Salvador, J. J. Dannenberg, S. Dapprich, A. D. Daniels, O. Farkas, J. B. Foresman, J. V. Ortiz, J. Cioslowski, and D. J. Fox, Gaussian, Inc., Wallingford CT, **2013**.
18. (a) Lu, T.; Chen, F. *J. Comput. Chem.* **2012**, *33*, 580; (b) Lu, T.; Chen, F. *J. Mol. Graphics Modell.* **2012**, *38*, 314.
19. (a) Foley, S. R.; Zhou, Y.; Yap, G. P. A.; Richeson, D. S. *Inorg. Chem.* **2000**, *39*, 924; (b) Karwasara, S.; Siwatch, R. K.; Jha, C. K.; Nagendran, S. *Organometallics* **2015**, *34*, 3246.
20. Maaß, C.; Andrada, D. M.; Mata, R. A.; Herbst-Irmer, R.; Stalke, D. *Inorg. Chem.* **2013**, *52*, 9539.

CHAPTER 4

Acyclic α-Borylamido-Germylene and Stannylene

Synthesis and Application in Hydroboration Reaction

4.1 Introduction

There is a growing number of recent developments showcasing the use of compounds with main group elements as catalysts or pre-catalysts for organic transformation driven by the non-toxicity, low synthetic cost, and most importantly high terrestrial abundance of main group elements.[1,2] In organic chemistry, hydroboration is an efficient route for synthesizing alcohols from the corresponding aldehydes and ketones. Several research group across the globe has successfully employed the transition and rare earth metal's complexes in hydroboration reactions.[3] In recent years, compounds with group 13-15 elements have also been explored in hydroboration of carbonyl compounds thanks to the contributions from the groups of Roesky,[4a] Kinjo,[4b] Aldridge,[4c] Jones,[4d] Nembenna,[4e] Sen,[4f] Zhao,[4g] Wesemann,[4h] Melen,[4i] and others (*Chart 4.1*).[4]

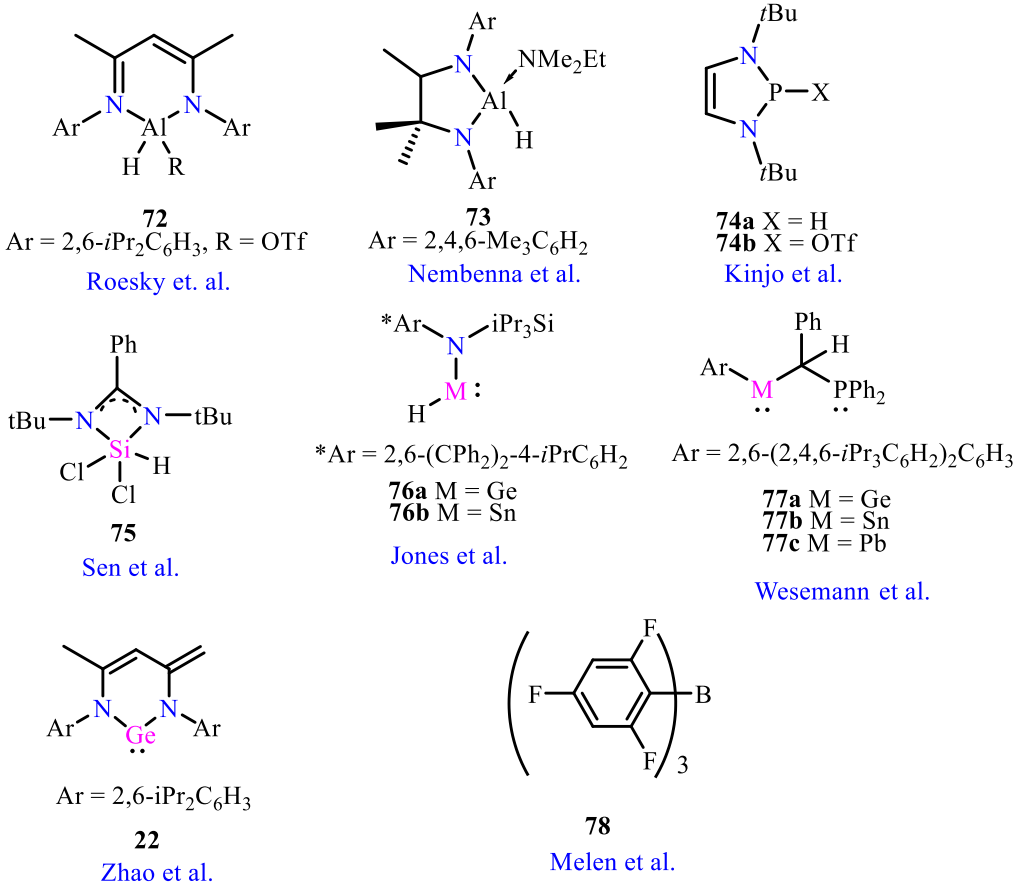

Chart 4.1 *Selected examples of catalysts derived from p-block elements for hydroboration of aldehydes and ketones.*

The current state of the art germylene and stannylene chemistry is very rich but primarily restricted to the structural characterization, bonding elucidation, and small molecule activation.[5] However, as seen in *chart 4.1*, there are recent pioneering works from the groups of Jones, Zhao, and Wesemann, who used low valent group 14 compounds as single-site catalysts for hydroboration reactions. While the Jones' group have used germylene and stannylene hydrides, Zhao et al. explored the utility of a previously reported N-heterocyclic germylene, and Wesemann and co-workers reported the hydroboration with intramolecularly stabilized tetrylenes (Ge-Pb) Lewis pairs. It is of note here that the substrate scope for Wesemann's catalyst is very limited. Theoretical calculations on α-phosphinoamido-germylene, [(2,6-*i*Pr$_2$C$_6$H$_3$NPPh$_2$)$_2$Ge],[6] discussed in the previous chapter, divulged that the HOMO of this germylene resides on the phosphorus atom and thereby the nucleophilicity of the P center is greater than the Ge center with a HOMO-LUMO gap of 59.73 kcal/mol. We envisaged that if we could replace the P atom with an electron deficient element, then the HOMO may shift to the Ge center. To verify our hypothesis, we have replaced the P atom with B and prepared acyclic α-borylamido-germylene and stannylene of composition (2,6-*i*Pr$_2$C$_6$H$_3$NBCy$_2$)$_2$E (E= Ge (**4.2**), Sn (**4.3**)). Subsequent theoretical calculations confirm our hypothesis. In a further step, we have used them for selective hydroboration of aldehydes.

4.2 Experimental section

4.2.1 General remarks

All the experiments were performed under inert atmosphere using standard Schlenk techniques. MBRAUN solvent purification system MB SPS-800 was used for drying the solvents (Toluene, Ether and *n*-Pentane). Diisopropylaniline was distilled over KOH before use. All other chemicals purchased from Sigma-Aldrich were used without further purification. $CDCl_3$ or C_6D_6 was used to record the NMR spectra using Bruker 400 MHz spectrometer. NMR spectra were referenced to external $SiMe_4$ (^1H, and ^{13}C). Mass spectra were recorded using AB Sciex, 4800 plus MALDI TOF/TOF mass spectrometer.

4.2.2 Synthesis

4.2.2.1 Synthesis of Ligand, 2,6-*i*Pr$_2$C$_6$H$_3$NHBCy$_2$ (**4.1**)

Diisopropylaniline (1.79 g, 1.89 mL, 10 mmol) was taken in a 250 mL flask with 100 mL of diethyl ether, and 5 mL of 2M solution of n-BuLi was added to the cooled (-78 ^{o}C). The

solution was then allowed to come to the room temperature and further stirred for 1 hr. After stirring for 1 hr, the reaction mixture was cooled again to -78 ^{o}C and 10 mL of 1M solution of chlorocyclohexylboarne was added. After 12 hrs stirring solution was filtered and the solvent was evaporated to get the viscous liquid of ligand **4.1**. Yield: 2.8 g (80 %). ^{1}H NMR (400 MHz, $CDCl_3$) δ 7.29 -7.11(m, 6H, *Ph*), 5.1 (s, 1H, -N*H*), 3.37 – 3.22 (m, 1H, -C*H*), 1.87- 0.77 (m, 22H, -Cy), 1.28 (d, J = 6.9 Hz, 6H, -CH_3), 1.18 (d, J = 6.9 Hz, 6H, -CH_3); ^{13}C NMR (101 MHz, $CDCl_3$): δ 145.03, 137.72, 125.80, 122.74, 29.96, 28.07, 27.41, 26.98, 24.53, 22.42; ^{11}B NMR (128 MHz, $CDCl_3$): δ 48.10.

4.2.2.2 Synthesis of (2,6-*i*Pr$_2$C$_6$H$_3$NBCy$_2$)$_2$Ge (**4.2**)

1 mL of *n*-BuLi (2M) was added to the solution of ligand **4.1** (0.71 g, 2 mmol) in ~ 60 mL of Et_2O and stirred for overnight. After that, 0.231 g (1 mmol) of $GeCl_2$·dioxane was added to the reaction mixture and left for stirring for additional 12 hrs. The reaction mixture was then filtered and the filtrate was reduced to ~15 mL. The concentrated solution was kept for crystallization at 0 ^{o}C. Yield: 0.3 g (38 %). Melting Point: decomposes around ~70-80 ^{o}C. ^{1}H NMR (400 MHz, $CDCl_3$): δ 7.28- 7.13 (6H, Ph), 3.46 (sept, 4H, -C*H*), 1.80-1.11 (m, 44H, -Cy), 1.36 (d, J = 6.8 Hz, 12H,-CH_3), 1.09 (d, J = 6.8 Hz, 12H, -CH_3); ^{13}C NMR (101 MHz, $CDCl_3$): δ 145.0, 135.0, 125.7, 124.6, 122.7, 29.6, 28.0, 27.7, 27.1, 26.7, 25.8, 24.5, 22.4; ^{11}B NMR (128 MHz, $CDCl_3$): δ 47.67. MALDI MS (m/z) calculated for $C_{48}H_{78}B_2GeN_2$ = 777.33; mass observed (m/z) = 800.46 $[M+Na]^+$. Elemental Analysis (%): calcd. C 74.52, H 10.19, N 3.64. Found C 74.82, H 9.89, N 3.28.

4.2.2.3 Synthesis of (2,6-*i*Pr$_2$C$_6$H$_3$NBCy$_2$)$_2$Sn (**4.3**)

4.1 (1.42 g, 4 mmol) was dissolved in ~60 mL of Et_2O and 2 mL of 2M solution of *n*-BuLi (at room temperature) was added to the reaction mixture. After stirring of 12 hrs, $SnCl_2$ (0.380 g, 2 mmol) was added to the reaction mixture. The reaction mixture was filtered after 12 hrs and filtrate was reduced to ~15 mL. The concentrated solution was kept for crystallization at 0 ^{o}C. Yield: 1.2 g (75%). Melting Point: 140 ^{o}C. ^{1}H NMR (400 MHz, $CDCl_3$) δ 7.2-7.1 (6H, Ph), 3.5 (m, 4H, -C*H*), 1.8-0.5 (m, 68H, -Cy and –CH_3); ^{13}C NMR (101 MHz, C_6D_6) δ; 144.8, 137.5, 126.3, 122.9, 118.6, 29.9, 28.1, 27.7, 27.3, 25.7, 24.4, 22.4,^{119}Sn NMR (149 MHz, C_6D_6) δ 327.22; ^{11}B NMR (128 MHz, C_6D_6) δ 47.69. MALDI MS (m/z) calculated for $C_{48}H_{78}B_2SnN_2$ = 823.43; mass observed (m/z) = 847.45 $[M+Na]^+$. Elemental Analysis (%): calcd. C 70.01, H 9.55, N 3.40. Found C 69.72, H 9.32, N 3.25.

4.2.3 X-ray crystallography details

The X-ray diffractions for compound **4.2** and **4.3** were recorded on the Bruker Venture D8 at the 150 ˚C temperature using molybdenum x-ray source. The structures of **4.2** and **4.3** were solved by direct methods and refined by full-matrix least-squares methods against F^2 (SHELXL-2014/6).[7] Crystallographic data file (including structure factors) for the **4.2** and **4.3** have been deposited with the Cambridge Crystallographic Data Centre. The CCDC numbers are 1835429 and 1835428 for **4.2**and **4.3** respectively. Copies of the data can be obtained free of charge upon application to the CCDC, 12 Union Road, Cambridge CB2 1EZ, U.K. (fax (international) + 44(1223)336-033; e-mail deposit@ccdc. cam.ac.uk).

4.2.4 Computational methodology

All the structures are optimized by DFT at the M06/def2-TZVPP//BP86/Def2-TZVPP level of theory[8] *Gaussian 09* program packages[9]. All the geometrical parameter are in good agreement with experimentally observed values. To calculate the orbital composition, NBO calculations were performed at the M06/Def2-TZVPP level of theory in *NBO 3.0* suite integrated into *Gaussian09*. The orbital composition was analyzed using *Multiwfn* program.[10]

4.3 Results and discussions

4.3.1 Synthesis and characterization

The tetrelylenes **4.2** and **4.3** were synthesized by treating the lithium salt of **4.1** with 0.5 equivalent of $GeCl_2$·dioxane or $SnCl_2$ respectively (*Scheme 4.1*). Both the compounds crystallize in toluene and give dark orange crystals. The ^{1}H NMR spectrum of **4.2**, shows two doublet peaks at δ 1.36 (J = 6.8 Hz) and 1.09 (J = 6.8 Hz) for –CH_3 group and the signal for cyclohexyl (Cy) protons appear in the range of δ 1.80-1.11 ppm. The septet peak of –C*H* is observed at δ 3.46 ppm. In the ^{11}B NMR spectrum of **4.2**, a single peak appears at δ 47.67 ppm, which matches well with tri-coordinated borane compounds[11] and substantially downfield shifted as compared to four-coordinated germanium-borane adducts.[12] The ^{1}H spectrum of **4.3** shows similar resonances as those of **4.2** (*vide infra*). The resonance for the boron atom appears at δ 47.69, which is shifted downfield compared to those in [Sn{B(NDippCH)$_2$}$_2$H$_2$] (δ 28.3 ppm), [Sn{B(NDippCH)$_2$}$_2$(H)(SiH$_2$Ph)] (δ 28.1 ppm) and [Sn{B(NDippCH)$_2$}$_2$(H) (BH$_2$·NMe$_3$)]

(δ 31.9 for 3-coordinate boryl, −8.26 for BH_2NMe_3) where the tin atom is directly bonded to the boron atom.[13] A singlet peak at δ 327.22 ppm is observed in the ^{119}Sn NMR spectrum of **4.3**, shifted downfield compared to [HC(CMeNDipp)$_2$]Sn(*t*-Bu) (δ 259 ppm)[13] and 1,2-C_6H_4[N(CH_2*t*-Bu)]Sn (δ 269 ppm)[14] but upfield than those reported for Sn[N($SiMe_3$)(Dipp)]$_2$ (δ 440 ppm) and Sn[N($SiMe_2Ph$)$_2$]$_2$ (δ 501 ppm).[15]

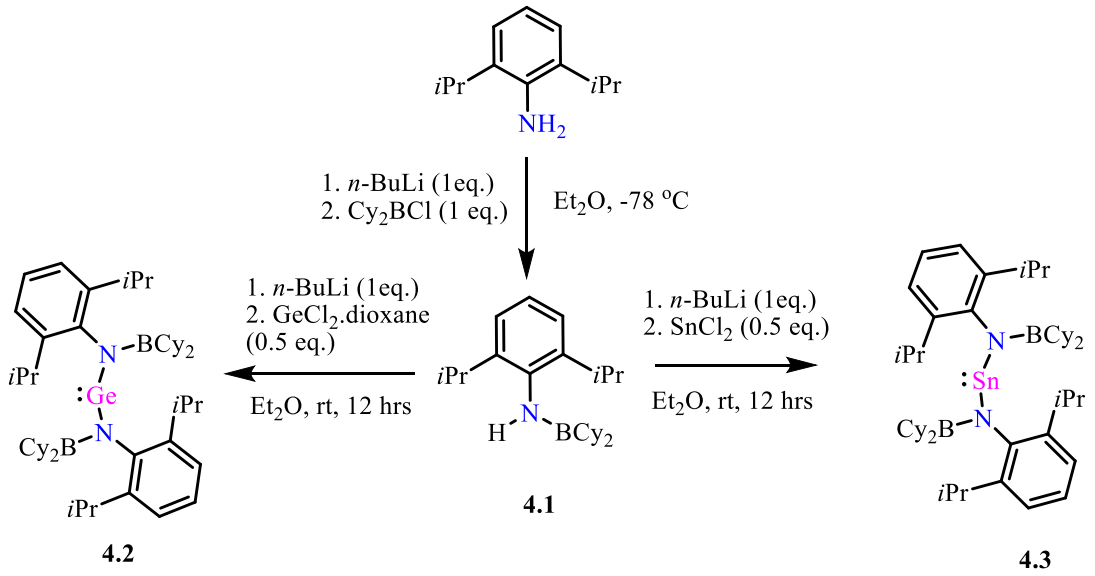

***Scheme 4.1**. Synthesis of borylamido-germylene **4.2**, and stannylene **4.3**.*

Figures 4.1 displays the molecular structures of **4.2** and **4.3**. Both the compounds crystallize in orthorhombic space group, *Pccn*.[7] Both **4.2** and **4.3** are monomeric. The Ge center is three coordinate (considering the lone pair of electrons on Ge). The two Ge-N bond lengths are identical (1.938(1) Å) and the N1-Ge1-N1 bond angle is of 106.78° The Ge1-N1 bond length is slightly greater than the average Ge-N bond length in the previously reported α-phosphinoamido-germylene (1.865 Å).[6] The difference in the bond lengths can be attributed to the replacement of the P atom by the B atom which pulls off the electron density from the adjacent N atom leading to the lengthening of the Ge-N bond in **4.2**.

The geometry around the Sn atom in **4.3** is similar to that in **4.2** with slight changes in the bond lengths and angles. The Sn1-N1 bond of **4.3** is 2.141 Å, and the N1-Sn1-N1 bond angle is 104.17°. The Sn1-N1 bond length is well matching with the values observed in

$Sn[N(SiMe_3)(Dipp)]_2$ (Sn-N_{avg} 2.094Å) and $Sn[N(SiMe_2Ph)_2]_2$ (Sn-N_{avg} 2.129 Å).[15] The B-N bond distances in **4.2** and **4.3** are 1.404(3) and 1.401(4) Å, respectively, which are substantially shorter than the B–N dative bond (~1.58 Å),[16] but match well with the N-B bond reported in $[N(2,6\text{-}i Pr_2C_6H_3)(PPh_2)(BCy_2)]$ (1.457(2) Å).[11]

Figure 4.1 *The molecular structure of* ***4.2*** *(left) and* ***4.3*** *(right) with 50% probability level of the thermal ellipsoids. Hydrogen atoms are omitted for clarity. Selected bond length (Å) and angles (degree). Calculated values given in square brackets: for compound* ***4.2*** *Ge1-N1 1.938(1)[1.99], N1-B1 1.404(3)[1.43]; N1-Ge1-N1 106.78[110.36], C1-N1-Ge1 115.0[112.00], C1-N1-B1 126.0(2)[126.75], Ge1-N1-B1 114.3[115.90]; for compound* ***4.3*** *Sn1-N1 2.141 (1)[2.198], N1-B1 1.401(4)[1.419]; N1-Sn1-N1 104.17[110.87], C1-N1-Sn1 115.1[111.134], C1-N1-B1 127.0(2)[128.28], Sn1-N1-B1 114.0[116.17].*

4.3.2 Theoretical calculations

The NBO calculations show that the HOMOs of **4.2** and **4.3** reside on lone pair of Ge (27.1 %), N (28.5 %) and Sn (19.2 %), N (29.0%), respectively and also partially delocalized over phenyl ring of dipp moieties (*Figure 4.2*). The LUMOs for both complexes are majorly comprised of the vacant *p*-orbitals of Ge (75.3 %) and Sn (62.0 %). The HOMO-LUMO energy gaps are 48.43 kcal/mol (2.10 eV) and 48.69 kcal/mol (2.11 eV) for **4.2** and **4.3**, respectively, and these energy gaps are much lower than that reported for phosphinoamido-germylene (59.73 kcal/mol).

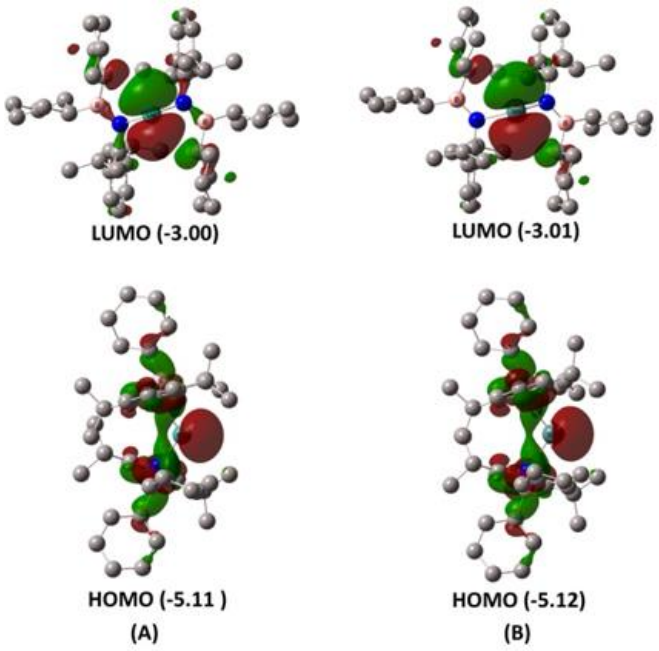

Figure 4.2 *The molecular orbitals surface diagrams (isosurface value 0.03) of (A)* ***4.2*** *and (B)* ***4.3*** *at the BP86/Def2TZVPP level of theory.*

4.3.3 Hydroboration of aromatic aldehydes using 4.2 and 4.3 as catalyst

With the two new tetrelylenes, we investigated their potential as hydroboration catalysts for aldehydes. The optimization of reaction conditions is given in Table 4.1. The benzaldehyde was used as a substrate for optimizing the reaction condition. Both **4.2** and **4.3** show fairly good conversion of benzaldehyde to the corresponding borate ester (**4.4a**) (*Scheme 4.2*), however, the higher catalyst loading is required for **4.2** (2.5 mol%) than that of **4.3** (0.5 mol %).

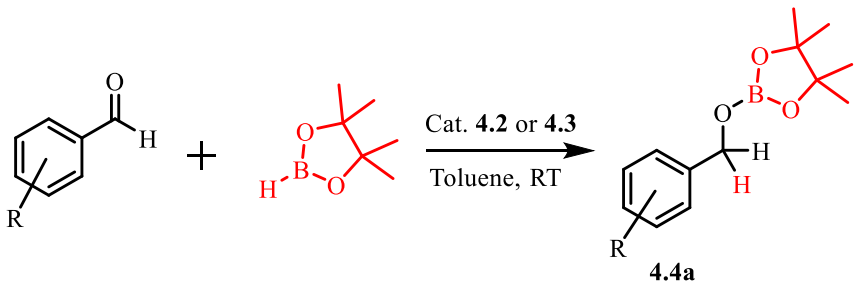

Scheme 4.2. *Hydroboration of aromatic aldehydes catalyzed by* ***4.2*** *and* ***4.3****.*

The lowering of mol% of **4.2** leads to the dropping of the yield (*Table 4.1*). For the comparison purpose, we also did the hydroboration of benzaldehyde, catalyzed by α-phosphinoamido-germylene (**3.3**) which is reported in chapter 3, and it is found to be equally efficient as **4.2**. The α-phosphinoamido-germylene gives the 98% yield of hydroborated product of benzaldehyde in 4 hrs reaction time with 2.5 mol% of catalyst loading (please see the Supporting Information). This mirrors that the diminishment in the HOMO-LUMO gap does not affect the catalytic attributes. After optimizing the reaction conditions, we investigated the substrate scopes for both **4.2** and **4.3** (*Chart 4.2*). Electron-donating (**4.4h, 4.4j, 4.4k**) as well as -withdrawing groups (**4.4b-f**, **4.4i**) show tolerance towards hydroboration.

Table 4.1 *Optimization of reaction conditions for the catalyst (a)* ***4.2*** *and (b)* ***4.3.***

Entry	Catalyst	Cat.(mol %)	Time	Yields (%)[b]
1	**4.2**	1.0	12 hrs	10
2	**4.2**	2.5	6 hrs	>99
3	**4.2**	2.5	4 hrs	62
4	**4.2**	2.5	2 hrs	14
5	**4.3**	2.5	12 hrs	>99
6	**4.3**	1.0	12 hrs	>99
7	**4.3**	1.0	3 hrs	>99
8	**4.3**	0.5	3 hrs	>99
9	**4.3**	0.5	15 min	>99
10	**4.3**	0.5	5 min	45
11	**4.3**	0.1	30 min	21

[a]Reaction conditions: Benzaldehyde (0.25 mmol), HBpin (0.25 mmol) and toluene (2 mL) as solvent. Catalyst loading is relative to benzaldehyde. b1H NMR spectroscopy was used to determine the yield using mesitylene as an internal standard.

The position of the substituent hardly affects the catalysis, as seen from the smooth conversion of all *o*-, *m*-, *p*-bromo benzaldehydes to their corresponding borate esters (**4.4b-d**). The hydroboration of bromo-benzaldehydes (*o-, m-,* and *p-)* is limited and only known with a Ca-based catalyst.[17] We observed quantitative hydroboration of bromo benzaldehydes (**4.4b**-**4.4d**) with **4.2** and **4.3**, which was thus far not known with germylene or stannylene as a catalyst. The hydroboration of salicylaldehyde occurred at the aldehyde functional group, and hydroxylborane dehydrocoupling did not take place.

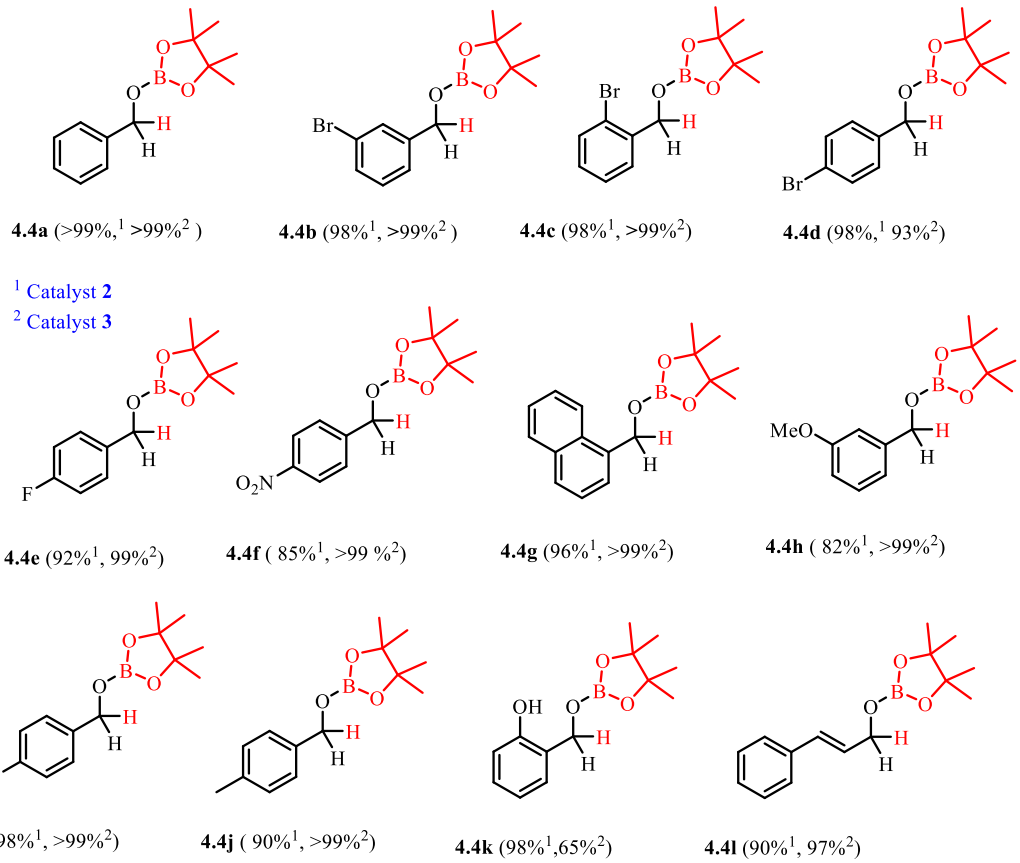

*[a]Reaction Conditions: Aldehydes (0.25 mmol), HBpin (0.25 mmol) and toluene (2.0 mL) as solvent. Catalyst loading for **4.2** and **4.3** are 2.5 mol % and 0.5 mol %, respectively. Time: 6 hrs for cat. **4.2** and 15 min for cat. **4.3**. Yields are calculated by [1]H NMR spectroscopy (mesitylene was used as internal standard) and are given below the products ([1]for cat. **4.2** and [2]for cat. **4.3**).*

***Chart 4.2** The scope of hydroboration of aldehyde substrates.*

Similar phenomenon was observed for the Ca-catalyzed hydroboration of aldehydes and ketones with hydroxyl functionalities.[18] Lastly, an electron-deficient cinnamaldehyde derivative exclusively gives hydroboration at carbonyl group (**4.4l**). Unfortunately, the hydroboration of ketones using **4.2** or **4.2** was found to be not productive, and only 40-50% yields were recorded. For chemoselective hydroboration, we reacted equimolar amount of PhCHO and $PhCOCH_3$ (*Scheme 4.3*). The reaction resulted in quantitative hydroboration of benzaldehyde and complete acetophenone recovery.

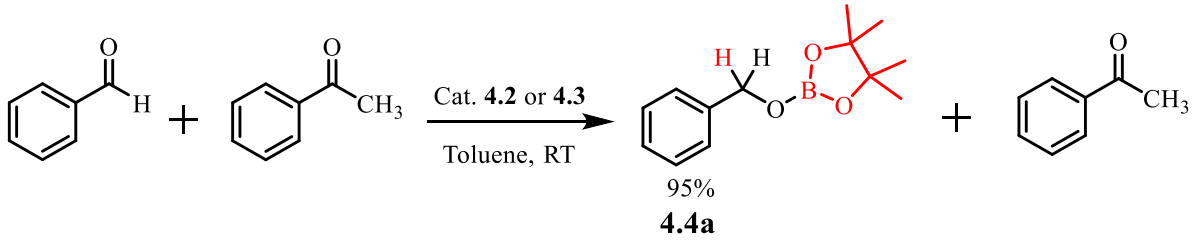

Scheme 4.3 *Selective hydroboration of benzaldehyde in the presence of acetophenone.*

A number of stoichiometric reactions were performed to propose the plausible mechanism for the hydroboration catalyzed by compound **4.2** and **4.3**. 1:1 reaction of benzaldehyde and **4.2**/**4.3** showed no change in the respective NMR spectrum, suggesting that there is no interaction of **4.2** and **4.3** with benzaldehyde first. This observation rules out the possibility of an adduct formation between the catalyst and benzaldehyde. On the contrary, the analogous reactions of **4.2** or **4.3** with HBpin show a multiplate at 22.20 for **4.2** and a singlet 21.44 ppm for **4.3**. Moreover, the ^{119}Sn NMR of **4.3** and HBpin reaction mixture show a signal at 310.0 ppm. This low-field shift with regard to that of **4.3** reflects a slight increase of electron density on the Sn atom. These additional signals in ^{11}B and ^{119}Sn NMR spectra suggest the interaction of the catalysts with HBpin. Based on the recent mechanism reported by Sen and coworkers for their organolithium compound catalyzed hydroboration of carbonyl compounds,[19] we propose that the first step involves the attack of the oxygen atom of HBpin to the Ge or Sn atom resulting that the B atom of HBpin is more electrophilic (*Scheme 4.4*).

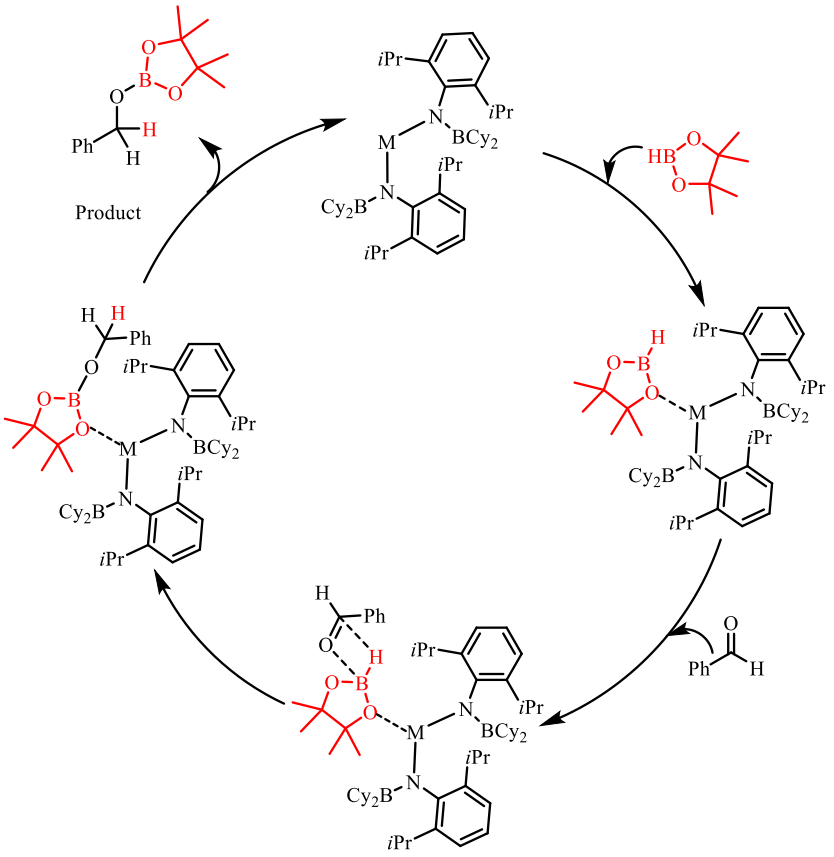

Scheme 4.4 *Tentative mechanism for the catalysis of hydroboration using catalyst* ***4.2*** *and* ***4.3****.*

The slight upfield shift in the ^{119}Sn NMR indicates such weak complex formation. Subsequently, the oxygen atom of aldehyde undergoes nucleophilic reaction with the boron atom of HBpin. A four-membered transition state can be postulated where the hydride moved to the carbonyl carbon. Such mechanistic pathway is consistent with the recent works of Zhi, Roesky, Sen, and others.[4a, 4f, 19]

4.4 Conclusions

In summary, taking inspiration from the electronic structures of our previous reported phosphinoamido-germylene, we have herein prepared new acyclic α-borylamido-germylene, **4.2** and stannylene, **4.3** by substituting the electron-rich P atom with electron deficient boron atom. Such a switch led to a substantial decrease in the HOMO-LUMO gap of **4.2** and **4.3**. Both **4.2** and **4.3** are well characterized by multinuclear NMR spectroscopy and single crystal X-ray studies. Subsequently, we have employed them for the hydroboration of aldehydes.

4.5 References

1. (a) Stennett, T. E.; Harder, S. *Chem. Soc. Rev.* **2016**, *45*, 1112; (b) Hill, M. S.; Liptrot, D. J.; Weetman, C. *Chem. Soc. Rev.* **2016**, *45*, 972; (c) Blake, A. J.; Cunningham, A.; Ford, A.; Teat, S. J.; Woodword, S. *Chem. Eur. J.* **2000**, *6*, 3586; (d) Yadav, S.; Saha, S.; Sen, S. S. *ChemCatChem* **2016**, *7*, 486.
2. (a) Hadlington, T. J.; Driess, M.; Jones C. *Chem. Soc. Rev.* **2018**, *47*, 4176; (b) Leitao, E. M.; Jurca, T.; Manners, I. *Nat. Chem*. **2013**, *5*, 817; (c) Siwatch, R. K.; Ngendran, S. *Chem. Eur. J.* **2014**, *20*, 13551; (d) Wang, W.; Luo, M.; Li, J.; Pullarkat, S. A.; Ma, M. *Chem. Commun.* **2018**, *54*, 3042; (e) Leszczyńska, K.; Mix, A.; Berger, R. J. F.; Rummel, B.; Neumann, B.; Stammler, H.-G.; Jutzi, P. *Angew. Chem., Int. Ed*. **2011**, *50*, 6843.
3. (a) Chong, C. C.; Kinjo, R. *ACS Catal*. **2015**, *5*, 3238; (b) Oshima, K.; Ohmura, T.; M. Suginome, M. *J. Am. Chem. Soc.* **2012**, *134*, 3699; (c) Burgess, K.; Ohlmeyer, M. J. *Chem. Rev.* **1991**, *91*, 1179; (d) Dudnik, A. S.; Weidner, V. L.; Delferro, M.; Motta, A.; Marks, T. J. *Nat. Chem.* **2014**, *6*, 1100; (e) Chen, S.; Yan, D.; Xue, M.; Hong, Y.; Yao, Y.; Shen, Q. *Org. Lett.* **2017**, *19*, 3382; (f) Weidner, V. L.; Barger, C. J.; Delferro, M.; Lohr, T. L.; Marks, T. J. *ACS Catal.* **2017**, *7*, 1244.
4. (a) Yang, Z.; Zhong, M.; Ma, X.; De, S.; Anusha, C.; Parameswaran, P.; Roesky, H. W. *Angew. Chem. Int. Ed.* **2015**, *54*, 10225; (b) Chong, C. C.; Hirao, H.; Kinjo, R. *Angew. Chem., Int. Ed*. **2015**, 54, 190; (c) Abdalla, J. A. B.; Riddlestone, I. M.; Tirfoin, R.; Aldridge, S. *Angew. Chem. Int. Ed.* **2015**, *54*, 5098; (d) Hadlington, T. J.; Hermann, M.; Frenking, G.; Jones, C. *J. Am. Chem. Soc.* **2014**, *136*, 3028; (e) Jakhar, V. K.; Barman, M. K.; Nembenna, S. *Org. Lett.* **2016**, *18*, 4710; (f) Bisai, M. K.; Pahar, S.; Das, T.; Vanka, K.; Sen, S. S. *Dalton Trans.* **2017**, *46*, 2420; (g) Wu, Y.; Shan, C.; Sun, Y.; Chen, P.; Ying, J.; Zhu, J.; Liu, L.; Zhao, Y. *Chem. Commun.* **2016**, *52*, 13799; (h) Schneider, J.; Sindlinger, C. P.; Freitag, S. M.; Schubert, H.; Wesemann, L. *Angew. Chem. Int. Ed.*, **2017**, *56*, 333; (i) Lawson, J. R.; Wilkins, L. C.; Melen, R. L. *Chem. Eur. J.* **2017**, 23, 10997.
5. Peng, Y.; Guo. J.; Ellis, B. D.; Zhu, Z.; Fettinger, J. C.; Shigeru Nagase, S.; Power, P. P. *J. Am. Chem. Soc.* **2009**, *131*, 16272; (b) Jana, A.; Roesky, H. W.; Schulzkeb, C. *Dalton Trans.*, **2010**, *39*, 132; (c) Mizuhata, Y.; Sasamori, T.; Tokitoh, N. *Chem. Rev.* **2009**, *109*, 347; (d) Nagendran, S.; Roesky, H. W. *Organometallics* **2008**, 27, 457.
6. Pal, S.; Dasgupta, R.; Khan, S. *Organometallics* **2016**, *35*, 3635.
7. (a) Kottke, T.; Stalke, D. *J. Appl. Crystallogr*. **1993**, *26*, 615; (b) Stalke, D. *Chem. Soc. Rev.* **1998**, *27*, 171; (c) Sheldrick, G. M. *Acta Crystallogr.,* **2015**, *A71*, 3; (d) Sheldrick,

G. M. *Acta Crystallogr.* **2015**, *C71*, 3; (e) Krause, L.; Herbst-Irmer, R.; Sheldrick, G. M.; Stalke, D. *J. Appl. Crystallogr.* **2015**, *48*, 3.

8. (a) Becke, A. D., *Phys. Rev. A* **1988**, 38, 3098; (b) Perdew, J. P. *Phys. Rev. B* **1986**, 33, 8822; (c) Zhao, Y.; Truhlar, D. G. *Theor. Chem. Acc.* **2008**, 120, 215; (d) Weigend, F.; Ahlrichs, R. *Phys. Chem. Chem. Phys.* **2005**, 7, 3297.
9. Gaussian 09, Revision D.01, M. J. Frisch, G. W. Trucks, H. B. Schlegel, G. E. Scuseria, M. A. Robb, J. R. Cheeseman, G. Scalmani, V. Barone, B. Mennucci, G. A. Petersson, H. Nakatsuji, M. Caricato, X. Li, H. P. Hratchian, A. F. Izmaylov, J. Bloino, G. Zheng, J. L. Sonnenberg, M. Hada, M. Ehara, K. Toyota, R. Fukuda, J. Hasegawa, M. Ishida, T. Nakajima, Y. Honda, O. Kitao, H. Nakai, T. Vreven, J. A. Montgomery, Jr., J. E. Peralta, F. Ogliaro, M. Bearpark, J. J. Heyd, E. Brothers, K. N. Kudin, V. N. Staroverov, T. Keith, R. Kobayashi, J. Normand, K. Raghavachari, A. Rendell, J. C. Burant, S. S. Iyengar, J. Tomasi, M. Cossi, N. Rega, J. M. Millam, M. Klene, J. E. Knox, J. B. Cross, V. Bakken, C. Adamo, J. Jaramillo, R. Gomperts, R. E. Stratmann, O. Yazyev, A. J. Austin, R. Cammi, C. Pomelli, J. W. Ochterski, R. L. Martin, K. Morokuma, V. G. Zakrzewski, G. A. Voth, P. Salvador, J. J. Dannenberg, S. Dapprich, A. D. Daniels, O. Farkas, J. B. Foresman, J. V. Ortiz, J. Cioslowski, and D. J. Fox, Gaussian, Inc., Wallingford CT, **2013**.
10. (a) Lu, T.; Chen, F. *J. Comput. Chem.* **2012**, *33*, 580; (b) Lu, T.; Chen, F. *J. Mol. Graphics Modell.* **2012**, *38*, 314.
11. Dasgupta, R.; Panda, A.; Pal, S.; Muhasina, P. V.; De, S.; Parameswaran, P.; Khan S. *Dalton Trans.* **2017**, *46*, 15190.
12. (a)Wing-Por Leung, W.; Chiu, W.; Mak, T. C. W. *Organometallics* **2012**, *31*, 6966; (b) Ding, Y.; Hao, H.; Roesky, H. W.; Noltemeyer, M.; Schmidt, H.- G. *Organometallics* **2001**, *20*, 4806; (c) Drost, C.; Hitchcock, P. B.; Lappert, M. F. *Organometallics* **1998**, *17*, 3838; (d) Rupar, P. A.; Jennings, M. C.; Ragogna, P. J.; Baines, K. M. *Organometallics* **2007**, *26*, 4109.
13. Protchenko, A. V.; Bates, J. I.; Saleh, L. M. A.; Blake, M. P.; Schwarz, A. D.; Kolychev, E. L.; Thompson, A. L.; Jones, C.; Mountford, P.; Aldridge, S. *J. Am. Chem. Soc.* **2016**, *138*, 4555.
14. Braunschweig, H.; Gehrhus, B.; Hitchcock, P. B.; Lappert, M. F. *Z. anorg. allg. Chem*. **1995**, *621*, 922.
15. Babcock, J. R.; Liable-Sands, L.; Rheingold, A. L.; Sita, L. R. *Organometallics* **1999**, *18*, 4437.

16. Jonas, V.; Frenking, G. *J. Chem. Soc. Chem. Commun*. **1994**, *0*, 1489. (b) Østby, K. A.; Gundersen, G.; Haaland, A.; Nöth, H. *Dalton Trans.* **2005**, *0*, 2284.
17. Yadav, S.; Pahar, S.; Sen, S. S. *Chem. Commun*. **2017**, *53*, 4562.
18. Romero, E. A.; Peltier, J. L.; Jazzar, R.; Bertrand, G. *Chem. Commun.*, **2016**, *52*, 10563.
19. Bisai, M. K.; Das, T.; Vanka, K.; Sen, S. S. *Chem. Commun.* **2018**, *54*, 6843.

CHAPTER 5

$Sn_{19}I_6{\cdot}6PPh_3$: A High-nuclearity Metalloid Tin Cluster

5.1 Introduction

Since, the observation of first metalloid cluster $[Pb_9]^{4-}$ in 1980 by Joannis, extensive progress has been achieved in the field of ligand-free naked polyanionic metalloid clusters which are commonly known as zintl ions.[1] However, the field of group 14 ligand-stabilized metalloid cluster was ignored for several decades until the isolation of *t*-butyldimethylsilyl- stabilized octasilacubane type cluster, $Si_8(t\text{-}BuMe_2Si)_8$, by Matsumoto *et al.* in 1988.[2] After this breakthrough in group 14 cluster chemistry, the exploration of new ligand-stabilized metalloid cluster is continued.[3] Generally ligand-stabilized metalloid clusters fall under two categories- $(EL)_n$ and E_nL_m, where n>m (E= metal or metalloid, L = ligand) (*Type II and III, Figure 5.1*). Among them, the metalloid clusters of E_nL_m (n>m, E=Si, Ge, Sn, Pb, R= Ligand) type, where the number of metal-metal (E-E) bond exceeded than metal-ligand (M-L) bond, attracted much attention than other type of metalloid clusters (*i.e.* zintl cluster, (EL)n, E=metal , L=ligand)).[4] The presence of both the metal as well as ligand-bonded metal atom in E_nL_m (n>m) type of clusters give the average oxidation state of metal in between 0 and 1, and consequently they exhibit interesting chemical and physical properties which are different from that of molecular species and bulk elemental solid.

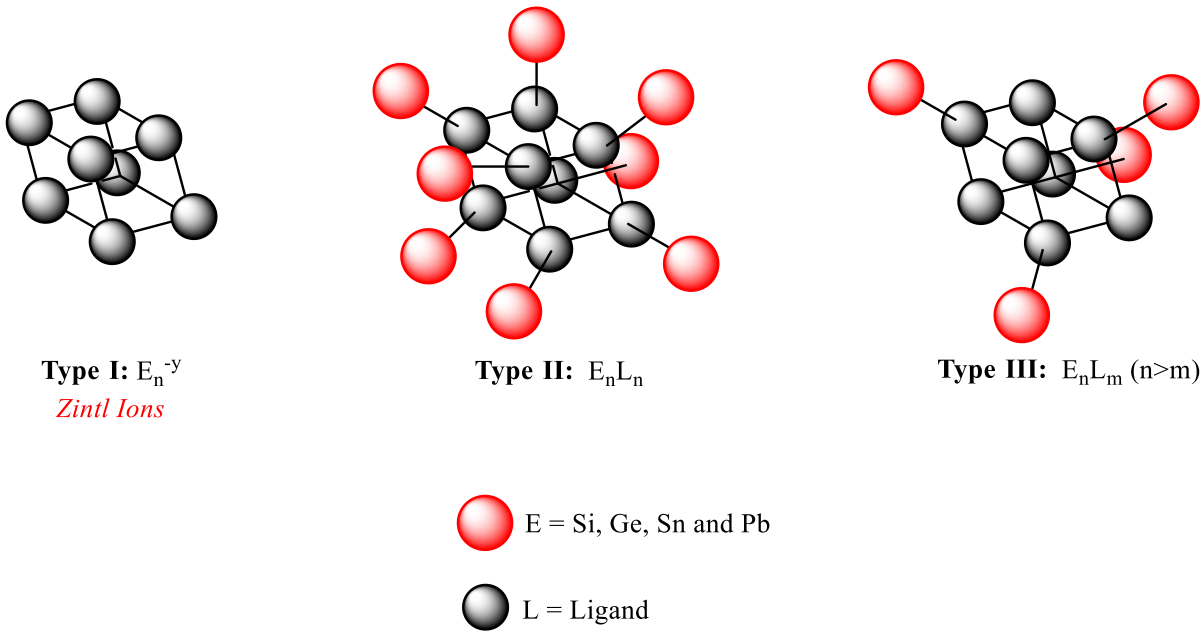

Figure 5. 1 *Graphical representation of three types of group 14 clusters*

To date several metalloid tin clusters, with up to ten metal atoms in core *i. e.* $Ge_2Sn_4Ar_2$ (Ar = 2,6-(2,6-*i*PrC_6H_3)C_6H_3),[5a] $Sn_8Ar^*_4$ (Ar^* = 2,6-$Mes_2C_6H_3$),[5b] $Sn_9Ar^\#_3$ (Ar^2 = 2,6-(2,4,6-iPr_3-C_6H_2)C_6H_3), and $Sn_{10}Ar''_3{}^+$ [5c] *etc.*, have been reported but there are only selected examples of structurally characterized tin clusters with high nuclearity (n ≥ 15). Synthetic strategy, popularly applied to synthesize the tin clusters, is mainly based on reductive coupling reaction of LSnX or $LSnX_3$ (L= ligands, X= Cl, Br, I) alone or in the presence of SnX_2 (X= Cl, Br, I). Recently M. Brynda *et. al.* reported a tin cluster of high nuclearity by reduction of [Sn[N(2,6-*i*$Pr_2C_6H_3$)($SiMe_3$)](μ-$Cl)_2$] with KC_8 which afforded [Sn_{15}{N(2,6-*i*Pr_2-C_6H_3)($SiMe_3$)}$_6$] (**79**) where the nine central tin atoms are arranged in bcc fashion and six ligand bonded tin atoms are on the six faces of cube.[6]

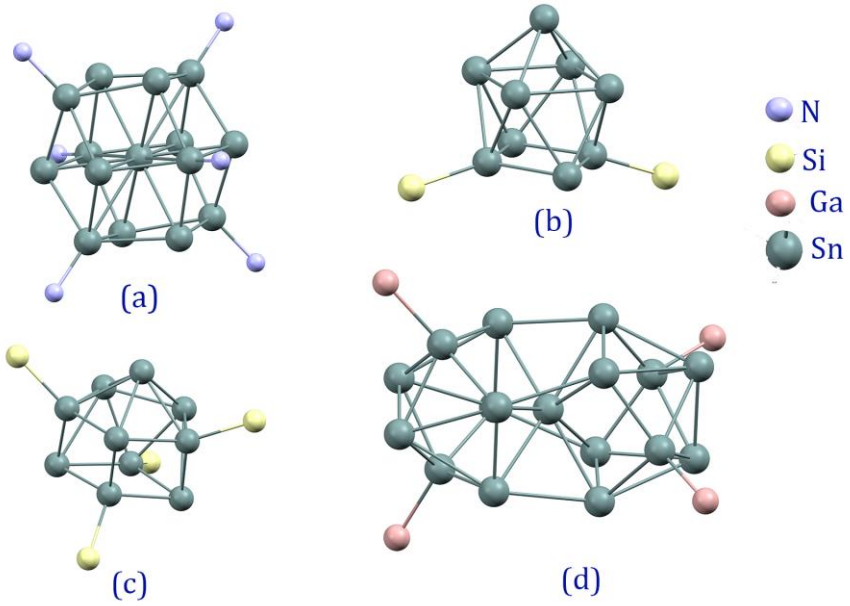

Figure 5.2 *The ball and stick representation of largest available tin cluster: (a)* ***79,*** *Sn_{15}{N(2,6-iPr_2-C_6H_3)($SiMe_3$)}$_6$, (b)* **80,** *{Sn_9[Si($SiMe_3$)$_3$]$_2$}$^{2-}$, (c)* ***81****, {Sn_{10}[Si($SiMe_3$)$_3$]$_4$}$^{2-}$, (d)* ***82****, Sn_{17}{GaCl(ddp)}$_4$ (ddp = HC(CMeNC_6H_3-2,6-iPr_2)$_2$). The substituents on N, Si and Ga are removed for clarity.*

Another synthetic approach to synthesize the tin cluster is the utilization of the disproportionation reaction of sub-valent tin halides in the presence of some stabilizing ligands (*Figure 5.3*).

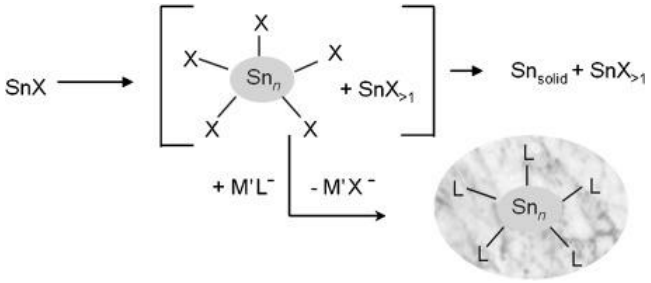

Figure 5.3 *Synthetic concept for the preparation of a metalloid tin cluster applying the disproportionation reaction of a sub-valent halide*. (reprinted with the permission)

Recently, Andreas Schnepf *et al.* reported dianionic cluster, $\{Sn_9[Si(SiMe_3)_3]_2\}^{2-}$ (**80**) and $\{Sn_{10}[Si(SiMe_3)_3]_4\}^{2-}$ (**81**) by disproportionation reaction of sub-valent tin chloride, SnCl, in the presence of $LiSi(SiMe_3)_3$.[7] The largest tin cluster reported to date is $Sn_{17}\{GaCl(ddp)\}_4$ (ddp = $HC(CMeNC_6H_3\text{-}2,6\text{-}i Pr_2)_2$) (**82**) by Fischer *et al.* in 2008. The tin cluster, **82**, could be considered as the dimer of Sn_9 cluster unit.[8]

In the present chapter, we utilized the benefits of disproportionation reaction of SnI_2 in the presence of PPh_3 ligand to synthesize the unique tin cluster **5.1**, $Sn_{19}I_6{\cdot}6PPh_3$. It is characterized by hetero-nuclear NMR spectroscopy, Raman spectroscopy, and X-ray crystallography.

5.2 Experimental section

5.2.1 General remarks

All the experiments were performed under inert atmosphere using standard Schlenk techniques. THF and n-Pentane were distilled over sodium and dried over molecular sieves before used. All other chemicals purchased from Sigma-Aldrich were used without further purification. THF-d_8 was used to record the NMR spectra using Bruker 400 MHz spectrometer. NMR spectra were referenced to external $SiMe_4$ (^1H, and ^{13}C), H_3PO_4 (^{31}P) and $SnMe_4$ (^{119}Sn).

5.2.2 Synthesis

In 100 mL of Schleck flask, 0.378 g (1.0 mmol) of SnI_2 was taken with 0.789 g (3.0 mmol) of PPh_3. In this solid mixture, 20 mL of dried THF was added, and the reaction mixture was stirred for 48 hrs. Over the period of stirring color of the reaction mixture changed

from red to reddish-orange. After stirring, the reaction mixture was filtered, and the solvent was evaporated to 15 mL, and 3 mL of pentane was added dropwise. The solution was kept at room temperature for crystallization. Orange colored and cube-shaped crystals were obtained. Yield: 150 mg; Melting Point: 138 °C. ^{1}H NMR (400 MHz, THF-d_8) δ 7.8-7.5 (90H, Ph, PPh_3); ^{13}C NMR (101 MHz, THF-d_8) δ 133.96, 128.9; ^{119}Sn NMR (149 MHz, THF-d_8) δ 315.70; ^{31}P NMR (128 MHz, THF-d_8) δ 31.71 (m).

5.2.3 X-ray crystallography

The X-ray diffractions for $Sn_{19}I_6{\cdot}6PPh_3$ were recorded on the Bruker Venture D8 at the 150 °C temperature using Mo Kα radiation (λ = 0.71073 A). The diffraction was very weak, and hence we had to record the diffraction at high exposure time *i. e.* 120 sec/frame. Data were corrected for absorption effect using the multi-scan method (SADABS). The structure of **5.1** was solved by direct methods and refined by full-matrix least-squares methods against F2 (SHELXL-2014/6).[9] X-ray crystallographic data are given in Appendix 5, Table 5A.1.

5.3 Results and discussion

The treatment of PPh_3 and SnI_2 in the 3:1 ratio results in the formation of $Sn_{19}I_6{\cdot}6PPh_3$ (*Scheme 5.2*). The compound **5.1** is very sensitive to oxygen and moisture. On exposing to the air, within a few minutes the orange color changes to the blackish-grey which probably indicates the decomposition of the compound.

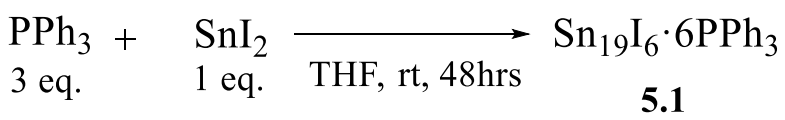

Scheme 5.2 *Synthesis of compound* ***5.1****,* $Sn_{19}I_6{\cdot}6PPh_3$

Compound **5.1** is also sparingly soluble in THF, and DMSO but insoluble in most of the common solvents like benzene, toluene, pentane, dichloromethane, and chloroform. In The THF or DMSO solutions, it begins to decompose after a few hours of solution preparation. The NMR of cluster **5.1** was tried to record in DMSO-d_6, but slow decomposition was observed with the formation of tin oxide cluster, [Sn_4O_6·12DMSO-

$d_6]^{4+}4I^-$(**5.2**) supported by DMSO-d_6 (*Figure 5.6*). After the failure of NMR data acquisition in DMSO-d_6, the NMR spectra was recorded in THF-d_8. Considerable efforts were made to record the NMR spectra as soon as the sample was prepared but the compound started to decompose during the acquisition of the data and therefore in the ^{31}P NMR spectrum, we observed the impurity of PPh_3. The ^{31}P NMR spectrum shows a multiplet at δ 31.7 ppm which is originating from the interaction of three tin nuclei with the phosphorus center (*Appendix 5, Figure 5A.1*). The ^{1}H NMR spectrum of **5.1** shows signal for phenyl proton of PPh_3 moiety in range of δ 7.8 to 7.5 ppm. In ^{119}Sn NMR, a broad singlet peak is observed at δ 315.7 ppm indicating that all the nineteen tin atoms are magnetically equivalent (*Appendix 5, Figure 5A.2)*. It has been observed that tin nuclei in ^{19}Sn NMR spectra of such types of high nuclearity tin clusters remain silent.[5c, 6, 7a, 10] Upon storage of the solution of **5.1** in THF-d_8 for 12 hrs under inert condition (in glove box), it decomposes to some unidentified product in which there is no donation from PPh_3, and it was confirmed by recording the ^{31}P NMR (peak observed at δ -5.46 ppm which is a peak for free PPh_3) (*Appendix 5, Figure 5A.3)*. We have tried to record the mass spectrum of compound **5.1** but we could not observe any molecular peak.

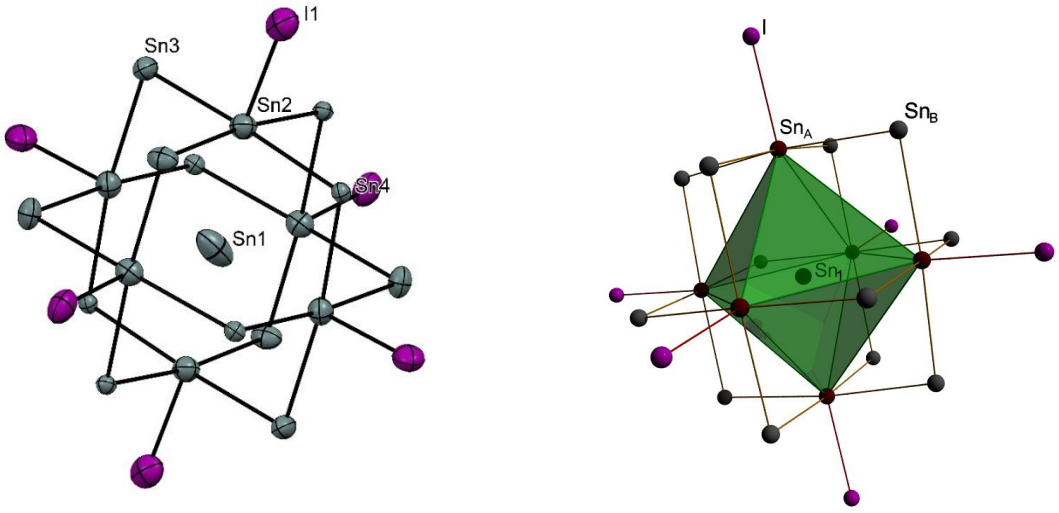

(a) (b)

Figure 5.4 *(a) The molecular structure of complex $Sn_{19}I_6$. Thermal ellipsoids are shown at the probability level of 50%. The PPh_3 moieties are omitted for clarity. Selected bond lengths (Å) and*

bond angles (deg): Sn2-Sn3 3.187(4), Sn2-Sn4 3.187(4), Sn1-Sn2 3.371(4), Sn2-I1 2.906(4); Sn3-Sn2-Sn4 174.9(1), I1-Sn2-Sn4 90.7(1), I1-Sn2-Sn1 172.6, I1-Sn2-Sn3 93.5(1), I1-Sn2-Sn4 90.9(1). (b) Polyhedral presentation of $Sn_{19}I_6$. Sn atoms located on octahedron vertices and on edges are shown dark-brown (Sn_A) and grey (Sn_B) in colour respectively.

The compound **5.1**, crystallizes in cubic space group *Pa-3*. The molecular structure of **5.1** in *Figure 5.4* which reveals that it consists of an octahedron geometry where six Sn atom (denoted as Sn_A) are on six vertices and bonded to iodine atom while other twelve Sn atoms (denoted as Sn_B) are located on twelve edges of the octahedron. There is one Sn atom (denoted as Sn1) which is located in the center of the octahedron. The phosphorus atom of PPh_3 moiety donates its lone pair of electron to the centre of triangular faces of octahedron created by three adjacent tin atoms (*Figure 5.5*). The average distance value of Sn_A-Sn_B is 3.187 Å and it matches with the value reported for $[Sn_9\{Sn(NRR')\}_6]$ (3.01 Å) and $[Sn_{17}\{GaCl(ddp)\}_4]$(3.124 Å). The average interaction distance between central tin (Sn1) atom and Sn_A atom is 3.37 Å which is considerably longer than the value reported for $[Sn_9\{Sn(NRR')\}_6]$ (3.10 Å).

In Raman spectrum of compound **5.1**, the appearance of vibrational bands at ~111 cm−1 (Sn-Sn stretching) and 141 cm−1 (Sn-I stretching) confirm the presence of Sn-Sn and Sn-I bonds in cluster (*Figure 5.7*). The observed Sn-Sn vibrational band for **5.1** falls in the order of the vibrational bands reported for $Me_3SnSnMe_3$ (190 cm^{-1}) and $Ph_3SnSnPh_3$ (138 cm^{-1}).[11]

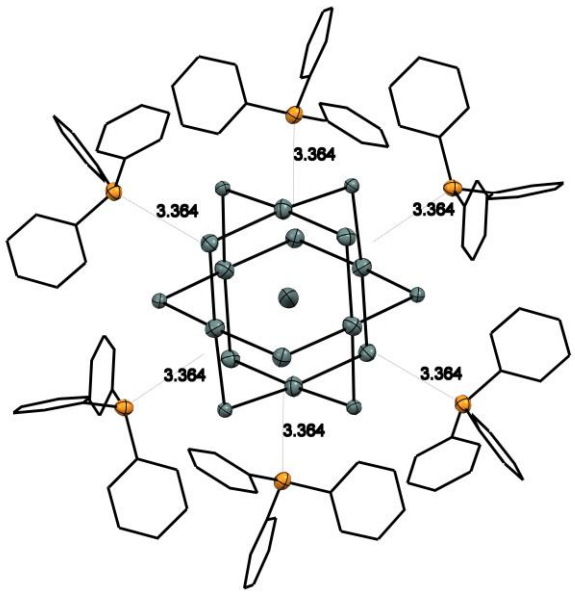

Figure 5.5 *The representation of interaction of PPh_3 with $Sn_{19}I_6$ core in compound **5.1**.*

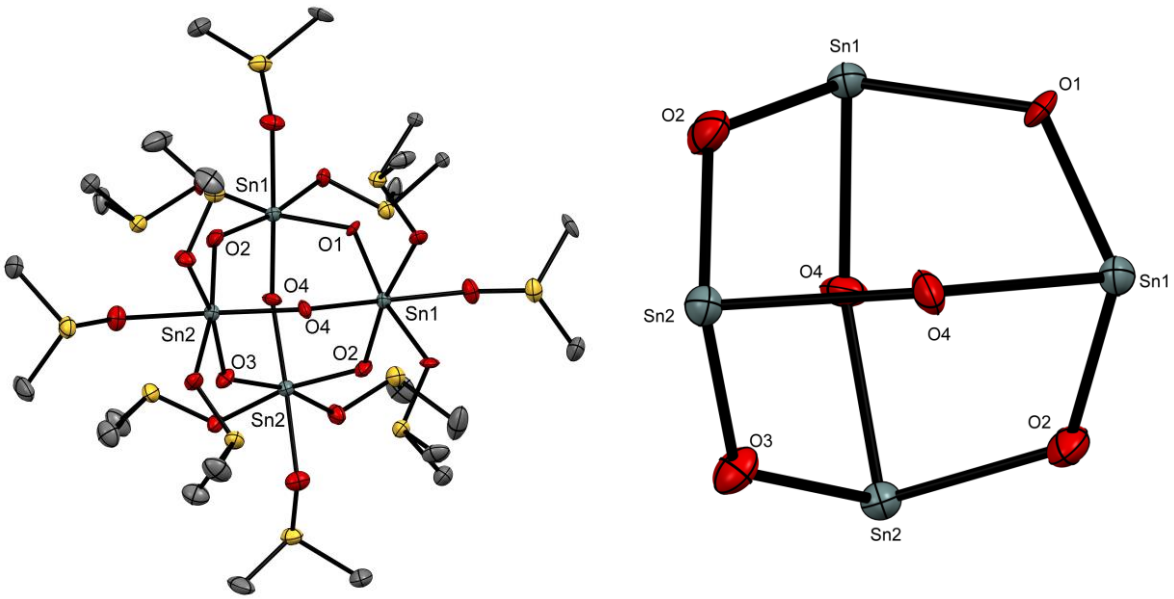

(a) (b)

Figure 5.6 *The molecular structure of* ***5.2*** *at probability level of thermal ellipsoid with 50%. Hydrogen atoms and iodide counter anion are omitted for clarity, (b) representation of Sn_4O_6 core without DMSO molecules.*

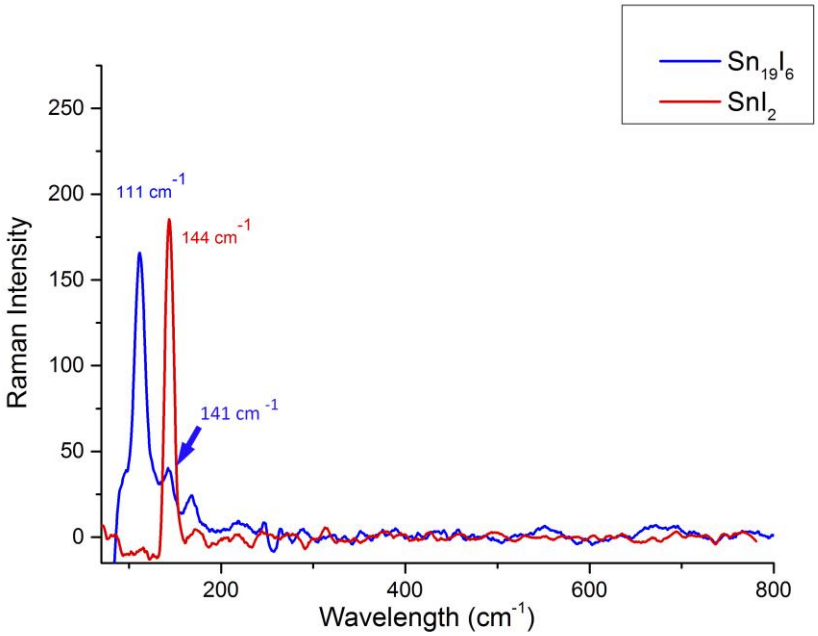

Figure 5.7 *Raman spectra of $Sn_{19}I_6 \cdot 6PPh_3$ and SnI_2.*

To know the vibrational frequency of Sn-I bond , we have also recorded the Raman spectrum of pure SnI_2 and it was observed at 144 cm^{-1} which is very close to the vibrational frequency observed for Sn-I bond (141 cm^{-1}) present in compound **5.1**.

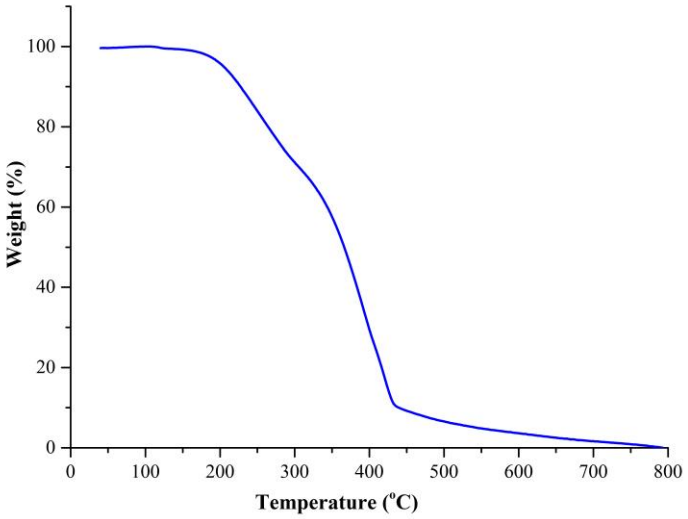

Figure 5.8 *TGA curve for the* $Sn_{19}I_6 \cdot 6PPh_3$

The thermogravimetric analysis was also carried out to know the thermal response of **5.1.** There no clear weight loss was observed which suggests that iodine molecules present in crystal packing do not liberated and the cluster decomposes as a whole (*Figure 5.8*). It started to decompose around 140 °C and lost the 90% weight around 450 °C.

5.4 Conclusions

In this chapter we have isolated the tin cluster, $Sn_{19}I_6 \cdot 6PPh_3$ of highest nuclearity reported to date. The compound **5.1**, was confirmed by XRD, NMR and Raman spectroscopy. The cluster is very sensitive to the air and moisture and insoluble in most of the solvent except THF with very low solubility. The cluster **5.1** in DMSO is very soluble but it slowly decompose and forms $Sn_4O_6 \cdot 12DMSO\text{-}d_6]^{4+}4I^-$(**5.2**) cluster.

5.5 References

1. (a) Zintl, E.; Harder, A.; *Z. Phys. Chem. Abt. A* **1931**, 154, 47; (b) Smyth, F. H.; *J. Am. Chem. Soc.* **1917**, 39, 1299; (c) Zintl, E. ; Goubeau, J. ; Dullenkopf, W. *Z. Phys. Chem.*

Abt. A **1931**, 154, 1; (d) Kraus, C. A.; *J. Am. Chem. Soc.* **1922**, *44*, 1216; (e) Peck, E. B.; *J. Am. Chem. Soc.* **1918**, *40*, 335.

2. Matsumoto, H.; Higuchi, K.; Hoshino, Y.; Koike, H.; Naoi, Y.; Nagai, Y. *J. Chem. Soc., Chem. Commun.* **1988**, 1083.
3. (a) Purath, A.; Köppe, R.; Schnöckel, *H. Angew. Chem. Int. Ed.* **1999**, *38*, 2926; (b) Schnepf, A.; Schnöckel, H. *Angew. Chem. Int. Ed.* **2002**, *41*, 3532; (c) Linti, G.; Schnöckel, H.; Uhl, W.; Wiberg, N. *Molecular Clusters of the Main Group Elements* (Eds.: M. Driess, H. Nöth), Wiley-VCH, Weinheim, **2004**, chap. 2.3, 126; (d) Schnepf, A. *Angew. Chem. Int. Ed.* **2004**, *43*, 664; (e) Wiberg, N.; Power, P. P. *Molecular Clusters of the Main Group Elements* (Eds.: M. Driess, H. Nöth), Wiley-VCH, Weinheim, **2004**, chap. 2.2, 188; (f) Schnöckel, H. *Dalton Trans.* **2005**, 0, 3131.
4. (a) Corbett, J. D. *Angew. Chem. Int. Ed.* **2000**, *39*, 670; (b) Fassler, T. F. *Coord. Chem. Rev.* **2001**, *215*, 347.
5. (a) Richards, A. F.; Hope, H.; Power, P. P. *Angew. Chem., Int. Ed.*, **2003**, *42*, 4071; (b) Eichler, B. E.; Power, P. P. *Angew. Chem., Int. Ed.,* **2001**, *40*, 796; (c) Richards, A. F.; Eichler, B. E.; Brynda, M.; Olmstead, M. M.; Power, P. P.; *Angew. Chem., Int. Ed.*, **2005**, *44*, 2546.
6. Brynda, M.; Herber, R.; Hitchcock, P. B.; Lappert, M. F.; Nowik, I.; Power, P. P.; Protchenko, A. V.; Růžička A.; Steiner, J. *Angew. Chem. Int. Ed.* **2006**, *45*, 4333.
7. (a) Schrenk, C.; Winter, F.; Pöttgen, R.; Schnepf, A.; *Inorg. Chem.* **2012**, *51*, 8583; (b) Schrenk, C.; Winter, F.; Pöttgen, R.; Schnepf, A. *Chem. Eur. J.* **2015**, *21*, 2992.
8. Prabusankar, G.; Kempter, A.; Gemel, C.; Schröter, M-K; Fischer R. A. *Angew. Chem. Int. Ed.* **2008**, *47*, 7234.
9. (a) Kottke, T.; Stalke, D. *J. Appl. Crystallogr*. **1993**, *26*, 615; (b) Stalke, D. *Chem. Soc. Rev.*, **1998**, *27*, 171; (c) Sheldrick, G. M. *Acta Crystallogr.* **2015**, *A71*, 3; (d) Sheldrick, G. M. *Acta Crystallogr.* **2015**, *C71*, 3; (e) Krause, L.; Herbst-Irmer, R.; Sheldrick, G. M.; Stalke, D. *J. Appl. Crystallogr.* **2015**, *48*, 3.
10. (a) Schrenk, C.; Schellenberg, I.; Pöttgen, R.; Schnepf A. *Dalton Trans.* **2010**, *39*, 1872; (b) Chapman, D. J.; Sevov S. C. *Inorg. Chem.* **2008**, *47*, 2006.
11. Davies G. A. *Organotin Chemistry, John Wiley & Sons.* **2006**, 29.

Summary

In summary, the thesis presents the synthesis of group 14 low valent compounds and their reactivity, and catalytic applications. In chapter 2, amidinato-phosphinoamido-supported tetrelylenes *i. e.* amidinato-phosphinoamido-silylene, germylene, and stannylene, were synthesized. Out of these tetrelylenes, the only silylene show the coordination to gold (I) chloride which shows that the silylene is more nucleophilic that other two tetrelylenes. This experimental observation was further investigated theoretically.

In chapter 3, we chose the phosphinoamido- ligands of the previous chapter to synthesize the dimeric phosphinoamido-chlorogermylenes and monomeric phosphinoamido-germylenes. Both the compounds were fully structurally characterized. The theoretical calculation shows that in the phosphinoamido-germylenes, P-center is more nucleophilic than germenium center and it was supported by experimental observation of reactivity with $AuCl{\cdot}SMe_2$ and Me_3NO. The NBO analysis shows that the HOMO is based on phosporus rather than germanimum atom while LUMO is located on germanium center.

In the chapter 4, we sythesized the borylamido-germylene and stannylene to sift both the HOMO and LUMO on Ge/Sn center, unlike phosphinoamido-germylene where they were observed on two different centers. The borylamido-germylene/stannylene and phosphinoamido-germylene were employed as catalyst for hydroboration of aldehydes. The borylamido-germylene and phosphinoamido-germylene show a moderate catalyst loading (2.5 mol%) whereas borylamido-stannylene catalyse the same reactions at very low catalyst loading (0.5 mol%) and reaction time (15 min).

In the last chapter we reported the high-nuclearity tin cluster ($Sn_{19}I_6{\cdot}6PPh_3$) which is synthesised via the disproportionation reaction of SnI_2 in presence of 3 equivalent of PPh_3. The cluster is very sensitive to moisture and oxygen.

Appendix

Table 2A.1 Crystallographic data for **2.2**, **2.3** and **2.4**

	2.2	**2.3**	**2.4**
Formula	$C_{39}H_{50}N_3PSi$	$C_{40}H_{52}AuCl_3N_3PSi$	$C_{80}H_{104}Au_2Cl_4F_{12}N_6P_2Sb_2Si_2$
Formula weight	619.88	937.22	2275.07
T, K	150(2)	150(2)	150(2)
Color, habit	Pale yellow, block	colorless, block	colorless, plate
Crystal system	triclinic	Triclinic	triclinic
Space group	*P*-1	*P*-1	*P*-1
a, Å	9.8573(12)	11.933(11)	12.058(6)
b, Å	10.9843(13)	12.334(13)	14.762(9)
c, Å	19.208(2)	17.499(16)	15.001(9)
α, deg	93.409(3)	81.27(3)	116.997(14)
β, deg	98.295(3)	82.82(2)	104.713(14)
γ, deg	115.316(3)	65.87(2)	95.716(14)
V, Å^3	1843.2(4)	2318(4)	2228(2)
Z	2	2	2
d_{calcd}, g cm^{-3}	1.117	1.343	1.695
Wavelength	0.71073	0.71073	0.71073
Absorption coefficient	0.137	3.435	4.133
Theta range [°]	2.31° to 25.25°	2.15° to 27.5°	2.31° to 24.25°
Index ranges	-11 ≤ h ≤ 11, -13 ≤ k ≤ 13, -23 ≤ l ≤ 23	-15 ≤ h ≤ 15, -16 ≤ k ≤ 16, -22 ≤ l ≤ 22	-13 ≤ h ≤ 13, -17 ≤ k ≤ 17, -17 ≤ l ≤ 17
Reflections collected	43905	38188	89255
Independent reflections	6666[*R*(int)= 0.0868]	10080[$R_{(int)}$=0.0812]	7185 [$R_{(int)}$= 0.2448]
Completeness	1.000	0.947	0.999
Parameters	407	452	494
R1 (*R1* all data)[a]	0.0541(0.1082)	0.0752 (0.0982)	0.0571 (0.0985)
wR2 (*wR2* all data)[b]	0.1205(0.1462)	0.2087 (0.2296)	0.1046 (0.1210)
GOF	0.950	1.047	1.028
max., min. peaks [eÅ^{-3}]	0.343, -0.204	3.306, -1.545	1.321, -1.030,

Table 2A.2 Crystallographic data for **2.7** and **2.8**

	2.7	2.8
Formula	$C_{49}H_{53}GeN_3P$	$C_{39}H_{50}SnN_3P$
Formula weight	664.38	710.48
T, K	150(2)	150(2)
Color, Habit	pale yellow, block	Pale yellow, block
Crystal System	Triclinic	Monoclinic
Space Group	*P*-1	$P2_1/c$
a, Å	9.9786(7)	10.799(4)
b, Å	10.5777(7)	35.449(13)
c, Å	19.9436(13)	10.262(4)
α, deg	92.444(2)	90
β, deg	95.808(2)	111.010(8)
γ, deg	91.228(2)	90
V, Å^3	2091.6(2)	3667(2)
Z	2	4
d_{calcd}, g cm^{-3}	1.055	1.287
Wavelength [Å]	0.71073	0.71073
μ (MoKα) [mm-1]	0.796	0.770
Crystal size [mm3]	0.1*0.1*0.1	0.1*0.1*0.1
Θ limits [°]	2.143 to 25.248	2.202 to 25.249
Completeness to Θ (%)	99.9	99.7
Reflns measured	56776	77803
Independent reflns[a]	6730 [$R_{(int)}$0.0549]	4132 [$R_{(int)}$ 0.1732]
Restraints	12	0
Parameters	407	407
R_1(R_1all data) [b]	0.0327 (0.0391)	0.0856(0.1478)
wR_2(wR_1all data)[c]	0.0748 (0.0770)	0.1618 (0.1831)
GOF	1.039	1.140
max., min peaks [eÅ-3]	0.753 (-0.269)	0.706 (-0.799)

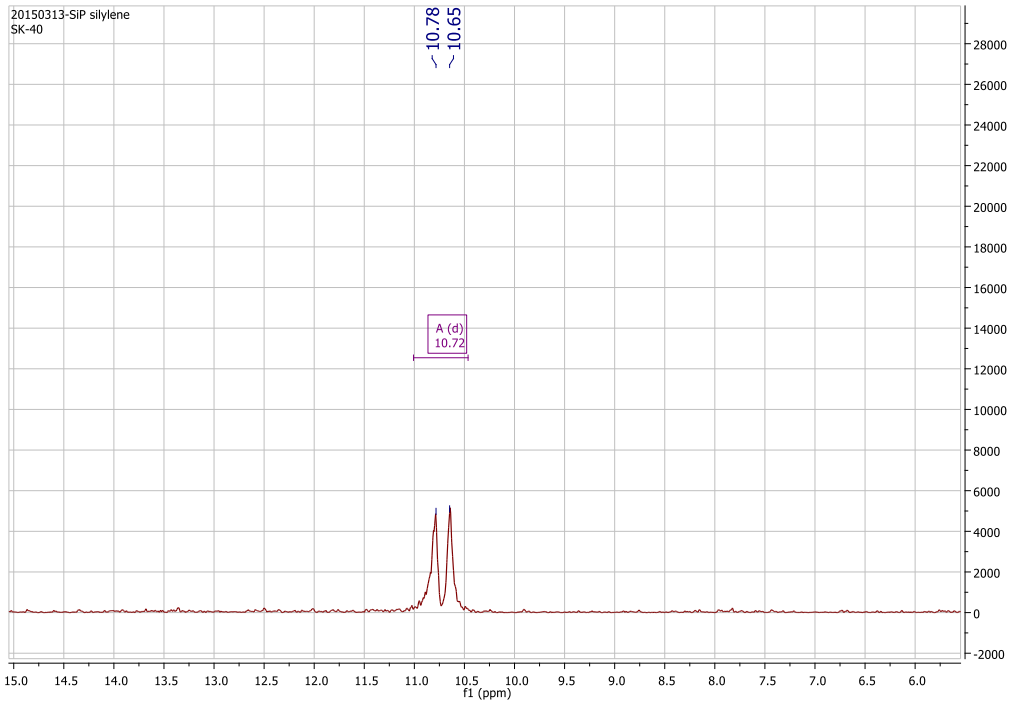

Figure 2A.1 ^{29}Si NMR (C_6D_6) of **2.2**

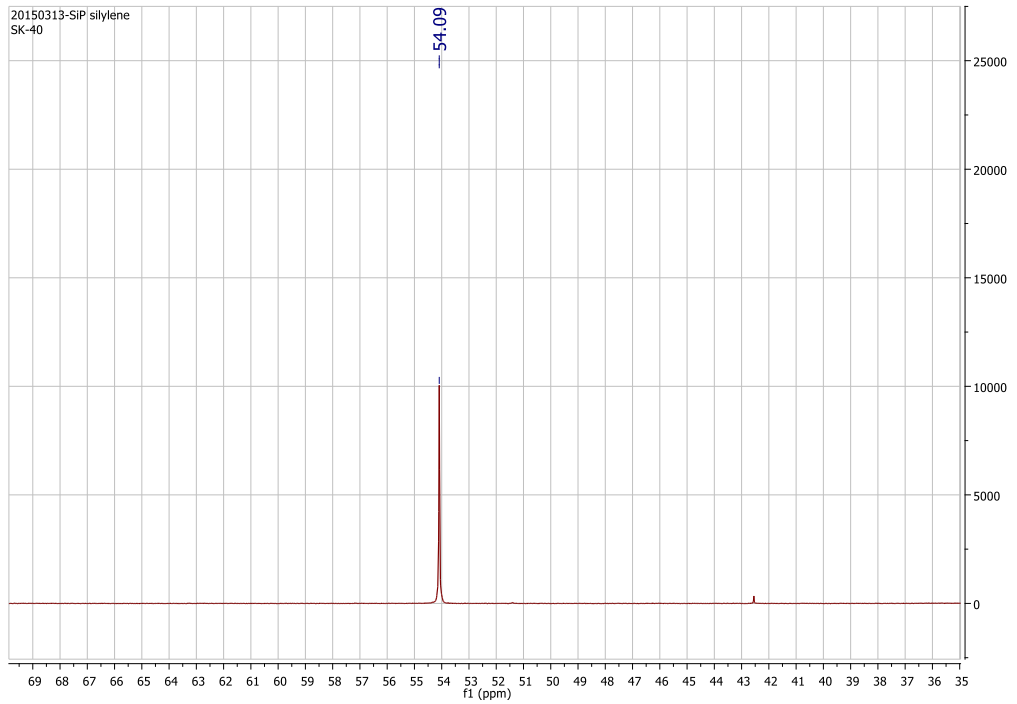

Figure 2A.2 ^{31}P NMR (C_6D_6) of **2.2**

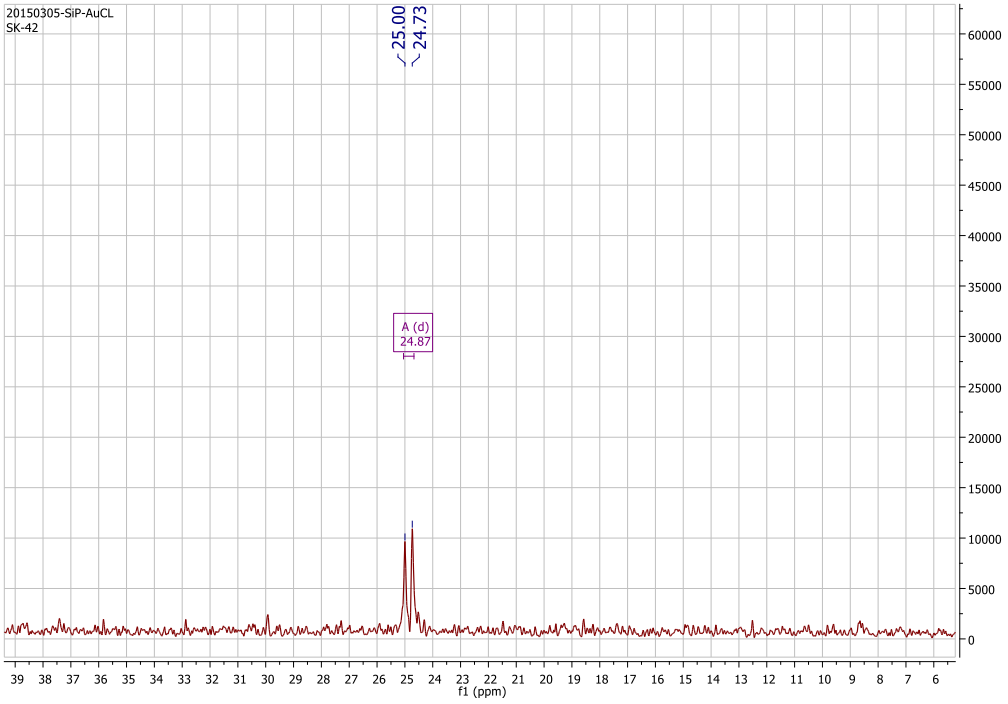

Figure 2A.3 ^{29}Si NMR (CD_2Cl_2) of **2.3**

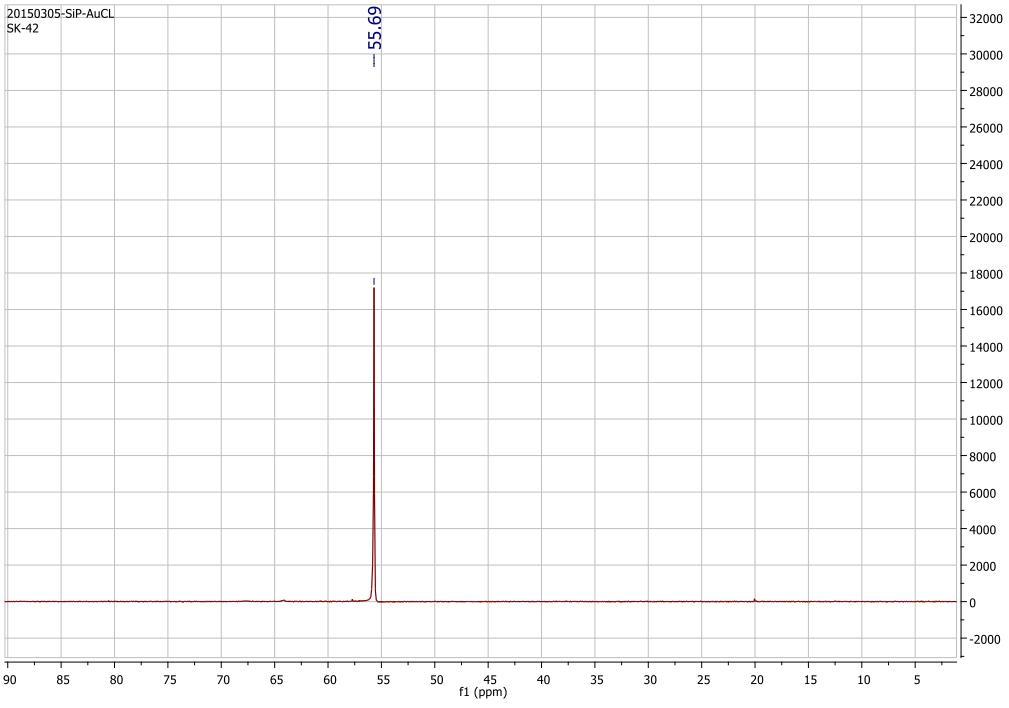

Figure 2A.4 ^{31}P NMR (CD_2Cl_2) of **2.3**

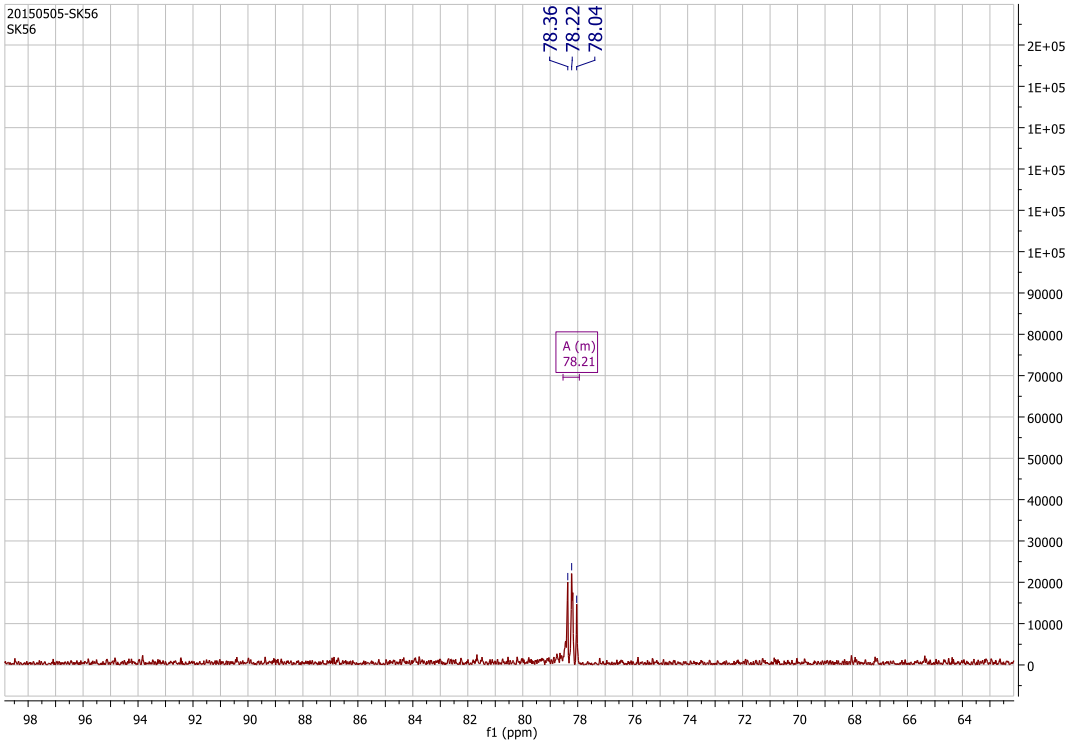

Figure 2A.5 ^{29}Si NMR (CD_2Cl_2) of **2.4**

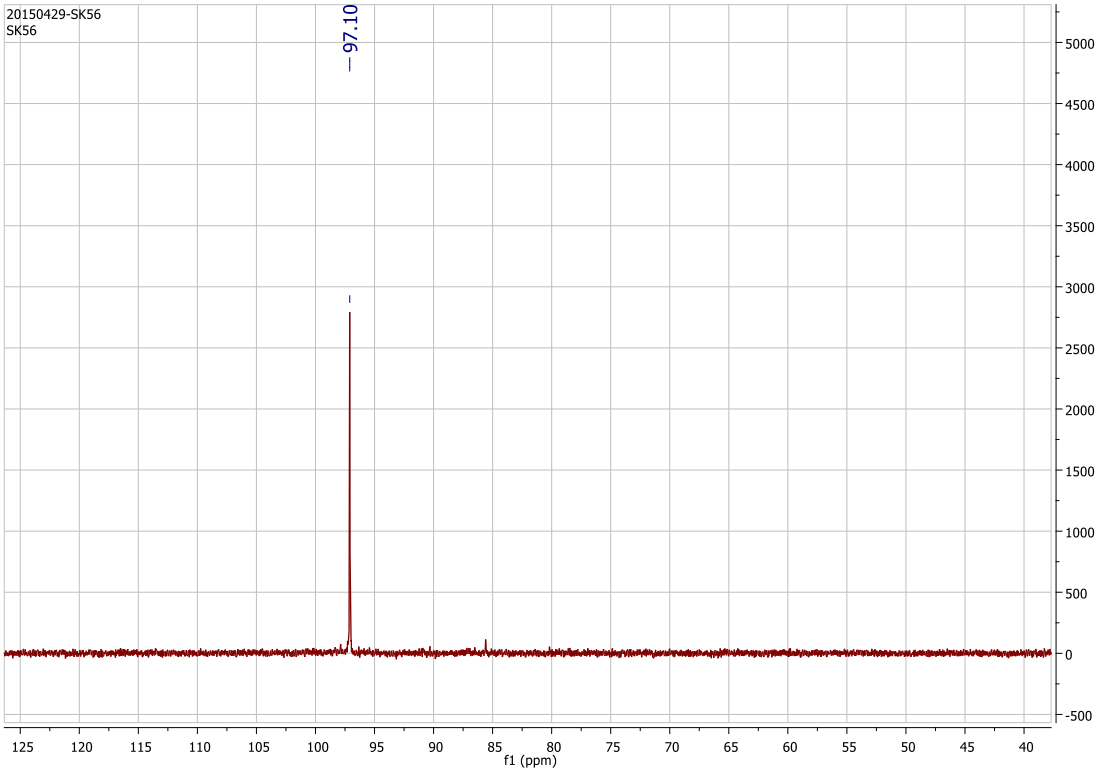

Figure 2A.6 ^{31}P NMR (CD_2Cl_2) of **2.4**

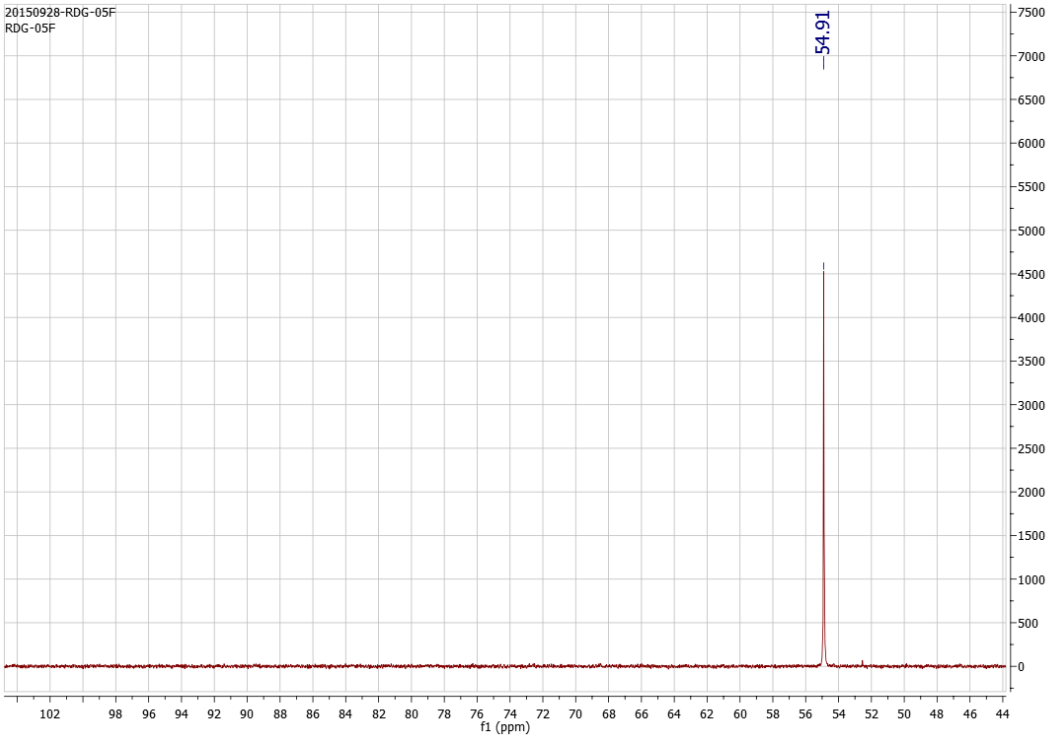

Figure 2A.7 ^{31}P NMR (CD_2Cl_2) of **2.7**

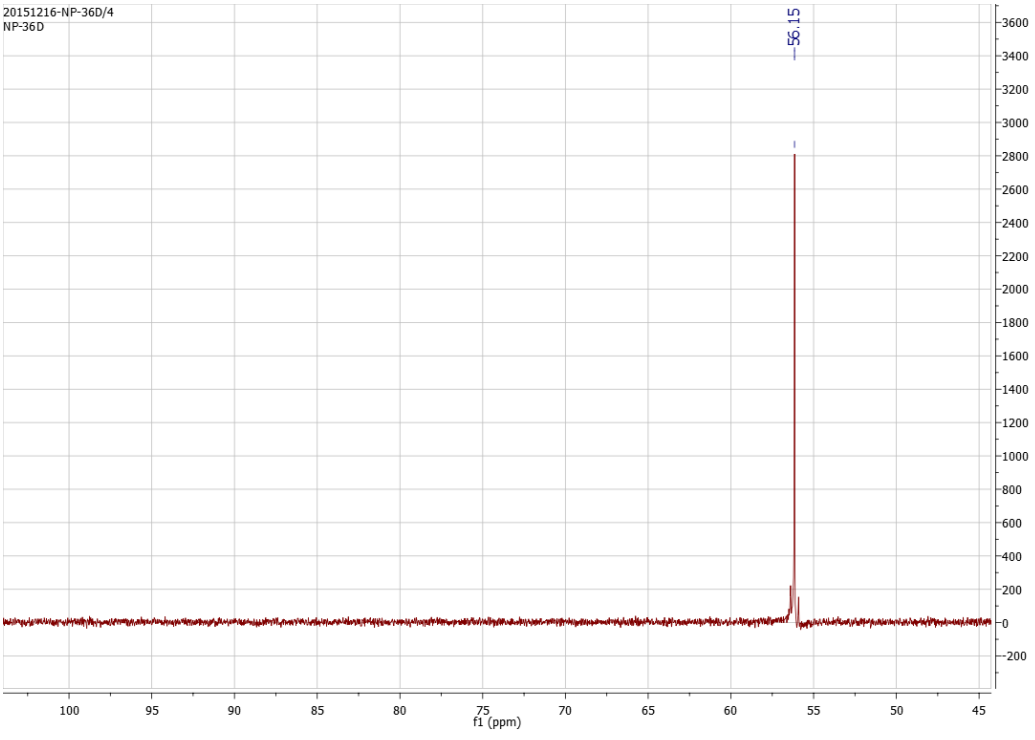

Figure 2A.8 ^{31}P NMR (CD_2Cl_2) of **2.8**

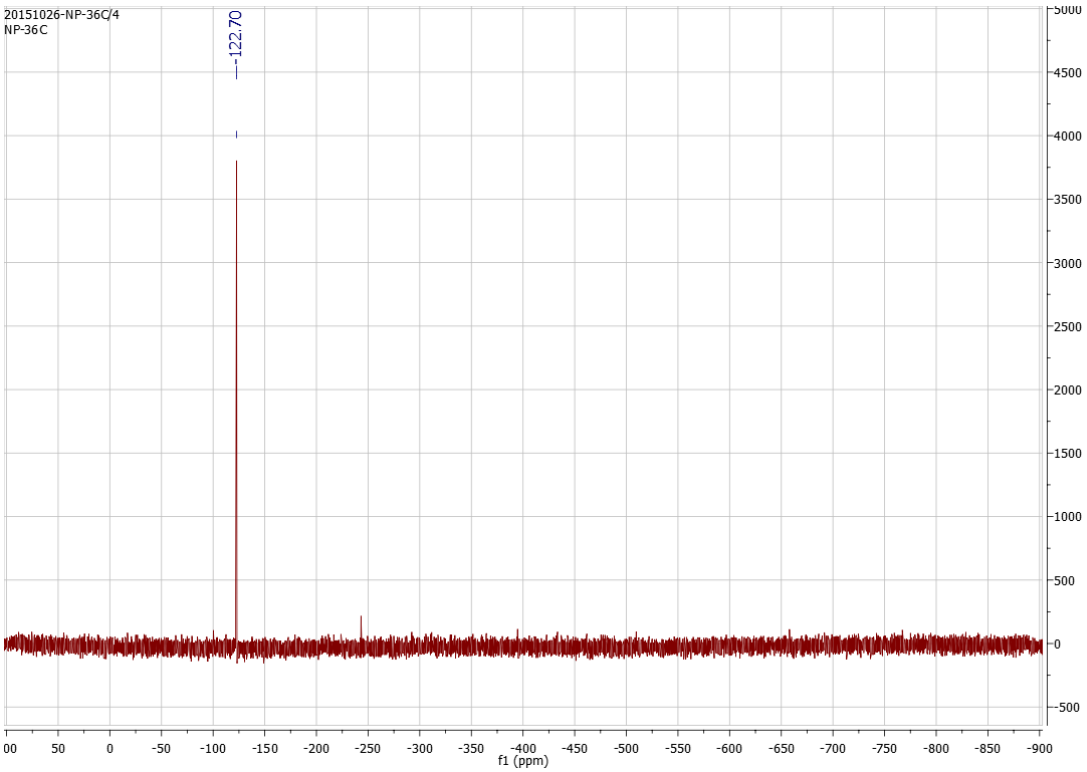

Figure 2A.9 ^{119}Sn NMR (CD_2Cl_2) of **2.8**

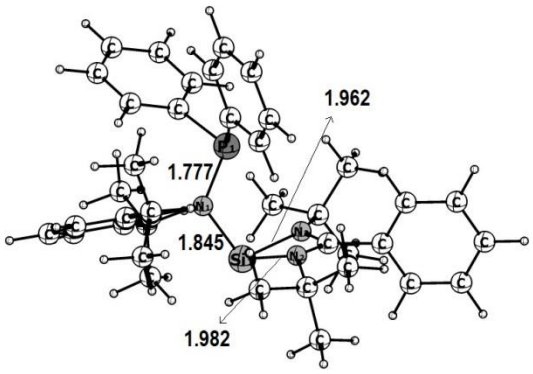

2.2

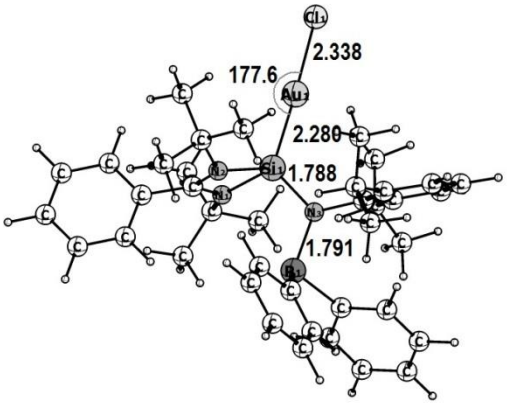

2.3

0.0

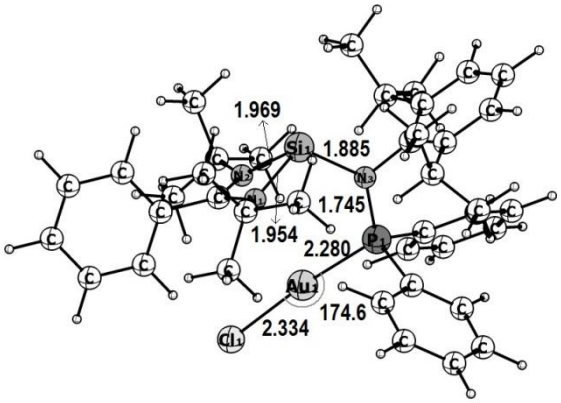

2.3'

14.5

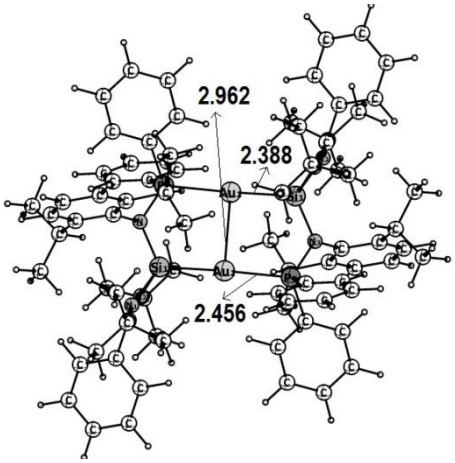

2.4

Figure 2A.10: Optimized geometries and important geometrical parameters of **2.2**, **2.3**, **2.3'** and **2.4** at the M06/def2-TZVPP//BP86/def2-SVP level of theory. Relative energies of **2.3** and **2.3'** are in kcal/mol.

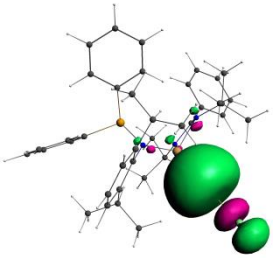

Ψ_{-1}(-0.56)

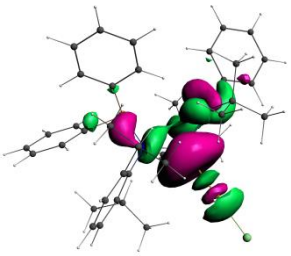

Ψ_1(0.56)

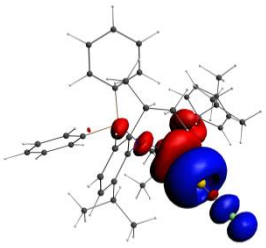

$\Delta\rho_1$
(ΔE = -28.6 kcal/mol)

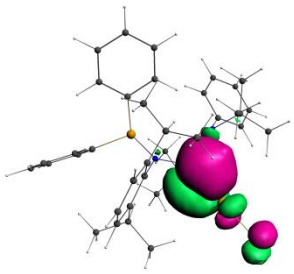

$\Psi_{-2}(-0.22)$

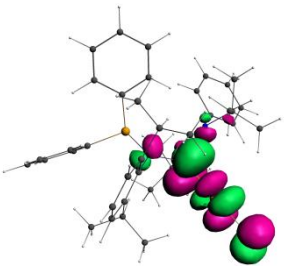

$\Psi_{2}(0.22)$

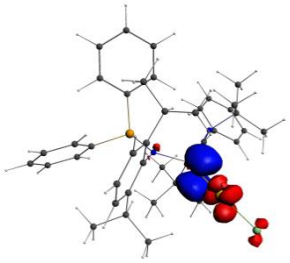

$\Delta\rho_2$
(ΔE = -6.9 kcal/mol)

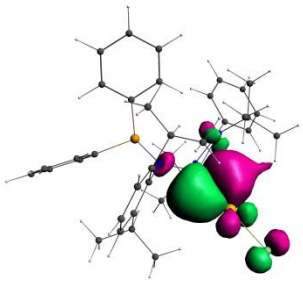

$\Psi_{-3}(-0.20)$

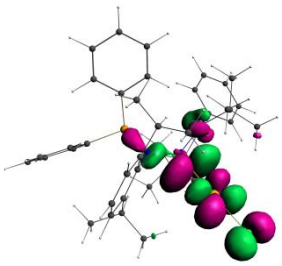

$\Psi_{3}(0.20)$

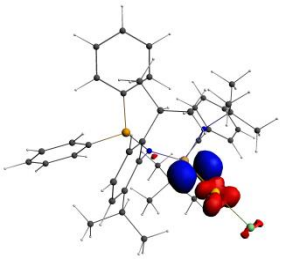

$\Delta\rho_3$
(ΔE = -6.2 kcal/mol)

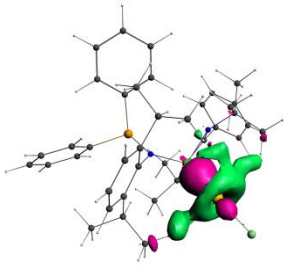

$\Psi_{-4}(-0.18)$

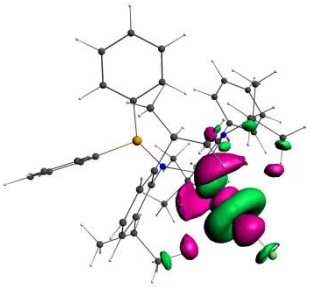

$\Psi_{4}(0.18)$

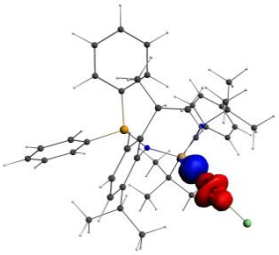

$\Delta\rho_4$
(ΔE = -7.8 kcal/mol)

Figure 2A.11: NOCV pair of orbitals with their eigen values in parenthesis, the associated deformation density plots (Δρ) and orbital stabilization energies ΔE for Si–Au bond of **2.3** at the BP86/TZ2P level of theory. The direction of the charge flow in the deformation density plot Δρ is from red → blue. Isosurface value for NOCV pair orbitals is 0.03 and that for deformation density is 0.001.

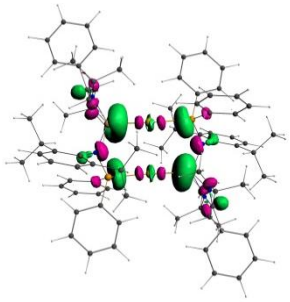

Ψ_{-1}(-1.00)

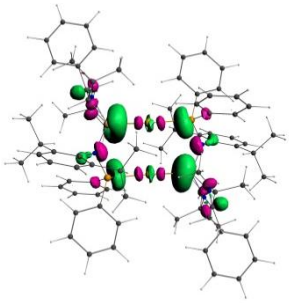

Ψ_{1}(1.00)

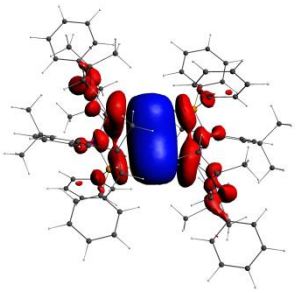

$\Delta\rho_1$

($\Delta E_{\sigma_{1(L\rightarrow Au)}}$= -102.4 *kcal/mol)*

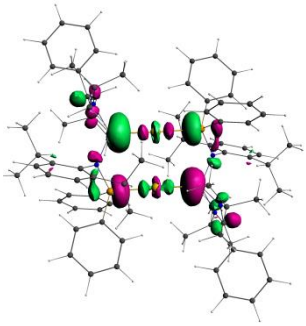

Ψ_{-2}(-0.89)

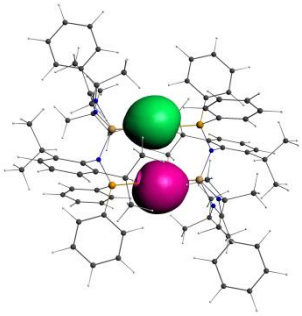

Ψ_{2}(0.89)

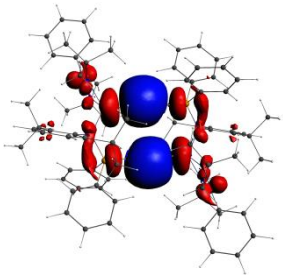

$\Delta\rho_2$

($\Delta E_{\sigma_{2(L\rightarrow Au)}}$= -77.5 kcal/mol)

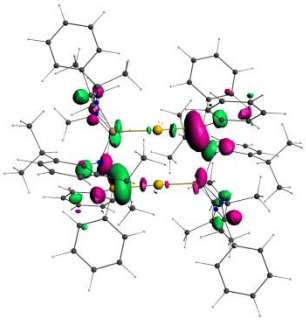

Ψ_{-3}(-0.51)

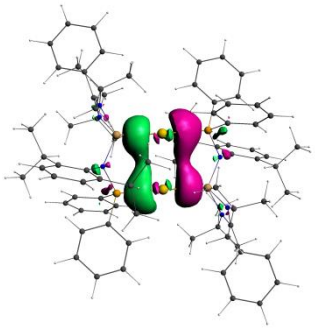

Ψ_{3}(0.51)

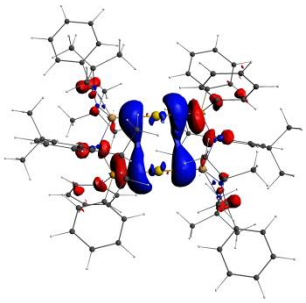

$\Delta\rho_3$

$\Delta E_{\sigma_{3(L\rightarrow Au)}}$= -34.3 kcal/mol)

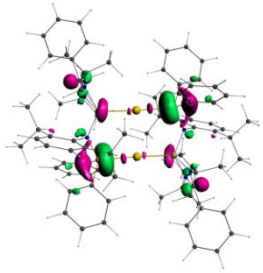

Ψ_{-4}(-0.49)

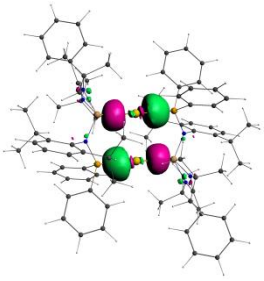

Ψ_{4}(0.49)

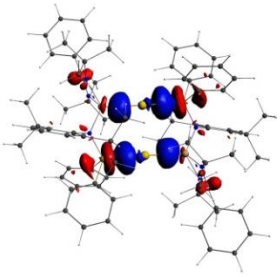

$\Delta\rho_4$

($\Delta E_{\sigma_{4(L\rightarrow Au)}}$=-34.0 kcal/mol

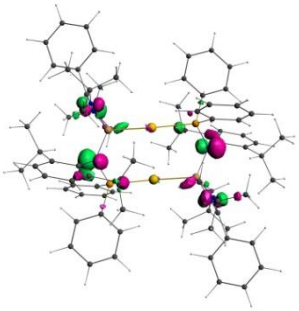

Ψ_{-5}(-0.35)

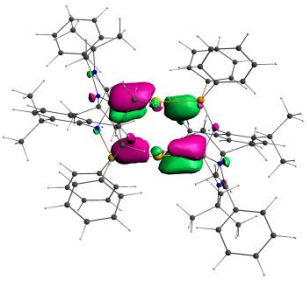

Ψ_{5}(0.35)

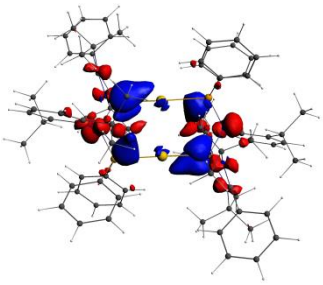

$\Delta\rho_5$
($\Delta E_{5(L\rightarrow L)}$=-12.3 kcal/mol)

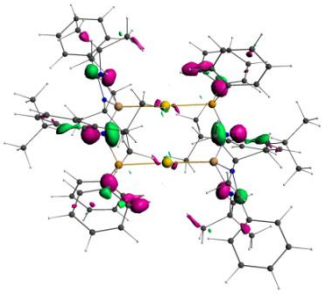

Ψ_{-6}(-0.30)

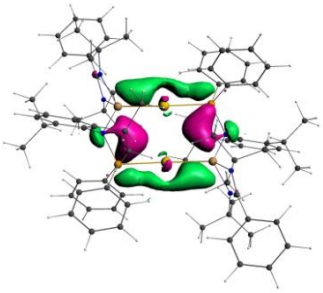

Ψ_{6}(0.30)

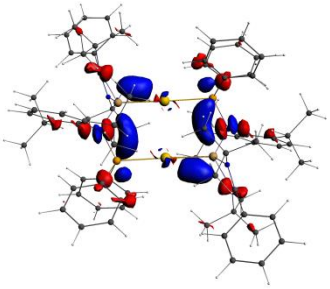

$\Delta\rho_6$
($\Delta E_{6(L\rightarrow L)}$=-9.9 kcal/mol)

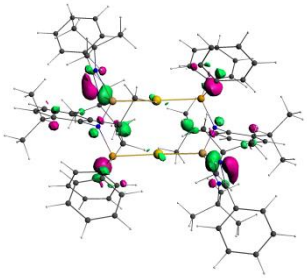

Ψ_{-7}(-0.26)

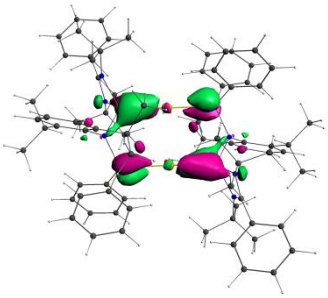

Ψ_{7}(0.26)

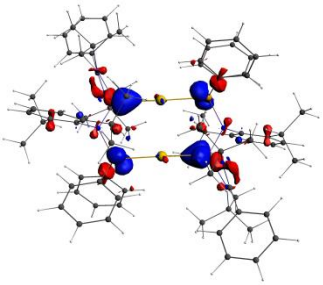

$\Delta\rho_7$
($\Delta E_{7(L\rightarrow L)}$=-8.5 kcal/mol)

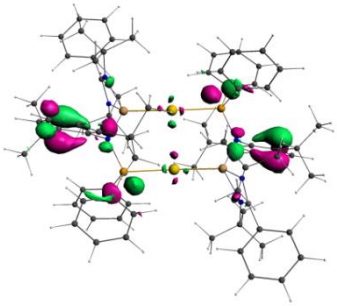

Ψ_{-8}(-0.25)

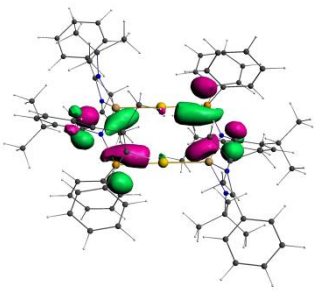

Ψ_{8}(0.25)

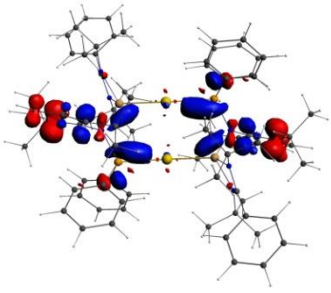

$\Delta\rho_8$
($\Delta E_{7(L\rightarrow L)}$= -8.1 kcal/mol)

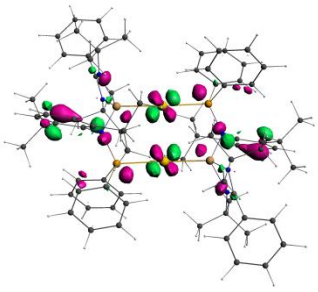

Ψ_{-9}(-0.24)

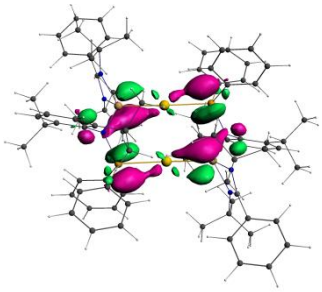

Ψ_{9}(0.24)

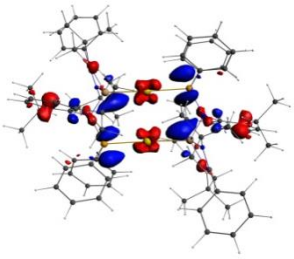

$\Delta\rho_{9}$
($\Delta E_{\sigma_{9(Au\rightarrow L)}}$=-8.2 kcal/mol)

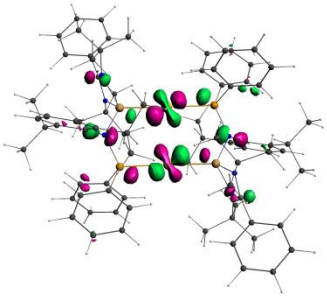

Ψ_{-10}(-0.22)

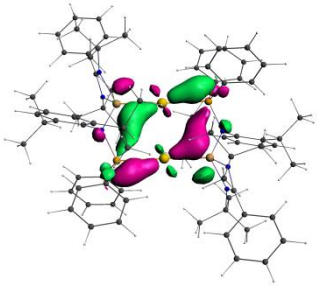

Ψ_{10}(0.22)

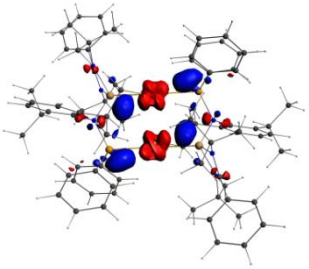

$\Delta\rho_{10}$
($\Delta E_{\sigma_{10(Au\rightarrow L)}}$=-9.1 kcal/mol)

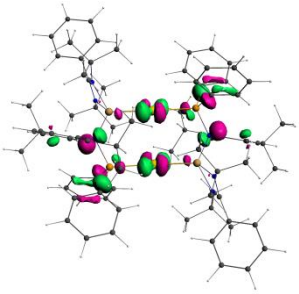

Ψ_{-11}(-0.22)

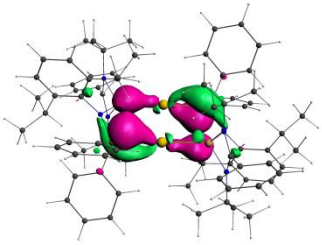

Ψ_{11}(0.22)

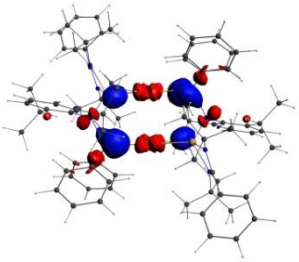

$\Delta\rho_{11}$
($\Delta E_{\sigma_{11(Au\rightarrow L)}}$=-8.7 kcal/mol)

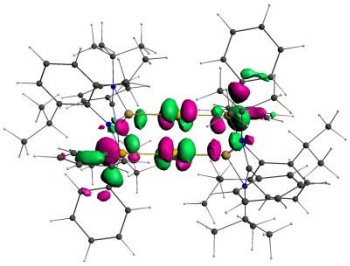

Ψ_{-12}(-0.21)

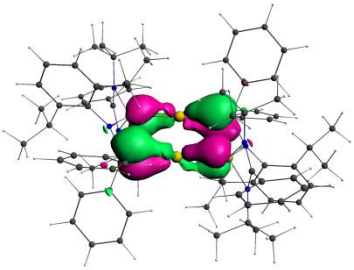

Ψ_{12}(0.21)

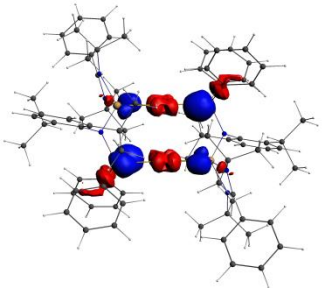

$\Delta\rho_{12}$
($\Delta E_{\sigma_{12(Au\rightarrow L)}}$=-8.6 kcal/mol)

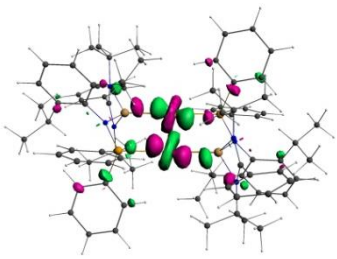

Ψ_{-13}(-0.19)

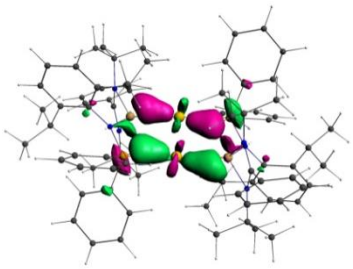

Ψ_{13}(0.19)

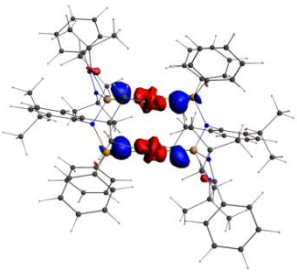

$\Delta\rho_{13}$ ($\Delta E_{\sigma_{13(Au\rightarrow L)}}$=-8.5 kcal/mol)

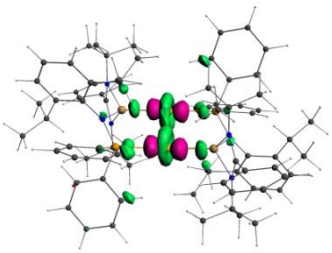

Ψ_{-14}(-0.18)

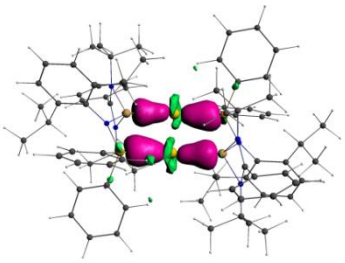

Ψ_{14}(0.18)

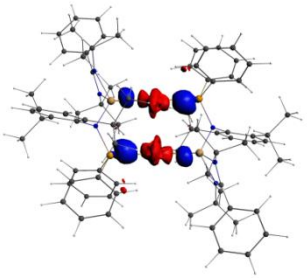

$\Delta\rho_{14}$ ($\Delta E_{\sigma_{14(Au\rightarrow L)}}$=-8.5 kcal/mol)

Figure 2A.12: NOCV pair of orbitals with their eigen values in parenthesis, the associated deformation density plots Δρ and orbital stabilization energies ΔE of **2.4** at the BP86/TZ2P level of theory. The direction of the charge flow in the deformation density plot Δρ is from red → blue. Isosurface value for NOCV pair orbitals is 0.03 and that for deformation density is 0.001 up to $\Delta\rho_4$ and 0.0005 for $\Delta\rho_5$-$\Delta\rho_{14}$. $\Delta\rho_5$-$\Delta\rho_8$ corresponds to the polarization of electron density within the fragments.

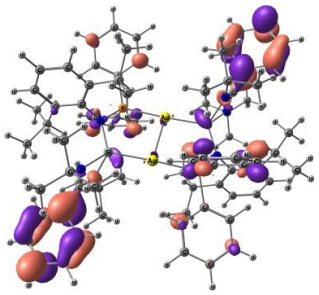

LUMO+6
-2.43

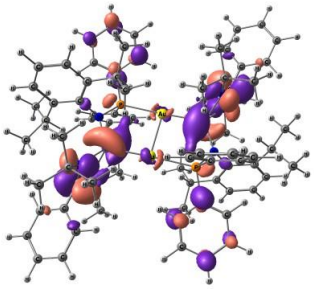

LUMO+5
-2.52

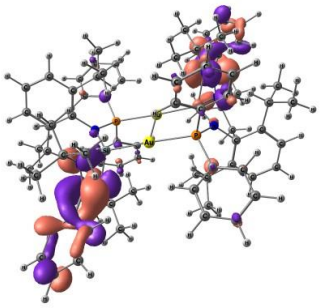

LUMO+4
-2.72

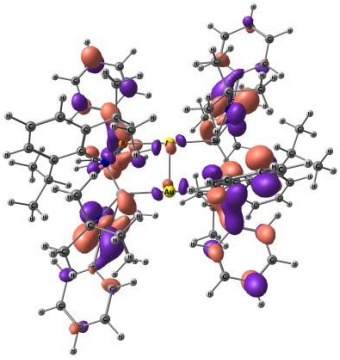

LUMO+3
-2.88

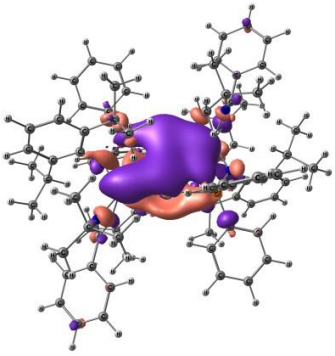

LUMO+2
-2.94

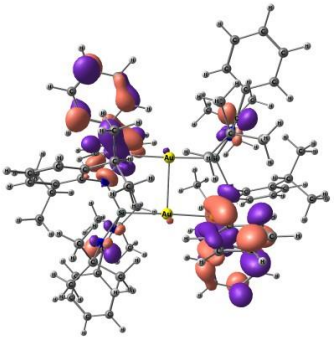

LUMO+1
-3.01

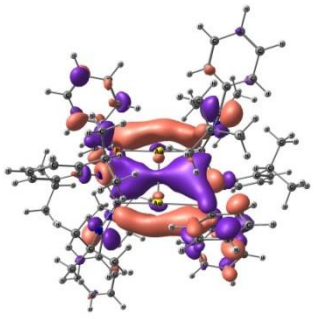

LUMO
-3.27

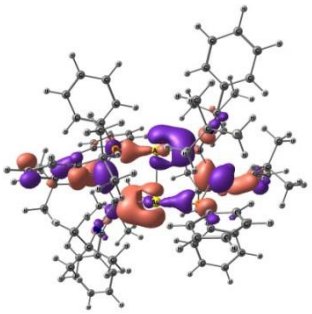

HOMO
-6.22

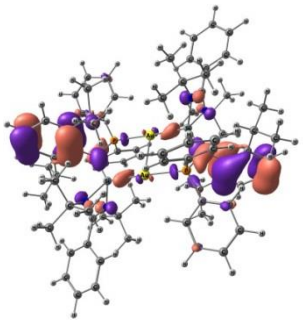

HOMO-1
-6.50

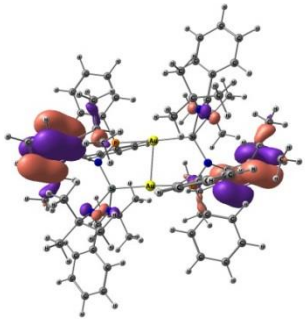

HOMO-2
-6.54

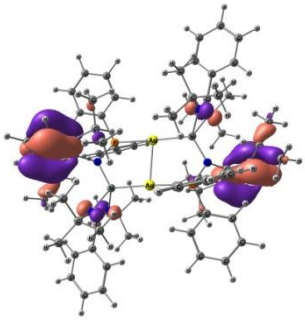

HOMO-3
-6.55

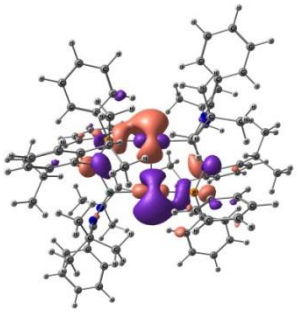

HOMO-4
-6.62

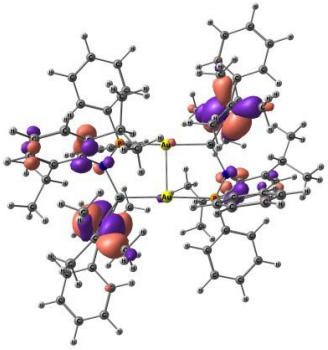

HOMO-5
-6.69

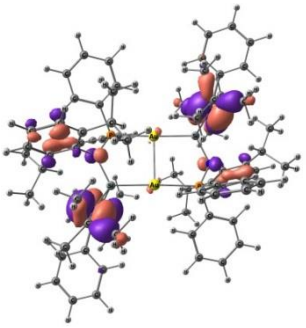

HOMO-6
-6.74

Figure 2A.12: Plot of important molecular orbitals of **2.4** at the BP86/def2-SVP level of theory including implicit solvent model.

Table 2A.3: EDA-NOCV results for the Si–Au bond of **2.3** at the BP86/TZ2P level of theory. Energies are in kcal/mol.

ΔE_{int}	ΔE_{Pauli}	ΔE_{elstat} [a]	ΔE_{orb} [a]	ΔE_1 [b]	ΔE_2 [b]	ΔE_3 [b]	ΔE_4 [b]	ΔE_{rest} [b,c]	ΔE_{prep}	ΔE(-De)
-63.7	219.5	-214.6 (75.8%)	-68.5 (24.2%)	-28.6 (41.7%)	-6.9 (10.1%)	-6.2 (9.1%)	-7.8 (11.4%)	-19.0 (27.7%)	1.5	-62.2

[a]Values in parenthesis give the percentage contribution to the total attractive interactions $\Delta E_{Elstat}+\Delta E_{Orb}$. [b]Values in parenthesis give the percentage contribution to orbital interaction ΔE_{Orb}. [c]$\Delta E_{rest} = \Delta E_{Orb} - (\Delta E_1 + \Delta E_2 + \Delta E_3 + \Delta E_4)$.

Table 2A.4: EDA-NOCV results for the Si–Au and P–Au bonds of **2.4** at the BP86/TZ2P level of theory. Energies are in kcal/mol**.**

ΔE_{int}	ΔE_{Pauli}	ΔE_{elstat} [a]	ΔE_{orb} [a]	$\Delta E_{\sigma(L\rightarrow Au)}$ [b]	$\Delta E_{\sigma(Au\rightarrow L)}$ [b]	ΔE_{rest} [b,c]	ΔE_{prep}	ΔE ($-D_e$)
-516.2	510.7	-536.2 (52.2%)	-490.7 (47.8%)	-248.2 (50.6%)	-51.6 (10.5%)	-190.9 (38.9%)	140.7	-375.5

[a]Values in parenthesis give the percentage contribution to the total attractive interactions $\Delta E_{elstat}+\Delta E_{orb}$. [b]Values in parenthesis give the percentage contribution to orbital interaction ΔE_{orb}. [c]$\Delta E_{rest} = \Delta E_{orb} - (\Delta E_{\sigma(L\rightarrow Au)} + \Delta E_{\sigma(Au\rightarrow L)} + \Delta E_{\sigma_3} + \Delta E_{\sigma_4} + \Delta E_p + \Delta E_b)$. $\Delta E_{\sigma(L\rightarrow Au)}$ is the energy corresponding to σ donation from ligand to Au and $\Delta E_{\sigma(Au\rightarrow L)}$ is the energy corresponding to back donation from Au to ligand.

Table 2A.5 Charge distribution given by the Natural Bond Orbital Analysis for **2.2**, **2.3** and **2.4** complex at the M06/def2-TZVPP//BP86/def2-TZVPP level of theory.

2.2		2.3		2.4	
Atom	Charge	Atom	Charge	Atom	Charge
P	1.03	P	1.03	P1	1.18
Si	1.18	Si	1.47	P2	1.18
N1	-1.20	Au	0.11	Si1	1.57
N2	-0.73	Cl	-0.58	Si2	1.57
N3	-0.71	N1	-1.22	Au1	-0.05
		N2	-0.72	Au2	-0.05
		N3	-0.76	N1	-1.23
				N2	-1.23

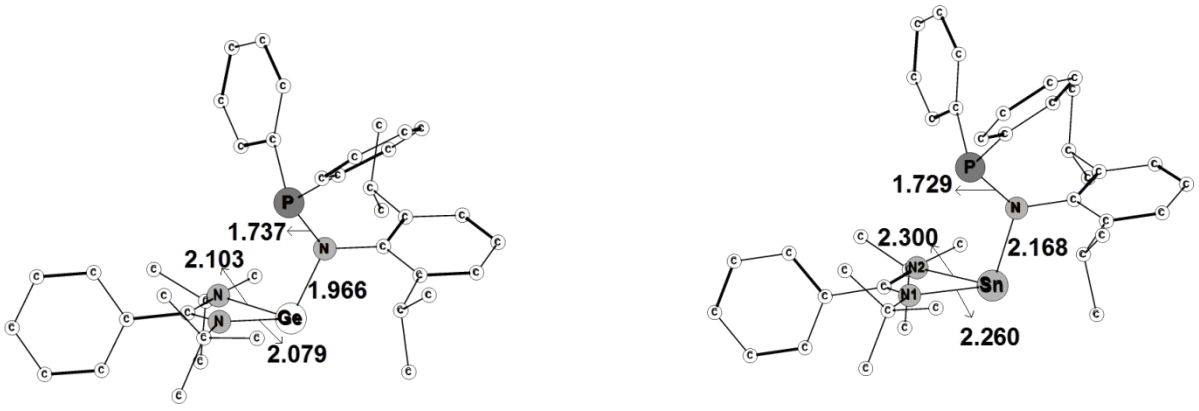

2.7 **2.8**

Figure 2A.13 Optimized geometries of germylene, **2.7** stannylene, **2.8** at the BP86/def2-TZVPP level of theory. Hydrogen atoms are omitted for clarity. Distances are given in Angstroms.

Table 2A.6 Atomic charge on the selected atoms of silylene (**2.2**), germylene (**2.7**) and stannylene (**2.8**) by natural bond orbital analysis at the M06/def2-TZVPP//BP86/def2-TZVPP[a] level of theory.

Atom	Atomic charge		
	X = Si	**X = Ge**	**X = Sn**
X	1.18	1.17	1.40
N1	-0.73	-0.71	-0.76
N2	-0.71	-0.68	-0.75
N	-1.20	-1.19	-1.26
P	1.03	1.04	1.04

[a]For **2.2** the natural bond order analysis was performed at the M06/def2-TZVPP//BP86/def2-SVP level of theory.

Table 3A. 1 Crystallographic data for **3.2**, **3.3** and **3.4**

	3.2	3.3	3.4
Chemical formula	$C_{48}H_{54}Cl_2Ge_2N_2P_2$	$C_{48}H_{54}GeN_2P_2$	$C_{48}H_{54}Ge_2N_2OP_2$
Formula weight	936.95 g/mol	793.46 g/mol	882.05 g/mol
Temperature	150(2) K	150(2) K	150(2) K
Wavelength	0.71073 Å	0.71073 Å	0.71073 Å
Crystal system	monoclinic	triclinic	triclinic
Space group	*P*n	*P* -1	*P* -1
Unit cell dimensions	*a* = 10.559(5) Å	*a* = 10.754(2) Å	*a* = 9.348(5) Å
	b = 14.185(7) Å	*b* = 17.660(3) Å	*b* = 12.975(6) Å
	c = 18.025(9) Å	*c* = 22.507(4) Å	*c* = 19.947(9) Å
	α = 90°	*α* = 95.526(5)°	*α* = 105.161(12)°
	β = 104.966(12)°	*β* = 91.930(6)°	*β* = 94.562(13)°
	γ = 90°	*γ* = 90.621(5)°	*γ* = 105.937(13)°
Volume	2608(2) Å^3	4252.0(14) Å^3	2215.4(18) Å^3
Z	2	4	2
Density (calculated)	1.193 g/cm^3	1.239 g/cm^3	1.322 g/cm^3
Absorption coefficient	1.347 mm^{-1}	0.830 mm^{-1}	1.466 mm^{-1}
F(000)	968	1672	916
Theta range for data collection	2.34 to 25.25°	2.25 to 25.25°	2.27 to 25.25°
Index ranges	-12<=h<=12, -17<=k<=17, -21<=l<=21	-12<=h<=12, -21<=k<=21, -26<=l<=27	-11<=h<=11, -15<=k<=15, -23<=l<=23
Reflections collected	65453	80912	85853
Independent reflections	9426[R(int)= 0.1986]	15370[R(int)= 0.1910]	8026[R(int)=0.0899]
Completeness to θ (%)	99.9%	99.9%	99.9%

Function minimized	Σ w(Fo² - Fc²)²	Σ w(Fo² - Fc²)²	Σ w(Fo² - Fc²)²
Data / restraints / parameters	9426 / 26 / 513	15370/ 0 / 971	8026 / 0 / 504
Goodness-of-fit on F²	0.968	1.013	1.089
Δ/σ max	0.017	0.001	0.001
Final R indices	6022 data; [I>2σ(I)] R1 = 0.0684, wR2 = 0.1315	8612 data[I>2σ(I)], R1 = 0.0644, wR2 = 0.1276	6263 data[I>2σ(I)], R1 = 0.0414, wR2 = 0.0878
	all data , R1 = 0.1151, wR2 = 0.1458	all data , R1 = 0.1447, wR2 = 0.1577	all data, R1 = 0.0629, wR2 = 0.0957
Largest diff. peak and hole	0.431 and -0.398 eÅ^{-3}	1.367 and -0.780 eÅ^{-3}	0.573 and -0.536 eÅ^{-3}
R.M.S. deviation from mean	0.081 eÅ^{-3}	0.085 eÅ^{-3}	0.061 eÅ^{-3}

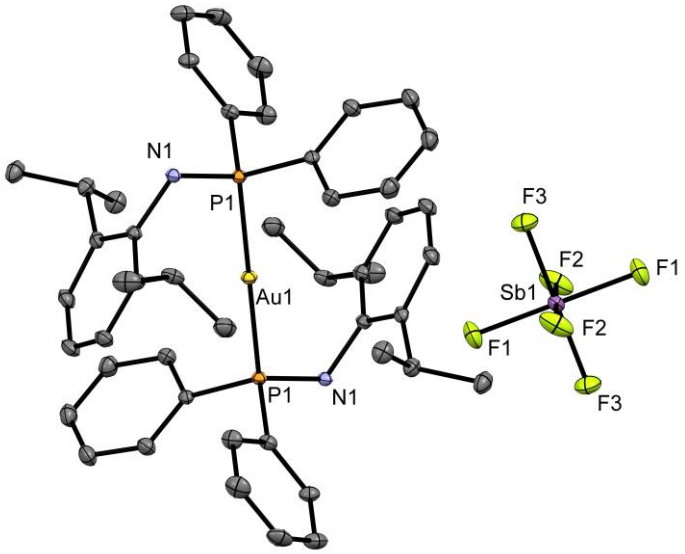

Figure 3A.1 Molecular structure of **3.5** at probability level of 50 %. Hydrogen atoms are omitted for clarity. Selected bond lengths (Å) and bond angles (deg). N1-P1 1.71(9) P1-Au1 2.33(5); P11-Au1-P1 180.

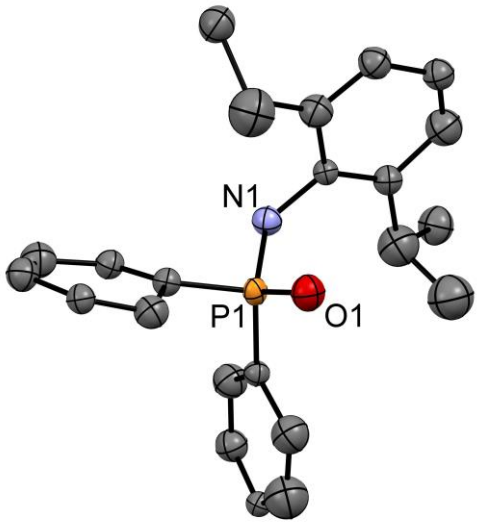

Figure 3A.2 Molecular structure of **3.6** at probability level of 50 %. Hydrogen atoms are omitted for clarity. Selected bond lengths (Å) and bond angles (deg). N1-P1 1.70(1) P1-O1 1.46(1); N1-P1-O1 113.0(7).

Table 4A.1 Crystallographic data for **4.2** and **4.3**

	4.2	4.3
Chemical formula	$C_{48}H_{78}B_2GeN_2$	$C_{48}H_{78}B_2N_2Sn$
Formula weight	777.33 g/mol	823.43 g/mol
Temperature	100(2) K	100(2) K
Wavelength	0.71073 Å	0.71073 Å
Crystal system	orthorhombic	orthorhombic
Space group	Pccn	Pccn
Unit cell dimensions	a = 12.6728(15) Å	a = 12.833(4) Å
	b = 18.474(2)Å	b = 18.606(6) Å
	c = 18.982(2) Å	c = 18.857(7) Å
	α = 90°	α = 90°
	β = 90°	β = 90°
	γ = 90°	γ = 90°
Volume	4444.0(9) Å^3	4502(3) Å^3
Z	4	4
Density (calculated)	1.162 g/cm^3	1.215 g/cm^3
Absorption coefficient	0.723 mm^{-1}	0.601 mm^{-1}
F(000)	1688	1760
Theta range for data collection	2.21 to 25.00°	2.16 to 25.25°
Index ranges	-15<=h<=15, -21<=k<=21, -22<=l<=22	-15<=h<=15, -22<=k<=22, -22<=l<=22
Reflections collected	113805	171519
Independent reflections	3912 [R(int) = 0.1449]	4087 [R(int) = 0.1382]
Completeness to Θ (%)	99.9%	100.0%
Absorption correction	multi-scan	multi-scan
Refinement method	Full-matrix least-squares on F2	Full-matrix least-squares on F2
Refinement program	SHELXL-2014/7 (Sheldrick, 2014)	SHELXL-2014/7 (Sheldrick, 2014)
Function minimized	Σ w(Fo2 - Fc2)2	Σ w(Fo2 - Fc2)2
Data / restraints / parameters	3912 / 0 / 244	4087/ 0 / 244
Goodness-of-fit on F2	1.052	1.050
Δ/σmax	0.001	0.000
Final R indices	2822 data; [I>2σ(I)] $R1$ = 0.0330, w$R2$ = 0.0679	3065 data[I>2σ(I)], $R1$ = 0.0340, w$R2$ = 0.0810
	all data , $R1$ = 0.0638, wR2 = 0.0810	all data , $R1$ = 0.0550, w$R2$ = 0.0919
Largest diff. peak and hole	0.349 and -0.352 eÅ^{-3}	0.574 and -0.815 eÅ^{-3}

R.M.S. deviation from mean	0.057 eÅ^{-3}	0.71 eÅ^{-3}

Table 4A.2 NMR data for hydroborated products catalysed by **4.2**

(i) **PhCH$_2$OBpin (4.4a)** ^{1}H NMR (400 MHz, $CDCl_3$) δ 7.43-7.26 (m, 5H, *Ph*), 5.02 (s, 2H, pinBOC*H$_2$*), 1.35 (s, 12H, Bpin-C*H$_3$*); ^{13}C NMR (101 MHz, $CDCl_3$) δ 139.4, 129.2, 128.4, 127.5, 126.9, 125.5, 83.1, 66.8, 24.7.

(ii) **3-BrPhCH$_2$OBpin (4.4b)** ^{1}H NMR (400 MHz, $CDCl_3$) δ 7.54-7.18 (m, 4H, *Ph*), 4.91 (s, 2H, pinBOC*H$_2$*), 1.29 (s, 12H, Bpin-C*H$_3$*); ^{13}C NMR (101 MHz, $CDCl_3$) δ 141.4, 130.3, 129.65, 128.5, 125.0, 122.3, 83.0, 65.7, 24.5.

(iii) **2-BrPhCH$_2$OBpin (4.4c)** ^{1}H NMR (400 MHz, $CDCl_3$) δ 7.56-7.23(m, 4H, *Ph*), 5.05(s, 2H, pinBOC*H$_2$*), 1.34 (s, 12H, Bpin-C*H$_3$*); ^{13}C NMR (101 MHz, $CDCl_3$) δ 137.9, 131.8, 128.2, 127.1, 124.9, 121.1, 82.7, 65.8, 24.2.

(iv) **4-BrPhCH$_2$OBpin (4.4d)** ^{1}H NMR (400 MHz, $CDCl_3$) δ 7.53-7.23(m, 4H, *Ph*), 4.94 (s, 2H, pinBOC*H$_2$*), 1.34 (s, 12H, Bpin-C*H$_3$*); ^{13}C NMR (101 MHz, $CDCl_3$) δ 138.29, 131.4, 129.1, 128.5, 125.4, 121.3, 83.1, 66.0, 24.7.

(v) **4-FPhCH$_2$OBpin (4.4e)** ^{1}H NMR (400 MHz, $CDCl_3$) δ 7.38-7.09 (m, 4H, *Ph*), 4.95 (s, 2H, pinBOC*H$_2$*), 1.33 (s, 12H, Bpin-C*H$_3$*); ^{13}C NMR (101 MHz, $CDCl_3$) δ 163.3, 128.6, 125.3, 115.1, 83.1, 66.1, 24.6.

(vi) **4-(NO$_2$)PhCH$_2$OBpin** (**4.4f**) ^{1}H NMR (400 MHz, $CDCl_3$) δ 8.43-7.23 (m, 4H, *Ph*), 5.08(s, 2H, pinBOC*H$_2$*), 1.34 (s,12H, Bpin-C*H$_3$*); ^{13}C NMR (101 MHz, $CDCl_3$) δ 146.6, 130.5, 128.3, 126.9, 123.6, 83.4, 65.6, 24.6.

(vii) **C$_6$H$_5$PhOBpin** (**4.4g**) ^{1}H NMR (400 MHz, $CDCl_3$) δ 8.15-7.29(m, 7H, *Ph*), 5.53(s, 2H, pinBOC*H$_2$*), 1.39 (s, 12H, Bpin-C*H$_3$*); ^{13}C NMR (101 MHz, $CDCl_3$) δ 134.8, 133.7, 131.1, 129.2, 128.7, 128.3, 126.0, 125.5, 125.0, 123.6, 83.2, 65.2, 24.8.

(viii) **3-(OCH_3)$PhCH_2OBpin$** (**4.4h**)) ^{1}H NMR (400 MHz, $CDCl_3$) δ 7.55-7.02 (m, 4H, Ph), 5.00 (s, 2H, pinBOCH2), 3.88 (s, 3H, -C*H*$_3$), 1.35 (s, 12H, Bpin-CH3); ^{13}C NMR (101 MHz, $CDCl_3$) δ 160.2, 130.1, 128.3, 123.6, 121.6, 112.1, 83.2, 66.6, 55.5, 24.5.

(ix) **4-CN$PhCH_2OBpin$** (**4.4i**) ^{1}H NMR (400 MHz, $CDCl_3$) δ 7.65-7.47(m, 4H, *Ph*), 5.02 (s, 2H, pinBOC*H*$_2$) 1.32 (s, 12H, Bpin-C*H*$_3$); ^{13}C NMR (101 MHz, $CDCl_3$) δ 144.6, 132.2, 128.7, 125.3, 118.9, 111.1, 83.3, 65.8, 24.6.

(x) **4-(CH_3)$PhCH_2OBpin$** (**4.4j**) ^{1}H NMR (400 MHz, $CDCl_3$) δ 7.33-7.21(m, 4H, *Ph*), 4.97 (s, 2H, pinBOC*H*$_2$), 2.41 (s, 3H, -C*H*$_3$), 1.34 (s,12H, Bpin-C*H*$_3$); ^{13}C NMR (101 MHz, $CDCl_3$) δ 136.6, 129.7, 129.0, 128.3, 125.4, 82.9, 66.6, 24.7, 21.2.

(xi) **2-(OH)$PhCH_2OBpin$** (**4.4k**) ^{1}H NMR (400 MHz, $CDCl_3$) δ 7.28-6.96(m, 4H, *Ph*), 5.03 (s, 2H, pinBOC*H*$_2$), 1.32 (s,12H, Bpin-C*H*$_3$); ^{13}C NMR (101 MHz, $CDCl_3$) δ 155.1, 129.7, 128.8, 125.3, 120.3, 117.0, 83.7, 64.7, 24.5.

(xii) **PhC_3H_4OBpin (4.4l)** ^{1}H NMR (400 MHz, $CDCl_3$) δ 7.37-7.22 (m, 5H, *Ph*), 4.59 (dd, J = 5.4, 1.6 Hz, 2H, pinBOC*H*$_2$), 1.33 (s, 12H, Bpin-C*H*$_3$); ^{13}C NMR (101 MHz, $CDCl_3$) δ 137.0, 130.8, 129.2, 128.7, 128.4, 127.6, 126.6, 125.4, 83.1, 65.4, 24.7.

Table 4A.3 NMR data for hydroborated products catalysed by **4.3**

(i) **$PhCH_2OBpin$ (4.4a)** ^{1}H NMR (400 MHz, $CDCl_3$) δ 7.39-7.29 (m, 4H, *Ph*), 4.96 (s, 2H, pinBOC*H*$_2$), 1.29 (s, 12H, Bpin-C*H*$_3$); ^{13}C NMR (101 MHz, $CDCl_3$) δ 139.4, 129.2, 128.4, 127.5, 125.5, 83.1, 66.8, 24.8.

(ii) **3-Br$PhCH_2OBpin$ (4.4b)** ^{1}H NMR (400 MHz, $CDCl_3$) δ 7.57-7.22 (m, 4H, *Ph*), 4.93 (s, 2H, pinBOC*H*$_2$), 1.31 (s, 12H, Bpin-C*H*$_3$); ^{13}C NMR (101 MHz, $CDCl_3$) δ 141.6, 130.5, 129.9, 128.7, 125.3, 122.6, 83.3, 65.9, 24.7.

(iii) **2-Br$PhCH_2OBpin$ (4.4c)** ^{1}H NMR (400 MHz, $CDCl_3$) δ 7.55-7.18 (m, 4H, *Ph*), 5.01 (s, 2H, pinBOC*H*$_2$), 1.30 (s, 12H, Bpin-C*H*$_3$); ^{13}C NMR (101 MHz, $CDCl_3$) δ 138.4, 132.4, 128.7, 127.7, 125.4, 121.6, 83.3, 66.4, 24.7.

(iv) **4-Br$PhCH_2OBpin$ (4.4d)** ^{1}H NMR (400 MHz, $CDCl_3$) δ 7.85-7.29 (m, 4H, *Ph*), 4.94 (s, 2H, pinBOC*H*$_2$), 1.34 (s, 12H, Bpin-C*H*$_3$); ^{13}C NMR (101 MHz, $CDCl_3$) δ 138.3, 131.4, 128.5, 121.3, 83.1, 66.0, 24.7.

(v) **4-FPhCH$_2$OBpin (4.4e)** ^{1}H NMR (400 MHz, $CDCl_3$) δ 7.37-7.05 (m, 4H, *Ph*), 4.92 (s, 2H, pinBOC*H$_2$*), 1.30 (s, 12H, Bpin-C*H$_3$*); ^{13}C NMR (101 MHz, $CDCl_3$) δ 163.4, 137.7, 132.3, 128.7, 126.9, 116.3, 115.0, 83.1, 66.1, 24.6.

(vi) **4-(NO$_2$)PhCH$_2$OBpin** (**4.4f**) ^{1}H NMR (400 MHz, $CDCl_3$) δ 8.26-7.56 (m, 4H, *Ph*), 5.08 (s, 2H, pinBOC*H$_2$*) 1.37 (s,12H, Bpin-C*H$_3$*); ^{13}C NMR (101 MHz, $CDCl_3$) δ 147.3, 146.6, 126.9, 123.6, 83.4, 65.6, 24.6.

(vii) **C$_6$H$_5$PhOBpin** (**4.4g**) ^{1}H NMR (400 MHz, $CDCl_3$) δ 8.15-7.26 (m, 7H, *Ph*), 5.49 (s, 2H, pinBOC*H$_2$*), 1.36 (s,12H, Bpin-C*H$_3$*); ^{13}C NMR (101 MHz, $CDCl_3$) δ 136.7, 135.3, 134.7, 133.6, 131.0, 129.1, 128.4, 126.0, 125.4, 124.9, 123.5, 83.1, 76.8, 65.1, 25.0

(viii) **3-(OCH$_3$)PhCH$_2$OBpin** (**4.4h**) ^{1}H NMR (400 MHz, $CDCl_3$) δ 7.31-6.88 (m, 4H, Ph), 4.99 (s, 2H, pinBOCH_2), 3.87 (s, 3H, -C*H$_3$*), 1.34 (s,12H, Bpin-CH_3); ^{13}C NMR (101 MHz, $CDCl_3$) δ 159.8, 140.9, 129.3, 118.9, 113.2, 111.9, 83.0, 66.6, 55.2, 24.7

(ix) **4-CNPhCH$_2$OBpin** (**4.4i**) ^{1}H NMR (400 MHz, $CDCl_3$) δ 8.01-7.29 (m, 4H, *Ph*), 5.03(s, 2H, pinBOC*H$_2$*), 1.33 (s, 12H, Bpin-C*H$_3$*); ^{13}C NMR (101 MHz, $CDCl_3$) δ 144.6, 132.2, 129.1, 126.9, 118.9, 111.2, 83.4, 65.8, 24.6.

(x) **4-(CH$_3$)PhCH$_2$OBpin** (**4.4j**) ^{1}H NMR (400 MHz, $CDCl_3$) δ 7.33-7.20 (m, 4H, *Ph*), 4.97 (s, 2H, pinBOC*H$_2$*) 2.41 (s, 3H, -C*H$_3$*), 1.34 (s, 12H, Bpin-C*H$_3$*); ^{13}C NMR (101 MHz, CDCl3) δ 136.4, 129.1, 126.9, 82.9, 66.8, 24.6, 21.4.

(xi) **2-(OH)PhCH$_2$OBpin** (**4.4k**) ^{1}H NMR (400 MHz, $CDCl_3$) δ 7.22-6.93 (m, 4H, *Ph*), 5.02 (s, 2H, pinBOC*H$_2$*), 1.31 (s,12H, Bpin-C*H$_3$*); ^{13}C NMR (101 MHz, $CDCl_3$) δ 155.1, 129.6, 128.6, 125.2, 120.2, 116.9, 83.6, 64.6, 24.5.

(xii) **PhC$_3$H$_4$OBpin (4.4l)** ^{1}H NMR (400 MHz, $CDCl_3$) δ 7.62-7.26(m, 5H, *Ph*), 6.72 (m, 1H, -CH=C*H*-), 6.38 (m, 1H, -C*H*=CH-), 4.63 (dd, *J* = 5.4, 1.7 Hz, 2H, pinBOC*H$_2$*), 1.35 (s, 12H, Bpin-C*H$_3$*); ^{13}C NMR (101 MHz, $CDCl_3$) δ 136.9, 130.7, 128.6, 127.5, 126.9, 126.5, 83.0, 65.3, 24.6.

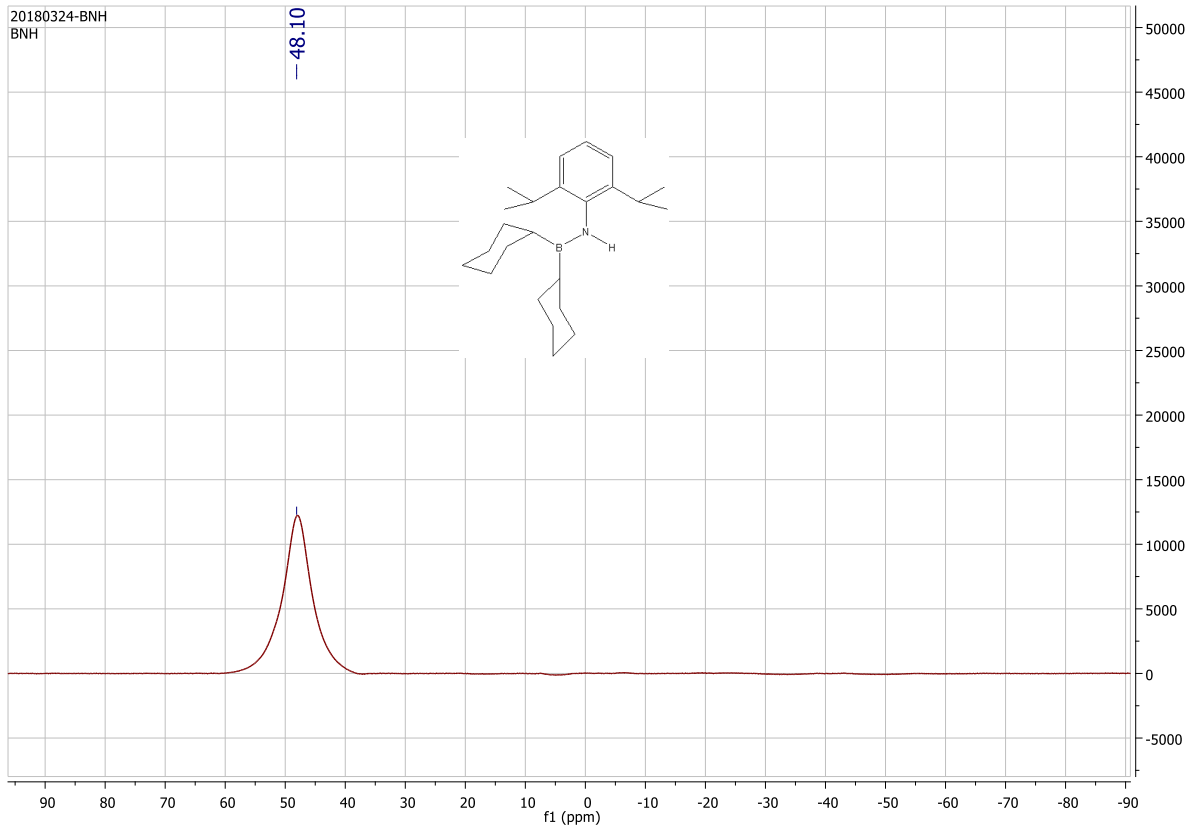

Figure 4A.1 ^{11}B NMR of **4.1** in $CDCl_3$

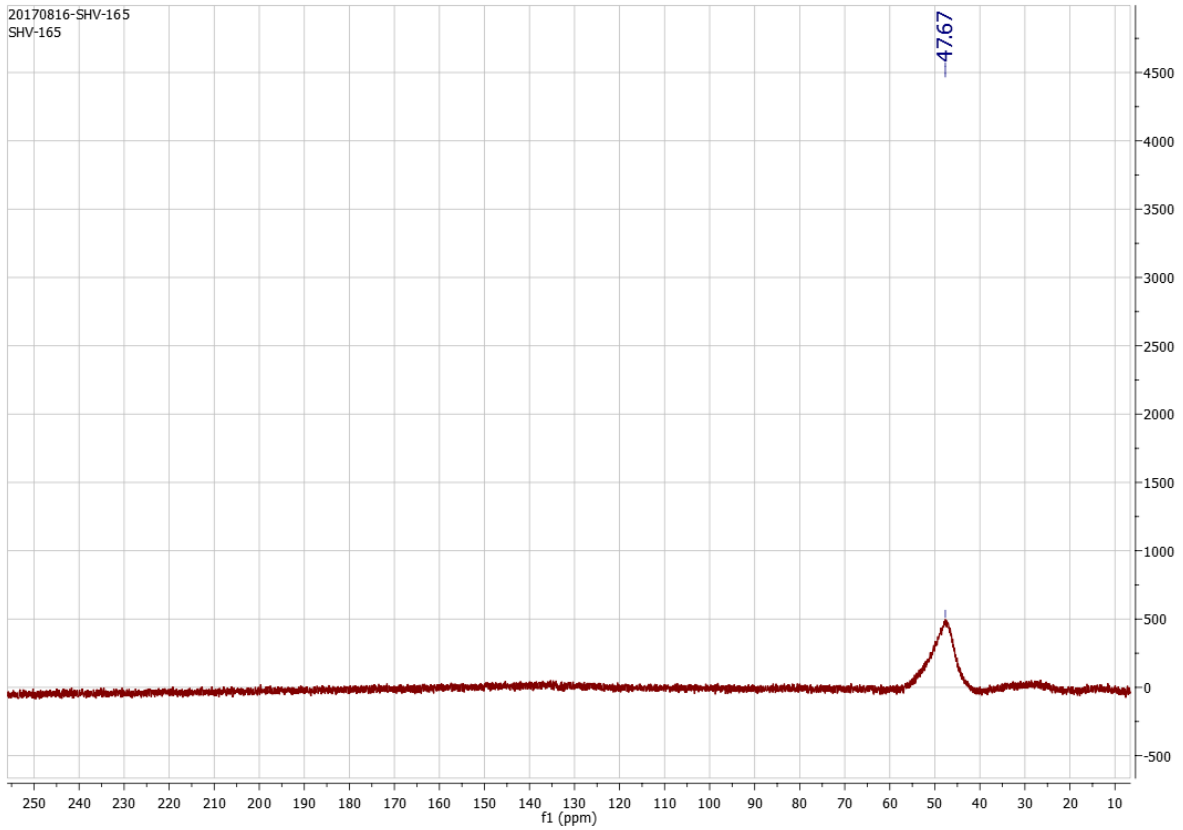

Figure 4A.2 ^{11}B NMR of **4.2** in $CDCl_3$

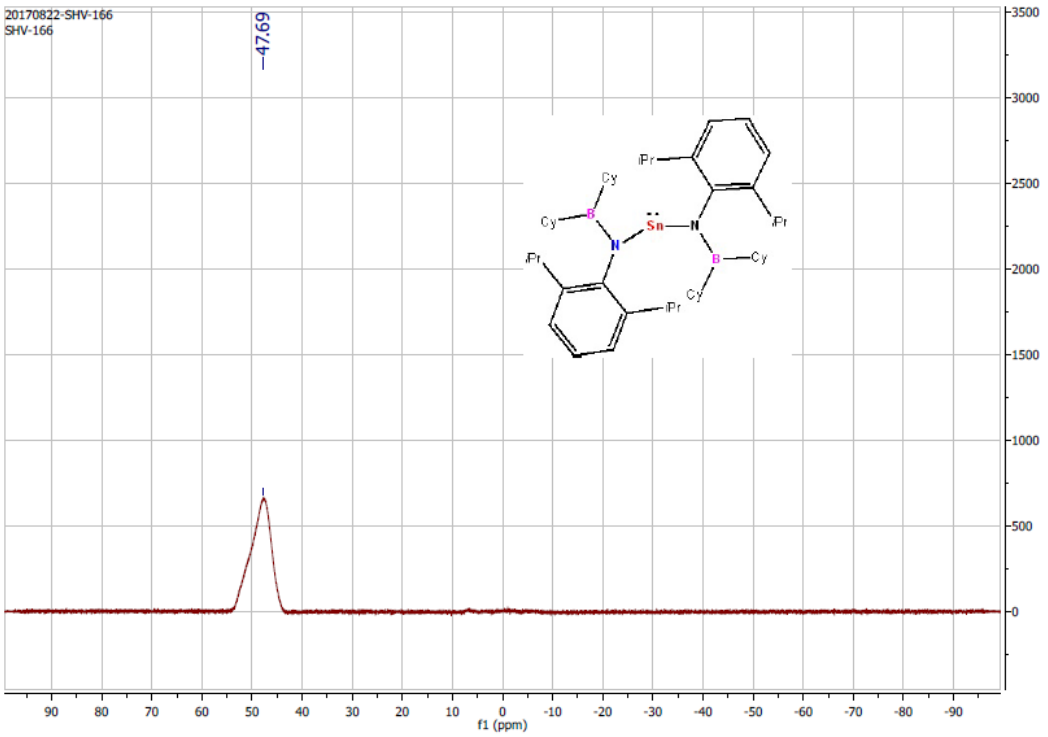

Figure 4A.3. ^{11}B NMR of **4.3** in C_6D_6

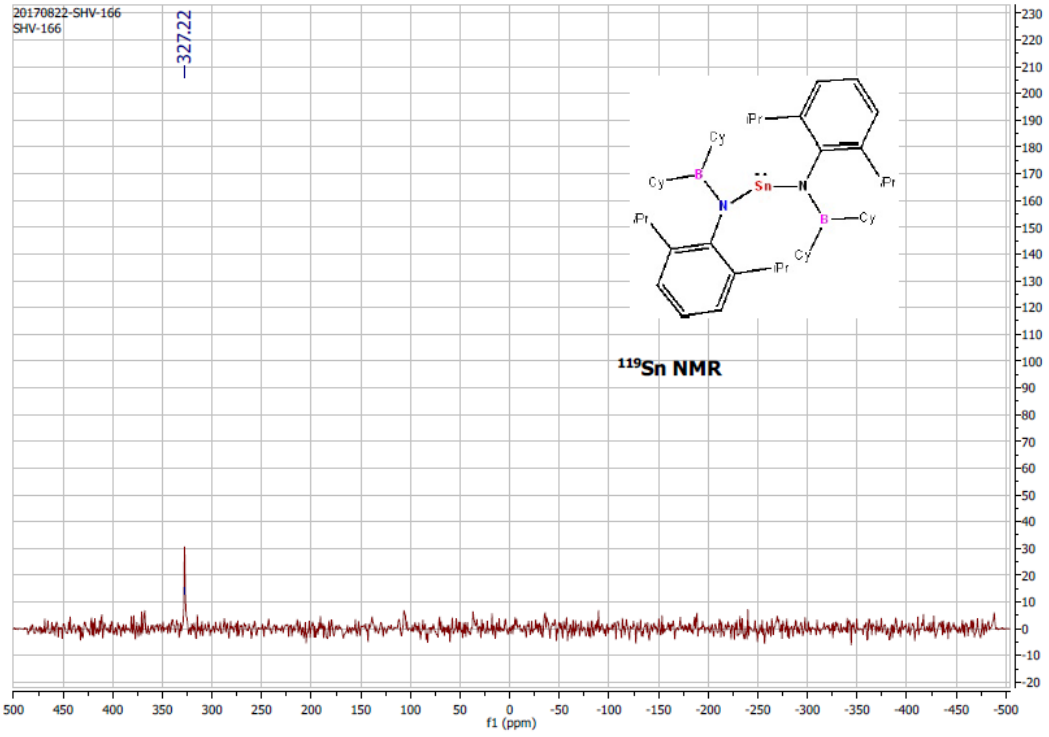

Figure 4A.4 ^{119}Sn NMR of **4.3** in C_6D_6

^{1}H NMR spectra for optimization of reaction conditions using catalyst 4.2

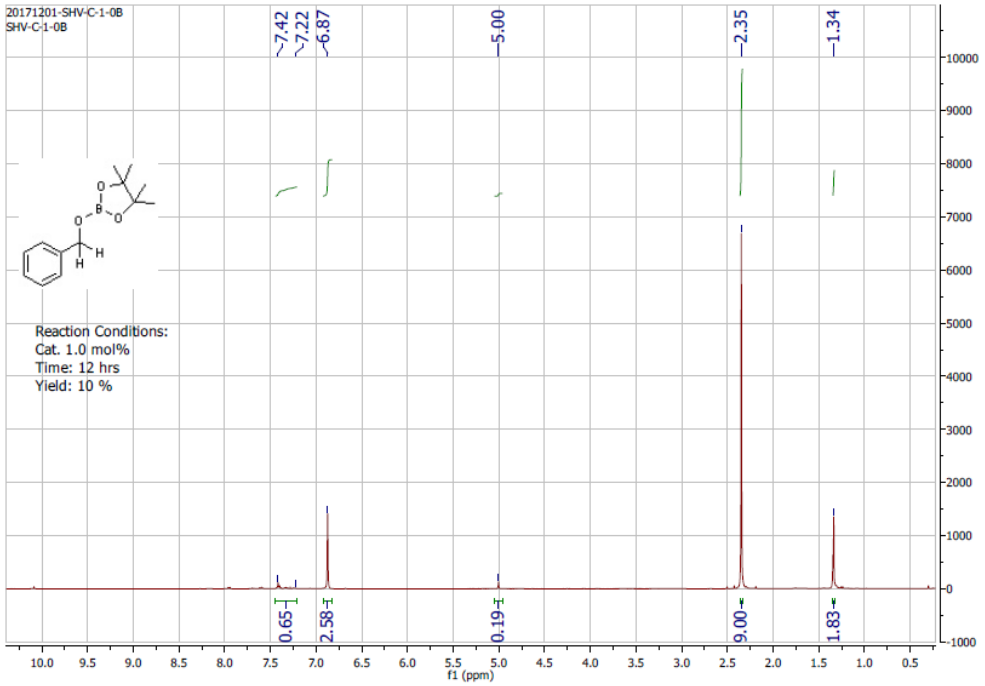

(a)

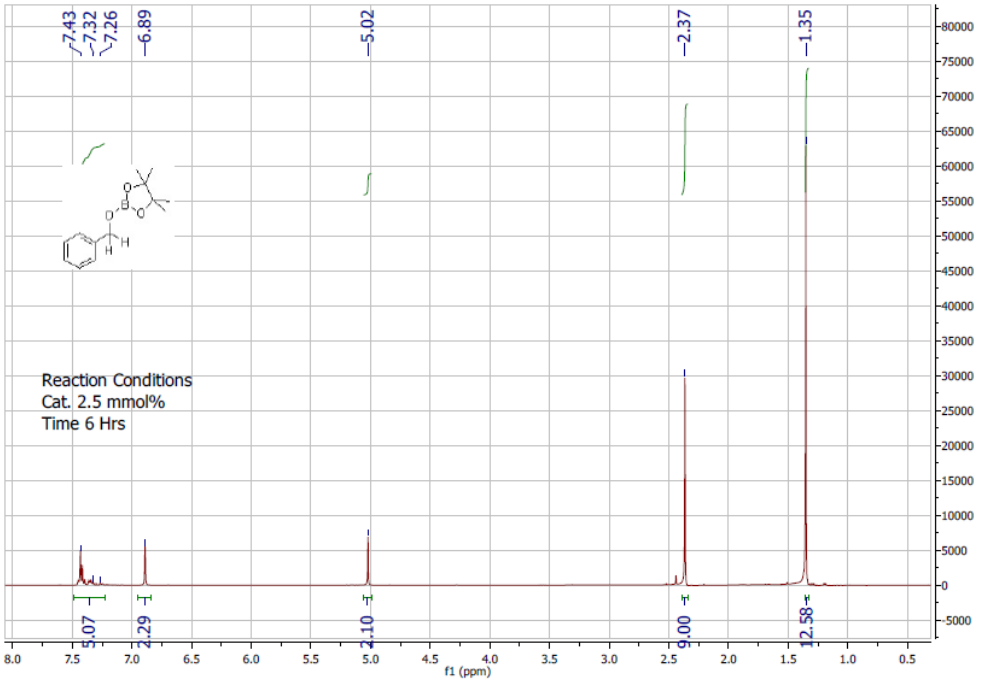

(b)

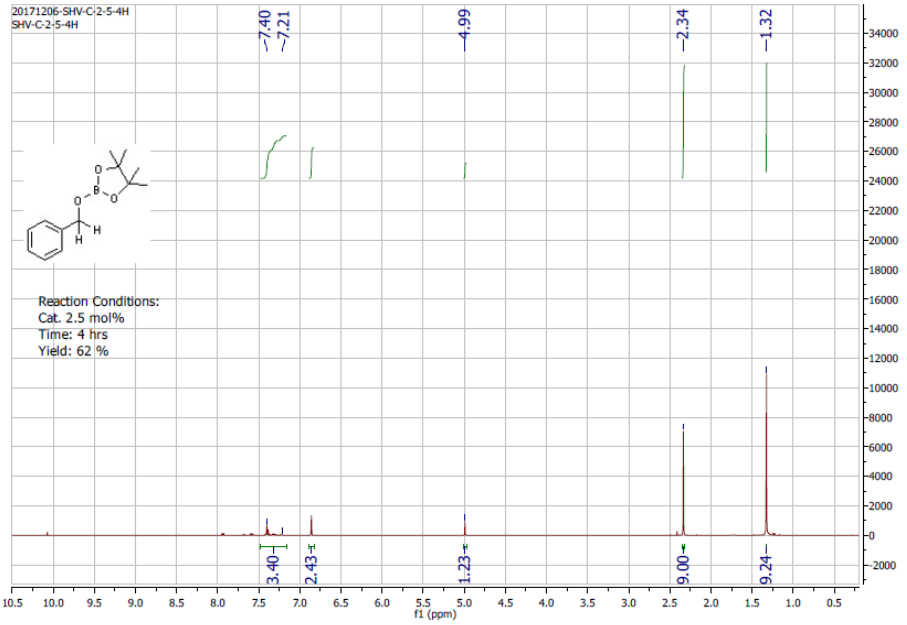

(c)

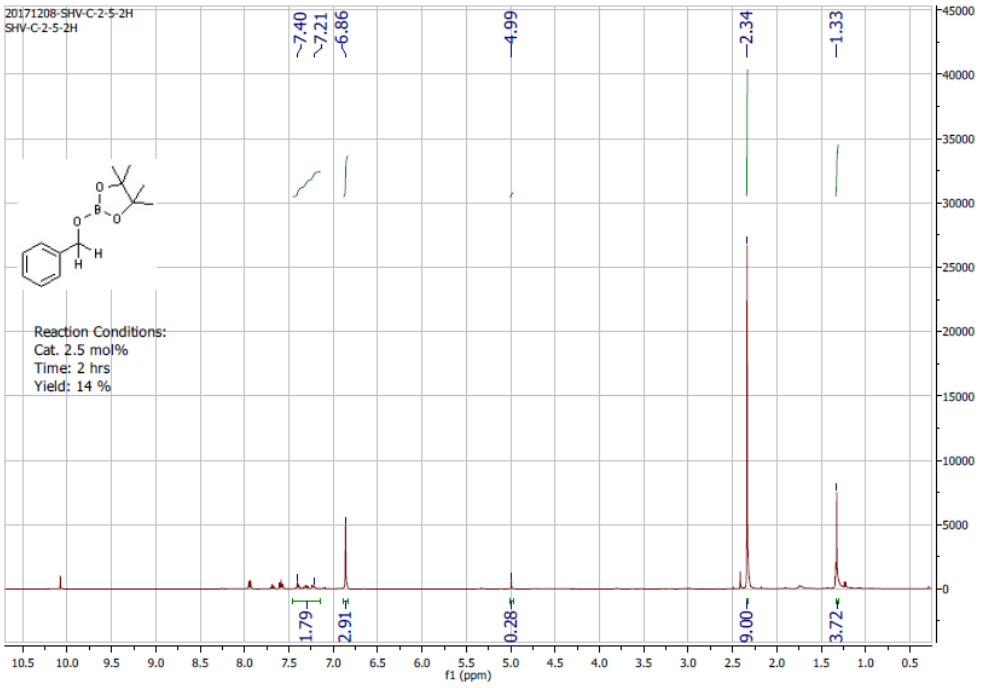

(d)

Figure 4A.5 ^{1}H NMR for optimization of reaction conditions using catalyst **4.2** at the reaction conditions of (a) cat. 1 mol%, 12hrs, (b) cat. 2.5 mol%, 6hrs (c) cat. 2.5 mol%, 4hrs (d) cat. 2.5 mol%, 2 hrs

^{1}H NMR spectra for optimization of reaction conditions using catalyst 4.3

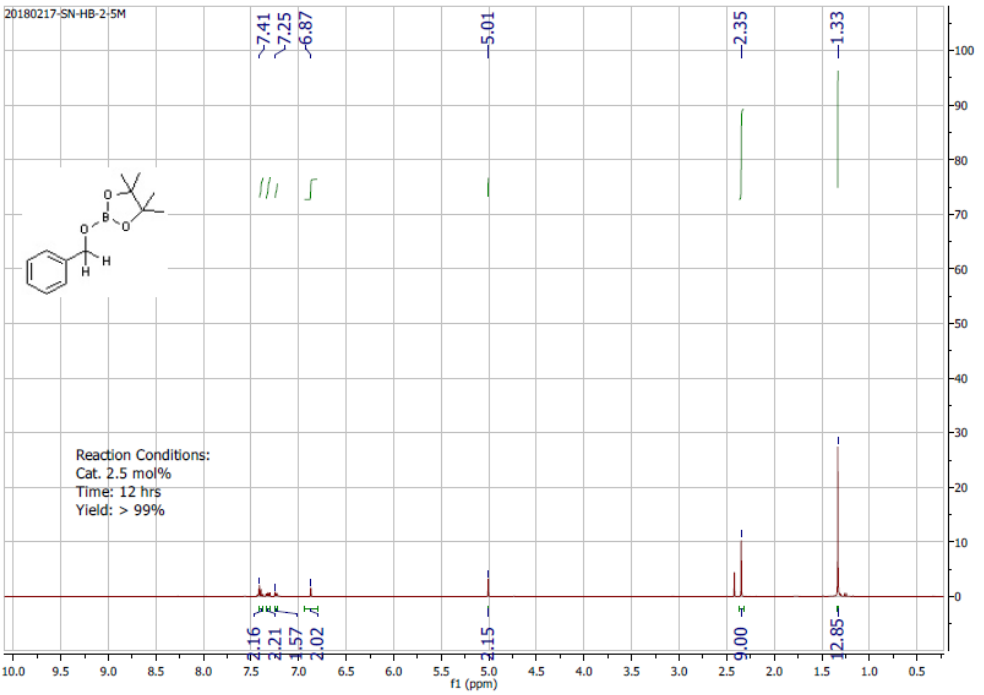

(a)

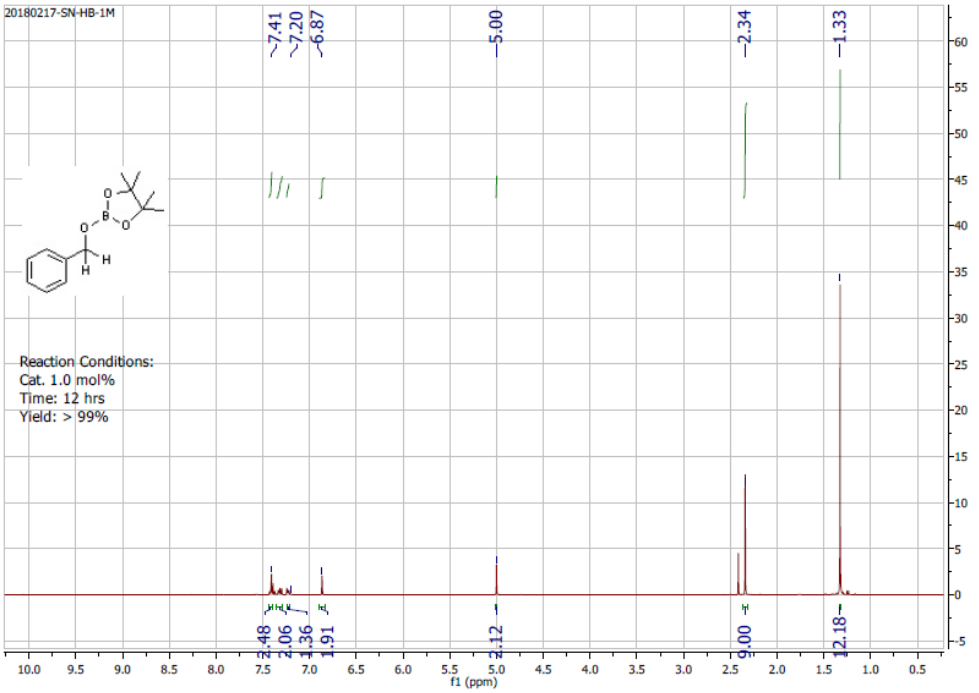

(b)

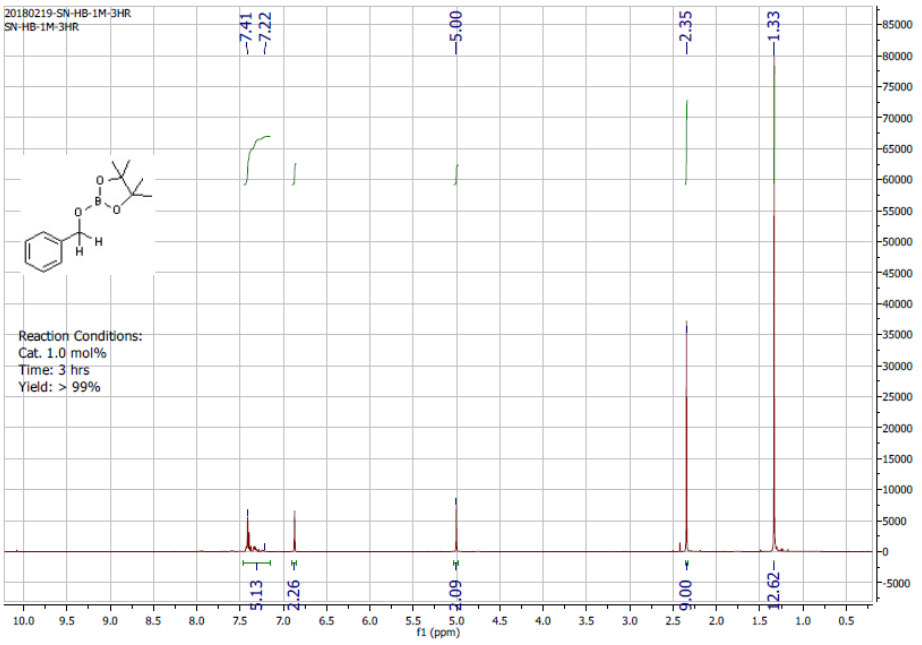
20180219-SN-HB-1M-3HR
SN-HB-1M-3HR
7.41
7.22
5.00
2.35
1.33
Reaction Conditions:
Cat. 1.0 mol%
Time: 3 hrs
Yield: > 99%
5.13
2.26
2.09
9.00
12.62
f1 (ppm)

(c)

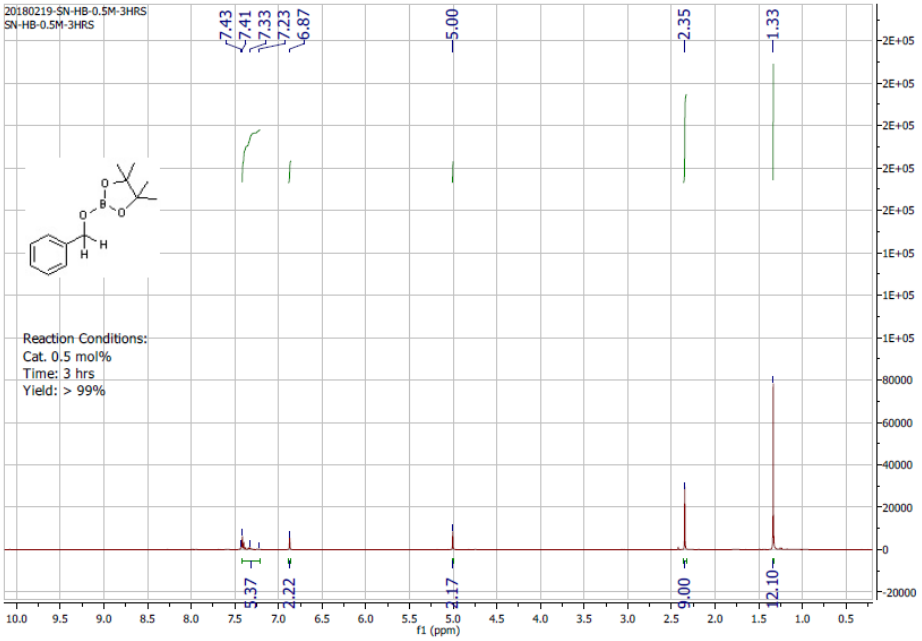
20180219-SN-HB-0.5M-3HRS
SN-HB-0.5M-3HRS
7.43
7.41
7.33
7.23
6.87
5.00
2.35
1.33
Reaction Conditions:
Cat. 0.5 mol%
Time: 3 hrs
Yield: > 99%
5.37
2.22
2.17
9.00
12.10
f1 (ppm)

(d)

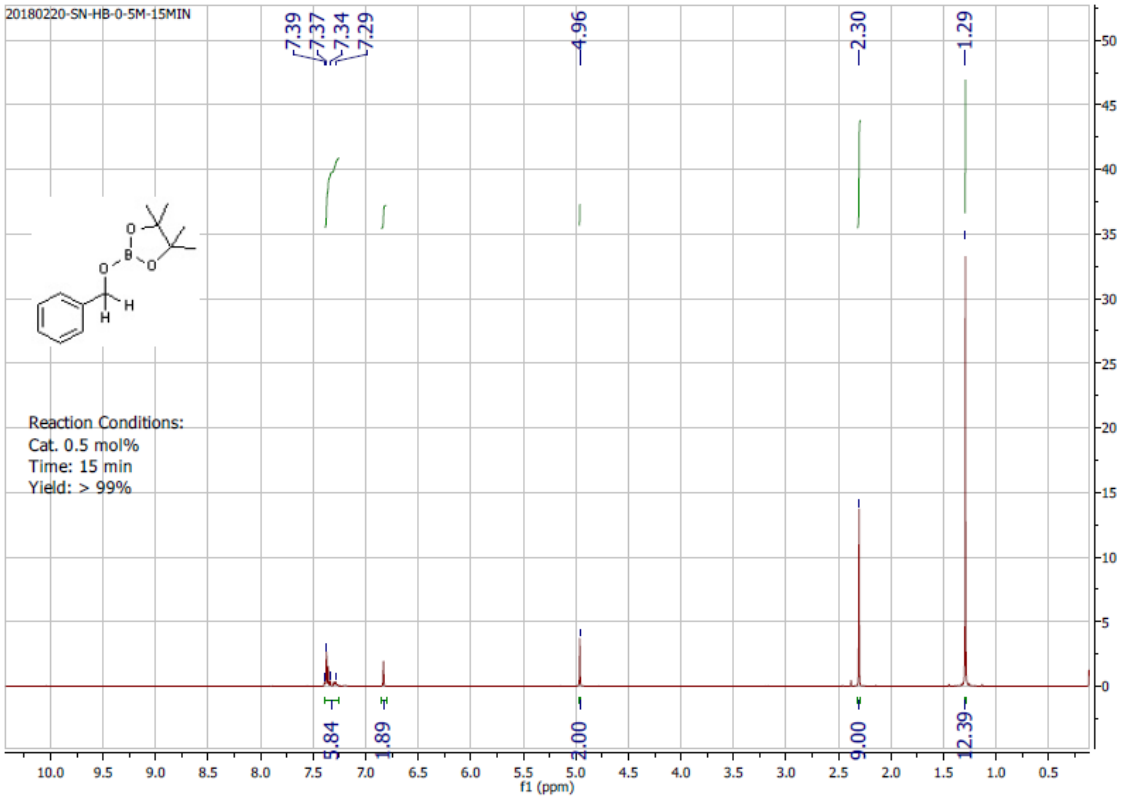
20180220-SN-HB-0-5M-15MIN
7.39
7.37
7.34
7.29
4.96
2.30
1.29
Reaction Conditions:
Cat. 0.5 mol%
Time: 15 min
Yield: > 99%
5.84
1.89
2.00
9.00
12.39
f1 (ppm)

(e)

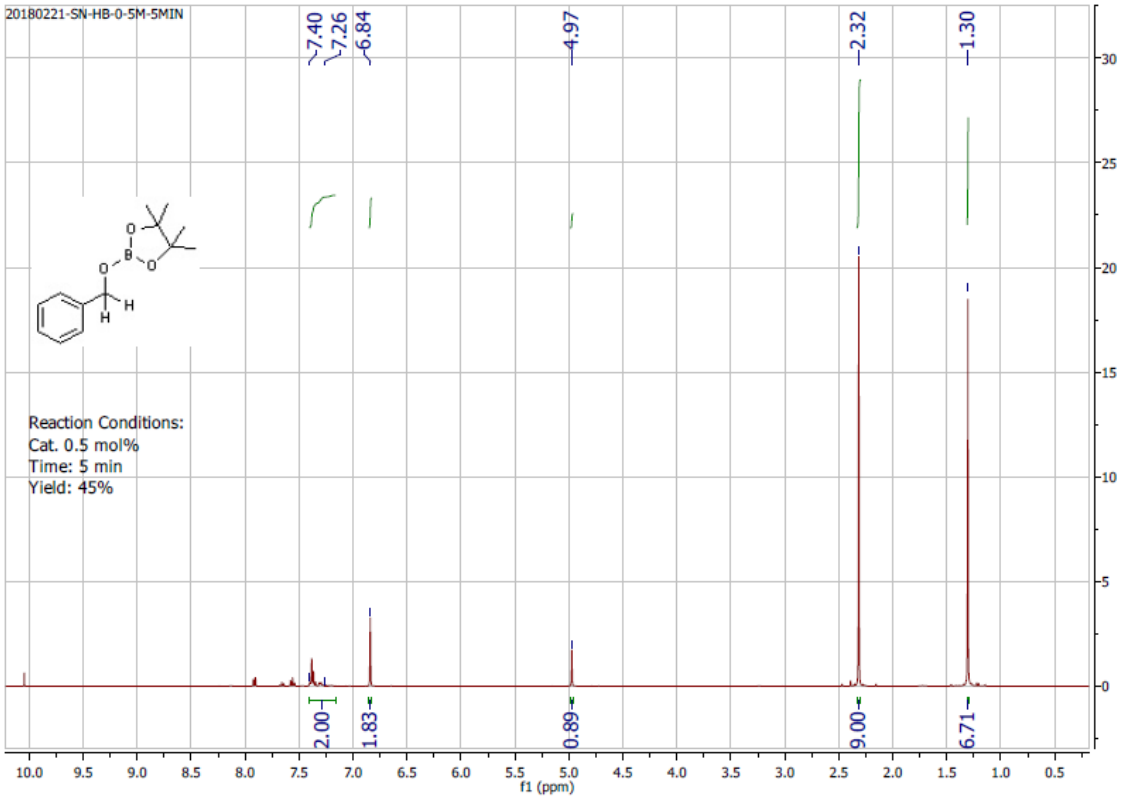
20180221-SN-HB-0-5M-5MIN
7.40
7.26
6.84
4.97
2.32
1.30
Reaction Conditions:
Cat. 0.5 mol%
Time: 5 min
Yield: 45%
2.00
1.83
0.89
9.00
6.71
f1 (ppm)

(f)

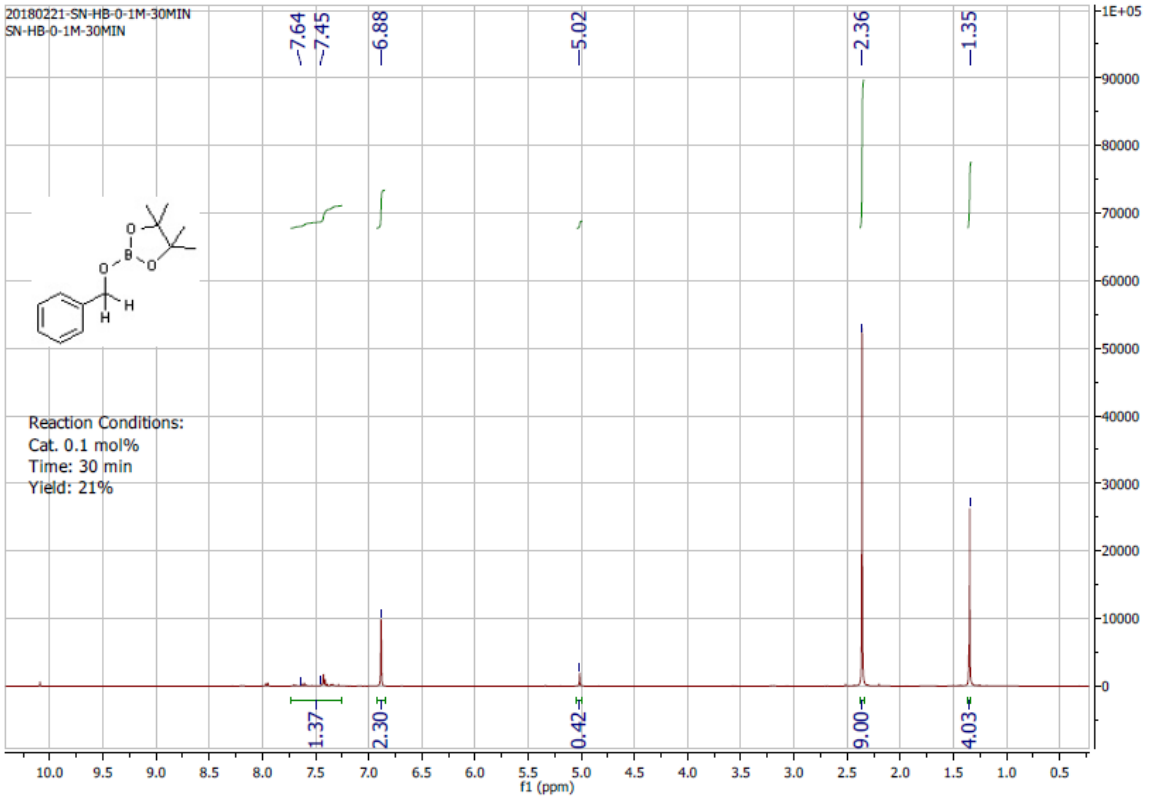

(g)

Figure 4A.5 ^{1}H NMR for optimization of reaction conditions using catalyst **4.3** at the reaction conditions of (a) cat. 2.5 mol%, 12hrs, (b) cat. 1.0 mol%, 12 hrs (c) cat. 1.0 mol%, 3hrs (d) cat. 0.5 mol%, 3 hrs (e) cat. 0.5 mol%, 15 min (f) cat. 0.5 mol%, 5 min (g) cat. 1.0 mol%, 30 min

Hydroboration of benzaldehyde using α-phosphinoamido-germylene (3.3) as catalyst

The same procedure which is employed for catalysis using **4.2** and **3.3**, is followed for catalysis using phosphinoamido-germylene (**3.3**). The optimization table and the ^{1}H NMR Spectra are given below

Entry	Cat.(mol %)	Time	Yields (%)[b]
1	2.5	12 hrs	98
2	1.0	12 hrs	66
3	2.5	4 hrs	97
4	2.5	1 hrs	18

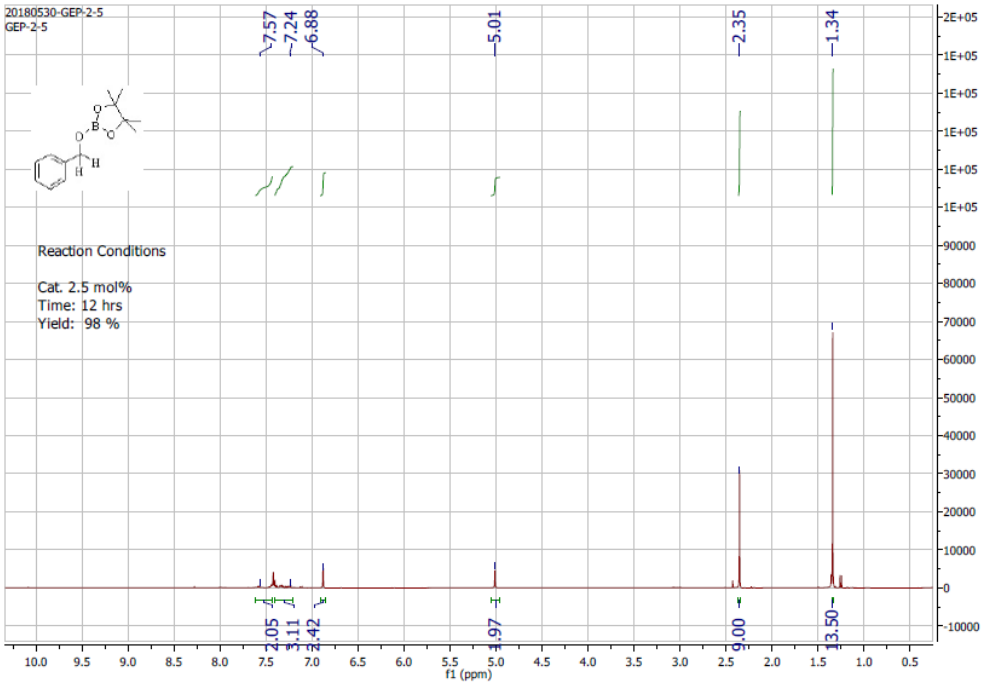
20180530-GEP-2-5
GEP-2-5
7.57
7.24
6.88
5.01
2.35
1.34
Reaction Conditions
Cat. 2.5 mol%
Time: 12 hrs
Yield: 98 %
2.05
3.11
2.42
1.97
9.00
13.50
f1 (ppm)

(a)

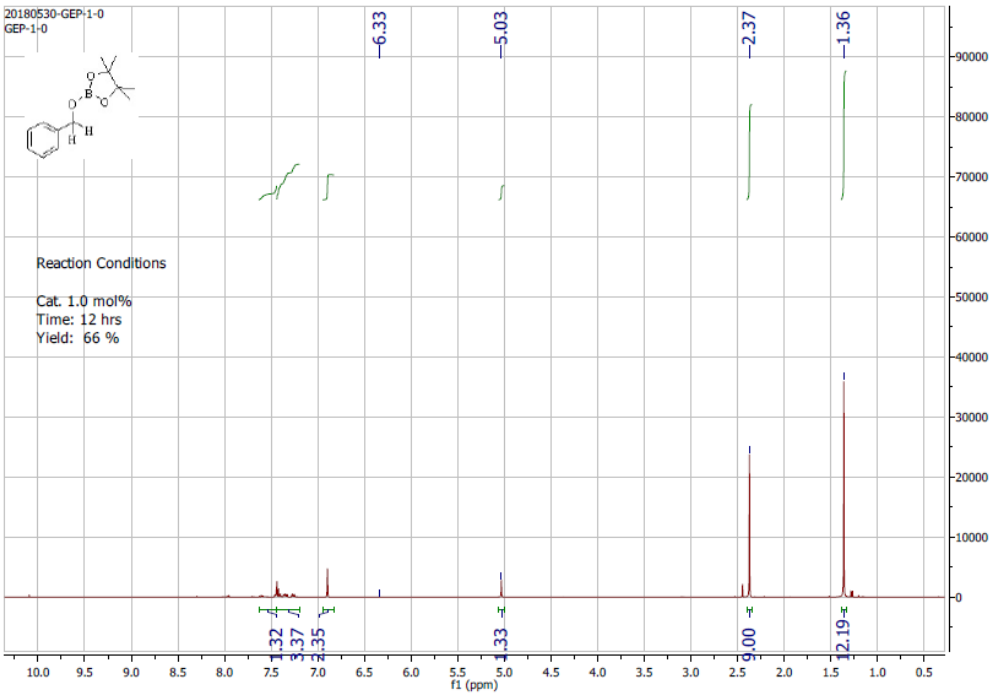
20180530-GEP-1-0
GEP-1-0
6.33
5.03
2.37
1.36
Reaction Conditions
Cat. 1.0 mol%
Time: 12 hrs
Yield: 66 %
1.32
3.37
2.35
1.33
9.00
12.19
f1 (ppm)

(b)

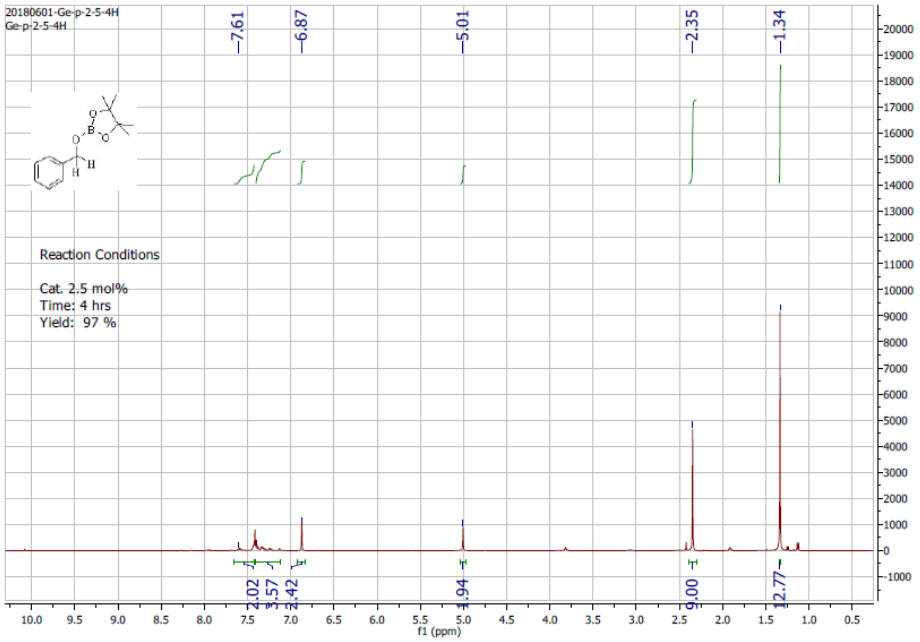

(c)

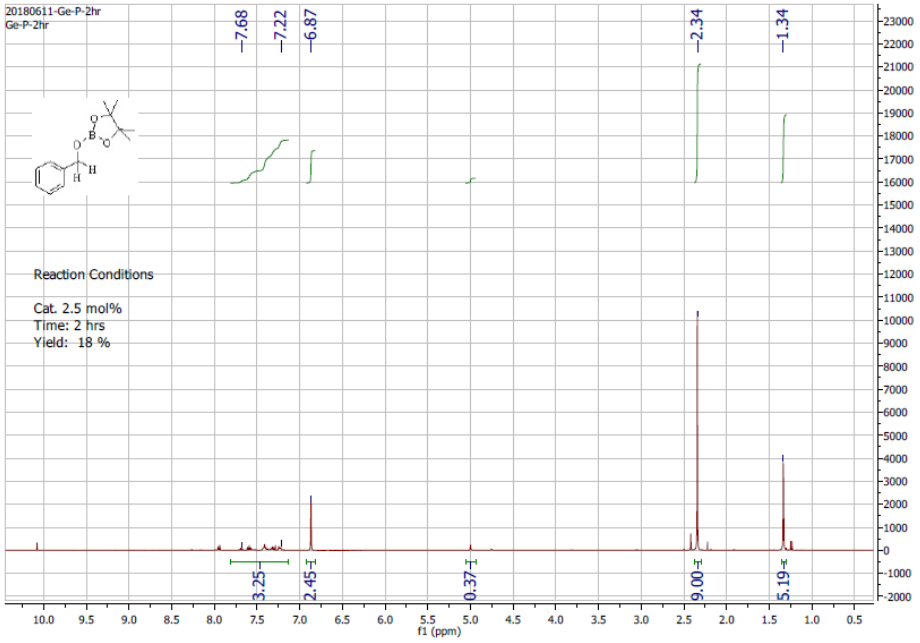

(d)

Figure 4A.6 ^{1}H NMR for optimization of reaction conditions using catalyst **3.3** at the reaction conditions of (a) cat. 2.5 mol%, 12hrs, (b) cat. 1.0 mol%, 12 hrs (c) cat. 2.5 mol%, 4hrs (d) cat. 2.5 mol%, 2 hrs.

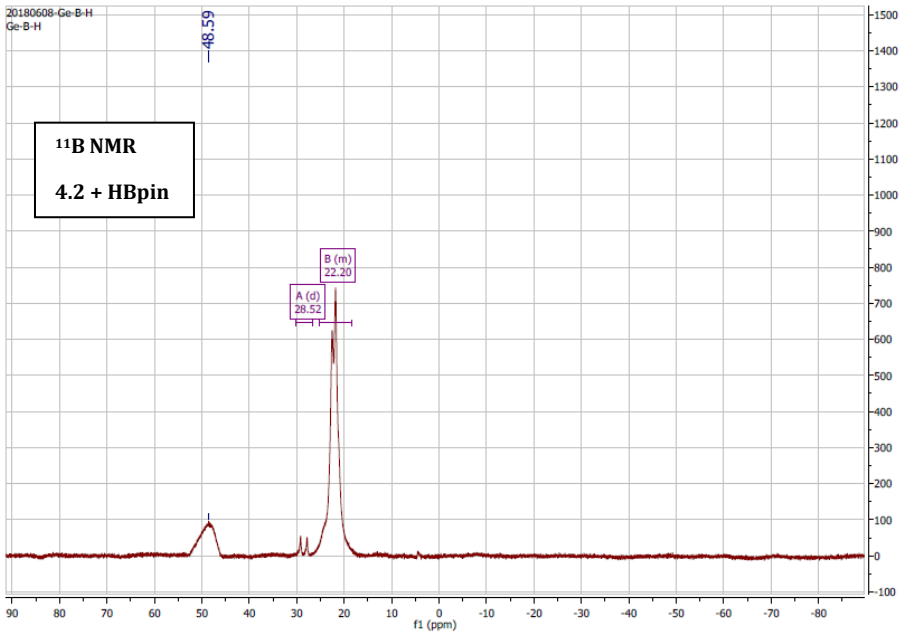
20180608-Ge-B-H
Ge-B-H
48.59
11B NMR
4.2 + HBpin
B (m)
22.20
A (d)
28.52
f1 (ppm)

(a)

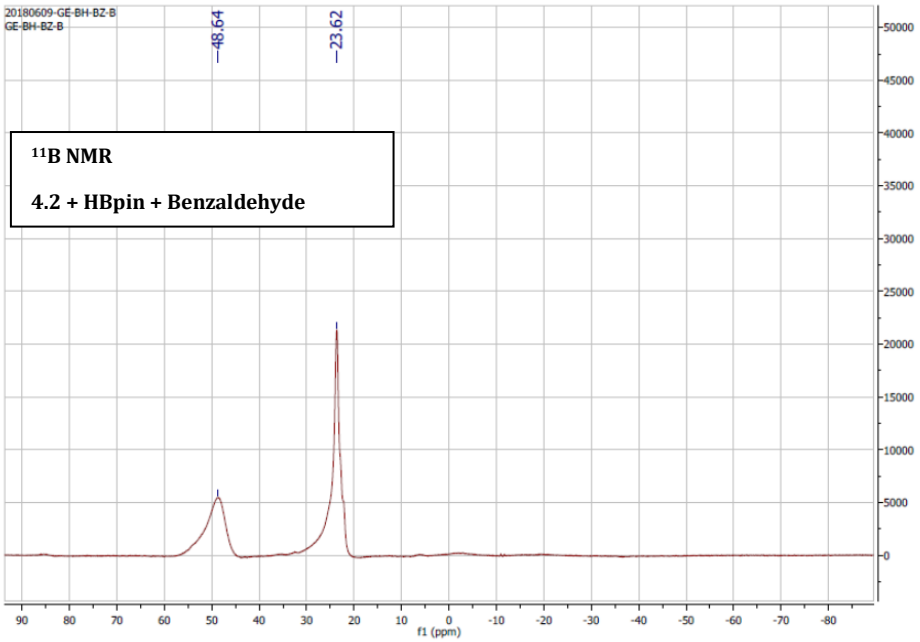
20180609-GE-BH-BZ-B
GE-BH-BZ-B
48.64
23.62
11B NMR
4.2 + HBpin + Benzaldehyde
f1 (ppm)

(b)

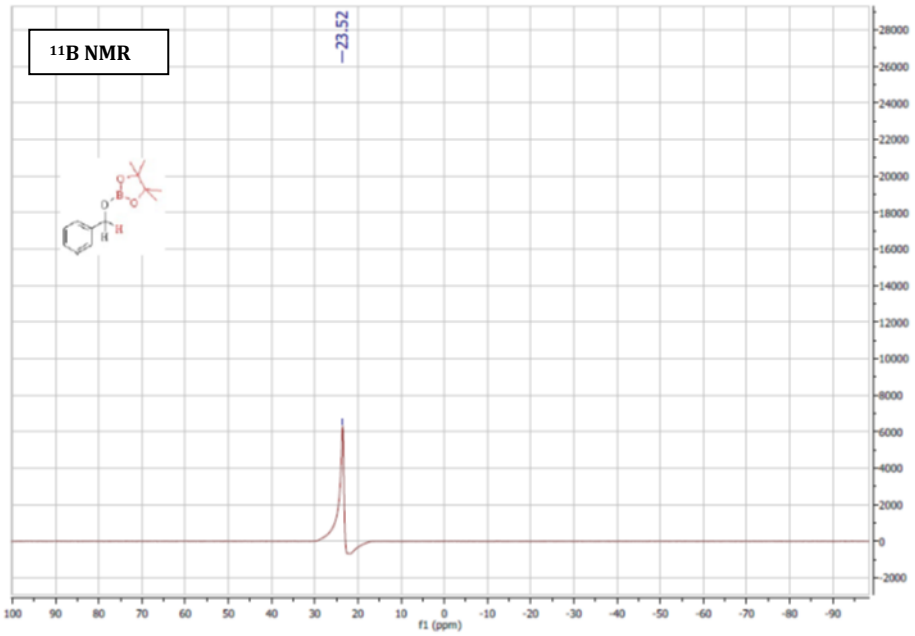

(c)

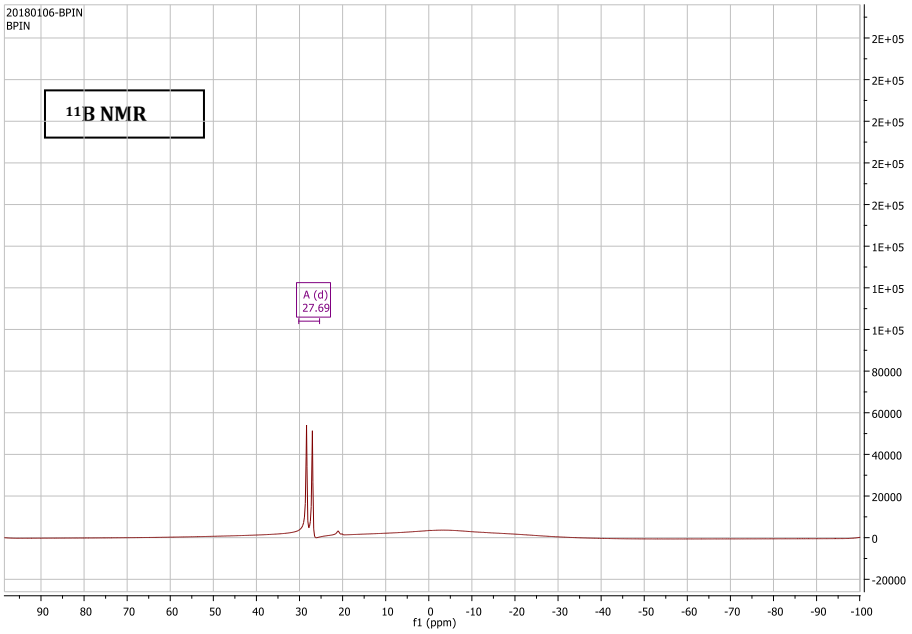

(d)

Figure 4A.7 ^{11}B NMR of reaction mixture of (a) **4.2** + HBPin; (b) **4.2** + HBPin + Benzaldehyde; (c) hydroborated product of benzaldehyde; (d) HBpin

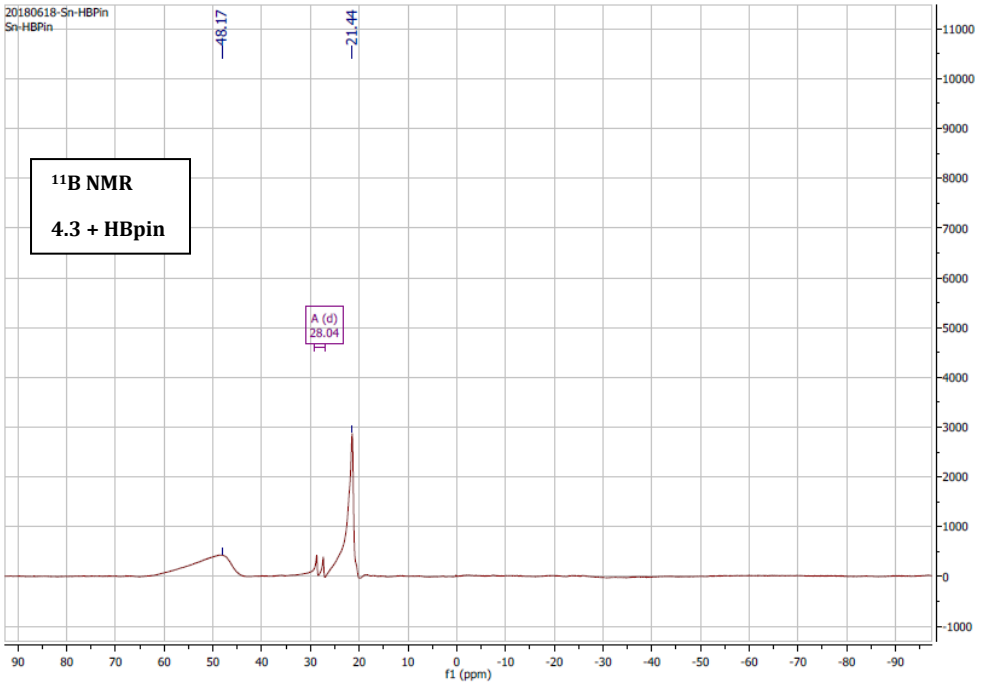

(a)

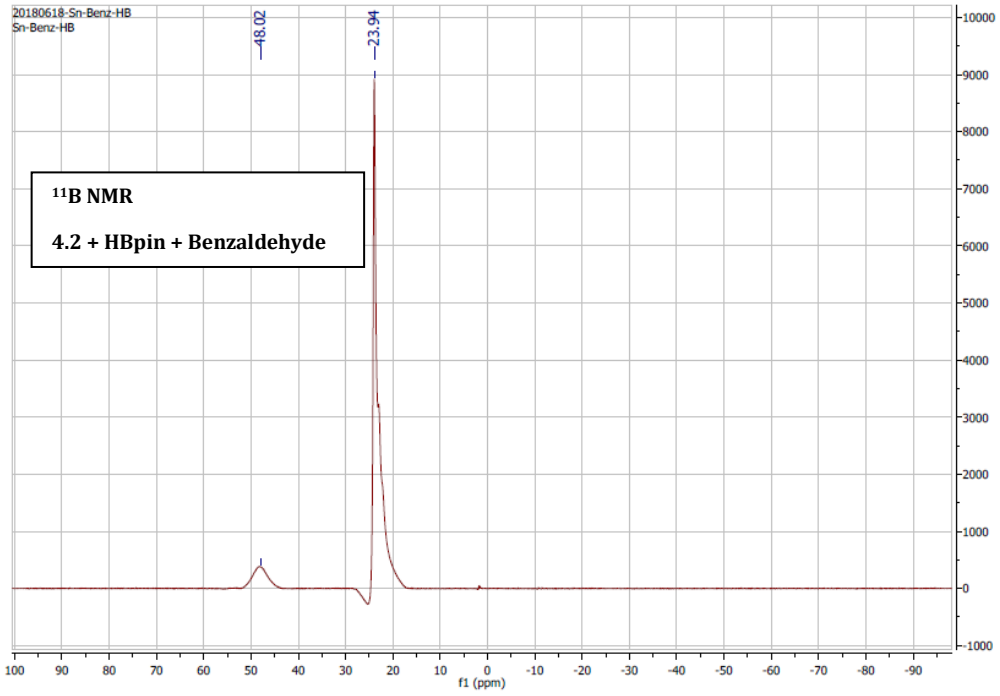

(b)

Figure 4A.8 ^{11}B NMR of reaction mixture of (a) **4.3**+ HBPin; (b) **4.3** + HBPin + Benzaldehyde

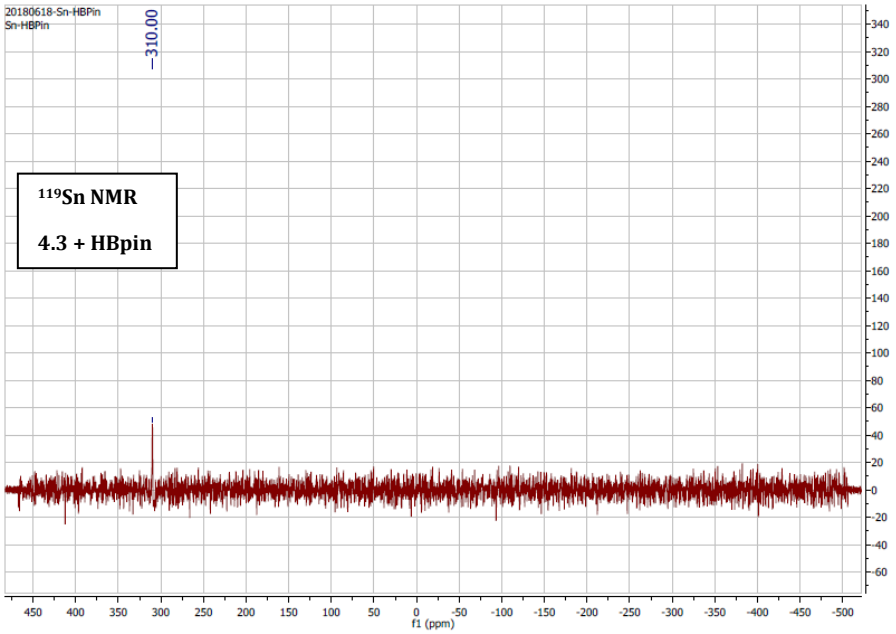

(a)

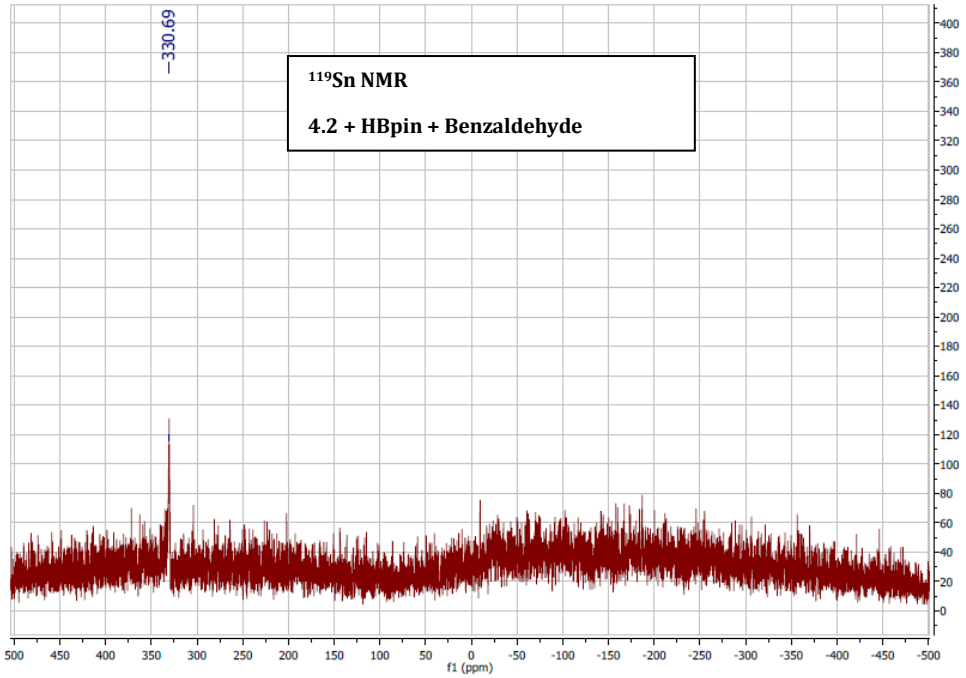

(b)

Figure 4A.9 ^{119}**Sn** NMR of reaction mixture of (a) **4.3** + HBPin; (b) **4.3** + HBPin + Benzaldehyde

Table 5A.1 Crystallographic data for tin cluster **5.1**

	5.1
Chemical formula	$C_{108}H_{90}I_8P_6Sn_{19}$
Formula weight	4843.92 g/mol
Temperature	100(2) K
Wavelength	0.71073 Å
Crystal system	orthorhombic
Space group	Pa-3
Unit cell dimensions	a = 23.931(4) Å
	b = 23.931(4) Å
	c = 23.931(4) Å
	α = 90°
	β = 90°
	γ = 90°
Volume	13705 (7) Å^3
Z	4
Density (calculated)	2.348 g/cm^3
Absorption coefficient	5.303 mm^{-1}
F(000)	8808
Theta range for data collection	2.40 to 21.89°
Index ranges	-25<=h<=25, -25<=k<=25, -25<=l<=25
Reflections collected	105128
Independent reflections	2778 [R(int) = 0.1449]
Completeness to Θ (%)	99.9%
Absorption correction	multi-scan
Refinement method	Full-matrix least-squares on F2
Refinement program	SHELXL-2014/7 (Sheldrick, 2014)
Function minimized	Σ w(Fo2 - Fc2)2
Data / restraints / parameters	2778 / 6 / 234
Goodness-of-fit on F2	1.130
Δ/σmax	0.001
Final R indices	1911 data; [I>2σ(I)] $R1$ = 0.0421, w$R2$ = 0.0814
	all data , $R1$ = 0.0889, wR2 = 0.1013
Largest diff. peak and hole	1.861 and -1.281 eÅ^{-3}
R.M.S. deviation from mean	0.152 eÅ^{-3}

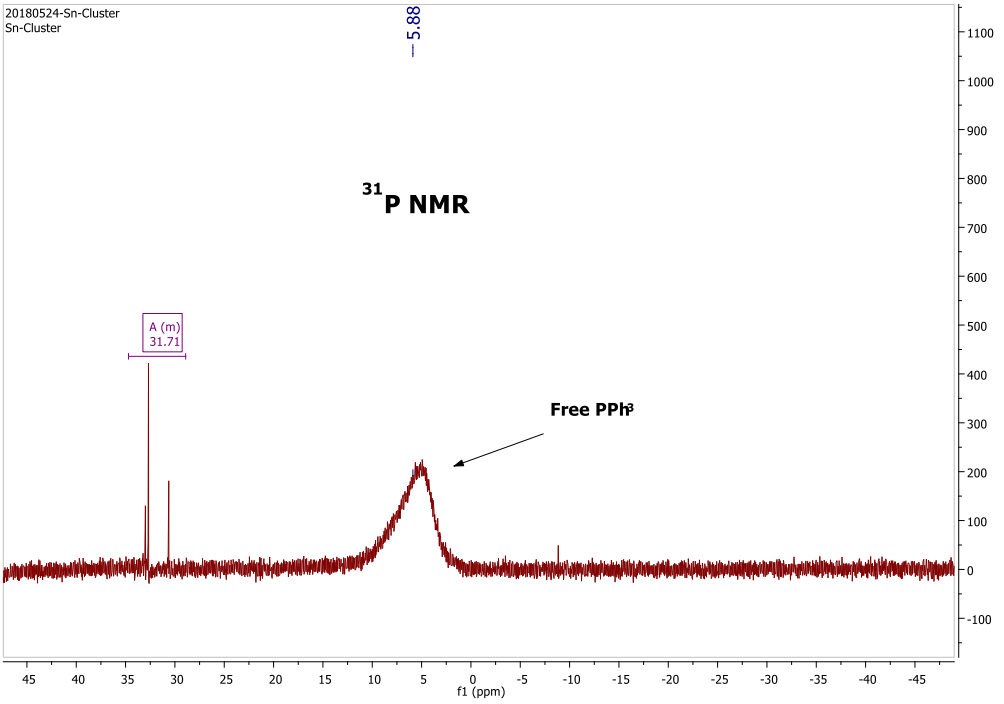

Figure 5A.1 ^{31}P NMR of tin cluster **5.1** in THF-d_8

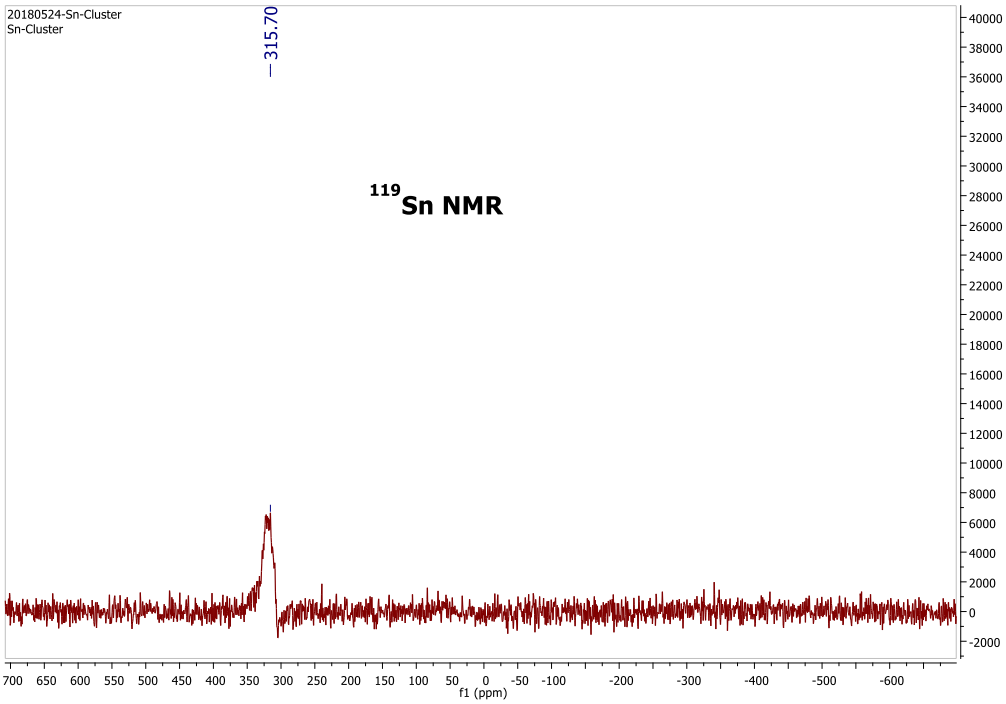

Figure 5A.2 ^{119}Sn NMR of tin cluster **5.1** in THF-d_8

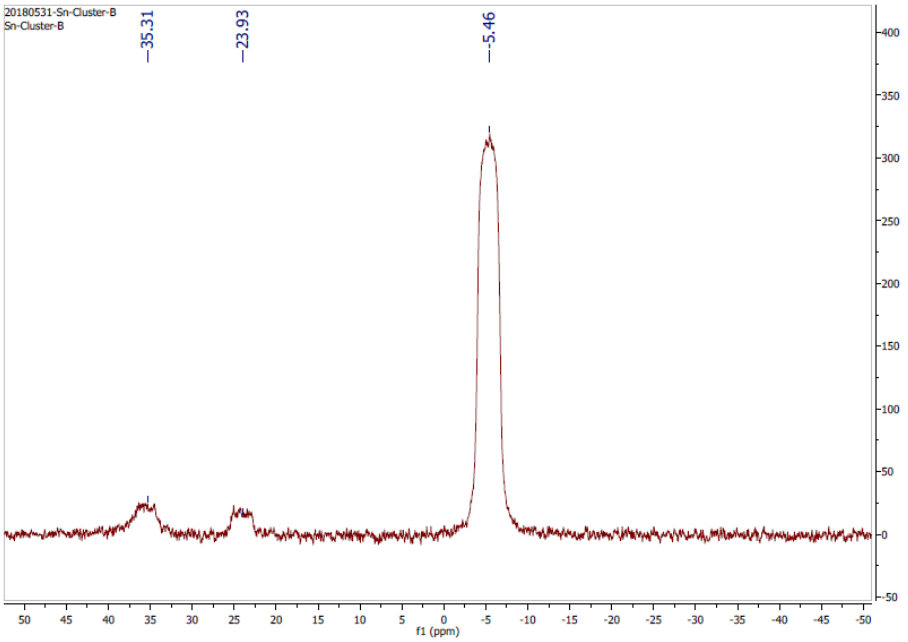

(a)

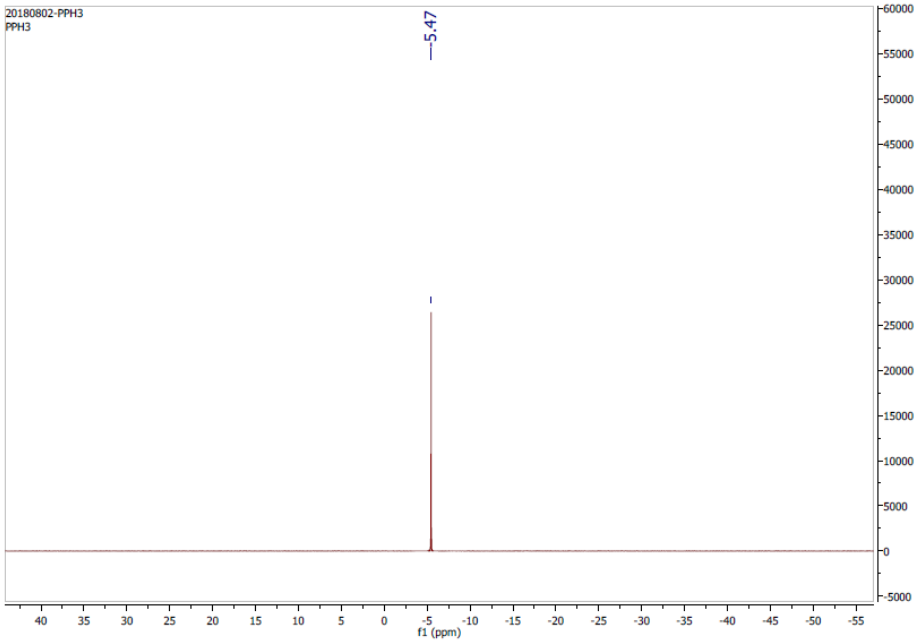

(b)

Figure 5A. 3 ^{31}P NMR of (a) Solution of tin cluster **5.1** after keeping the solution for 12 hrs under inert atmosphere (the solution turned to colourless form orange) (b) pure PPh

Rights and Permissions

9/19/2018 RightsLink® by Copyright Clearance Center

Copyright Clearance Center RightsLink®

Home | Create Account | Help

ACS Publications Most Trusted. Most Cited. Most Read.

Title: Acyclic α-Phosphinoamido-Germylene: Synthesis and Characterization

Author: Shiv Pal, Rajarshi Dasgupta, Shabana Khan

Publication: Organometallics

Publisher: American Chemical Society

Date: Oct 1, 2016

Copyright © 2016, American Chemical Society

LOGIN

If you're a copyright.com user, you can login to RightsLink using your copyright.com credentials.

Already a **RightsLink user** or want to learn more?

PERMISSION/LICENSE IS GRANTED FOR YOUR ORDER AT NO CHARGE

This type of permission/license, instead of the standard Terms & Conditions, is sent to you because no fee is being charged for your order. Please note the following:

- Permission is granted for your request in both print and electronic formats, and translations.
- If figures and/or tables were requested, they may be adapted or used in part.
- Please print this page for your records and send a copy of it to your publisher/graduate school.
- Appropriate credit for the requested material should be given as follows: "Reprinted (adapted) with permission from (COMPLETE REFERENCE CITATION). Copyright (YEAR) American Chemical Society." Insert appropriate information in place of the capitalized words.
- One-time permission is granted only for the use specified in your request. No additional uses are granted (such as derivative works or other editions). For any other uses, please submit a new request.

BACK | CLOSE WINDOW

Copyright © 2018 Copyright Clearance Center, Inc. All Rights Reserved. Privacy statement. Terms and Conditions.
Comments? We would like to hear from you. E-mail us at customercare@copyright.com

JOHN WILEY AND SONS LICENSE TERMS AND CONDITIONS

Sep 21, 2018

This Agreement between INDIAN INSTITUTE OF SCIENCE EDUCATION AND RESEARCH, PUNE, INDIA -- SHIV PAL ("You") and John Wiley and Sons ("John Wiley and Sons") consists of your license details and the terms and conditions provided by John Wiley and Sons and Copyright Clearance Center.

License Number	4432540517567
License date	Sep 19, 2018
Licensed Content Publisher	John Wiley and Sons
Licensed Content Publication	ChemistrySelect
Licensed Content Title	Comparing Nucleophilicity of Heavier Heteroleptic Amidinato-Amido Tetrelylenes: An Experimental and Theoretical Study
Licensed Content Author	Nasrina Parvin, Shiv Pal, Vallyanga Chalil Rojisha, et al
Licensed Content Date	Jun 27, 2016
Licensed Content Volume	1
Licensed Content Issue	9
Licensed Content Pages	5
Type of Use	Dissertation/Thesis
Requestor type	Author of this Wiley article
Format	Print and electronic
Portion	Full article
Will you be translating?	No
Title of your thesis / dissertation	Synthesis, Structural Elucidation, and Application of Tetrelylenes
Expected completion date	Oct 2018
Expected size (number of pages)	150
Requestor Location	INDIAN INSTITUTE OF SCIENCE EDUCATION AND RESEARCH, PUNE, INDIA NEW HOSTEL IISER CAMPUS PUNE, MAHARASTRA 411008 India Attn: shiv pal
Publisher Tax ID	EU826007151
Total	**0.00 USD**
Terms and Conditions	

TERMS AND CONDITIONS

This copyrighted material is owned by or exclusively licensed to John Wiley & Sons, Inc. or one of its group companies (each a"Wiley Company") or handled on behalf of a society with which a Wiley Company has exclusive publishing rights in relation to a particular work (collectively "WILEY"). By clicking "accept" in connection with completing this licensing transaction, you agree that the following terms and conditions apply to this transaction (along with the billing and payment terms and conditions established by the Copyright Clearance Center Inc., ("CCC's Billing and Payment terms and conditions"), at the time that you opened your RightsLink account (these are available at any time at http://myaccount.copyright.com).

JOHN WILEY AND SONS LICENSE TERMS AND CONDITIONS

Sep 21, 2018

This Agreement between INDIAN INSTITUTE OF SCIENCE EDUCATION AND RESEARCH, PUNE, INDIA – SHIV PAL ("You") and John Wiley and Sons ("John Wiley and Sons") consists of your license details and the terms and conditions provided by John Wiley and Sons and Copyright Clearance Center.

License Number	4433630282702
License date	Sep 21, 2018
Licensed Content Publisher	John Wiley and Sons
Licensed Content Publication	Chemistry - A European Journal
Licensed Content Title	{Sn10[Si(SiMe3)3]4}2−: A Highly Reactive Metalloid Tin Cluster with an Open Ligand Shell
Licensed Content Author	Claudio Schrenk, Florian Winter, Rainer Pöttgen, et al
Licensed Content Date	Nov 27, 2014
Licensed Content Volume	21
Licensed Content Issue	7
Licensed Content Pages	6
Type of use	Dissertation/Thesis
Requestor type	University/Academic
Format	Print and electronic
Portion	Figure/table
Number of figures/tables	2
Original Wiley figure/table number(s)	Scheme 1 and Figure 2
Will you be translating?	No
Title of your thesis / dissertation	Synthesis, Structural Elucidation, and Application of Tetrelylenes
Expected completion date	Oct 2018
Expected size (number of pages)	150
Requestor Location	INDIAN INSTITUTE OF SCIENCE EDUCATION AND RESEARCH, PUNE, INDIA NEW HOSTEL IISER CAMPUS PUNE, MAHARASTRA 411008 India Attn: shiv pal
Publisher Tax ID	EU826007151
Total	0.00 USD
Terms and Conditions	

TERMS AND CONDITIONS

This copyrighted material is owned by or exclusively licensed to John Wiley & Sons, Inc. or one of its group companies (each a"Wiley Company") or handled on behalf of a society with which a Wiley Company has exclusive publishing rights in relation to a particular work (collectively "WILEY"). By clicking "accept" in connection with completing this licensing